



Durham E-Theses

The structure and evolution of the Wessex Basin.

Lake, S.D.

How to cite:

Lake, S.D. (1985) *The structure and evolution of the Wessex Basin.*, Durham theses, Durham University. Available at Durham E-Theses Online: <http://etheses.dur.ac.uk/1215/>

Use policy

The full-text may be used and/or reproduced, and given to third parties in any format or medium, without prior permission or charge, for personal research or study, educational, or not-for-profit purposes provided that:

- a full bibliographic reference is made to the original source
- a [link](#) is made to the metadata record in Durham E-Theses
- the full-text is not changed in any way

The full-text must not be sold in any format or medium without the formal permission of the copyright holders.

Please consult the [full Durham E-Theses policy](#) for further details.

**THE STRUCTURE AND EVOLUTION OF THE
WESSEX BASIN**

by

STUART DAVID LAKE B.Sc.

VOL 1

A thesis submitted to the University of Durham
for the degree of Doctor of Philosophy.

The copyright of this thesis rests with the author.
No quotation from it should be published without
his prior written consent and information derived
from it should be acknowledged.

Department of Geological Sciences, December 1985.



15. APR. 1986

BEST COPY

AVAILABLE

Variable print quality



FRONTISPIECE

Stair Hole and Lulworth Cove along the Dorset Coast.

I dedicate this thesis to my sister Fiona,
and her brave fight against cancer.

There are some heights in Wessex, shaped as if by a kindly hand
For thinking, dreaming, dying on, and at crises when I stand,
Say, on Inqpen Beacon eastward, or on Wyllys-Neck westwardly,
I seem where I was before my birth and after death may.

Thomas Hardy. 1896. "Wessex Heights"



Abstract

The subsidence form of many sedimentary basins consist of two discrete phases of basin development: a rapid subsidence phase related to rifting of the crust and thinning of the sub-crustal lithosphere followed by a thermal or flexural subsidence phase. In marked contrast to this simple models prediction, some basins exhibit a complicated subsidence history consisting of one or more phases of extension and thermal recovery (construction phase). These phases may in turn be followed by phases of destruction (inversion) which could introduce an additional driving subsidence.

The Wessex Basin is such an example. Polyphase reactivation of basement thrusts and wrench (or transfer) faults tended to compartmentalize the basement, thereby leading to the initiation of discrete (Permian-Cretaceous) pull-apart depocentres opening along northwest-southeast faults. On the basis of structural and subsidence data, the Wessex Basin has been interpreted as the result of thin skinned crustal extension above an intracrustal late Variscan listric detachment surface, with significantly reduced extension of the sub-crustal lithosphere and is not the result of simple lithospheric stretching as described previously. The same detachment surface facilitated inversion and hence the destruction of the basin, beginning in the late Cretaceous-early Tertiary.

The structural development of the Wessex Basin, both during extension and compression, was ultimately controlled by the plate motion of Africa relative to Europe. Such plate motions successfully predict the observed northwest-southeast sinistral motion in the Stephanian-Aptian, east-west sinistral motion during the Aptian-Cenomanian, and northwest-southeast dextral motion and inversion from the Cenomanian to the Present day.



Acknowledgements

I am sincerely grateful to Professor John F. Dewey for his stimulating and patient supervision of this study throughout the past three years. I am particularly indebted to Dr. Garry Karner for his help, encouragement and the many fruitful and sometimes heated discussions throughout this study and for his willingness to write and develop the thermo and mechanical computer programs used in this study. I would also like to thank Garry and Lois for their many evenings of entertainment and games of Trivial Pursuit.

I would like to thank the following companies/organisations and their employees for the many fruitful discussions and access to their data: British Geological Survey, Dr. A. Chadwick, Dr. G. Day, Dr. J. Edwards and Dr. S. Holloway, British Petroleum, in particular Dr. I. Vann and Dr. R. Clarke; Clyde Petroleum, Dr. C. Fletcher; Department of Energy, Dr. Aitken; Elf Aquitaine U.K.; Esso; Geomorphological Services Ltd., Dr. J. Craig; Geophysical Services International; Goaf Petroleum, Dr. J. Donato; Nigel Press Associates, W. Duncan; R.T.Z., Dr. C. Brooks; Shell, Dr. K. Glennie, Dr. B. Van Hoorn and Dr. P. Zieqler; and Teneco U.K., Dr. P. Woodroof. The views and interpretations expressed in this thesis are not necessarily those of the companies.

Additionally I would like to thank Dr. T. Bevan, Dr. D. Donovan, Dr. P. Drummond, Dr. P. Hancock, Dr. G. Johnson, Dr. R. Mortimore, Dr. G. Plint, Dr. W.G. Townson, Dr. M. Tucker, Dr. I. West and Dr. R. Wilson and the help and co-operation provided by local Dorset Geologists in particular Paul Ensom and Hugh Prudden. I would also like to thank Nutty and Mich for their hospitality during the 9 months fieldwork.

My appreciation of help and support is also extended to Dr. H. Emeleus,

Dr. D. Hutton, Dr. G. Karner and Dr. T. Munday for proof reading the typescript through its various developments, Andy Reid and Shell International B.V. for the draughting of some text figures, Alan Carr and Gerry Dresser for the photographic work, and especially Dave Asbery for his help throughout the 3 years.

I would like to take this opportunity to thank my parents and all the past and present research students and postdoctorates in particular Ian Alsop (alias Thuq), Alistair Baird, Colin 'Budgie' Bradshaw (critic and flatmate), Kevin Brown, Dr. Rob Butler, Antony Dixon, John Faithful, Ian Goldsmith, Mark Helman, Kevin Hird, Neville Hollingworth, Anthony Lewis, Dr. Jim 'on your bike' Pindell, Ashley Price, Webster Mohriak (and his computer program), Dr. D. Southwood and Colin Bradshaw again (he likes to be mentioned).

The work for this thesis was done while the author was under the tenureship of an N.E.R.C. research studentship which is gratefully acknowledged.

Lastly I would like to thank Mrs. Carole Blair for typing various contributions at short notice and express my sincere thanks to my girlfriend Nicola Bruce for her willingness at all hours to type this work and her help in keeping me sane during the months of turmoil writing this contribution.

ABSTRACT	I
ACKNOWLEDGEMENTS	II
CONTENTS	IV
LIST OF TEXT FIGURES	VII
LIST OF PLATES	XIV
LIST OF TABLES	XVI
LIST OF ENCLOSURES IN VOLUME 2	XVIII
DECLARATION AND COPYRIGHT	XX
 CHAPTER 1	
INTRODUCTION	1
 CHAPTER 2	
BASIN EVOLUTION	12
2.1 Introduction	13
2.2 Regional Geology and Structure	16
2.3 Structure of the English Channel	19
A. Introduction	19
B. The Channel Basin	21
C. The Cherbourg High	35
D. The Hampshire Dieppe High	36
E. The Western Approaches Basin	40
F. Conclusions	41
2.4 Reactivation	42
A. East-west structures	42
1. Thrust reactivation in Lyme Bay	43
B. Northwest-southeast structures	51
C. Discussion	51
2.5 Basin formation mechanisms	53
A. Introduction	53
B. Lithospheric stretching model	54
C. Crustal stretching model	56
1. Cyclicity	83
a. Introduction	83
b. Sedimentary cyclicity	85
c. Climatic cyclicity	86
d. Tectonic and eustatic cyclicity	90
e. Discussion	93
2.6 Conclusions	97
 CHAPTER 3	
STRUCTURE, EVOLUTION AND INVERSION TECTONICS	104
3.1 Introduction	105
3.2 Structural setting	106

3.3	Structural configuration, basement structure and basin stratigraphy	108
A.	Pre-basinal phase	108
1.	South West Approaches Traverse (SWAT)	110
B.	Basinal phase	121
3.4	Structural evolution of the basin	125
3.5	Inversion	138
A.	Timing of Inversion	138
B.	Evidence for Laramide Inversion	138
3.6	Present structural style	149
3.7	Conclusions	153
CHAPTER 4	RELATIONSHIP OF THE WESSEX BASIN TO THE TECTONICS OF WESTERN EUROPE	158
4.1	Introduction	159
A.	Western Approaches Basin	163
B.	Bristol Channel Basin	164
C.	Porcupine Basin, Slyne Trough, Erris Trough, and Donegal Basins	165
D.	Fasnet Basin	165
E.	Celtic Sea and Cardigan Bay Basins	166
F.	Kish Bank Basin	168
G.	Cheshire, Irish Sea, Solway, Ulster, Rathlin Trough and Loch Indall Basins	168
H.	West Scottish and Shetland Basins	168
I.	Moray Firth Basin	169
J.	North Sea Basin	169
K.	Sole Pit and Cleveland Basins	169
L.	Worcester Basin	170
M.	Paris Basin	170
4.2	Discussions	172
CHAPTER 5	LOCAL STRUCTURES AND BRITTLE MICROTECTONICS	181
5.1	Local Structures	182
A.	Introduction	182
B.	Folding	182
1.	Introduction	182
2.	Pre-Aptian	183
3.	Post-Aptian	183
C.	Faulting	184
1.	Introduction	184
2.	Pre-Aptian	184
3.	Post-Aptian	187
D.	Conclusions	187
5.2	Brittle Microtectonics	193
A.	Introduction	193
B.	Data Collection and Analysis	193
C.	Kinematic indicators	194
1.	Bedding	194

	2. Shear Zones	197
	3. Kink Bands	203
	4. Stylolites	204
	5. Veins	204
	6. Fissures	207
	7. Sediment filled mesofractures	210
	8. Superficial structures	212
	9. Jointing	213
D.	Conclusions	227
CHAPTER 6	HYDROCARBON OCCURENCES	228
	6.1 Introduction	229
	6.2 Source rocks	229
	6.3 Maturation and Migration	233
	6.4 Reservoirs	235
	6.5 Hydrocarbon Plays	237
	1. Introduction	237
	2. Primary Plays (1)	237
	A. Play 1A Pre-Aptian/Albian tilted fault blocks	237
	B. Play 1B Stratigraphic path cuts	238
	C. Play 1C Roll overs, Hanging wall drapes, monoclinial flexures and folds	239
	D. Play 1D Strike Slip related structures	240
	3. Secondary Plays (2)	240
	A. Play 2A Horsts	240
	B. Play 2B Buried Fans	241
	4. Wytch Farm Oilfield: Example	241
	6.6 Future Exploration	242
	6.7 Conclusions	242
REFERENCES		244
APPENDICES		266
APPENDIX A	LIST OF LOCALITIES	266
APPENDIX B	LIST OF BOREHOLES AND WELLS	275
APPENDIX C	BOREHOLES	279
APPENDIX D	LANDSAT INTERPRETATION	292
APPENDIX E	BRECCIATED PIPES AND THE BROKEN BEDS	311
APPENDIX F	EVIDENCE FOR BATHONIAN AND TITHONIAN SYNSEDIMENTARY FAULT MOVEMENT IN DORSET	321

FRONTISPIECE

Stair Hole and Lulworth Cove along the Dorset Coast.

Chapter 1

Fig. 1.1	Map of the British Isles, showing the area of study.	5
Fig. 1.2	Stratigraphic column of the Wessex Basin.	6
Fig. 1.3	Solid Geology of the western Wessex Basin.	10

Chapter 2

Fig. 2.1	The major Mesozoic structural features in the Wessex Basin, Southern England. (Based on Stoneley, 1982; Sellwood et al., 1985; Whittaker, 1985).	15
Fig. 2.2	Chrono-lithostratigraphic column along a north-south transect in the western portion of the Wessex Basin. A. Vale of Pewsey fault, B. Mere Fault, C. Cranbourne Fault and D. Purbeck-Isle of Wight Fault. Data compiled from many sources.	17
Fig. 2.3	Top Penarth Group structural map of the English Channel, based on a G.S.I. non-exclusive seismic survey.	20
Fig. 2.4	North-south seismic section and interpretation across the Weymouth anticline.	23
Fig. 2.5	Aeromagnetic anomaly map of the Wessex Basin and surrounding areas, 1:625,000 scale. (From the Aeromagnetic Map of Great Britain sheet 2, England and Wales, compiled by the Geological Survey, 1st Edition, 1965).	25
Fig. 2.6	North-south seismic section and interpretation across the Mid-Channel fault.	28
Fig. 2.7	Five serial seismic sections across the Pay de Bray fault and their respective interpretations.	31
Fig. 2.8	North-south seismic section and interpretation across the Channel Basin and Purbeck-Isle of Wight fault.	32
Fig. 2.9	A. Interpreted north-south seismic section showing basement topography overlapped to the south by presumed Permo-Triassic sedimentary sequences on the southern	37

- edge of the Channel Basin. 37
- B. North-south seismic section and interpretation across the Western Approaches Basin, depicting a south dipping partially inverted half graben.
- Fig. 2.10 Two-way travel-time map of the persistent prominent reflectors in the Devonian/Carboniferous basement. Isochrons in seconds. 45
- Fig. 2.11 North-south seismic section and interpretation of reflector 2 (R2) controlling the development of a major northerly-dipping late Palaeozoic/Mesozoic half graben in Lyme Bay. 46
- Fig. 2.12 North-south seismic section and interpretation showing the ramp/flat geometry of reflector 2 (R2) controlling the development of a major northerly-dipping late Palaeozoic/Mesozoic half graben in Lyme Bay. The detailed structure of the Abbotsbury-Ridgeway fault zone is well displayed. 48
- Fig. 2.13 North-south seismic section and interpretation of reflector 1 (R1). The reflector extends well in to the footwall side of a major overlying late Palaeozoic/Mesozoic fault. The reflector is interpreted as a shallow southward-dipping Variscan thrust. 50
- Fig. 2.14 Lithospheric stretching initially modifies the thickness of both the crust and sub-crustal lithosphere: δ represents stretching above the decollement (usually considered to be the Moho) and β represents either stretching below the decollement or the degree of sub-crustal heating. The simplest model of basin formation is for depth-independent stretching ($\delta = \beta$) in which the pre-event lithospheric configuration and temperature structure (a) is modified to give (b). 55
- Alternatively, crustal thinning in the absence of sub-crustal extension significantly modifies the temperature structure of the lithosphere (c). The general model therefore, is for depth-dependent stretching across a decollement (d). (Modified from Karner & Dewey (1986)).
- Fig. 2.15 Procedure for calculating tectonic subsidence by backstripping. The Winterborne Kingston borehole was chosen as most representative. The porosity was recorded from the Winterbourne Kingston sonic log and used for the decompaction of all boreholes. 59
- Fig. 2.16 Subsidence plots for all the backstripped boreholes in southern England. Borehole numbers are summarized on Table 2.1. 61

- Fig. 2.17 Backstripped subsidence plots. Arne Gl-Brabourne boreholes. 63
- Fig. 2.18 Backstripped subsidence plots. Brighting - Cranbourne boreholes. 64
- Fig. 2.19 Backstripped subsidence plots. Elham - Herne boreholes. 65
- Fig. 2.20 Backstripped subsidence plots. Highworth - Nettlecombe boreholes. 66
- Fig. 2.21 Backstripped subsidence plots. Portsdown - Sonningeye boreholes. 67
- Fig. 2.22 Backstripped subsidence plots. Southampton - Warlingham boreholes - BH 98/22-2. 68
- Fig. 2.23 Backstripped subsidence plots based on regional (as opposed to well data). Bristol Channel - Weymouth Area. 70
- Fig. 2.24 Three examples of backstripped boreholes. Each borehole the actual basement subsidence, decompacted subsidence and backstripped tectonic driving subsidence are shown. Subsidence due to sediment loading is stippled. The observed and best fitting (in a least squares sense) porosity curve from Winterbourne Kingston No.1 is also shown. This curve was used for decompacting all the wells from the Wessex Basin. A 31.2 km crust and 125 km lithosphere were assumed to calculate the theoretical driving subsidence curves. 72
- Fig. 2.25 Four selected wells including the effects of decollement extension relaying and finite rifting subsidence plots as a function of delta and beta (i.e. $\delta = \beta$). Delta was determined by the maximum backstripped subsidence. Three different types shown Beta = 1 (no lithospheric involvement) Beta = Delta (Delta and Beta) = 1.4 73
- Fig. 2.26 Four selected wells - polyphase finite rerifting (i.e. $\delta = \beta$) 77
). Deltas and betas and finite rifting duration for each extension event are shown.
- Fig. 2.27 Calculated flexural-phase stratigraphy of a theoretical sedimentary basin in which the thermal and mechanical properties of the lithosphere are integrated with the McKenzie stretching model. Maximum stretching is 20% and predicts a 300 metre deep basin, 400-500 km wide. Marginal onlap is a direct consequence of an increasing T_e (elastic thickness) with time since rifting. The rapid onlap in this model reflects the failure of β to 80

appreciably reset the temperature structure of the lithosphere.	80
Fig. 2.28 North-south transect across the Wessex Basin using data from Whittaker (1985). A. Present-day observed structural configuration. B. Removal of inversion effects and thrust reactivation from section A to compare to forward modelled examples of the development. C. Forward modelling of the late Palaeozoic/lower Mesozoic development of the Wessex Basin using the magnetitude and distribution of stretching parameters on Table 2.1.	81
Fig. 2.29 The geologic correlation between polyphase extension events in a north-south transect across the Wessex Basin from borehole data to the large scale clay/sandstone/limestone cyclicity, and their correlation to tectonic events elsewhere.	84
Fig. 2.30 (a) Plan view of the stratigraphy in the central portion of the Wessex Basin showing onlap in the Tertiary at a time of world-wide sea level fall. (b) Relative sea-level variations estimated by Vail et al., (1977), Solid and Pitman (1978), dotted, compared with the Tertiary onlap and offlap patterns of the Wessex Basin. Numbered transgressions observed in the Vail et al., (1977) curve can be directly compared with the observed transgressional phases in the basin. Transgressions from Anderton et al., (1979) and Plint (1983).	99
 <u>Chapter 3</u>	
Fig. 3.1 Simplified regional tectonic map of the major Mesozoic structures in the Wessex Basin. Based on Whittaker (1985), Stoneley (1982), Sellwood et al., (1985), Kamerling (1979) and this thesis.	107
Fig. 3.2 Pre-Permian subcrop map of the Wessex Basin. Based in part on Wills (1973), Wallace (1983).	109
Fig. 3.3 Interpretation 1 of SWAT lines 10 and 11. (Inset map from BIRPS/ECORS 1986).	111
Fig. 3.4 Interpretation 2 of SWAT lines 10 and 11. (Inset map from BIRPS/ECORS, 1986).	112
Fig. 3.5 Postulated crustal profile across the Wessex Basin.	114
Fig. 3.6 Generalized lithological sequence of the Wessex basin and correlation of tectonic events to nearby (Ziegler,	122

Fig. 3.18	Tertiary evolution of the Sticklepath fault zone. Sinistral pull-apart development of the Tertiary basins, other more local deposits developed along the same structure.	147
Fig. 3.19	Detailed structure of the main features developed along the Sticklepath fault zone. Plan and cross section views of the Bovey and Petrockstow basins are shown. Terminology summarized on Fig. 3.18.	148
Fig. 3.20	Representative cross sections across the onshore portion of the Wessex Basin based on the isopachyte data of Whittaker (1985).	151
 <u>Chapter 4</u>		
Fig. 4.1	Late Palaeozoic/Mesozoic basin configuration of Western Europe (After Ziegler, 1982).	160
Fig. 4.2	Backstripped tectonic subsidence curves from selected basins in north-west Europe. (Bristol Channel - North Celtic Sea basins).	167
Fig. 4.3	Backstripped tectonic subsidence curves from selected basins in north-west Europe. (Rathlin Trough - Yorkshire (Cleveland) Basin).	171
Fig. 4.4	Late Palaeozoic/Mesozoic tectonic framework of north-west Europe. (Modified from Ziegler, 1982). Postulated Variscan fractures from this work are superimposed on the figure. These are postulated to have influenced the late Palaeozoic to Present day tectonic evolution of north-west Europe. (Numbered fractures are discussed in the text).	173
Fig. 4.5	Structural map of the late Variscan structure, from the Urals to the southern Appalachians. Heavy continuous and dashed lines represent the observed and inferred main fractures. Fit of continents after Le Pichon et al., (1977), Europe fixed. (Modified from Arthaud & Matte, 1977).	174
Fig. 4.6	Composite Bouguer Gravity image of north-west Europe. Preferential illumination from the northeast to the southwest to enhance the postulated northwest-southeast Variscan fractures. Figure 4.6 kindly supplied by G.D. Karner).	176

Chapter 5

Fig. 5.1	Contractional mesofaults. Examples (1) Kimmeridge Bay (N.G.R. SY 908 792), Kimmeridge Clay; (2) Ridgeway (N.G.R. SY 671 852), Purbeck Beds and (3) Horbarrow Bay 2 (N.G.R. SY 896 791) Kimmeridge Clay.	185
Fig. 5.2	Schematic profiles illustrating the geometry, kinematics, and dynamics of mesofaults developed in the Chalk of the steep-zone of the northern limb of the Weymouth anticline.	189
Fig. 5.3	A field sketch of the observed conjugate mesofaults within the Portland Beds at Dungy Head (N.G.R. SY 815 800) interpreted as indicative of layer-parallel extension.	190
Fig. 5.4	Plan view of mapped conjugate shear faults at Mupe Point (N.G.R. SY 844 792).	192
Fig. 5.5	Locality location map (Grid references in Appendix A).	195
Fig. 5.6	Additional Jurassic localities also visited during the research. (where no significant kinematic indicators were observed).	196
Fig. 5.7	Types of lineations and steps on mesofault surfaces. (a) Accretionary growth of crystal fibres (frictional type not shown) (B) Oblique pressure solution. (Redrawn from Hancock, 1985).	198
Fig. 5.8	Shear indicators (all examples are sinistral). Complex infillings also discussed. Infilling displays polyphase movement or one single incremental movement.	199
Fig. 5.9	Shear indicators continued, from Fig. 5.8.	200
Fig. 5.10	Shear indicators continued. (Number 16 = stylolitic margin still representing sinistral motion).	201
Fig. 5.11	Shear sense indicators spatially summarized (western Wessex Basin).	202
Fig. 5.12	Additional kinematic indicators spatially summarized (western Wessex Basin).	208
Fig. 5.13	Summary map of Ham Hill (N.G.R. ST 478 172) showing main kinematic indicators which are particularly well displayed at the locality. Superficial structures also indicated.	214
Fig. 5.14	Primary Joint summary map (western Wessex Basin).	216
Fig. 5.15	Secondary and Tertiary Joint summary map (western	217

	Wessex Basin).	217
Fig. 5.16	Joints, all orientations which are undefined. Summary map.	218
Fig. 5.17	A. Mesofaults and Joint summary block diagram represented basinwide (restoration of bedding to horizontal). B. Additional kinematic indicator summary block diagram represented basinwide restoration of bedding to horizontal. Compare both diagrams with Price (1966, Fig. 46).	223

Chapter 6

Fig. 6.1	Hydrocarbon Occurences in the Wessex Basin. Postulated mature and early mature source areas are shown concordant with reservoir distribution and postulated optimum reservoir location. (Lower insets indicate detailed structure of the Wytch Farm and Humbly Grove oilfields).	230
Fig. 6.2	Geothermal gradient of the Wessex Basin plotted from the Sherwood Sandstone. Based on temperature structure mapped by Allen & Holloway (1984).	234
Fig. 6.3	Simplified stratigraphic column of the Wessex Basin to scale. Source, Reservoir units are shown. Main hydrocarbon funds are summarized and th epossible play type they are associated with.	236

Plates

Plate 2.1	A view of the limestone/clay cyclicity at Lyme Regis (N.G.R. SY 328 909). The limestone nodule clearly is secondary in origin (post-compactional). These structures have been called by House (1985) 'Microrhythms', and are discussed more fully in Chapter 2. The microrhythms comprise laminated, dark, organic rich shale followed by lighter coloured calcareous shales and bioturbated limestone beds.	88
Plate 5.1	A side view of a contractional mesofault (thrust) within the 'Flat Stone Band' at Horbarrow Bay (N.G.R. SY 896 790). A duplex is evident in the footwall, while the hanging wall displays a local backthrust.	186
Plate 5.2	An oblique view of the 'Flats Stone Band' at Kimmeridge Bay (N.G.R. SY 898 788), showing thrust surface in plan. The hanging wall has been removed by erosion.	186

- Plate 5.3 An oblique view of two normal faults within the Kimmeridge Clay at Horbarrow Bay (N.G.R. SY 896 790). Local reverse antithetic faulting is displayed in the middle ground and discussed in more detail on Figure 5.1. Normal drag of the 'Flats Shone Band' in the foreground is clearly seen. 188
- Plate 5.4 Looking due east at a series of conjugate extension fractures in the Portland Beds at Dungey Head (N.G.R. SY 823 798) reflecting layer-parallel extension in the northern limb of the Weymouth anticline. The undulating basal contact of the Purbeck Beds clearly displays bedding plane slip. The detailed interpretation of these structures are described on Figure 5.3. 191
- Plate 5.5 Dextral calcite vein segments in the Kimmeridge Clay at Horbarrow ledges (N.G.R. SY 897 790). These displacement shears represent some lateral movement associated with fault zone. The fault breccia in the bottom left hand corner of the exposure corresponds to the same fault zone on Plate 5.13 and Figure 5.1. 205
- Plate 5.6 A north-south normal fault zone and flexure in the Kimmeridge Clay at Cuddle, Kimmeridge (N.G.R. SY 912 782). Outer arc extension is well displayed. 206
- Plate 5.7 A detailed view of extensional tilted fault block structures within the Bridport Sands under East Cliff, Bridport (N.G.R. SY 453 909). 211
- Plate 5.8 Looking along a north-south fault plane at Kimmeridge Bay (N.G.R. SY 908 792) which transects and offsets the hanging wall anticlines (displayed clearly as ridges) of the overlapping contractional mesofaults (thrusts) in the 'Flats Stone Band'. 225
- Plate 5.9 North-south dextral en-echelon hybrid fractures within the 'Flats Stone Band', at Kimmeridge Bay (N.G.R. SY 904 792). These are developed parallel to the fault plane displayed clearly in plate 5.8. 225
- Plate A.1 A view of a brecciated pipe within the Purbeck Beds extending up through the 'Cypris freestones' from the 'Broken Bed' horizon, Mupe rock, Bacon Hole (N.G.R. SY 840 797). The detailed description of this structure is outlined in Appendix E. 314
- Plate A.2 Strong asymmetric folds exposed in the Purbeck Beds at Bacon Hole, with short, (N.G.R. SY 840 797) almost vertical north limbs. Axial planes dip 30°S. The relative movement is implied to be down dip to the north. 314

- Plate A.3 A detailed view of the Bathonian section at Herbury (N.G.R. SY 611 810) reveals growth faulting within the Fullers Earth. This is exemplified by the thickening of the limestone in the centre of the section from left to right against the fault, and progressive onlap to the left of the picture, (see Appendix F). 324
- Plate A.4 Looking due west at the Tithonian growth fault described in Appendix F at Durlston Head (N.G.R. SZ 036 773). Fault 3 (see Appendix F) displayed in the centre of the picture. A major increase in thickness in the lower Purbeck stromatolitic units is displayed across the fault zone. The 'micrograben' which displays synsedimentary fault movement is displayed on the left side of the picture. 324

Tables

- Table 2.1 Resultant β (Beta) and δ (Delta) values for all the backstripped boreholes using finite rerifting plots. 75
- Table 2.2 The geologic correlation between the mechanical subsidence across the Wessex Basin from backstripped boreholes to the tectonic events in nearby areas. 75a
- Table 2.3 Wessex Basin cyclicity from the Permian-Present day compared to the regional cycles of Vail et al., (1977). T = transgressions and R = regressions. 94
- Table 2.4 Example sea-level correction for the Fordingbridge borehole. Removal of the apparent rift related subsidence (160-170 m.y. after rifting, upper Cretaceous) can be achieved with palaeobathymetry correction of Hancock (1975). Alternatively inversion induced subsidence may also account for both the upper Cretaceous and Tertiary rapid subsidence. (Sea level correction modified from Pitman, 1978 with a sea level maximum of 150 m). Tectonic subsidence assumed to account for the absent lower Cretaceous sedimentary section which was subsequently removed by the Aptian/Albian unconformity. 98
- Table 3.1 Summary of the symbols used in Figures 3.7 - 3.16. 141
- Table 3.2 Structural summary of the Channel Basin and Winterbourne Kingston Trough from Permian to Present. The terminology is summarized on Table 3.3 Tectonic events are also shown. 156
- Table 3.3 Structural summary of the Vale of Pewsey and Weald Basins from Permian to Present. 157

Table 4.1	List of all the basins and structural highs shown figure 4.4	161
Table 5.1	Joint frequency versus bed thickness for differing aged units and lithologies.	220
Table 5.2	Joint spacing for differing aged units and lithologies. (Numbers denote frequency at individual localities). Spacings greater than 3 m summarized.	221

VOLUME 2

- Fig.II.1.1 Western Wessex Basin, Solid Geology map, (1:250,000 scale).
- Fig.II.2.1 Previous north-south structural profile across the Wessex Basin, 1:100,000 scale based on data acquired prior to this study.
- Fig.II.2.2 Track lines of seismic reflection profiles based on G.S.I. non-exclusive seismic reflection survey and I.G.S. project 76/8 and 77/1 (part) used to compile a structural map of the Top Penarth Group in the English Channel.
- Fig.II.2.3 Top Penarth Group structural map of the English Channel. Interpretation by S.D. Lake. Based on G.S.I. non-exclusive seismic survey.
- Fig.II.2.4 Composite Bouguer Gravity anomaly map, Wessex Basin, 1:500,000 scale (Redrawn from B.G.S. Sources).
- Fig.II.2.5 Two-way time isochron map of dipping reflectors in Lyme Bay and associated active late Palaeozoic/Mesozoic faulting, (1:250,000 scale).
- Fig.II.3.1 Pre-Aptian subcrop map, (1:250,000 scale).
- Fig.II.3.2 Six serial north-south structural profiles across the Wessex Basin. Scale shown. Compiled from geological maps of the onshore British Isles by Whittaker, 1985.
- Fig.II.3.3 Chrono-lithostratigraphic column. Western Wessex Basin, S. England (Permian - Quaternary).
- Fig.II.5.1 Location map at 1:250,000 scale. Three insets of Lyme Bay, Bradstock and Kimmeridge at 1:50,000 scale.
- Fig.II.5.2 Additional Jurassic localities also visited during research.
- Fig.II.5.3 Shear sense indicators (1:250,000 scale). Three insets of Lyme Bay, Burton Bradstock and Kimmeridge at 1:50,000 scale. Dextral and sinistral movements distinguished (frequency also shown).
- Fig.II.5.4 Additional Kinematic indicators (1:250,000 scale). Three insets of the Lyme Regis, Burton Bradstock and Kimmeridge areas enlarged to 1:50,000 scale. The detailed orientation of calcite and pyrite veins and stylolites are also shown.

- Fig.II.5.5 Structures in the Bridport Sands, East Cliff, Bridport.
- Fig.II.5.6 Primary Joints 1:250,000 scale. Three insets of Lyme Bay, Bradstock and Kimmeridge at 1:50,000 scale. (Frequency also shown).
- Fig.II.5.7 Secondary and Tertiary Joints (1:250,000 scale). Three insets of the Lyme Regis, Burton Bradstock and Kimmeridge areas enlarged to 1:50,000. Clay or Calcite infill along joint planes are also distinguished.
- Fig.II.5.8 Joints all orientations undefined (1:250,000 scale). Three insets of the Lyme Regis, Burton Bradstock and Kimmeridge areas enlarged to 1:50,000 scale.
- Fig.II.6.1 Hydrocarbon occurrences in the Wessex Basin (1:625,000 scale).
 Inset 1. Detailed plan of the Wytch Farm Oilfield.
 Inset 2. Detailed plan of the Humbly Grove Oilfield.
 5 insets 1) Lower Lias Clay source rocks - showing areas of postulated maturity and early maturity.
 2) Kimmeridge Clay Source rock - showing areas of postulated maturity and early maturity.
 3) Sherwood Sandstone Reservoir - areas of reservoir distribution and postulated optimum reservoir location are also shown.
 4) Bridport Sands reservoir - areas of reservoir distribution and postulated optimum reservoir location are also shown.
 5) Great Oolite Limestone Formation reservoir - areas of reservoir distribution and postulated optimum reservoir location are also shown.
- Fig.II.A.1 Boreholes and wells in the western Wessex Basin, at 1:250,000 Scale (including exploration license blocks).
- Fig.II.A.2 Landsat MSS lineament map, path 216: row 24, path 217: row 24 (1:250,000 scale). Band 7 (0.8 - 1.10 m. Near Infra Red) Winter Imagery. Mosaic compiled by G.S.L. (Interpretation by S.D. Lake).
- Fig.II.A.3 Landsat TM lineament map, path 202: row 24, 1:250,000 scale. Band 5 (1.55 - 1.75 m Near Infra Red). Image taken 4.2.83. Processed on Dial system by Nigel Press Associates. Interpretation by S.D. Lake.
- Fig.II.A.4 TM lineament map, 1:250,000 scale of Dorset. Detail of the structures along the Dorset coast particularly well exemplified.

DECLARATION

The content of this thesis is the original work of the author (other people's work, where included, is acknowledged by reference). It has not been previously submitted for a degree at this or any other university.

S.D.LAKE

DURHAM

December 1985

COPYRIGHT

The copyright of this thesis rests with the author. No quotation from it should be published without his prior written consent and information derived from it should be acknowledged.

CHAPTER 1

INTRODUCTION

INTRODUCTION

In recent years, several models have been proposed to account for the driving mechanism and subsidence of intracratonic sedimentary basins; crustal doming and rifting (Sleep, 1971), phase changes or intrusion of dense material at depth (Falvey, 1974; Haxby et al., 1976; Royden et al., 1980); lithospheric stretching and loading (Artemjev & Artyushkov, 1971; McKenzie, 1978) and sub-crustal/sub-lithospheric tectonic erosion (Bott, 1971; Spohn & Neugebauer, 1978). It is possible that a mixture of these mechanisms may be responsible for basin initiation. However, the majority of these models either cannot explain the general decrease in subsidence with age of a basin, or such models require inappropriate local conditions which are generally not observed. The only model that systematically satisfies the geological history of intracratonic and rifted margin basins (excluding those basins associated with thrust loading), is the McKenzie (1978) model of lithospheric attenuation. This results in rapid fault-controlled rift subsidence followed by exponentially declining rates of subsidence associated with the cooling of the lithosphere. McKenzie characterised his model in terms of the function β , (Beta) the degree of lithosphere^{ic} thinning, which allows the prediction of the initial fault controlled subsidence, heat flow and thermally controlled subsidence. However the model assumed perfect Airy compensation with no flexural strength of the lithosphere. Whilst such an assumption might be expected during rifting and hence fracturing of the crust (Watts, 1982), the post-rift development of a sedimentary basin is generally characterised by increasing basin widths and complex basin edge stratigraphy which can most easily be explained in terms of an increasing lithospheric flexural rigidity (Watts et al., 1982). The

importance of flexural rigidity is further enhanced or reduced depending on the amount of heat added to the Crust and upper Mantle and the amount of crustal thinning that occurs during extension. Observed differences in these parameters around the world subsequently led to the development of an assortment of possible variations on the original model, such as the Royden & Keen (1980) model of depth-dependent stretching and the thin-skinned extensional model of Royden et al., (1983) whereby little or no heating need occur during basin extension.

In order to calculate the amount of crustal attenuation and heating with all these models, Royden et al., (1983) have shown that it is necessary to, (1) discriminate between the rift and thermal phases of basin formation, (2) quantify the magnitude of initial rift subsidence, and pre-rift elevations, (3) know the rates of thermal subsidence or heat flow, and lastly (4) estimate the pre-extensional crustal and lithospheric thickness (subsidence or uplift results from stretching depending on the ratio between them (Dewey, 1982)). Knowledge of the crustal/lithospheric thickness alone is sufficient to estimate the amount of extension. However, while some basins display a typical bimodal subsidence, many exhibit a polymodal subsidence record, reflecting a more complicated extensional history. Some authors, such as Chadwick, (1985a), have simply assumed that complications can be explained in terms of polyphase lithospheric extension. Yet this alone does not yield a unique determination of the rifting processes, nor does it adequately explain the detailed structural evolution of polyphase basins. Indeed, such models tend to overestimate the extension factors. Therefore, with this in mind, the purpose of the thesis was to integrate basin kinematics to the detailed structural evolution of a particular basin.

The Wessex Basin in southern England represents a particularly fine example of a basin with a multiple stretching and thermal recovery history (Fig. 1.1). The basin was initiated in the late Palaeozoic and contains a late Palaeozoic-Cenozoic sedimentary sequence of up to some 4 km in thickness (Fig. 1.2). The huge amount of surface and subsurface data available for the basin, combined with excellent biostratigraphic dating information, makes the basin one of the most tightly constrained in the region and as such, the area clearly merited further study to test if an integration between basin kinematics and the geologic/tectonic evolution was possible.

Previous workers have briefly attempted to evaluate the subsidence history of the region using the simple lithospheric attenuation model of McKenzie (1978). Dewey (1982) noted that the general basement onlap pattern that characterises the basin margin supposedly conforms to the increasing flexural strength of the lithosphere following rifting. Since all sedimentary basins are the result of the isostatic adjustment of the lithosphere to a tectonic driving force, it is possible to isolate the tectonic driving force by correcting for sedimentary loading (Watts & Ryan, 1976). The resulting tectonic subsidence can then be directly compared with subsidence curves predicted by various theoretical models. However, consideration of the polyphase subsidence history is complicated by the fact that the lithosphere contains residual heat from the previous event and a modified crustal/lithospheric thickness ratio. In addition, extension factors determined by ^{fault} geometries persistently — indicate low orders of extension relative to backstripping estimates. In an attempt to address this problem, Chapter 2 deals with the broad scale basin evolution of the area utilizing previous work and newly acquired

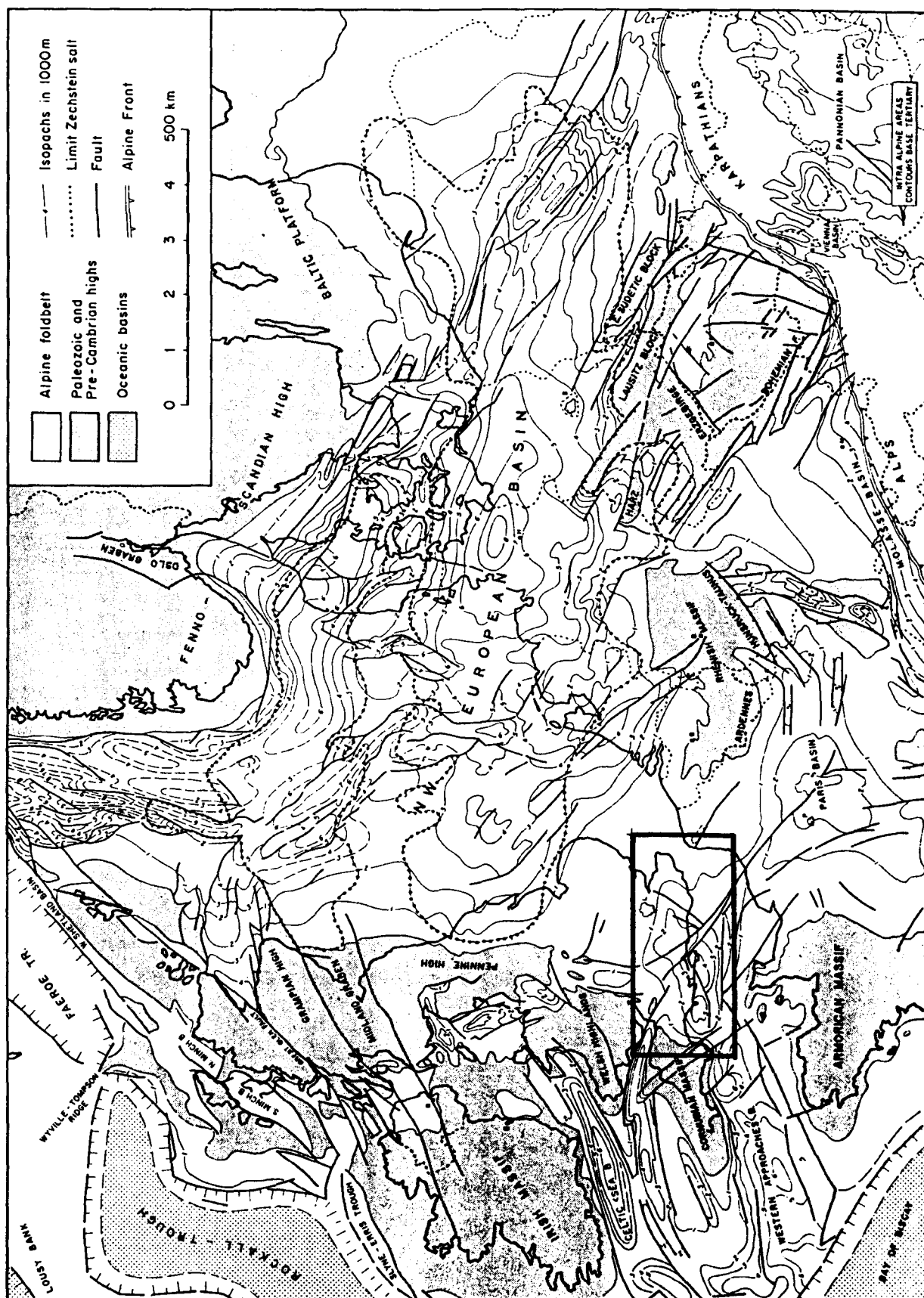


Fig. 1.1 Map of the British Isles, showing the area of study.
(from Ziegler, 1981).

ERA	SUB-ERA	EPOCH	AGE	M.A AGE	LITHOSTRATIGRAPHIC FORMATIONS	
CENOZOIC	QUATERNARY					
	NEOGENE	PLIOCENE		2.0		
		MIOCENE		5.1		
		OLIGOCENE		24.6	Hamstead Beds	
		EOCENE		38.0	Bembridge, Solent, Barton, Bracklesham Groups and London Clay	
		PALAEOCENE		54.6	Reading Beds	
	UPPER CRETACEOUS	SENONIAN	Maastrichtian	65.0		
			Campanian	73.0		
			Santonian	83.0	Upper Chalk	
			Coniacian	87.5		
				88.5		
			Turonian	91.0	Middle Chalk	
			Cenomanian	97.5	Lower Chalk	
			LOWER CRETACEOUS	Albian	113.0	Upper Greensand and Gault
				Aptian	119.0	Lower Greensand
				Barremian	125.0	
	NEOCOMIAN	Hauterivian		131.0	Wealden	
		Valanginian		138.0		
		Berriasian	144.0			
	JURASSIC	MALM	Tithonian	150.0	Purbeck Beds	
			Kimmeridgian	156.0	Portland Group Kimmeridge Clay	
			Oxfordian	163.0	Corallian Beds Oxford Clay and Kellaways Beds	
			Callovian	169.0		
		DOGGER	Bathonian	175.0	Great Oolite Series	
			Bajocian	181.0		
			Aalenian	188.0	Inferior Oolite	
				189.0		
		LIAS	Toarcian	194.0	Upper Lias	
			Piensbachian	200.0	Middle Lias	
Sinemurian			206.0			
Hettangian			213.0	Lower Lias		
TRIASSIC		UPPER	Rhaetian	219.0	Rhaetic	
			Norian	225.0		
	Carnian		231.0	Upper Keuper		
	MIDDLE	Ladinian	238.0	Lower Keuper (Keuper Marl. Waterstones) Upper Bunter (Bunter s/st. L. Keuper s/st)		
		Anisian	243.0			
	SCYTHIAN	Spathian				
		Smithian				
		Dienerian				
		Griesbachian	248.0	Lower and Middle Bunter (Budleigh Salterton Pebble Beds and Aylesbeare Group in part)		
	PERMIAN	LATE	Tatarian	253.0		
			Kazanian			
Ufimian			258.0			
Kungurian			263.0	(Aylesbeare Group in part local sands, mudstones and breccias)		
EARLY		Artinskian	268.0			
		Sakmarian				
		Asselian	286.0			
			BASEMENT			

Fig. 1.2 Stratigraphic column of the Wessex Basin.

seismic reflection data. Basically, Chapter 2 isolates the thermo-mechanical properties of the lithosphere during basin formation by analysing some 50 boreholes within the region, (using backstripping techniques to isolate the tectonic driving subsidence). This technique was applied to various types of thermo-mechanical models to test which one is more applicable. It is concluded that the observed subsidence is generally not a function of the conductive cooling of the lithosphere following rifting and that β seriously overestimates stretching within the basin. Locally high β values were confined to areas of polyphase active growth faulting which in turn were controlled by thrust reactivation within the underlying basement. The affect of this underlying basement control was further examined. First, by using newly acquired geophysical results in the region, it was found that the Moho does not vary appreciably between so called stretched and unstretched crust suggesting that sub-crustal lithospheric involvement was minimal. As an alternative quantitative model basin initiation utilizes the earlier basement structures with continuing extension only to the crust with the sub-lithosphere playing a reduced role. Strain compatibility is maintained by balancing local crustal extension by regional sub-lithospheric heating. Polyphase extensional events, the interaction of eustatic sea level and regional tectonics controlled the major cyclicity observed within the stratigraphic record. In addition lithospheric flexure as evidenced for example, by increasing basin widths, could not be resolved. Furthermore modelling subsidence in terms of polyphase, but instantaneous lithospheric thinning, showed a poor correlation to the driving subsidence obtained from boreholes. The inclusion of finite rifting and lateral heat flow (Cochran, 1983) in the rerifting process

showed an excellent correlation to the observed subsidence and predicted significantly lower orders of extension than those predicted using lithospheric failure model.

Given the general applicability of the modelled subsidence data to crustal finite rerifting models, Chapter 3 investigates the structural evolution of the region and in particular, the complicating effects introduced by baseⁱⁿ inversion and how the development is ultimately controlled by the plate motion of Africa relative to Europe. Chapter 3 therefore, examines the timing and effects of inversion on the development of the Wessex Basin.

Whilst realistic interpretations of lithospheric behaviour must combine analyses with structural data for the upper crust, geophysical data at deeper levels and regional tectonic data, such data must also be integrated with the analysis of other basins in comparable tectonic settings. Chapter 4 deals with integrating such data to nearby basins in north-west Europe and develops a general model which can be applied to such basins.

We have so far dealt with the direct link between basin formation mechanisms, the kinematic development of the basin and how such a model can be applied to other regions. However, it is salient to consider that perhaps an even more complex history can be unfolded, such that older sedimentary successions within the basin have been attenuated by stretching processes, while up succession, a progressive decrease in attenuation has occurred. This cannot be demonstrated by any of the techniques previously described, but requires a detailed structural analysis of faults, folds, joints and fissures etc, which may help in estimating rates and directions of extension, thus allowing the

restoration of the bed to the original sedimentary thicknesses. Such an analysis is outlined in Chapter 5, where a study of mesostructures has been completed. This study was confined to the western portion of the Wessex Basin (Figs 1.3 and II.1.1) and concludes that whilst theoretically such techniques can and have been applied to other areas, (Engelder, 1982), brittle microtectonic mesoscale structures within the Wessex Basin clearly occurred since the culmination of inversion. As such, they do not record basin geometry, sedimentary wedge patterns, sedimentation/compaction rates, nor do they record details of the lithospheric thinning mechanism such as would result if β and strain rates were large. Lastly, it can be demonstrated that modelling more complex extension mechanisms to determine β are unnecessary within the Wessex Basin, but that brittle microtectonics data generally modifies the post inversion/tectonic development of the region which in turn clarifies the closing phases of the kinematic development of the basin.

Although a series of new models have been developed and demonstrated, one may ask, what is the economic significance of the results, and more specifically, how can they be used as a hydrocarbon exploration tool in the region. Such applications are summarized in Chapter 6. While problems in predicting past temperature gradients may occur, emphasis is placed on the major areas of maturity and optimum reservoir location within the basin, in addition to an outline of prospective plays and future exploration strategies.

Appendices A, B and C, describe in detail some of the major data sources used in the work. Appendix D, specifically deals with the more detailed aspects of lineament mapping and analysis used in the region prior to developing a detailed structural model for the area, while

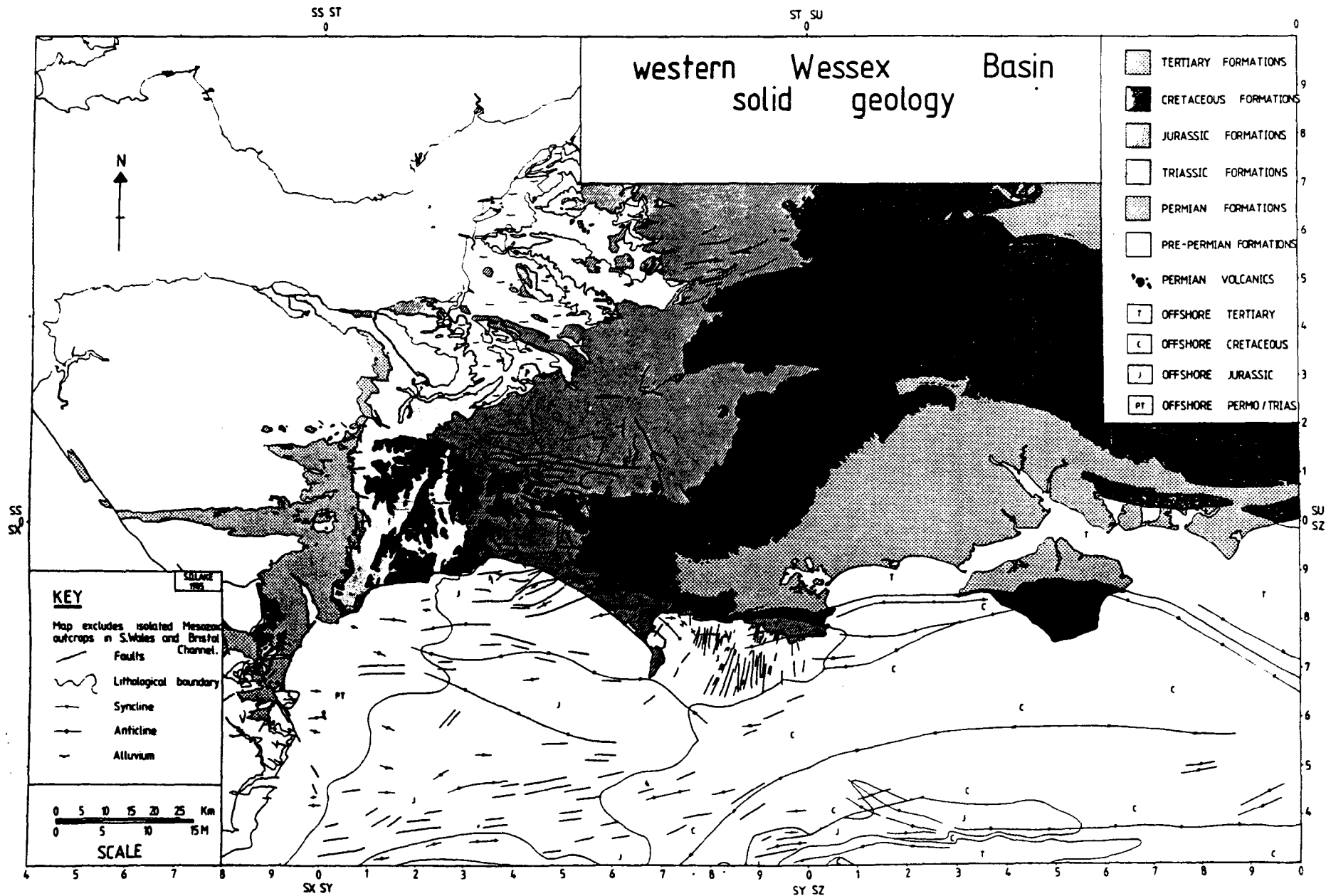


Fig. 1.3 Solid Geology of the western Wessex Basin.

appendices E and F attend to particular examples of mesoscale kinematic processes.

CHAPTER 2

BASIN EVOLUTION

2.1 Introduction

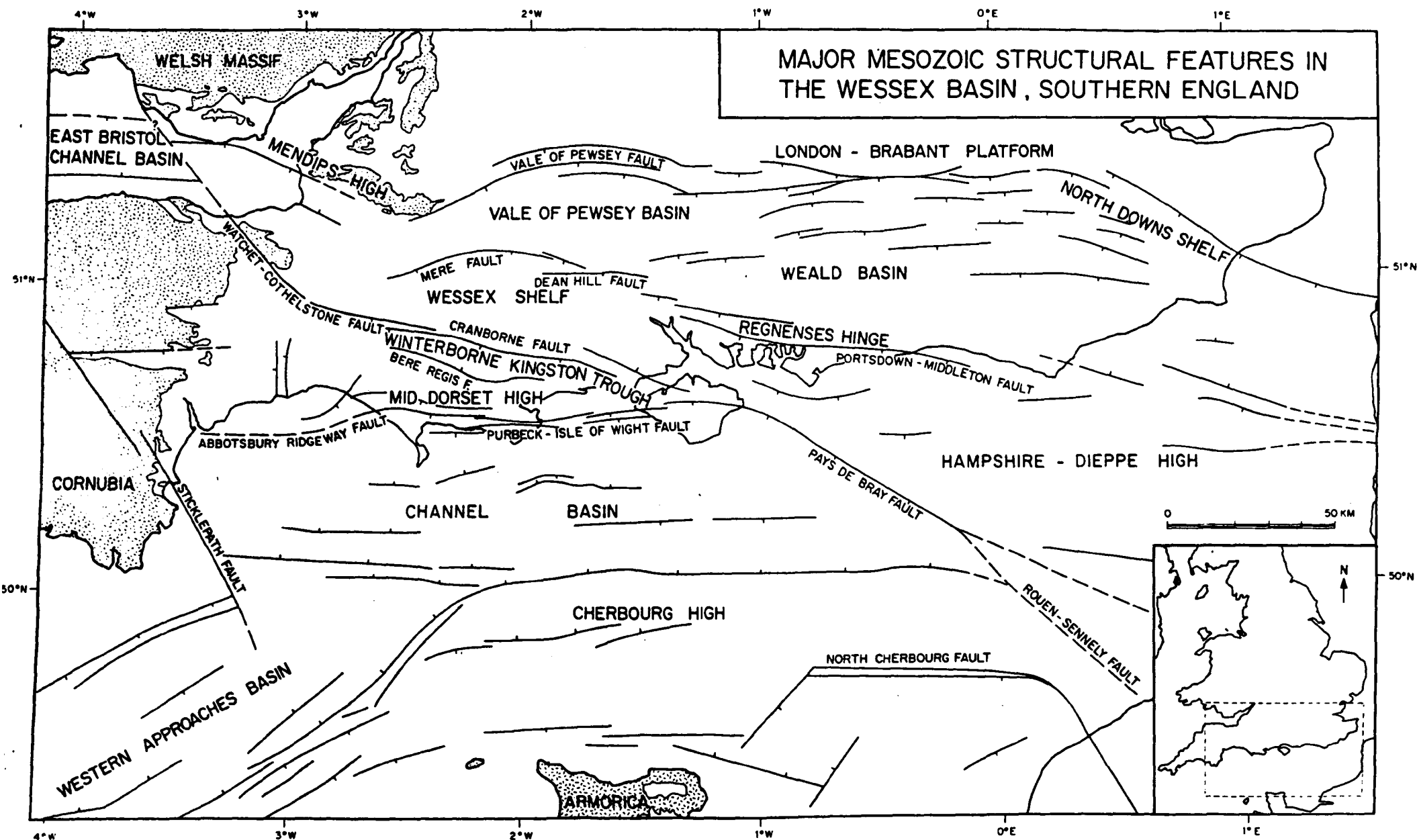
To date, the quantitative modelling of intracratonic sedimentary basins has been primarily concerned with the isostatic response of the lithosphere to extension. Lithospheric extension predicts two discrete phases of basin development, a rapid subsidence phase related to rifting of the crust and thinning of the sub-crustal lithosphere (i.e. the active phase), followed by a generally negative exponential subsidence phase associated with the conductive cooling of the lithosphere (i.e. the passive phase). In marked contrast to this simple model prediction, many basins exhibit a polyphase rifting history as characterised by episodes of renewed basin subsidence. Often, this renewed subsidence is very rapid and is followed by little, if any, thermal subsidence. However, not all active subsidence phases need be caused by rifting. A major complexity in basin development, especially within European basins, is the attempted destruction of the basin by inversion, that process by which a depocentre is transformed into a structural high (while structural highs become depocentres). The very nature of inverting structural highs into basin subsidence introduces an additional driving subsidence. Structural high inversion is the consequence of regionally generated compression (or transpression) acting across the same crustal faults which facilitated basin initiation.

Apart from the above complexities, basin modelling has generally failed to reproduce the simple (e.g. young, uni-extensional phase) basins, even when factors such as lithospheric flexure, lateral heat-flow, sediment compaction, and eustatic sea-level variations are taken into account. The purpose of this ^{chapter} ~~paper~~ is to investigate the response

of the lithosphere to polyphase extension and its implications on sedimentary basin development. We chose as a suitable example, the Wessex Basin of southern England and the English Channel.

The Wessex Basin (Kent, 1949) covers an area approximately 80,000 sq. km. The basin is bounded to the west by the Cornubian Massif, to the north and east by the London-Brabant Platform, and to the south by the Armorican Massif (Fig. 2.1). Basement largely consists of Devonian and Carboniferous molassic-type sediments deformed by the emplacement of thrust sheets during the Variscan Orogeny. Within the Wessex Basin, Palaeozoic, Mesozoic and Cenozoic sediments have been deposited with an average thickness of ca. 1500 m, locally exceeding 3500 m. The area is currently attracting considerable exploration interest in the light of recently discovered economic oil and gas reserves.

The stratigraphy, structure and sedimentology of the Wessex Basin has been reported by several authors (e.g. Strahan, 1898; Arkell, 1947; Falcon and Kent, 1950; Phillips, 1964; Drummond, 1970; Whittaker, 1975; Dewey, 1982; Drummond, 1982; Melville and Freshney, 1982; Stoneley, 1982; and Chadwick, 1985b). However there is still no clear agreement on the structural development of the basin and even less discussion on the mechanisms responsible for its development. Some authors have interpreted the Wessex Basin in the context of lithospheric stretching and crustal rifting (Whittaker, 1975; Dewey 1982 and Chadwick, 1985b), while others, notably Drummond (1970) have suggested that wrenching must play a fundamental role. No serious attempt has been made to integrate the entire development history of the basin (tectonic and stratigraphic) with a basin-formation mechanism. Given this, and the accessibility of new data (in particular, recently released borehole data and the deep seismic



reflection profiles of the British Institutions Reflection Profiling Syndicate (BIRPS) group), this ^{paper} attempts to integrate the geological and structural history of the Wessex Basin and the structure of the Variscan basement with the thermal and mechanical properties of the southern England lithosphere.

2.2 Regional geology and structure

The Wessex Basin was initiated in the late Carboniferous-early Permian (Knill, 1982) with the deposition of continental desert sediments, locally interbedded with Permian volcanics (Knill, 1969) (Fig. 2.2). Volcanic intrusives and extrusives are relatively rare in the Wessex Basin, the Permian volcanics represent the only significant occurrence. Continental sedimentation continued throughout most of the Permian and Triassic with sediment distribution being strongly controlled by late Variscan topography. The Rhaetian (upper Triassic) marine transgression marked the first onset of marine conditions within the Wessex Basin and the initiation of a marked limestone/sandstone/clay cyclicity which continued throughout the Jurassic (Hallam, 1975). Middle Jurassic bentonites are developed locally, perhaps associated with North Sea volcanism. During the late Jurassic, the seas began to shallow (Sellwood, 1978) with the area finally becoming emergent by the late Portlandian. The lower Cretaceous was dominated initially by non-marine fluviatile sands and clays, unconformably overlain by Aptian/Albian shallow marine sediments. Oil generation and migration was probably initiated during this period (Colter and Havard, 1981) as local oil saturated conglomerates exist within the Wealden (Arkell, 1947). The extensive regional distribution of the upper Cretaceous marine chalks is

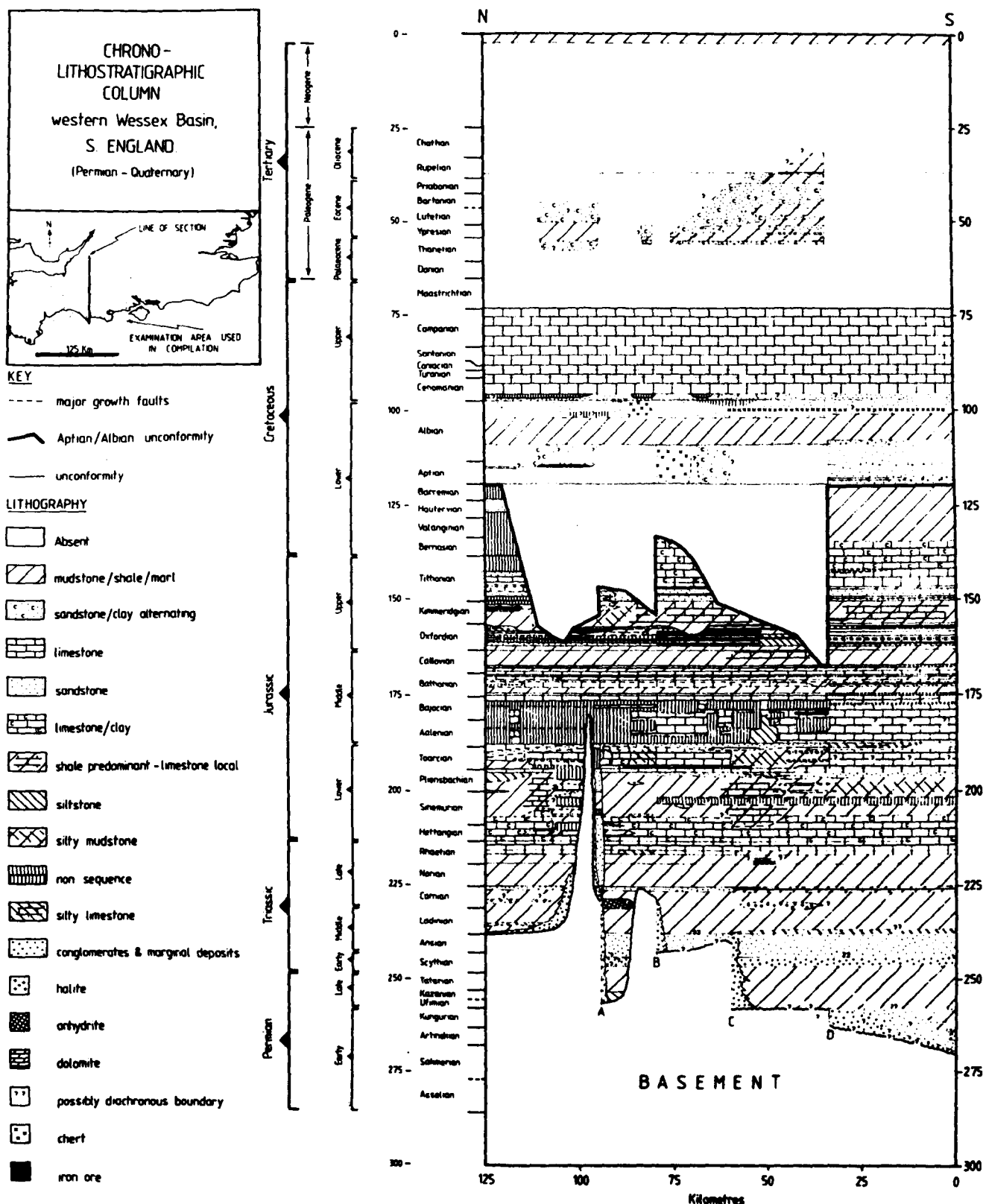


Fig. 2.2 Chrono-lithostratigraphic column along a north-south transect in the western portion of the Wessex Basin. A. Vale of Pewsey fault, B. Mere Fault, C. Cranbourne Fault and D. Purbeck-Isle of Wight Fault. Data compiled from many sources.

coincident with the global peak in eustatic sea-level (Hays and Pitman, 1973; Vail et al., 1977; Pitman, 1978), while shallow-marine to freshwater sands and clays dominate most of the Tertiary. The Alpine collision (Helvetic phase) in the late Oligocene effectively terminated the development of the Wessex Basin.

The basin comprises four main sub-basins (Fig. 2.1) of varying geometry which show similar structural controls and stratigraphic relationships. The Channel Basin developed as a half graben, the Winterborne Kingston Trough as a symmetric graben, the Vale of Pewsey Basin as a half-graben, while the Weald Basin is more typical of a sag-type basin, although westwards along strike it develops into a half graben. Whilst a considerable amount of knowledge has been acquired onshore on the deep structure, the following section summarizes the results of a major seismic survey recently completed in the English Channel.

2.3 Structure of the English Channel from Seismic Reflection Data

A. Introduction

Active exploration in southern England has resulted in the acquisition of a large seismic reflection data base. The amount of data that individual companies hold is largely dependent upon their exploration interest and financial backing. Previous publications on the structure of southern England have been hampered by the lack of access to seismic reflection lines therefore close co-operation was sought and provided by many oil companies actively involved in the area. Initially, access was given to a whole series of seismic reflection surveys which were then examined with a view to delineating major areas of interest and which merit^{cd} further studying. The results of this work are not directly summarized here because of their commercial nature. However, some of the interpretation presented has been broadly based upon this data.

Access was made available to a major Geophysical Service International (G.S.I.) non-exclusive survey covering most of the English Channel up to the international boundary between France and England. The whole survey was examined and sixty seismic lines were chosen to indicate the best structures and optimum locations. In addition fourteen GSI non-exclusive shallow water seismic reflection lines in Bournemouth Bay and south of Brighton, and four IGS seismic reflection lines from projects 76/8 and 77/7 were also analysed. All these reflection lines were incorporated in the compilation of the structural map of the Top Penarth Group at 1:250, 000, scale across the English Channel (Fig. 2.3, II.2.2 and II.2.3).

PULL

OUT

The G.S.I. non-exclusive survey was recorded at 1:50, 000 scale, and the shallow water survey (at 1:25, 000 scale) in 1983. The survey was recorded to 4 seconds two-way travel time (TWTT) with 36 fold coverage; the resultant filtered migrated sections were analysed and the main features are summarized below.

The Top Penarth Group reflection (base Jurassic) was contoured since it forms a distinctive marker of fairly constant thickness and facies across the basin and is cross cut by the most important structural features. The most appropriate scale was 1:250, 000 coincident with published British Geological Survey Solid Geology, magnetic and gravity maps. The isochrons were contoured at 100 millisecond intervals in two-way time, thus best indicative^e the structural style of the English Channel. Six boreholes, Arreton, Lulworth Banks, Middleton, Westham, Wytch Farm D5 and BH 98/22-1 were used to locate the reflector and as well ties, using the velocity information summarized on each seismic section. The Penarth subcrop and surficial faulting shown external to the subcrop were derived from surveys and published geological maps in order to indicate the lateral continuity of some of the more significant geological features.

The map area (Fig. 2.3) is clearly divisible into four areas (c.f. Fig. 2.1), the Channel Basin, the Cherbourg High, the Hampshire-Dieppe High and the Western Approaches Basin.

B. The Channel Basin

The Channel Basin essentially has a rhombohedral shape bounded to the north by the Purbeck-Isle of Wight and Abbotsbury-Ridgeway faults, to the south by the mid-Channel fault, and to the east and west by the Pays de Bray and Sticklepath faults respectively. The dominant structural

grain within the depocentre appears east-west, with increased fracturing in areas where the basement lies at shallow depths. Separate depocentres can be distinguished within the basin: immediately southwest of the Isle of Wight, due south of the Isle of Portland; and in a synuous symmetric trough south of the Isle of Purbeck (Fig. 2.3). The contoured Penarth reflector clearly shows the Channel Basin to be a northerly dipping half graben with asymmetry of the infill from east to west. The approximate north-south orientation of the Penarth contour in the west probably indicates Tertiary erosion because of the removal of the subsequent Jurassic and Cretaceous units above. However, the obliquity of the contours in the east particularly near the junction of the Pay de Bray and Purbeck-Isle of Wight faults, may reflect the original asymmetry produced by the postulated pull-apart development of the basin. Local highs are particularly well developed on the footwall side of fault blocks. In addition, periclinal highs are located along the Pay de Bray and Mid Channel faults and presumably reflect the inversion history of those structures due to their parallelism and age. Significant perturbation in the contours generally reflects folding, probably largely associated with the inversion which initiated the late Cretaceous (see Chapter 3). One significant high in Weymouth Bay clearly reflects a roll-over antiform above a listric fault, (Fig. 2.4) in broad agreement with the postulated roll-over structures of Stoneley (1982). The surface expression of this fault would coincide with the Purbeck-Isle of Wight fault, the precise lateral extent is more fully displayed on onshore seismic lines along strike. Figure 2.4 clearly shows the roll-over geometry accentuated by inversion related structures (see Phillips 1964) with clear thickening of most Jurassic units towards the

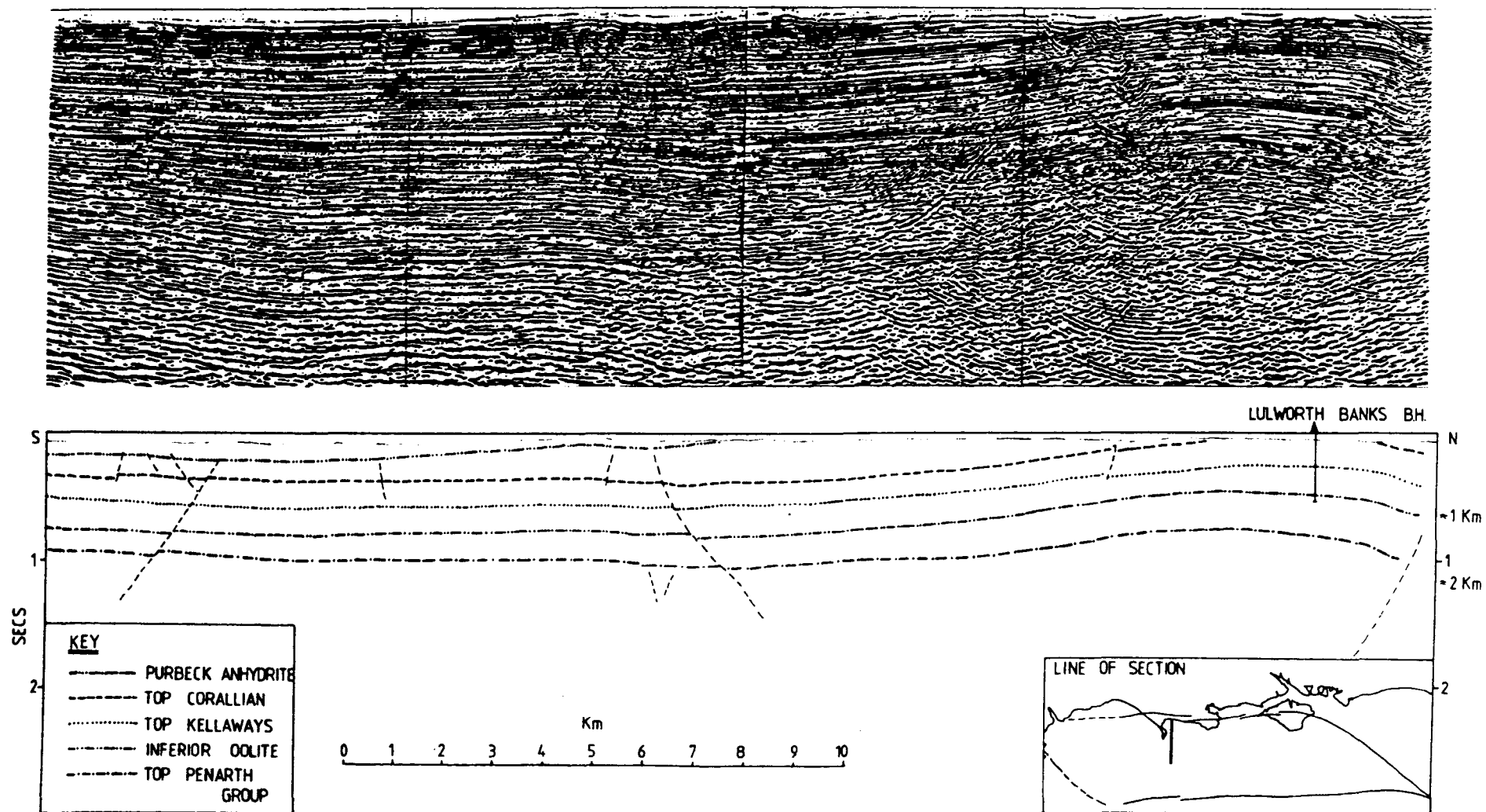
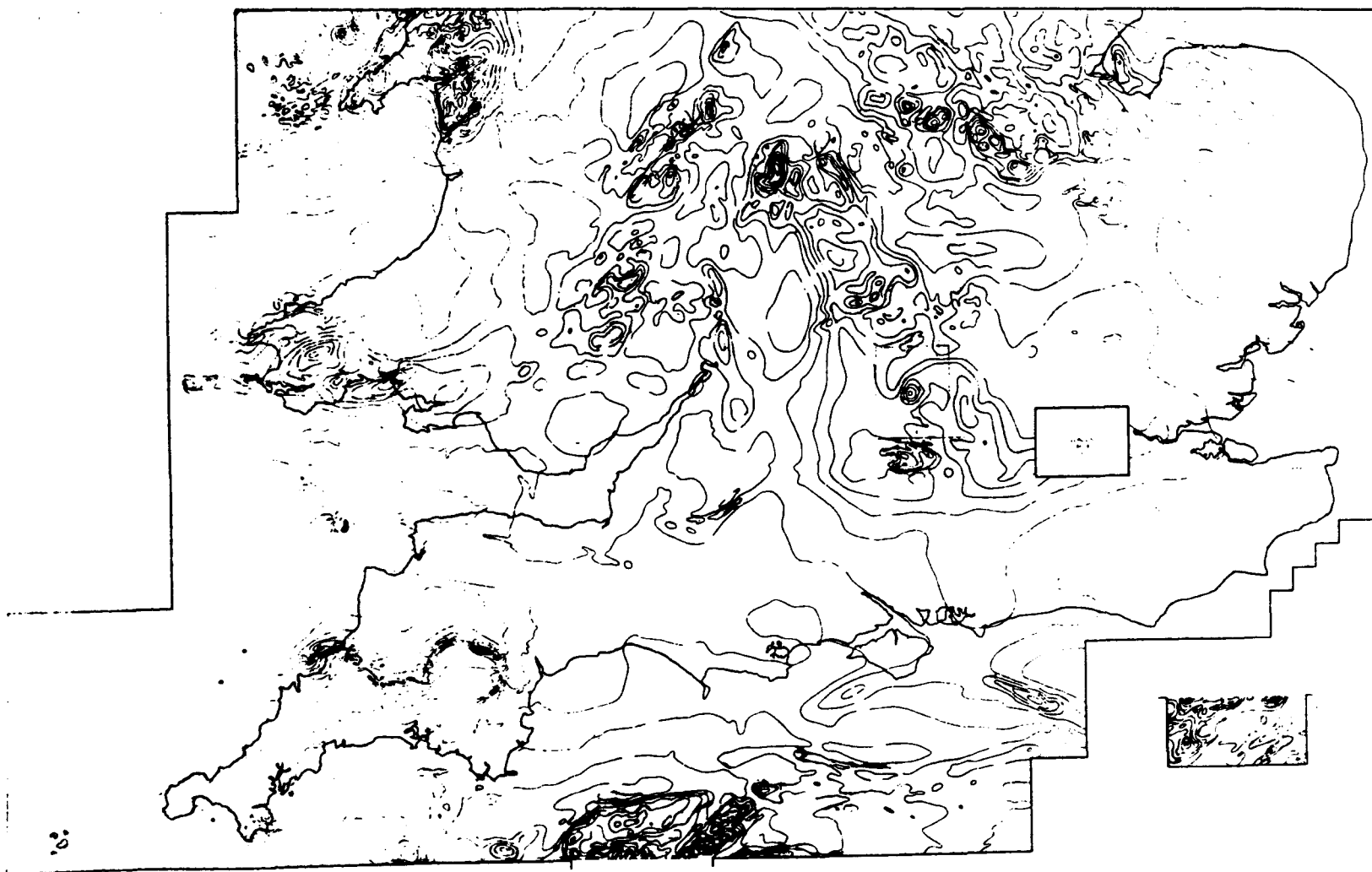


Fig. 2.4 North-south seismic section and interpretation across the Weymouth anticline.

north indicating the true growth nature of the Purbeck-Isle of Wight fault. Detailed three dimensional analysis of the Weymouth Bay area indicates onlap towards the west above most Jurassic limestone reflectors, again reflecting the original roll-over geometry. Onshore contour maps show thinning of units along the crest of the proto Weymouth anticline, for example the Inferior Oolite is approximately 1.8 m thick at Radipole (N.G.R. SY 663 811) on the west compared to over 20 metres at Winterborne Kingston (N.G.R. SY 847 980) (c.f. Penn 1982, fig. 9). Probably the lack of hydrocarbons in the Lulworth Banks borehole (N.G.R. SY 785 771) reflects a) the later inversion history, b) the north-south shallow faulting transecting the anticlinal culmination (see Donovan & Stride 1961) and c) the generally poor stratigraphic location (see Chapter 6). Local antithetic and synthetic faulting associated with the Purbeck-Isle of Wight fault is particularly well displayed along strike where a detailed analysis of the structure in Lyme Bay has been completed (see Chapter 2).

Further towards the southwest, a major transpressional flower structure is displayed and is presumably the offshore continuation of the Sticklepath Fault zone. Geological boundaries along the zone appear to be sinistrally offset, in contrast to the well document^{ed} dextral offset onshore (eg. Bristow & Hughes, 1971). Tight east-west to east-northeast-south-southwest^{fold^{ing} in} the area may be the result of the multiple history of the fault zone and/or the complex inversion history of the area. The Penarth Group boundary in the southwest portion of the basin approximately marks the westward continuation of the east-west-Mid-Channel fault zone which has downthrow to the north. Along the central portion of the fault belt, two major en^ochelon fault traces can be

Fig. 2.5 Aeromagnetic anomaly map of the Wessex Basin and surrounding areas, 1:625,000 scale. (From the Aeromagnetic Map of Great Britain sheet 2, England and Wales, compiled by the Geological Survey, 1st Edition, 1965).



identified. Their precise correspondence is uncertain, however magnetic and gravity maps (Figs. II.2.3, and 2.5) clearly show a major east-west structural, and presumably rheological, boundary along the centre of the Channel which is termed the Channel Magnetic Anomaly (Chauval et al., 1980). Detailed examination of this area shows strong magnetic anomalies varying between + 100-300 gammas and indicates that the Mid Channel fault splays into two strands, one trending northwest-southeast and probably controlling much of the development of the Western Approaches basin, and the other east-west trending which can be traced into the Sticklepath fault zone. Other, more localized, magnetic signatures trend west-northwest off the fault trace and are coincident with significant Mesozoic highs and local minor fault traces. The anomalies south of the fault have previously been variously interpreted as basement ridges (Hill & Vine, 1965), ophiolite thrust nappes (Lefort & Segnolfin, 1978), and lava flows of unknown date (Smith & Curry, 1975). The latter seems more likely (c.f. Day, in press) although a Permian age is doubted for these rocks because Permian volcanism in the Credition Trough in the Exeter area have, in contrast a poor magnetic signature. The Mid Channel fault also forms the boundary between high amplitude localized gravity lows (Fig. II.2.4) possibly related to granites (Day, pers comm) of unknown age which lie to the southern side of the fault. The Penarth reflector varies considerably in depth along strike. This has previously been used to postulate strike slip movement along the fault which Donato (Oral Comm.) has related to Mesozoic reactivation of the Great Glen shear system. However, because the Mid-Channel Fault is terminated at both ends by northwest-southeast fault zones (Fig. 2.1), it is unlikely to be a major linked strike-slip fault (particularly when local antithetic

faulting and complex inversion related structures could easily have been misinterpreted as transtensional or transpressional strike-slip induced structures). Onshore data along similar trends seemingly demonstrate upper Cretaceous small scale strike-slip motion (see Chapter 3). The reverse drag against the Mid-Channel fault on the hanging wall appears to be inversion related rather than directly due to roll-over geometry above a listric fault detachment. These highs post date oil migration; (Chapter 6). A rim synform along the axis of the Tertiary Cherbourg basin on the immediate footwall of the fault clearly indicates the relative uplift of the Channel basin in the upper Cretaceous/Tertiary (see Chapter 3). Areas where this synform is best developed (along the central part of the fault belt) generally reflect the greatest inversion. An interpretation of the structure across the fault is shown in figure 2.6. The form of the monoclinial flexuring in the Cretaceous sequence clearly indicates the northerly dipping subsurface geometry of the fault, as confirmed by the southwest Approaches (SWAT) profile 11 (Chapter 3). The fault seems to be a mirror image of the Purbeck-Isle of Wight fault. However, thickening of the sedimentary sequence on the hanging wall towards the north suggests a more complex history. It is postulated that the fault may have originally been a major northerly dipping growth fault (c.f. thickness variation between top Penarth and top Kellaways reflections Fig. 2.6) was thus a major controlling structure (Chapters 2 and 3). Alternatively it can be suggested that during the Permo-Triassic the hinge zone on the hanging wall block of the Channel Basin may have originally been located near Cherbourg; later obvious Jurassic extension resulting in brittle failure and major down to the north ^{movement} thus indicating the fault to a secondary structure. Regional considerations

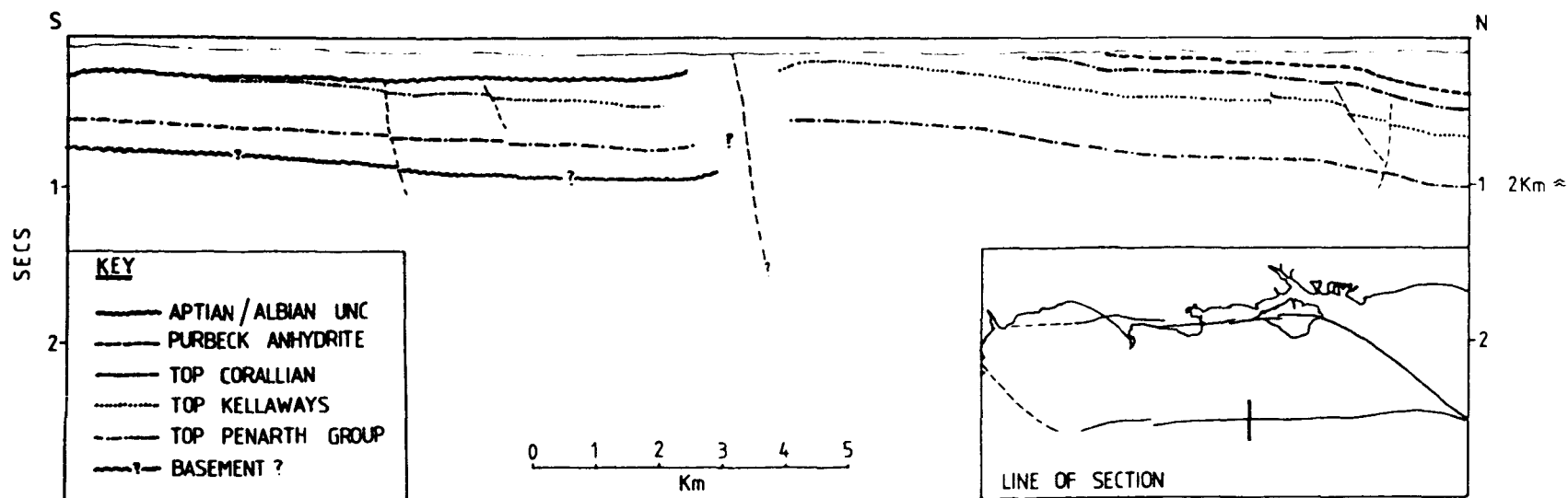


Fig. 2.6 North-south seismic section and interpretation across

of growth faulting would agree with the former model:, thus the Mid-Channel Fault represents the opposite side of the Channel Basin depocentre and influenced sediment distribution from Permian times onwards. Therefore the Channel Basin, bounded to the south by the Mid-Channel fault, can be considered a separate depocentre.

The Cherbourg basin is distinguished as a gravity low (Fig. II.2.4), however the amount of basin infill does not coincide with the magnitude. Thus Day (pers comm.) has speculated that granites are located immediately south of the fault. Additionally the upper Cretaceous unit appears to be abnormally attenuated compared to the sequence elsewhere, whilst the Aptian/Albian unconformity has eroded through most of the middle Jurassic sequence unlike the situation north of the Purbeck-Isle of Wight fault. This may reflect increasing uplift towards the Atlantic and Bay of Biscay associated with Aptian extension and peripheral bulge uplift (see Chapter 3). Alternatively but unlikely, it may indicate relative uplift of the postulated underlying granitic highs, similar to the Market Weighton Granite which influences Jurassic sedimentation in the Cleveland Basin further north.

The increase in brittle failure to the west may reflect increasing inversion on the thin sedimentary cover above shallow basement. The southern eastern portion of the Channel Basin clearly indicates the oblique dip of the basement comparable to basement topography in pull-apart basins (Karner & Dewey, 1986). The importance of this basement topography on subsequent sedimentation is emphasized by significant thinning of at least the Jurassic section in an easterly and southwesterly direction. The Mid-Channel fault seemingly terminates along the Rouen-Sennely fault system as interpreted by Stoneley (1982,

Fig. 2.1). The Sennely fault system clearly displays local periclinal uplift along its length, consistent with localized transpression associated with the strike-slip history of northwest-southeast orientated faults; in addition the fault is divisible into two separated segments which probably join up along strike and bound an area of relative downwarp (transtension).

The Pay de Bray fault is a significant structural boundary zone between the Channel Basin in the west and the Hampshire-Dieppe high to the east. The relative change in displacement towards the northwest along strike (Fig. 2.7) probably reflects increasing uplift and inversion towards the Isle of Wight where the fault links up the Purbeck-Isle of Wight fault coincident with this is an increase in monoclinial flexuring. The amount of vertical displacement increases northwestwards from some 10's of metres to at least half a kilometre. Increasing vertical displacement upwards reflects the original growth nature of the fault. Uplift probably initiated in the late Cretaceous (see Chapter 3) synchronous with the inception of inversion, thus most structures probably post date oil migration (see Colter & Havard, 1981), in particular the transpressional highs seen on Figure 2.7 (Sections A + B). The significant northwest-southeast magnetic anomaly along the same trend (Fig. 2.5) lies on the footwall side of the Pay de Bray fault and may reflect local volcanism (of unknown age).

Bournemouth Bay is undoubtedly an area of great interest to petroleum exploration companies because of the possible offshore continuation of the Wytch Farm oilfield (Britains biggest onshore discovery). The offshore continuity of the Wytch Farm horst is clearly displayed on Figure 2.8 and is located some 2.5 km north of the Purbeck-

Fig. 2.1). The Sennely fault system clearly displays local periclinal uplift along its length, consistent with localized transpression associated with the strike-slip history of northwest-southeast orientated faults; in addition the fault is divisible into two separated segments which probably join up along strike and bound an area of relative downwarp (transtension).

The Pay de Bray fault is a significant structural boundary zone between the Channel Basin in the west and the Hampshire-Dieppe high to the east. The relative change in displacement towards the northwest along strike (Fig. 2.7) probably reflects increasing uplift and inversion towards the Isle of Wight where the fault links up the Purbeck-Isle of Wight fault coincident with this is an increase in monoclinial flexuring. The amount of vertical displacement increases northwestwards from some 10's of metres to at least half a kilometre. Increasing vertical displacement upwards reflects the original growth nature of the fault. Uplift probably initiated in the late Cretaceous (see Chapter 3) synchronous with the inception of inversion, thus most structures probably post date oil migration (see Colter & Havard, 1981), in particular the transpressional highs seen on Figure 2.7 (Sections A + B). The significant northwest-southeast magnetic anomaly along the same trend (Fig. 2.5) lies on the footwall side of the Pay de Bray fault and may reflect local volcanism (of unknown age).

Bournemouth Bay is undoubtedly an area of great interest to petroleum exploration companies because of the possible offshore continuation of the Wytch Farm oilfield (Britains biggest onshore discovery). The offshore continuity of the Wytch Farm horst is clearly displayed on Figure 2.8 and is located some 2.5 km north of the Purbeck-

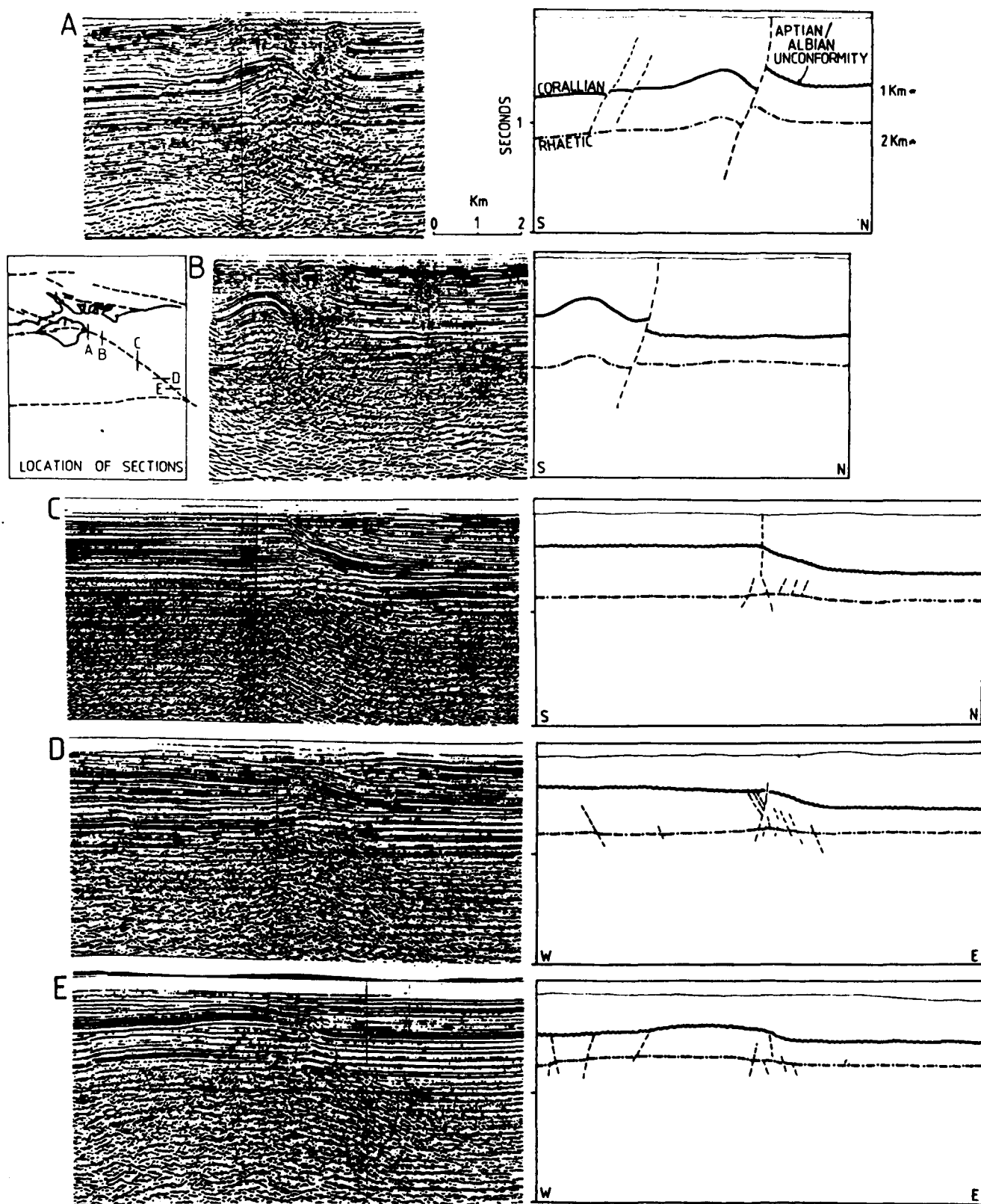


Fig. 2.7 Five serial seismic sections across the Pay de Bray fault and their respective interpretations.

Isle of Wight fault. Figure 2.8 clearly demonstrates that the Purbeck-Isle of Wight Fault is one of three major east-west growth faults, the other two lie to the south within a 5 km fault belt. The central fault belt, here called the Brixton fault belt, coincides with the Brixton anticline on the Isle of Wight although its lateral continuity onshore westwards into the Isle of Purbeck is doubted. The southern most fault belt, here called the Peveril fault belt, coincides with the major onshore disturbances at Peveril Point (N.G.R. SZ 040 787) and the Blashenwell disturbance (N.G.R. SY 955 201) along the Purbeck/Wealden boundary. All these fault belts display at least Jurassic and lower Cretaceous growth faulting. Thus recorded Wealden thickness on the Isle of Purbeck (c.f. Arkell 1947 p. 150) are attenuated whilst the full thickness of the Wealden succession is found immediately to the south of the Peveril fault belt. The Peveril fault belt may extend even further west at depth eventually coinciding with the Lulworth Cove disturbance (N.G.R. SY 828 798) and finally outcropping at Dungy Head (N.G.R. SY 815 799). The complex faulting south of the Purbeck-Isle of Wight fault undoubtedly reflects a complex history including oblique-slip extension, oblique-slip compression and local strike slip (see Chapter 3). The detailed geometry of each fault belt is comparable to upward divergent transpressional flower structures. Although this complex form is not well displayed in seismic sections (Fig. 2.8), onshore evidence, for example at Durlston Head (N.G.R. SZ 035 774), shows sub-horizontal slickensides along small east-west growth faults (see Appendix F). All these fault belts are undoubtedly listric at depth, in accordance with the postulated listricity of the Purbeck-Isle of Wight fault outlined by Stoneley (1982). This listricity is well demonstrated by reverse drag

(Fig. 2.8) along each fault belt and the onlapping sedimentary successions seen above the Penarth, Inferior Oolite and Corallian reflectors onto the active roll-overs in the hanging walls. More importantly the relative elevation of the hanging wall and footwall basement prior to inversion along the Purbeck-Isle of Wight fault would agree with the hypothesis of Colter & Havard (1981) that mature oil was generated from the Lias and Oxford Clay south of the fault in the early Cretaceous and then migrated northwards into the Bridport Sands and Triassic reservoirs. The actual mechanisms and migration patterns are undoubtedly complex, particularly since the three major growth faults and the resultant complex roll-over developments would have impeded migration. On the footwall, north of the Purbeck-Isle of Wight fault, the sedimentary successions are attenuated and active pre-Aptian faults are truncated by the Aptian/Albian unconformity: thus there is a clear change in structural style across the fault. Inversion resulted in the relative uplift of the southern side of the Purbeck-Isle of Wight fault whilst immediately north of fault inversion may locally result in northward facing monoclinal flexures (for example in The Solent (N.G.R. SZ 380 940)) above major basement involved faults.

Within the central portion of the Channel basin, a localized sinuous symmetric graben some 3 km wide and at least 35 km long is largely basement detached and may in part ^{be} soleing out into a Permo-Triassic salt horizon. Because this is a basement detached ⁺ structure it thus records the approximate true direction of extension ^{west} northeast-southwest ^{east}. Within the central portion of the basin localized folding and faulting to the west probably developed in response to the inversion. Immediately south of Durlston Head (N.G.R. SZ 035 773) on G.S.I. line EG51W, a major

truncation is recorded in the lower Jurassic reflectors. Considering the absence of the Aptian/Albian unconformity and the nature of the outcrops on the seabed, it seems likely that this truncation is the mid- Cimmerian unconformity since it correlates well with the base of the Kimmeridge Clay. Similar breaks are recorded elsewhere, both onshore in the Vale of Wardour (Chapter 3), the Broad Fourteens Basin (Ziegler, 1982) and in the Bristol Channel (Kamerling, 1979). In the latter case the break is disconformable whereas within the Wessex basin a more angular unconformity can be locally observed.

In conclusion the rhomboidal form of the Channel Basin, the geometry of the sediment/basement interface and the structures developed within the depocentre clearly indicate that the basin essentially developed as a pull-apart half graben. The major northwest-southeast Sticklepath and Pay de Bray faults facilitated this opening. Local faulting and folding probably developed in response to the inversion of this Basin which initiated in the late Cretaceous. Major synsedimentary faulting occurred around all the basin boundary faults with local antithetic and synthetic faulting and roll- over development well emphasized along the Purbeck-Isle of Wight fault. The major depocentre in Bournemouth Bay south of the Purbeck-Isle of Wight fault may reflect basement at about 4.5 km. Thus prior to inversion the depocentre may have been in excess of 5 km thick. Lastly the Mid-Channel fault probably developed above a major Variscan structure since it forms the boundary between strong magnetic and gravimetric variations within the basement.

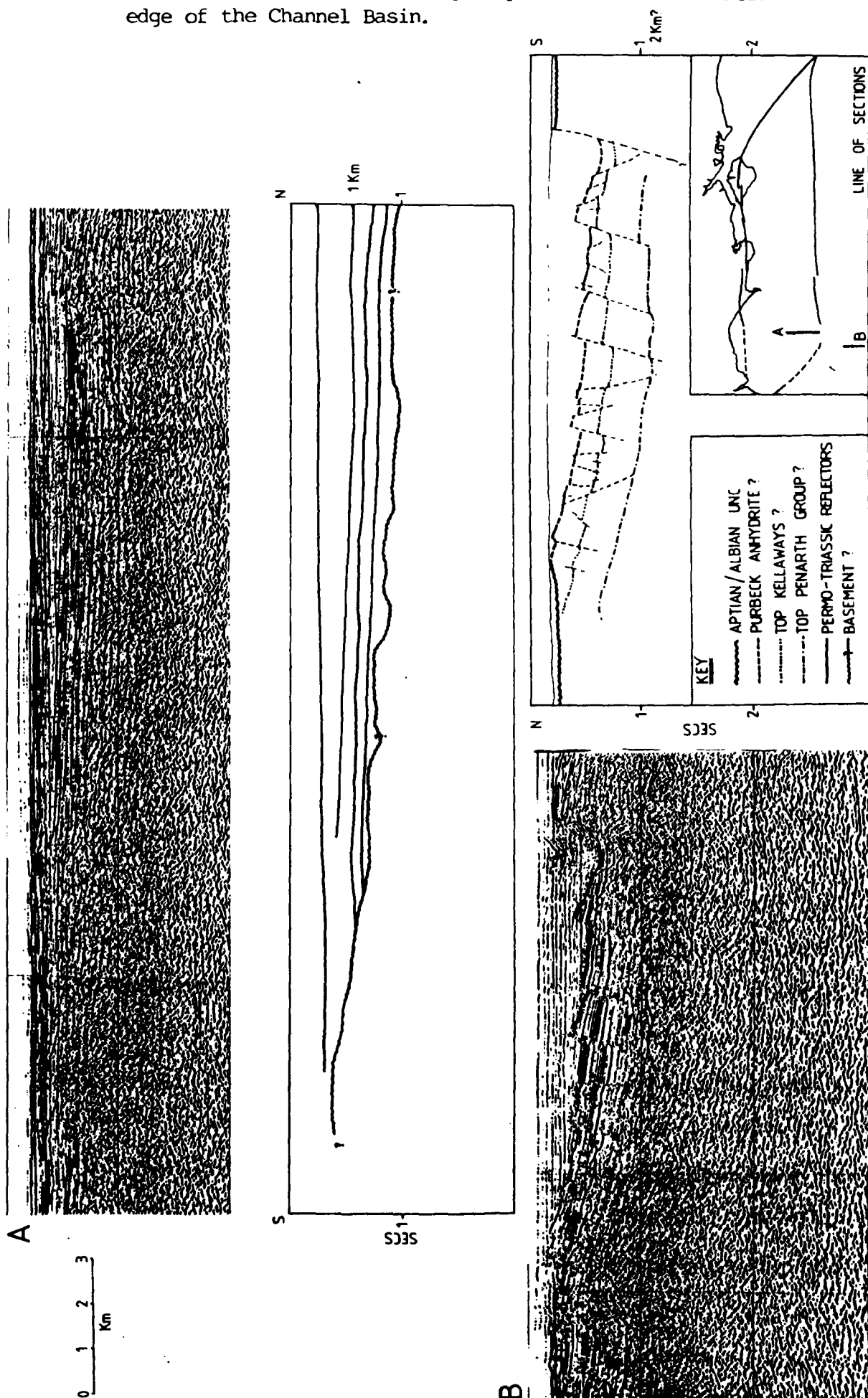
C. The Cherbourg High

This high represents a mirror image of the Mid Dorset High, to the

south side of the Mid-Channel fault. The highly magnetic basement lies at about 2 km depth and probably comprises lavas and intrusions of unknown age. The high developed on the footwall side of a major northward dipping growth fault (The Mid-Channel fault). This high undoubtedly developed synchronously with the development of the Channel Basin and was probably separated from ~~the~~ a high in the Le Havre area (at least during the Permo-Triassic and base Jurassic (in part) (c.f. Megnien, 1980)). Alternatively local transtension along the Pay de Bray fault (due to its west-northwest orientation with respect to northwest-southeast extension) would create a local elongate downwarp linking the Paris and Wessex basins similar to that encountered between the Sennely and Pay de Bray faults. The lateral continuity of the high with respect to the Western Approaches Basin is well displayed on Figure 2.9 and on SWAT profiles 10 and 11. The initiation of inversion resulted in the uplift of the Channel Basin, and the relative downwarp of the high leading to the subsequent development of a local east-west Tertiary depocentre developing immediately south of the Mid-Channel fault, (similar to the Tertiary Hampshire Basin on the Hampshire-Dieppe High). Thus the Cherbourg High probably represents an area of relative stability, in part comparable to the Mid-Dorset High, and therefore the whole Mesozoic sequence probably rarely exceeds 2 km. Accordingly the high has little hydrocarbon potential even taking into account the significant Aptian/Albian truncation. (no high structure)

D. The Hampshire - Dieppe High

This high is bounded to the south and west by the northwest-southeast Pay de Bray fault, to the north by the Portsdown-Middleton fault and to the east by the London-Brabant Platform and the attenuated



B. North-south seismic section and interpretation across the Western Approaches Basin, depicting a south dipping partially inverted half graben.

northeastern margin of the Paris Basin. The Penarth reflector does not generally reflect the importance of this high since inversion of the Weald basin has brought up the reflector to approximately similar elevations as the high. The importance of this high is however emphasized by the Aptian/Albian truncation, which is almost similar in magnitude to that encountered on the Cherbourg High (see Fig. 2.6) and approximately follows the postulated offshore continuation of the Portsdown-Middleton fault. Local folds, excluding those in the vicinity of the Pay de Bray fault, follow an east-west trend and essentially developed as monoclinial flexures above basement involved faults. These flexures face northward with steep short northern limbs located above major pre-Aptian southward dipping faults. This high undoubtedly strongly influenced the Jurassic and Cretaceous sedimentation (Taitt & Kent, 1958; Howitt, 1964) and separated the two major pull-apart depocentres (The Channel and Weald basins). Additionally the high is well identified by the presence of a Tertiary sedimentary basin (the limits of Tertiary deposition approximately marks the boundary of the high). This is similar to other highs such as the Cherbourg High, Mid-Dorset High, Hampshire-Dieppe High (Hampshire Basin) and the London-Brabant Platform (London Basin). A major ridge within the base Jurassic at about 600 milliseconds (TWTT) extends eastsoutheast from Beachy Head (N.G.R. TV 580 950) parallel to the magnetic signature, and is presumed to be the offshore continuation of the Regneses Hinge (see Sellwood et al., 1985). Structures north of the hinge essentially strike parallel to the axis of the Weald Basin which is located just southeast of Rye (N.G.R. TQ 950 180), and which plunges eastwards away from a low amplitude northeast-southwest boundary ridge which parallels the Sussex

coast immediately onshore. Further north, the basement shallows onto the London-Brabant Platform and Mesozoic units onlap onto it. Access to a regional non-exclusive G.S.I. survey across the London-Brabant Platform clearly displays increasing uplift, truncation and thinning towards the platform. The London-Brabant Platform area is approximately 150 km wide in this region, with the Aptian unconformity lying directly on Devonian/Carboniferous basement at approximately 500 milliseconds (TWT). The platform eventually terminates northwards off the Norfolk coast in the vicinity of Ipswich where it deepens towards the Sole Pit Basin and the West Netherlands Basin.

Further west near the Isle of Wight major pre-Aptian faulting truncated by the Aptian/Albian unconformity is clearly imaged. However the density of faulting undoubtedly reflects the amount and spacing of seismic data used in this summary. Some of these faults were undoubtedly reactivated in the Tertiary resulting in local northward facing monoclinial flexures. Others clearly display an arcuate form e.g. in the vicinity of the Pay de Bray and Purbeck-Isle of Wight fault bend. Moreover, pre-Aptian horst structures are developed close to and parallel with the Pay de Bray fault, thus ideally located for hydrocarbon generation in the Channel Basin and updip migration. Thus the Hampshire-Dieppe high separated two major subsidiary pull-apart basins and is clearly distinguished by the increasing truncation of the Aptian/Albian unconformity from around its margins towards the middle. Two major fault systems on the high, orientates^d east-southeast-west-northwest and northwest-southeast, probably reflect the strike of structures in the underlying basement. Local monoclinial flexures are developed above major pre-Aptian faults and may have developed as a result of late Cretaceous

inversion. The offshore continuation of the Regneses Hinge following the strike of the South Downs is well imaged. The high also displays clearly attenuated Mesozoic sedimentary sequences (which is in contrast to the depocentres on either side) as well as increasing inversion and uplift towards the major depocentres of the Channel and Weald Basins. Lastly, significant, and as yet undrilled, pre-Aptian structures are located in the vicinity of major mature source rocks, similar in structural style to the Wytch Farm Oilfield (see Chapter 6).

E. The Western Approaches Basin

This basin is more adequately dealt with in Chapter 4. However, one 4 second (TWTT) seismic section crossed the depocentre in addition to the SWAT profile 10 (which is summarized in Chapter 3). Both these surveys clearly image a southerly dipping, heavily fractured, northeast-southwest trending, inverted half graben. The Penarth Group reflector possibly lies at 1 second (TWTT), in contrast to thicker, deeper successions further southwest. The relative attenuation of the sequence possibly reflects the strong sedimentological control of, and thinning towards, the Sticklepath fault zone (the Start-Cherbourg Ridge of Naylor & Shannon, 1982). It is highly probable that a more comprehensive seismic survey of the Western Approaches Basin will reveal important northwest-southeast transfer zones, similar to those seen in Wessex (see Chapter 3) and the Bristol Channel (c.f. Kamerling, 1979) particularly when there is significant rapid variations in half graben geometry along strike (c.f. Ziegler, 1982 Fig. 15 D & E).

Thus the northeasterly portion of the Western Approaches clearly developed as a southerly dipping half graben which was infilled with a

significantly reduced sedimentary succession. This is in contrast to the observed sequences encountered further southwest along strike.

F. Conclusions

The detailed structure of the Channel and Western Approaches Basins, Cherbourg and Hampshire-Dieppe Highs have been described. Both the Channel and Western Approaches Basins are northward and southward dipping half grabens respectively. The geometry of the Channel Basin clearly reflects a pull-apart origin, with faults on at least three sides showing significant Mesozoic growth. Other extensional structures, in particular the three major synsedimentary fault belts in Bournemouth Bay and the along strike reactivated roll-overs above major listric faults are ^{clearly} closely imaged in seismic reflection data. Other structures within the basin undoubtedly formed during late Cretaceous and Tertiary when the depocentre was inverted. The Cherbourg high developed as a mirror image to the Mid-Dorset high, with the Tertiary basins developed on both highs separated by the inverting Channel Basin. The Hampshire-Dieppe high clearly shows marked attenuation of the Mesozoic sedimentary sequence and shows strong structural similarities to the Cherbourg and Mid Dorset Highs. Pre-Aptian faulting is clearly imaged on all seismic reflection lines where the Aptian/Albian unconformity truncates the structures. Localized monoclinal flexures in the overlying upper Cretaceous/Tertiary cover clearly indicate the approximately northerly directed compression associated with inversion and the major Mesozoic basement involved pre-Aptian growth faults. The offshore continuation of the Regneses Hinge and Weald Basins are seen in addition to significant, and as yet undrilled, pre-Aptian horsts which are located updip of mature source rocks.

2.4 Reactivation

A. East-west structures

Two fundamentally different interpretations have been suggested to explain the structural development of the Wessex Basin, and differ in the importance attached to the east-west and northwest-southeast trends which occur within the basin. Dewey (1982) and Stoneley (1982) considered the east-west structures to be fundamental to basin development and suggested that they represented major listric growth faults. Dewey (1982) identified three main phases of crustal rifting; a Triassic event, a more localised Toarcian event, and finally, a late Neocomian event. Chadwick et al., (1983) strengthened this interpretation by demonstrating that the east-west growth faults were generated by the normal reactivation of basement thrusts, possibly of Variscan age (Fig. II.2.1). Further support for a basement (i.e Variscan thrust) control on basin development was given by Day and Edwards (1983), who traced southward dipping intra-basement reflectors to surface thrusts, while Lake et al., (1984) identified lineament orientations within the central portion of the Wessex Basin (based on LANDSAT, MSS, and TM data sets) parallelling east-west Variscan basement trends. A more detailed study of basement reactivation along east-west trends is summarized in the next section.

1. Thrust Reactivation in Lyme Bay

Lyme Bay particularly well displays structural complications associated with the offshore continuation of the Abbotsbury-Ridgeway fault and the Mangerton tear fault.

The area was surveyed by Darton et al., (1981) using echo-sounding, sideways looking sonar and continuous seismic profiling. The latter, sparker surveys, rarely penetrated greater than 100 ms (milliseconds), therefore the deeper structure still remained speculative. However, the G.S.I. non-exclusive survey, which imaged to 4 seconds (TWTT), clearly depicts the deeper structure and shallow basement and its importance in aiding modelling the structural development of the region.

G.S.I. seismic lines throughout the area show clear subhorizontal reflectors locally truncated by, and onlapping onto, a presumed basement topography. These reflectors are interpreted as late Palaeozoic in age and are presumed to comprise largely of Permo-Triassic sands and clays. The similarity in lithology between the basin fill and the underlying Devonian/Carboniferous basement locally results in problems defining the basement/sediment interface. Displayed on at least nine profiles running north-south and east-west in Lyme Bay are number of other reflectors within the basement. These reflectors can be traced in all three dimensions proving they cannot be seismic reflection processing artifacts. The deepest dipping reflector can be traced to at least 3 seconds (TWTT) which is well in excess of 6 km depth. Comparison of the geometry of individual events on different trending profiles indicates that these reflectors strike approximately east-west and largely dip southwards.

Figure 2.10 and II.2.5 shows six identified reflectors in three dimensions contoured in two-way travel-time. Where possible depth conversion has been attempted from velocity data. These reflectors have a large lateral extent (at least 50 km). R2 (Fig. 2.11), immediately south of the Isle of Portland, appears approximately horizontal for 3 km across strike and 25-30 km along strike, thus reflecting a ramp/flat geometry to these structures locally. Updip, major east-west extensional structures controlling Mesozoic deposition, are generally located above these dipping events, such as the offshore continuation of the Abbotsbury-Ridgeway fault zone above the R1 reflector (Fig. 2.10). Similar dipping reflectors encountered on other seismic profiles elsewhere have been attributed to thrust faults, eg. Brewer & Smythe (1984) and Leveridge et al., (1984). The latter authors traced the dipping reflectors to inferred thrust locations onshore in south-west England. Depth conversion clearly indicates event R1 to have a true dip of 18° S whilst R2 has a true dip of 33° S, these dips are essentially minimum and maximum values. Most reflectors display a true dip of about 26° S (eg. R5 Fig. 2.10). These dips compare favourably with reflection events encountered elsewhere eg. Brewer & Smythe (1984) $20-25^{\circ}$ and Leveridge et al., (1984) 30° which they attributed to thrusts within the basement. However, more remarkable is the curved nature of the isochrons ~~is~~ comparable to observed thrust geometry in ^sSouth Cornwall and the western English Channel (c.f. Leveridge et al., 1984). Their geometry also compares extraordinarily well with onshore mapped thrusts on the BGS 1:50, 000 (Tavistock) sheet (see Issac et al., 1982) but clearly extend to greater depths, at least 6.8 km. One event R6 on figure 2.10 dips in a northerly direction and is interpreted as a small backthrust which has

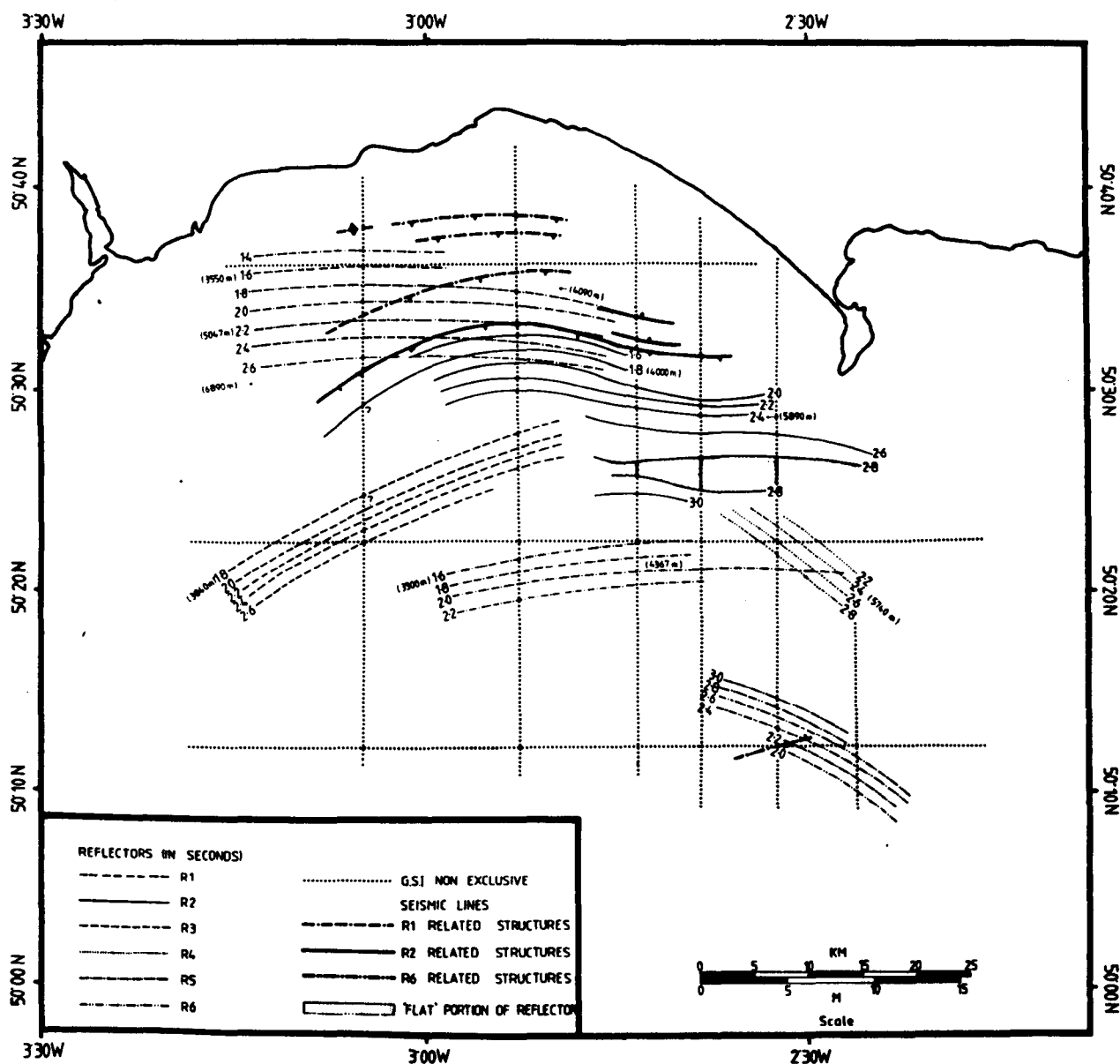


Fig. 2.10 Two-way travel-time map of the persistent prominent reflectors in the Devonian/Carboniferous basement. Isochrons in seconds.

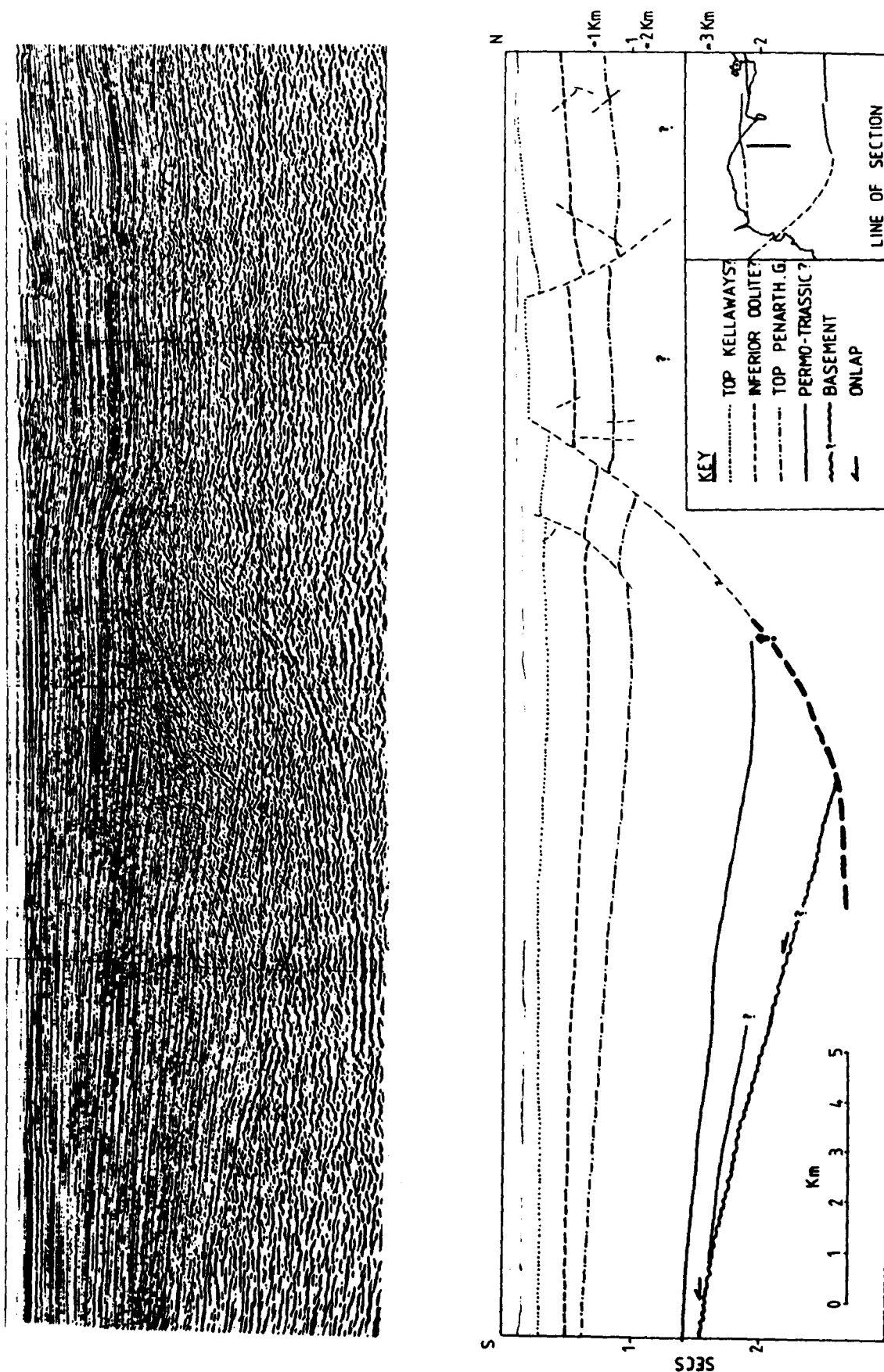


Fig. 2.11 North-south seismic section and interpretation of reflector 2 (R2) controlling the development of a major northerly-dipping late Palaeozoic/Mesozoic half graben in Lyme Bay.

been described further along strike by Shackleton et al., (1982).

Major normal faults are located in the hanging wall above the southward dipping reflectors. Figure 2.11 displays a major listric fault, or normally reactivated thrust, which seemingly controls the geometry of a northerly dipping half graben to the south. The basement interface is recognised by non uniform reflectors overlapped by an overlying sedimentary sequence and may indicate a depocentre greater than 5 km thick. On figure 2.11 the Penarth Group appears to be underlain by possibly at least 3 km of presumed Permo-Triassic sediments, within this sequence one reflector has been interpreted as the base of the Sherwood Sandstone Group due to the unconformable nature of the reflector (cf Colter & Havard, 1981, Wytch Farm oilfield). The hanging wall Mesozoic sequence above the Penarth reflector on figure 2.11 displays clear reverse drag partially associated with the original roll-over geometry above a listric detachment, plus local reverse movement probably associated with inversion. Figure 2.12, along strike to the west, displays a major unconformity within the sedimentary sequence above the same R2 reflector, again this may represent the Permo-Triassic unconformity (see Colter & Havard, 1981). The R2 reflector displays a ramp/flat geometry which corresponds with the major horizontal reflector interpreted as a flat identified on the two seismic lines immediately to the east (Fig. 2.10). Thus the R2 reflector may be either a normal listric growth fault initiating in the early Permian or, more likely, a normally reactivated Variscan thrust. Figure 2.12 is further complicated by upward diverging faults on the footwall side of R2. These have an approximately eastwest trend and could be interpreted as negative transtensional flower structures (using terminology of Harding, 1985)

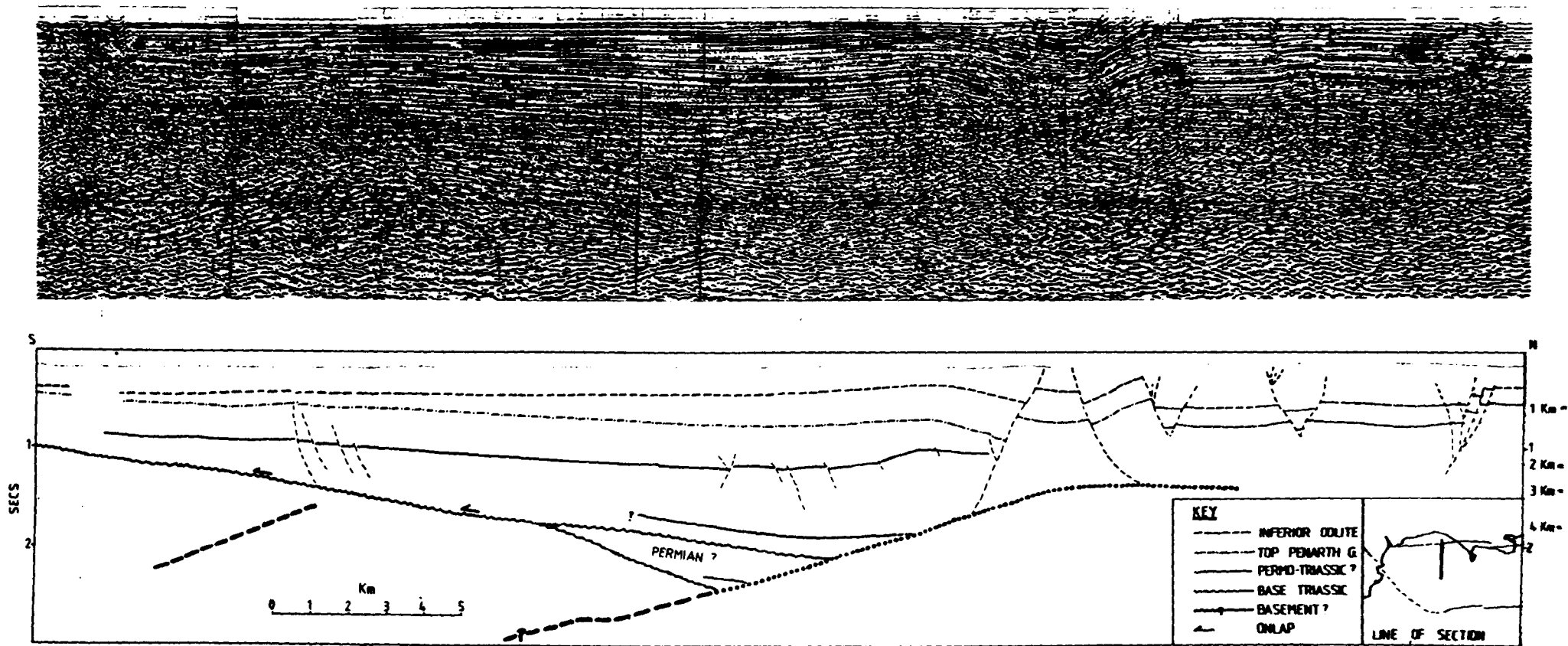
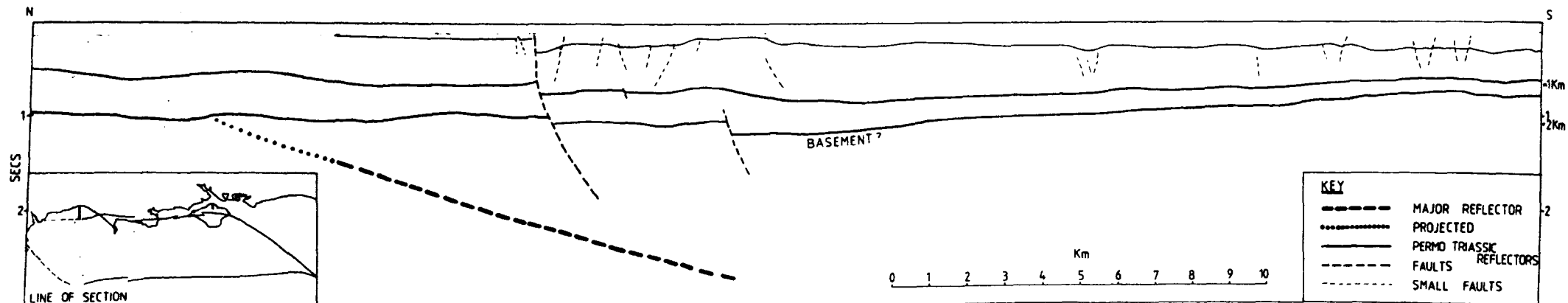
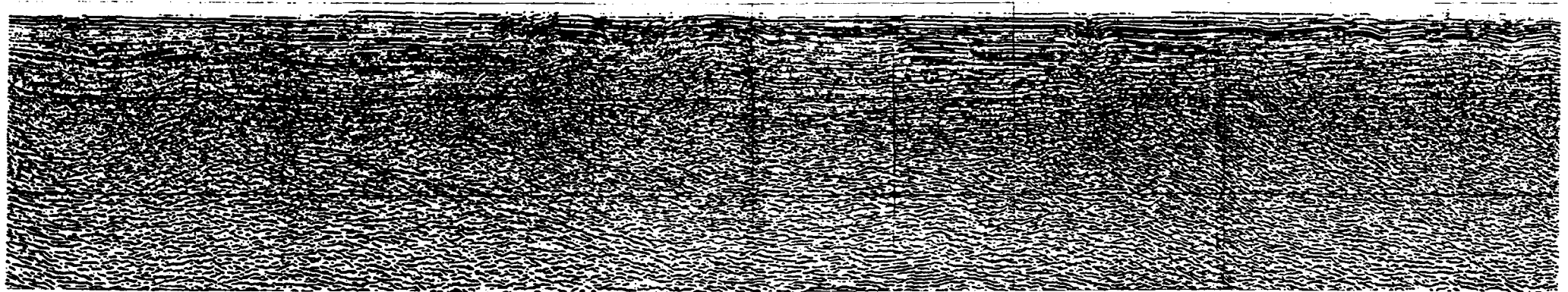


Fig. 2.12 North-south seismic section and interpretation showing the ramp/flat geometry of reflector 2 (R2) controlling the development of a major northerly-dipping late Palaeozoic/Mesozoic half graben in Lyme Bay. The detailed structure of the Abbotsbury-Ridgeway fault zone is well displayed.

indicating oblique extension during basin development.

Figure 2.13 shows clearly a major southward dipping reflector (R1) which extends at least 5 km into the footwall side of a major Mesozoic growth fault in the overlying sedimentary sequence. Updip projection of this reflector coincides with a major low amplitude antiform in the Mesozoic sequence presumably associated with reversed movement along this reflector during inversion. The dip ($\approx 18^\circ$ S) of the reflector combined with geometry and lateral extent (beyond Mesozoic growth faulting) implies reactivated Variscan thrusts controlling Mesozoic basin development. The other reflectors could be interpreted in the same light. The extent of Mesozoic faulting largely accords with the length of the reflectors, particularly in the case of R2 (Fig. 2.10), thereby implying a genetic relationship. The listric geometry of R2 is similar to Chadwick et al.'s (1983) T4 thrust controlling the Mere fault, whereas R1 (Fig. 2.13) accords more with their T3 reflector which controls the Vale of Pewsey fault. The listric nature of R2 accords with the postulated listric geometry of the Purbeck-Isle of Wight fault proposed by Stoneley (1982). Thus most, if not all, the major east-west growth faults sole out onto reactivated thrust detachments. Thus each thrust zone represents a significant weakness within the crust. Consequently any strain resulting from stress applied subsequently could be locally released most easily along, or in the vicinity of the fracture. In summary, it appears that the reflectors geometry, their locations and their relationship to overlying Mesozoic faulting can be viewed in the light of thrusts reactivated in a normal sense controlling the location and geometry of the subsequent Mesozoic depocentres. The results presented here are the first documented example of such structures based on three dimensional seismic control.

Fig. 2.13 North-south seismic section and interpretation of reflector 1 (R1). The reflector extends well in to the footwall side of a major overlying late Palaeozoic/Mesozoic fault. The reflector is interpreted as a shallow southward-dipping Variscan thrust.



B. Northwest-southeast structures

Alternatively, some authors have interpreted Wessex Basin development solely in terms of the reactivation of the second dominant trend within the basin, the northwest-southeast faults. These faults formed contemporaneously with the emplacement of Variscan thrust sheets (Coward and Smallwood 1984, Hobson and Sanderson 1983) and acted as transfer faults by facilitating thrust sheet offsets. For example, the southeastward continuation of the Sticklepath fault has acted as a transfer fault thereby allowing the independent development of the Western Approaches Basin relative to the Wessex Basins (Fig. 2.1). Within the Wessex Basin, the en-echelon arrangement of northwest-southeast trends suggests an east-west sinistral shear, and a complementary northwest-southeast dextral shear (Drummond, 1982) during basin formation.

C. Discussion

It would appear therefore, that the reactivation of both east-west and northwest-southeast faults have played a major role in basin development in that they tended to compartmentalize the basement and isolate individual depocentres (c.f. Issac 1983). The resulting geometry resembles a pull-apart basin (Fig. 2.1), in broad agreement with the wrench boundaries of the Wessex Basin (i.e. Sticklepath and Pays de Bray faults and the Purbeck-Isle of Wight and Mid-Channel faults). The apparent separation between these basin-boundary faults is of the order of 40 km. However, Stoneley (1982) has demonstrated that the maximum horizontal extension across the Purbeck-Isle of Wight fault was only ca. 2.5 km during the Jurassic-mid Cretaceous. While crustal extension, and

therefore basin initiation, is a consequence of sinistral motion across the northwest-southeast wrench faults, it is the collapse of the hanging wall block (or thrust sheet) which ultimately determines the basin width even when the absolute amount of extension is small. Localised half-grabens form as a consequence of hanging-wall collapse. However, on increasing extension, antithetic faulting becomes important and transforms the apparent half graben geometry to full symmetric grabens (e.g. Weald Basin).

While the northwest-southeast fault direction is obviously important in the development of the Wessex Basin, it also represents a major fabric which cross-cuts the Variscides of Europe and as such, has controlled the development of many western European basins (e.g. Ziegler, 1982; Lake and Karner, 1986). In summary, the structural evolution of the Wessex Basin is fundamentally the result of basement reactivation. The east-west faults, as a consequence of normal reactivation, compensate extension by the upward propagation of growth faulting into the overlying sedimentary cover. The northwest-southeast faults compartmentalised the basement, thereby producing rhomboidal-shaped depocentres. Intermittant movement along both either fault direction resulted in polyphase crustal extension and hence a punctuated basin subsidence.

Other lineament and fault trends, while existing, are generally considered insignificant, for example, the north-south trends south of the Purbeck-Isle of Wight fault (e.g. Arkell 1947, Donovan and Stride 1961). To the north of the Wessex Basin, the only feature with this trend is the Malvern axis, a probable Precambrian basement feature. As the strong magnetic signature of the axis does not continue southwards into the Wessex Basin (c.f. Hawkins 1942, Shackleton 1984), the basement of the

Wessex Basin is likely to be solely of Variscan age.

Basin initiation independent of a basement control has been suggested by Falcon and Kent (1950) in which the migration of large amounts of Triassic salt has allowed basin subsidence. Structures formerly attributed to salt movement, such as the Compton Valence anticline and the Fordingbridge high, proved to be, on drilling, low density intra-basement rocks at shallow depths rather than salt diapirs. Rhys et al., (1982) have also shown that in the areas of thickest salt accumulation (e.g. 30-50 metres, Winterborne Kingston Trough), there is virtually no disruption of bedding as evidenced by seismic reflection imaging.

2.5 Basin formation Mechanisms

A. Introduction

So far, we have been interested in the kinematic description of basin development. But mechanistically, how has the Wessex Basin formed and in particular, what role do the thermal and mechanical properties of the lithosphere play in Wessex Basin development? Sedimentary basins are the consequence of a driving mechanism, the form and distribution of which is mechanism dependent. The history of basin subsidence therefore, is a sensitive indicator of both the basin initiation mechanism, and the thermal and mechanical properties of the lithosphere, both in rifting, and during the subsequent conductive dissipation of rift-induced heat.

Rift basins can be divided into two main types, those resulting from lithospheric stretching (McKenzie 1978) and those resulting from crustal /upper crustal stretching (Royden et al., 1983; Karner and Dewey, 1986). Although the geometric surface expressions may be broadly similar, the subsidence history is sensitive to the degree of lithospheric heating during rifting and hence the role of the sub-crustal lithosphere. Litho-

spheric rifting introduces a significant amount of heat into the sub-crustal lithosphere (associated with the passive upwelling of hot asthenospheric material) relative to crustal rifting, which involves considerably less heat input during extension (Fig. 2.14).

B. Lithospheric stretching model

The lithospheric stretching model of McKenzie (1978) successfully reproduces the regional observations of intracratonic and rift/passive margin basins (e.g. Watts et al., 1982; Watts and Thorne, 1984). The degree of lithospheric stretching is parameterised by the factor β and predicts two phases of basin formation; an initial rifting phase associated with fault controlled subsidence, followed by a thermal subsidence phase related to the thermal contraction and cooling of the lithosphere (Fig. 2.14). As the lithosphere/asthenosphere boundary represents a temperature isotherm, any upward migration introduces a temperature perturbation into the lithosphere. The observed negative exponential form of rift basin subsidence (Sleep, 1971) is analogous to the exponential decay of oceanic crust subsidence (Parsons and Sclater, 1977). In most applications of this technique (e.g. Steckler and Watts, 1978; Christie and Sclater, 1980), lithospheric stretching model assumes perfect Airy compensation (local loading) that is, zero flexural strength of the lithosphere. Inclusion of a finite strength lithosphere helps to explain the overall increase of basin width with time and the progressive basement onlap forming the basin margin during the thermal subsidence phase (Watts et al., 1982).

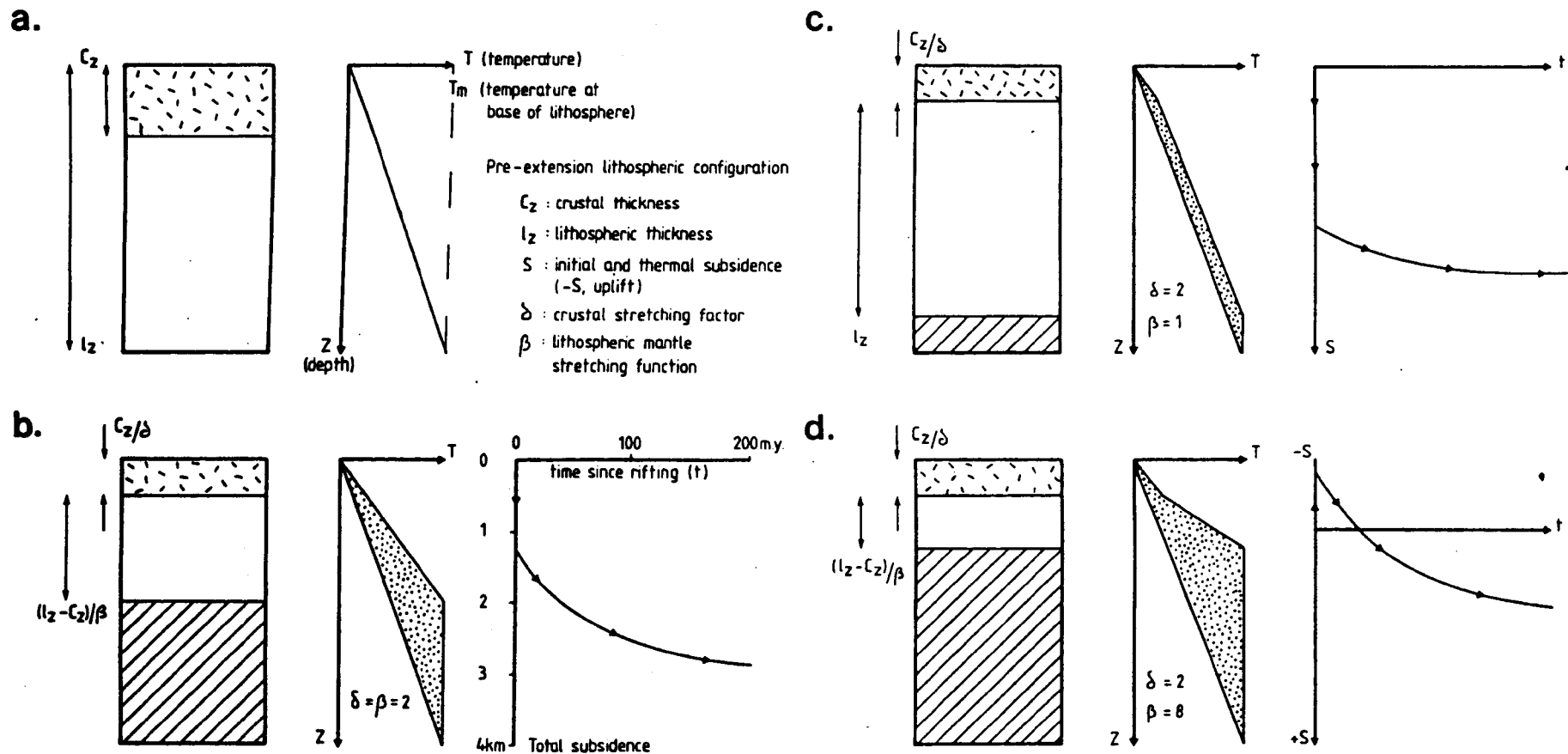


Fig. 2.14 Lithospheric stretching initially modifies the thickness of both the crust and sub-crustal lithosphere: δ represents stretching above the decollement (usually considered to be the Moho) and β represents either stretching below the decollement or the degree of sub-crustal heating. The simplest model of basin formation is for depth-independent stretching ($\delta = \beta$) in which the pre-event lithospheric configuration and temperature structure (a) is modified

Alternatively, crustal thinning in the absence of sub-crustal extension significantly modifies the temperature structure of the lithosphere (c). The general model therefore, is for depth-dependent stretching across a decollement (d). (Modified from Karner & Dewey (1986)).

C. Crustal stretching model

Crustal extension (Royden et al., 1983; Karner and Dewey, 1986) refers to the tectonic situation whereby extension is confined solely to the crust, the sub-crustal lithosphere playing an entirely passive role (Fig. 2.14). During extension, strain compatability must be maintained within the crust and is most simply accommodated by contemporaneous foreland basin formation or regional thrusting in adjacent regions (c.f. Karner and Dewey, 1986; Christie-Blick and Biddle, 1986). Although basins produced by crustal/upper crustal extension are probably common, little attention has been given to this model. Possible candidates include many of the British offshore basins (on the continental margin) that have been seismically imaged by BIRPS and show Palaeozoic and Mesozoic basins formed along earlier Caledonide and Variscan structural trends (e.g. Brewer and Smythe 1984). Other examples include the Triassic grabens and half-grabens formed within the collapsed hanging wall of reactivated Appalachian thrust sheets along the Eastern seaboard of the United States (e.g. the Connecticut, Newark, Culpepper, Riddeville, Bay of Fundy Basins and the Brunswick graben).

Strain compatability can be maintained in other ways, most notably by the relaying of extension across crustal/lithospheric detachments (e.g. Wernicke, 1985). Quantitative models for studying the development of basins above a detachment (e.g. Fig. 2.14) have been investigated by Royden and Keen (1980) and Hellinger and Sclater (1983). Though originally designed to investigate basins in which an excess amount of heat was required to explain the high ratio of post-rift to syn-rift sedimentation (i.e. $\delta < \beta$), by symmetry, it is equally applicable to basins in which only minor heating occurs, such as in continental pull-

apart basins or hanging wall basins (e.g. Vienna Basin and Limagne Graben respectively). The McKenzie model for which $\delta > 1$ and $\beta = 1$ characterises extension (Fig. 2.14) which is confined to the crust (δ defining the crustal stretching) with the sub-crustal lithosphere maintaining its thickness during stretching (β defining the stretching or degree of heating within the sub-crustal lithosphere). The resultant lithospheric temperature structure and subsidence for general detachment stretching is shown in Fig. 2.14 (with $\delta = \beta$ and in this example, a flat detachment at the Moho). Readjustment of the sub-crustal lithosphere introduces a minor thermal anomaly which, on dissipation, produces the usual negative exponential subsidence characteristic of the conductive dissipation of heat.

A variety of methods exist by which the amount of crustal (and hopefully lithospheric) extension can be estimated; (1) consideration of pre- and post-stretched crustal thicknesses, the most diagnostic of all but fails to address the history of stretching, only the cumulative stretching, (2) examination of fault geometries (e.g. Wernicke and Burchfiel, 1982) which tend to produce a minimum estimate of extension, and (3) by comparing the observed driving subsidence of a basin, obtained from isostatically removing or backstripping its sediments, with a theoretical determined driving subsidence. We will use all these techniques in an effort to define the magnitude, distribution, and history of lithospheric extension responsible for Wessex Basin formation and develop further the previous crustal configuration shown on figure II.2.1.

While the subsidence history of a sedimentary basin potentially contains information on the driving subsidence and hence initiating

mechanism, sedimentation tends to distort the basin subsidence such that a correction for sediment loading must be applied. The process of backstripping, as outlined by Steckler and Watts (1978), allows the isolation of the tectonic driving subsidence responsible for the development of a sedimentary basin (Fig. 2.15). Backstripping is a two part process; firstly, the sediments are decompacted so that an estimate of sediment density through time can be made (assuming that the present-day porosity/depth curve applies at all times during basin development), and secondly, the sediments are then progressively removed and the isostatic rebound of the basement monitored (Fig. 2.15). As is usual in backstripping studies, the isostatic rebound of the basement is assumed to be Airy. Airy isostasy refers to a lithosphere with a low flexural strength (Karner and Watts, 1982), and while it is an unrealistic description of lithospheric behaviour (except possibly early in basin development), it does not change the form of the subsidence curves (Bond and Kominz, 1984; Watts et al., 1982). The resultant backstripped subsidence history (e.g. Fig. 2.15) represents the driving subsidence responsible for basin development, and can be directly compared to theoretically determined subsidence curves, as for example, in figure 2.15 in which the simple one-layer stretching model of McKenzie (1978) has been used.

In order to predict the ^cresponse of the lithosphere to extension, the pre-stretching lithospheric and crustal thicknesses must be known. Lithospheric thickness is proportional to the thermal age of the basement (Karner et al., 1983), that is, the time since the last major thermal event. In southern England, the radiometric age of the low grade metamorphic basement is 337 ± 5 m.y. (K-Ar, Colter and Havard 1981).

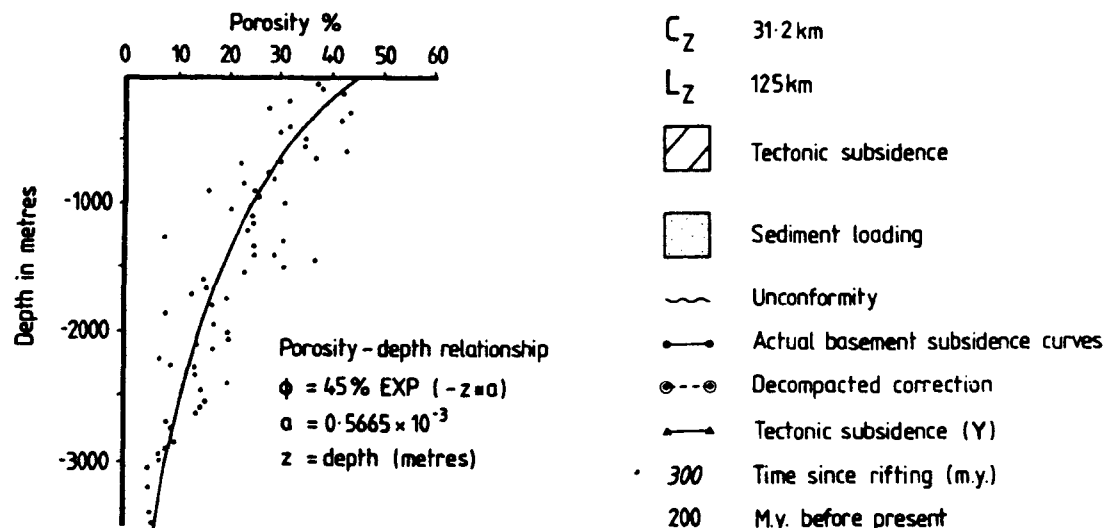
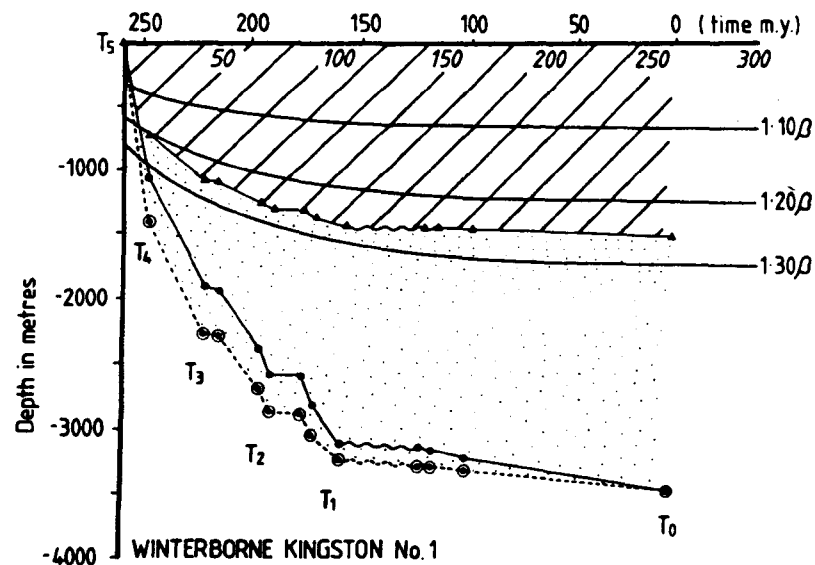
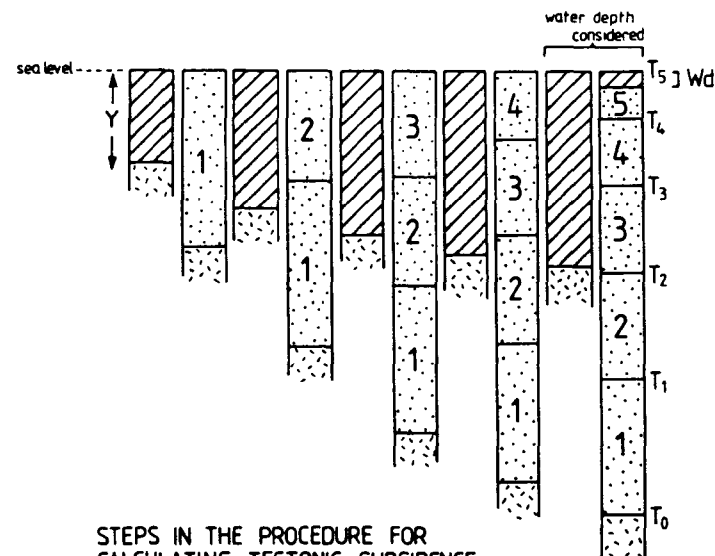


Fig. 2.15 Procedure for calculating tectonic subsidence by backstripping. The Winterborne Kingston borehole was chosen as most representative. The porosity was recorded from the Winterborne Kingston sonic log.



STEPS IN THE PROCEDURE FOR CALCULATING TECTONIC SUBSIDENCE

- Y = Tectonic subsidence
- S^* = Sediment thickness corrected for compaction
- ρ_s = Mean sediment density
- ρ_m = Density of mantle
- ρ_w = Density of water
- ΔSL = Sea level
- Wd = Water depth

$$Y = S^* \left(\frac{\rho_m - \rho_s}{\rho_m - \rho_w} \right) - \Delta SL \frac{\rho_m}{(\rho_m - \rho_w)} + Wd$$

- Layer 1 = Permian
- Layer 2 = Triassic
- Layer 3 = Lower Jurassic
- Layer 4 = Middle Jurassic
- Layer 5 = Upper Jurassic - Cretaceous

- T_n = in time steps
- Sediment fill corrected for compaction
- Basement

Similarly, the $\text{Ar}^{40}/\text{Ar}^{39}$ dating of the Middle Devonian basement in Arreton No2 borehole is 340 ± 8 m.y. Interpretation of seismic refraction and wide angle reflection data (e.g. Holder and Bott 1971, Brooks et al., 1984) over the Cornubian Massif suggests a pre-basin crustal thickness of 27-32 km (implying incidentally, that the original Variscan foredeep crust must have been relatively thin prior to the upper Carboniferous collision). Thus, the pre-extensional lithospheric and crustal thicknesses were approximately 90-125 km and 30.0 km respectively.

Fifty boreholes were backstripped in order to determine the driving subsidence of the Wessex Basin (Fig. 2.16 and Table 2.1). As is usual, Airy isostasy was assumed and the effects of eustatic sea-level variations, palaeobathymetry and erosion were ignored. Figure 2.16 shows that subsidence within the Wessex Basin is rather complex, with subsidence magnitude being a minimum in the northerly region of the basin and increasing towards the Channel. In some regions, the subsidence basically consists of a simple exponential shape punctuated by a number of rapid but small subsidence events (e.g. nos. 30, 35 and 47), whereas other regions show a gentle and continuous (almost linear) subsidence for the entire development history of the basin (e.g. 13, 30, 35 and 37). The truncation of subsidence within the Wessex Basin depocentres (e.g. 18, 23, 31, 46, 49 and 50) undoubtedly represents the effects of syn to post-upper Cretaceous inversion and subsequent erosion. Similarly, synchronous structural high inversion resulted in a renewed subsidence phase (e.g. 35, 36, 42 and 47). The initiation of Weald Basin subsidence shows an approximately 50 m.y. offset relative to the basin subsidence in the west (Fig. 2.16), suggesting a migration of rifting from west to east during the upper Palaeozoic-Mesozoic.



Fig. 2.16 Subsidence plots for all the backstripped boreholes in southern England. Borehole numbers are summarized on Table 2.1.

As the lithospheric stretching model of McKenzie (1978) has been useful in understanding the development of other intracratonic basins, we have used the same model for comparison with the observed subsidence of the Wessex Basin. Rather than showing all the backstripped subsidence curves of the Wessex Basin, (Figs. 2.17, 2.18, 2.19, 2.20, 2.21, 2.21, 2.22, 2.23), four representative examples have been chosen; Winterborne-Kingston (no. 44. Fig. 2.16), Southampton (no. 36), Arreton (no. 49) and Ashdown (no. 31) to follow through the modelling more easily. Figure 2.24 shows from the backstripping analysis of three wells that, in general, the observed backstripped subsidence transects the negative exponential subsidence predicted from the simple lithospheric stretching model (except Winterborne-Kingston) implying that during rifting, whole-lithospheric failure has not occurred. The degree of involvement of the sub-lithosphere during rifting is wavelength dependent and is necessarily regional (Karner and Dewey, 1986). Therefore, spatially local crustal rifting need not be related to the sub-crustal lithosphere in a one-to-one fashion as required by the McKenzie stretching model. Indeed, the lack of a significant Moho topography being developed between the basin and the surrounding massifs (e.g. Brooks et al., 1984; Holder and Bott, 1971; BIRPS/ECORS, 1986) during rifting strongly suggests that the upper and lower crusts are accommodating extension in a different way. In particular, we might expect that brittle extension in the upper crust (and hence local failure) is balanced by dominantly ductile extension in the lower crust/sub-crustal lithosphere (resulting in a broad, regional failure; e.g. Hellinger and Sclater, 1983; Karner, 1984). Alternatively, the flexural rigidity of the lithosphere has failed to be reset (as a consequence of $\beta < 1.25$) such that upper-crustal unloading (i.e. to form

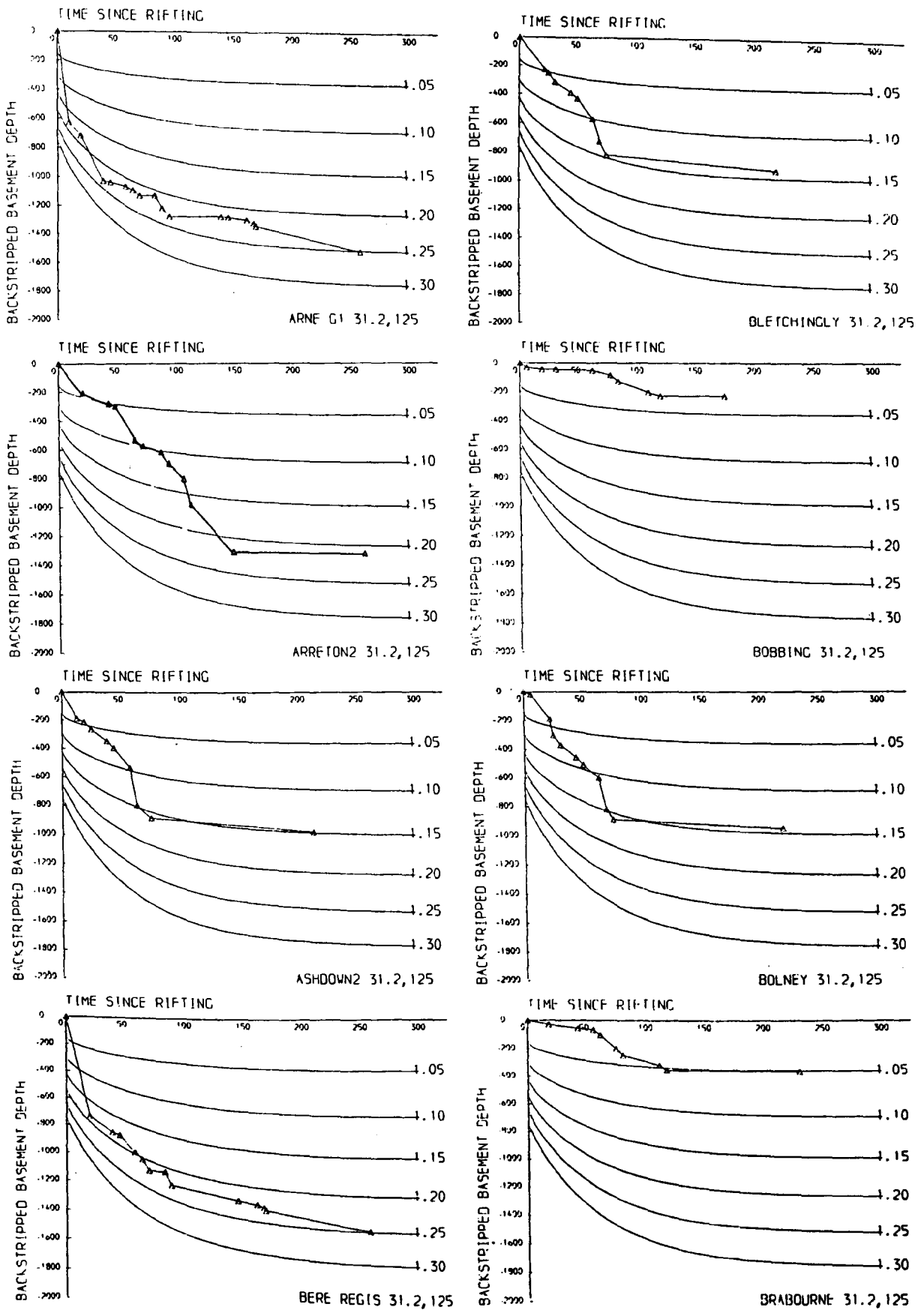


Fig. 2.17 Backstripped subsidence plots. Arne G1-Brabourne boreholes.

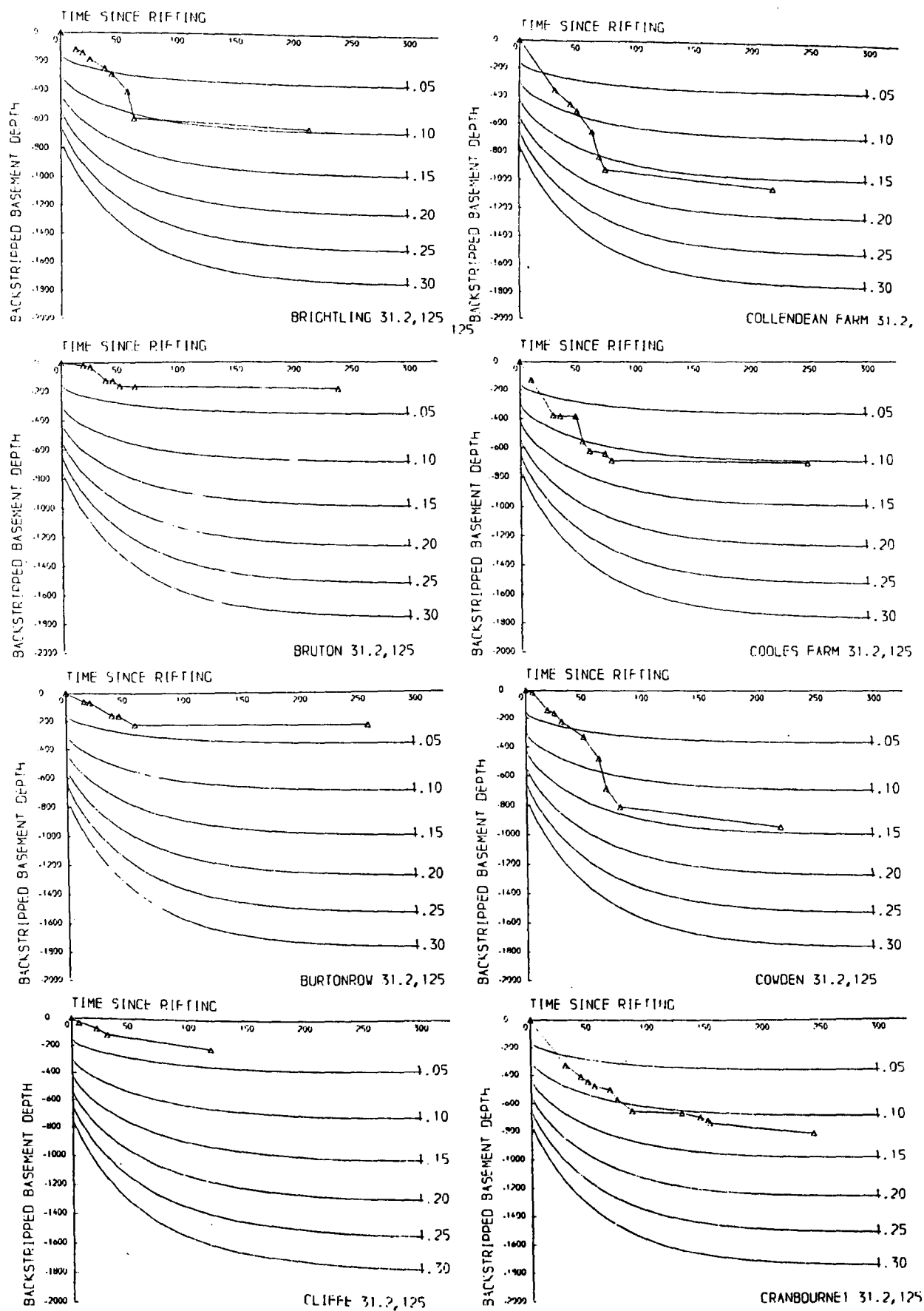


Fig. 2.18 Backstripped subsidence plots. Brighting - Cranbourne boreholes.

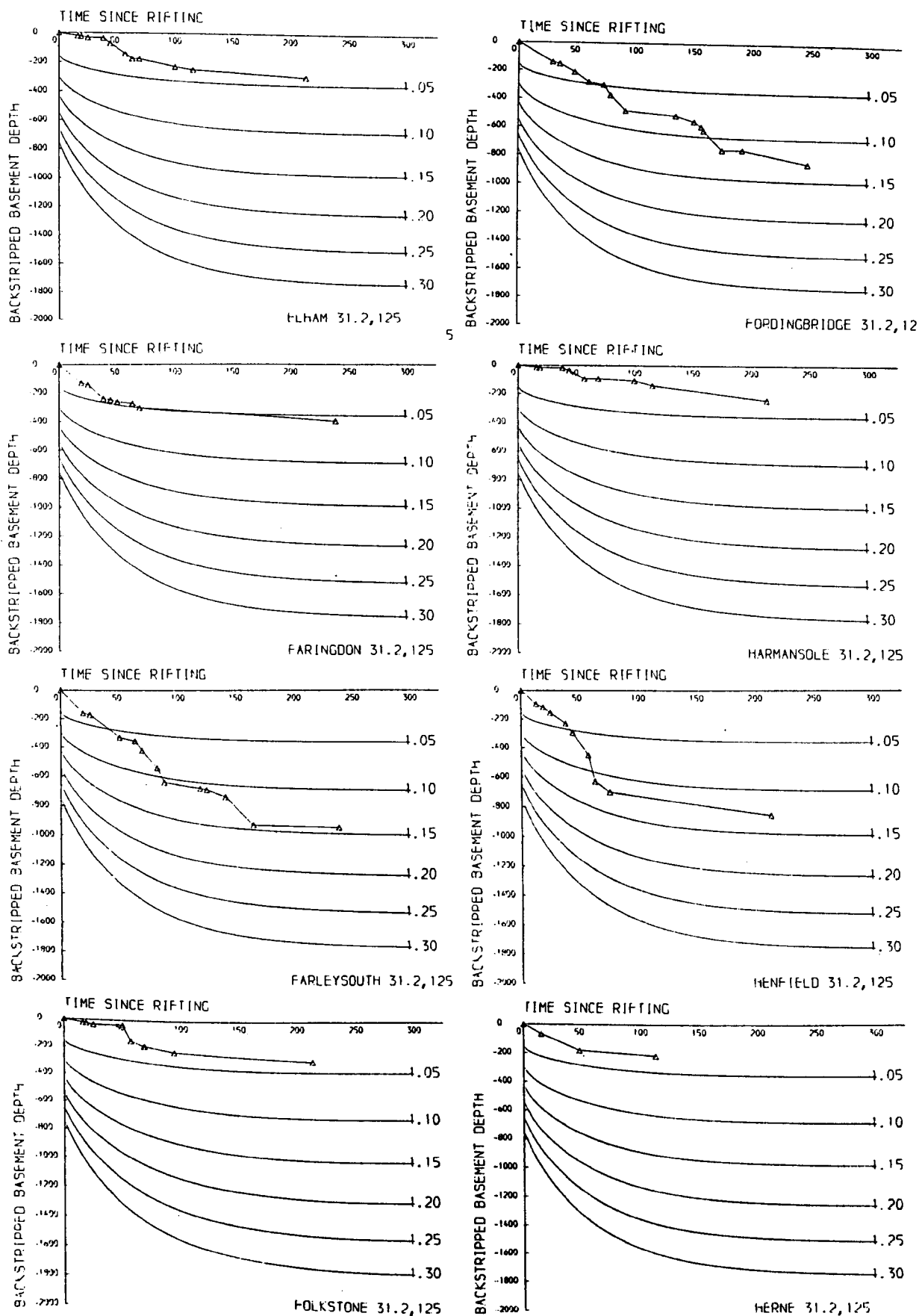


Fig. 2.19 Backstripped subsidence plots. Elham - Herne boreholes.

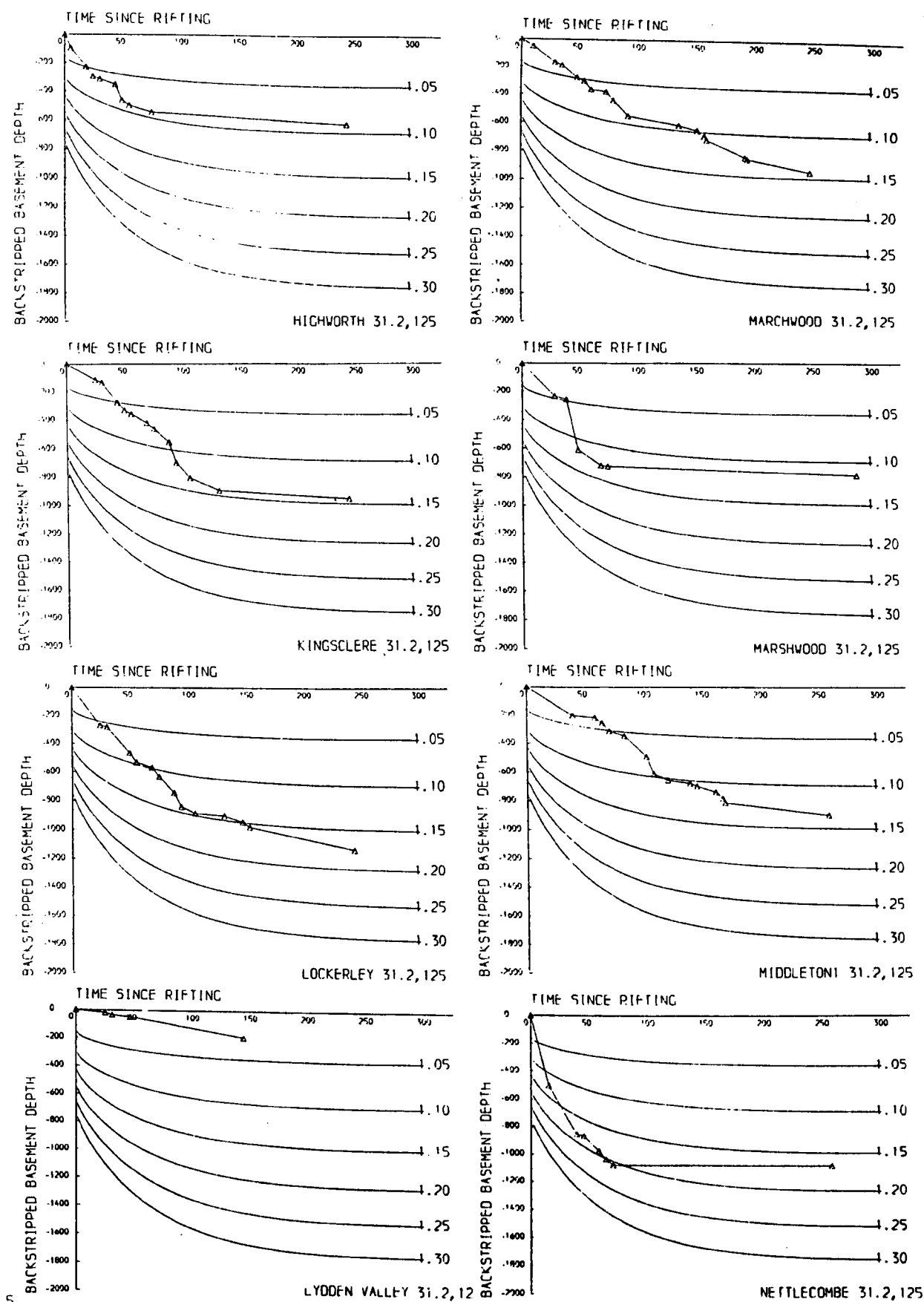
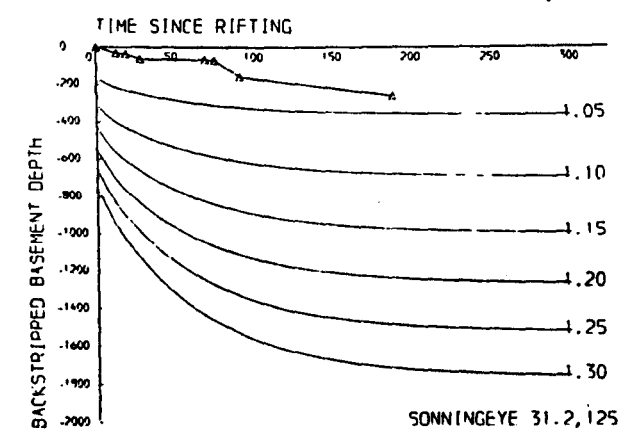
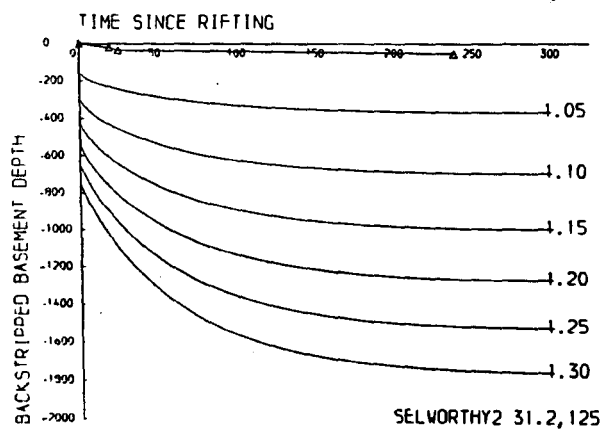
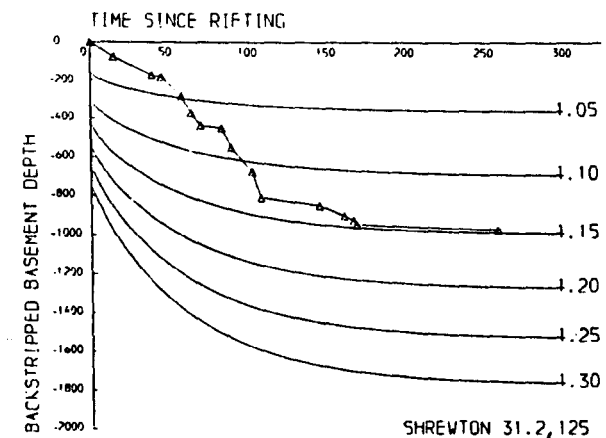
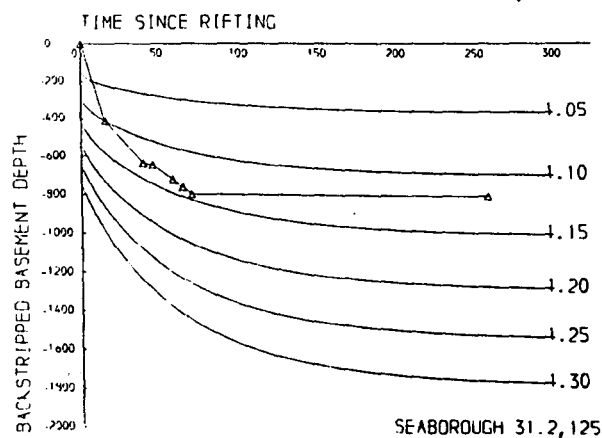
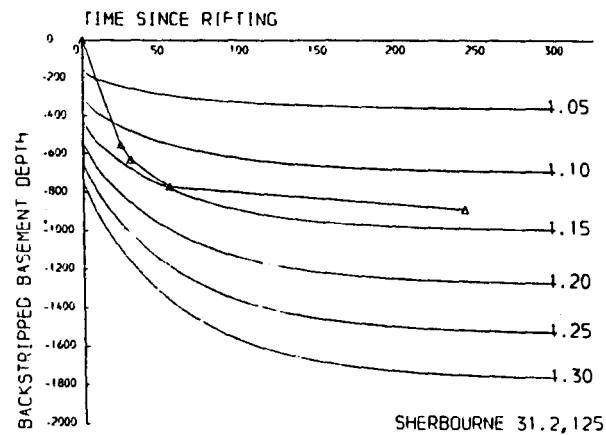
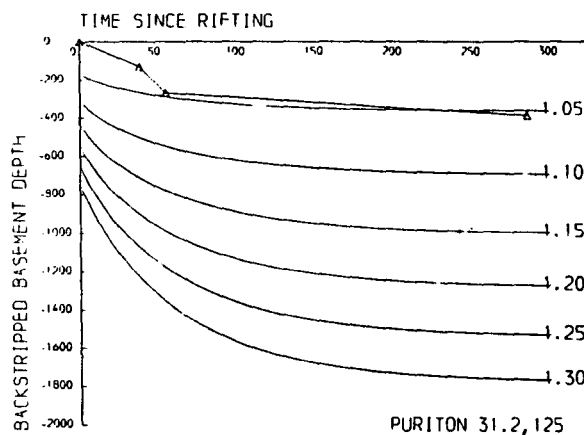
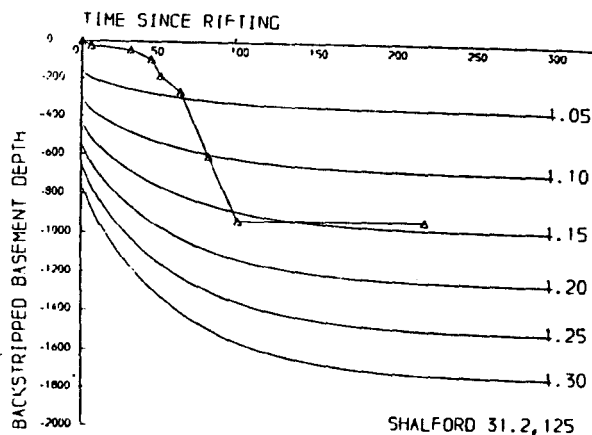
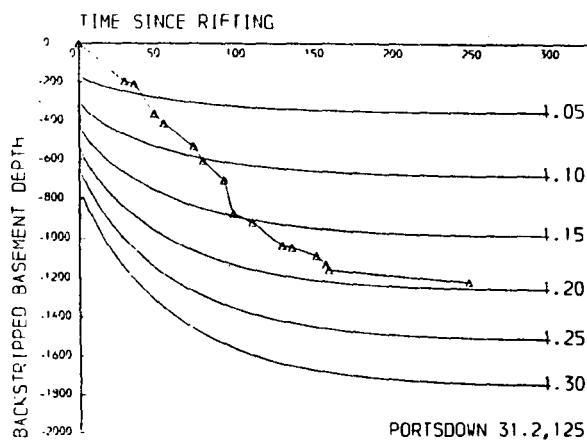


Fig. 2.20 Backstripped subsidence plots. Highworth - Nettlecombe boreholes.



Backstripped subsidence plots. Portsdown - Sonningeye boreholes.

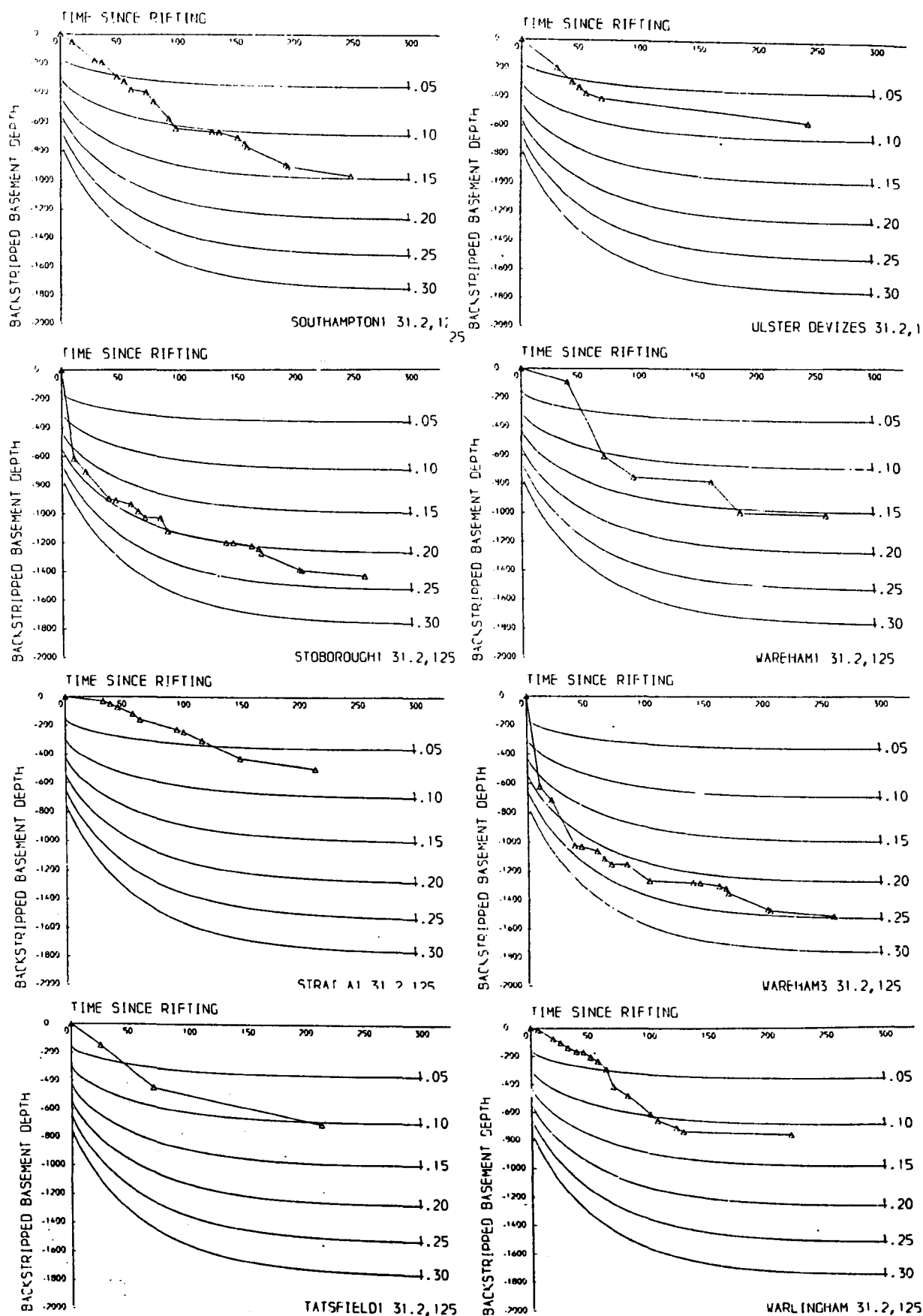


Fig. 2.22 Backstripped subsidence plots. Southampton - Warlingham boreholes.

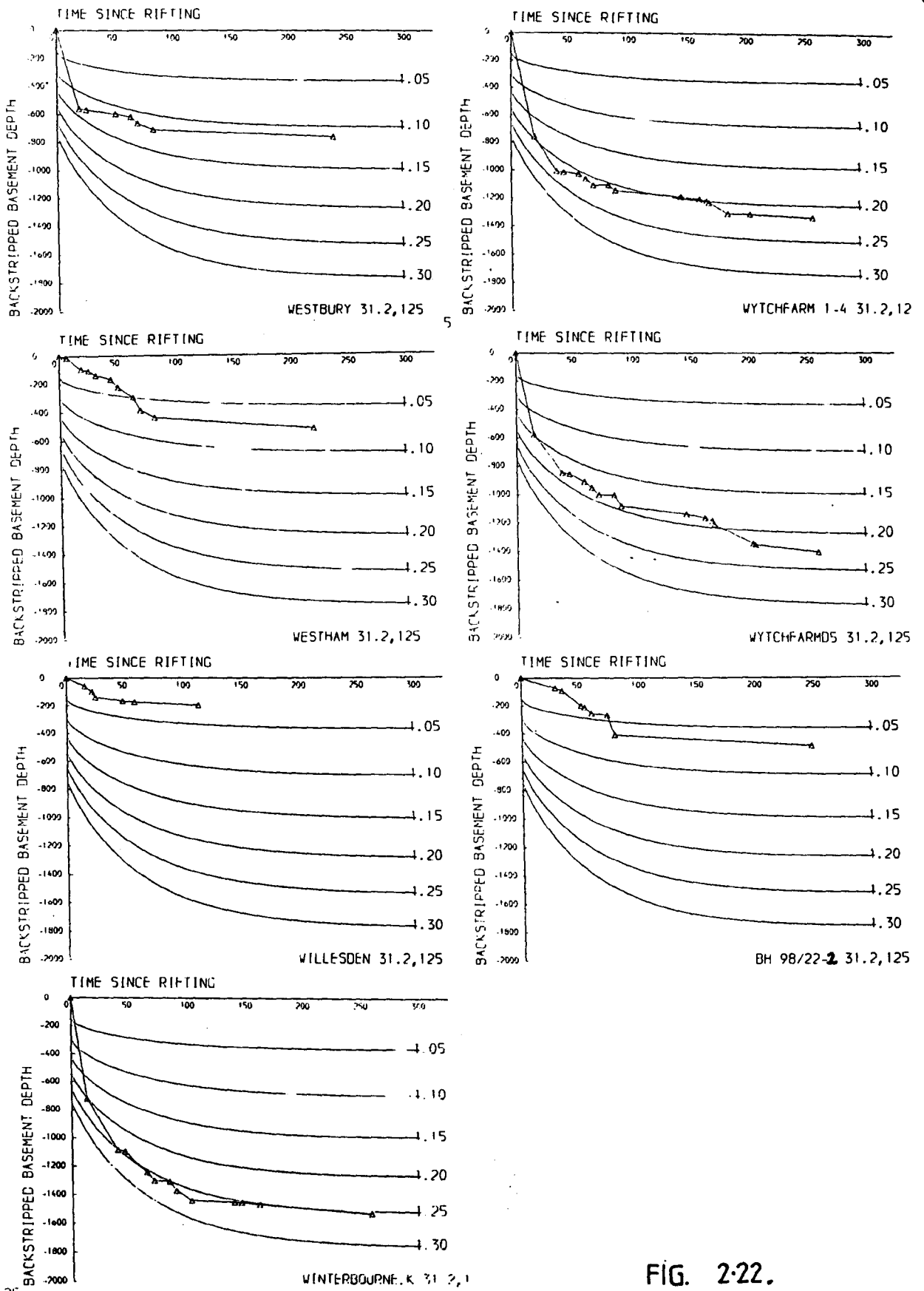


FIG. 2.22.

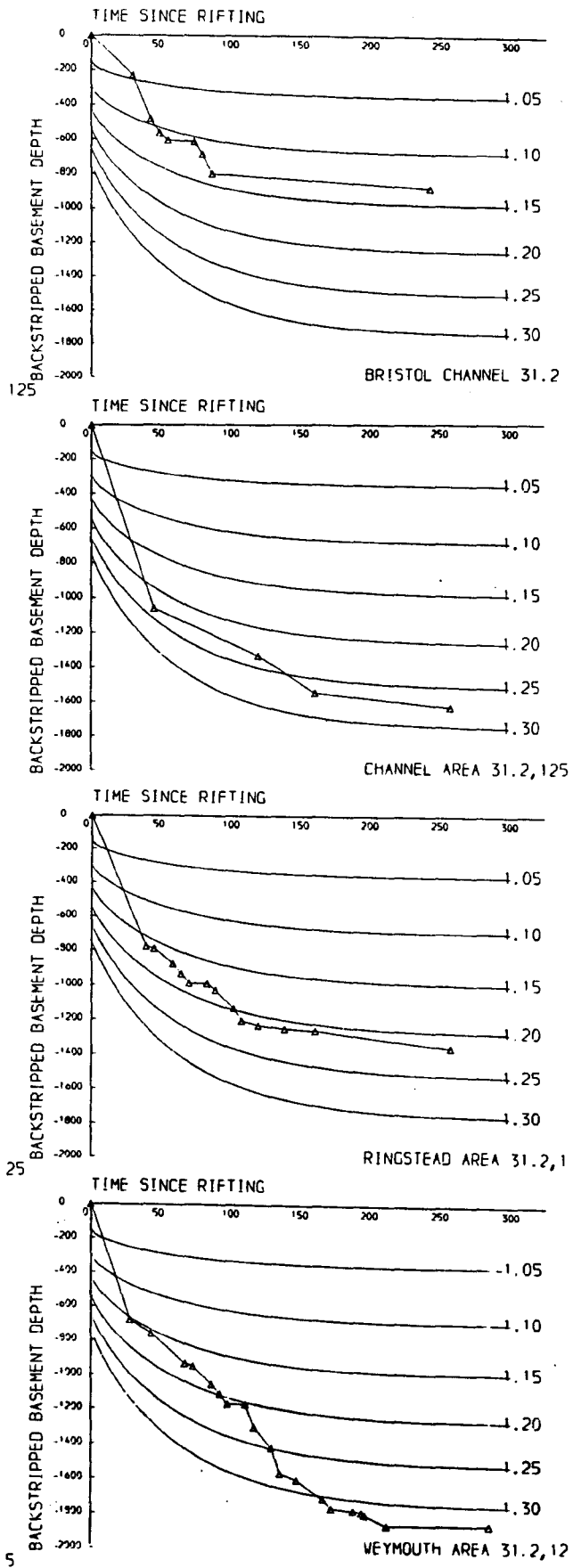


Fig. 2.23 Backstripped subsidence plots based on regional (as opposed to well data). Bristol Channel - Weymouth Area.

spatially local basins) by extension is isostatically compensated by a regional rebound of the lower crust/sub-crustal lithosphere (c.f. Karner and Dewey, 1986).

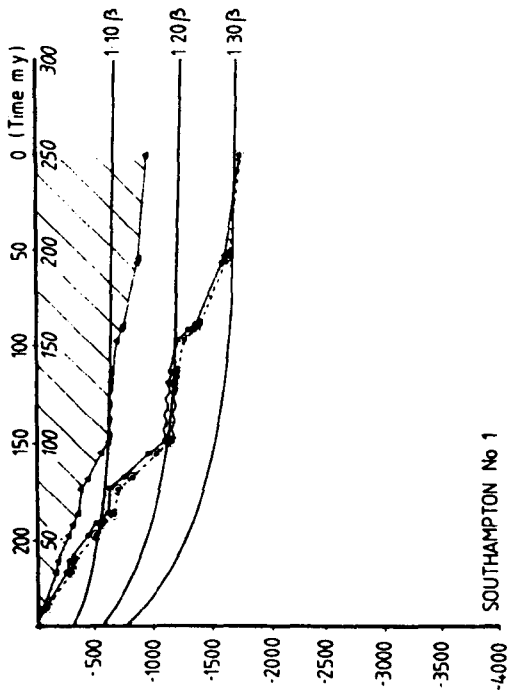
The estimation of β , as in figure 2.24, is somewhat problematical since it represents an estimate of the amount of heat introduced into the sub-crustal lithosphere during rifting. In the original McKenzie model, rifting was considered instantaneous and as such, tended to maximise the heating of the sub-crustal lithosphere and therefore the magnitude of the post-rift subsidence. More importantly, in this model the magnitude of the thermal subsidence is a direct measure of β . During finite rifting however, heat is conductively removed from the lithosphere, thereby accentuating the rift subsidence while diminishing the magnitude of the subsequent thermal subsidence. In this case, the thermal subsidence reflects the amount of heat residing in the lithosphere at the close of rifting. To accurately estimate β therefore, this heat loss needs to be accounted for. In addition, as basement fault reactivation along a listric detachment is known to have played a fundamental role in basin development, we utilised a lithospheric stretching model which included the effects of decollement extension relaying (see Chapter 3) and finite rifting (Fig. 2.25).

The estimation of δ , the crustal stretching, was relatively straightforward; it represents the maximum observed subsidence of the basin. For each well, δ was assigned according to the maximum backstripped subsidence, while the rifting interval was estimated from the major break in subsidence (thought to represent the rift/cooling transition). The depth to the intra-crustal detachment was assumed to be 15 km based on Williams and Brooks (1985) and Lake and Karner (1986). This information

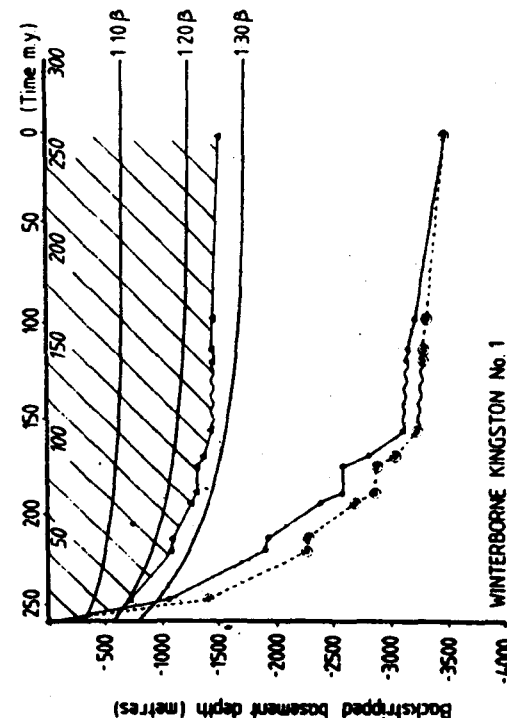
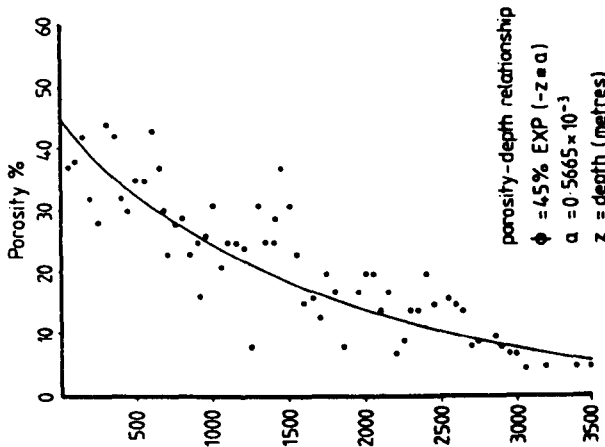
modified
10
(1986)

Three examples of backstripped boreholes. Each borehole the actual basement subsidence, decompacted subsidence and backstripped tectonic driving subsidence are shown. Subsidence due to sediment loading is stippled. The observed and best fitting (in a least squares sense) porosity curve from Winterbourne Kingston No.1 is also shown. This curve was used for decompacting all the wells from the Wessex Basin. A 31.2 km crust and 125 km lithosphere were assumed to calculate the theoretical driving subsidence curves.

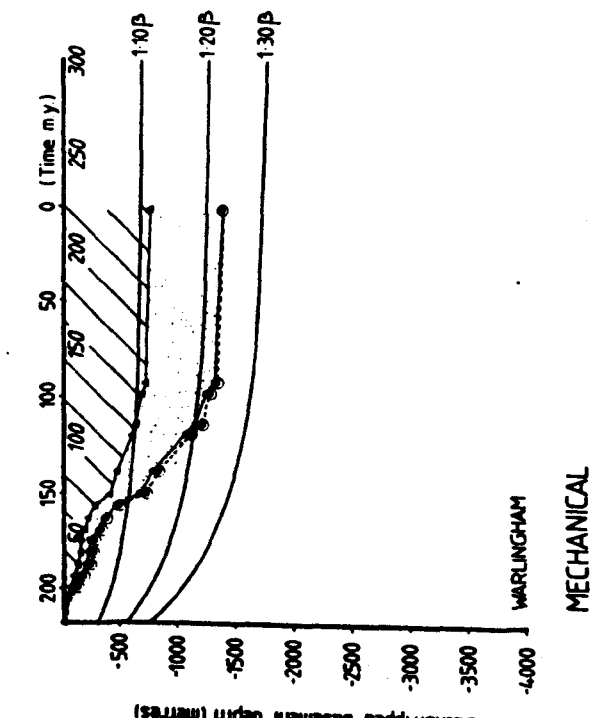
Fig. 2.24



THERMAL and MECHANICAL



THERMAL

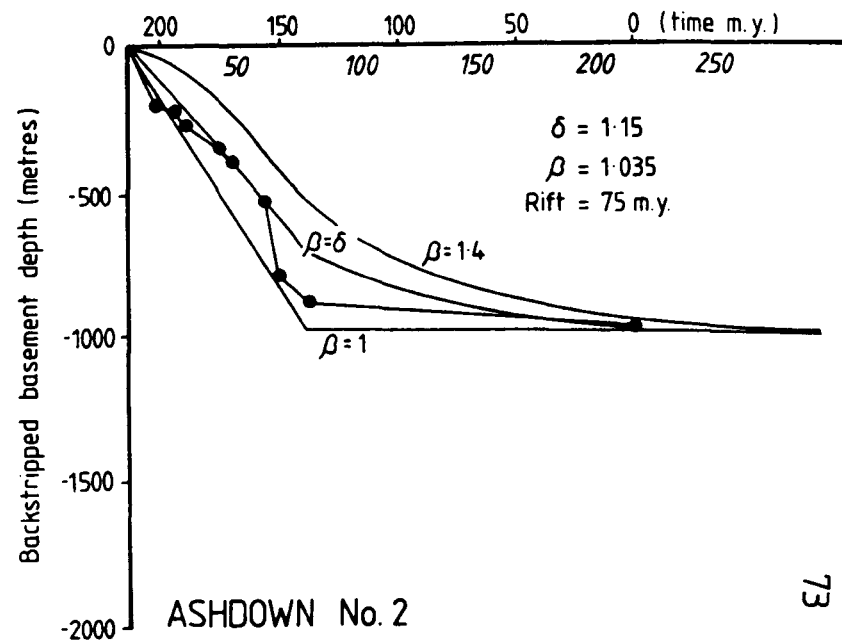
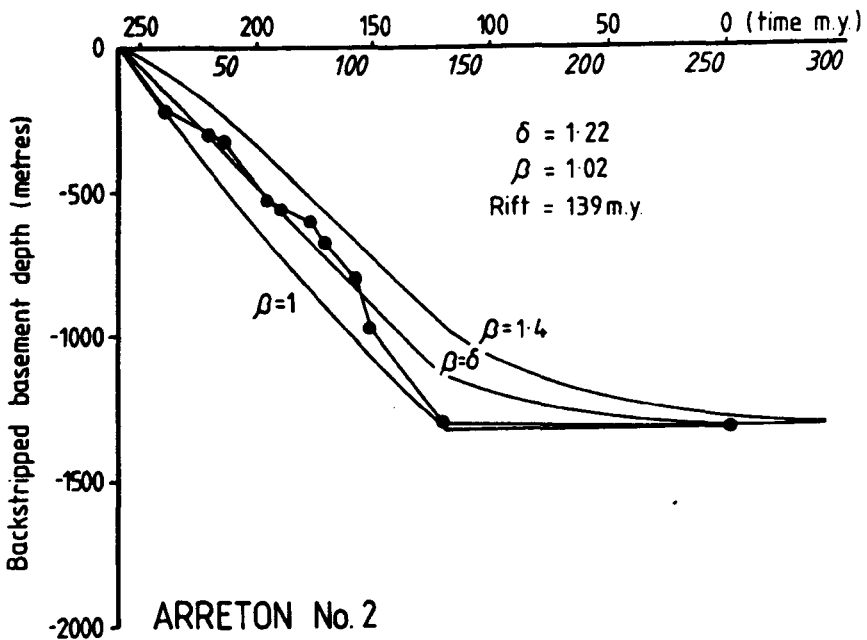
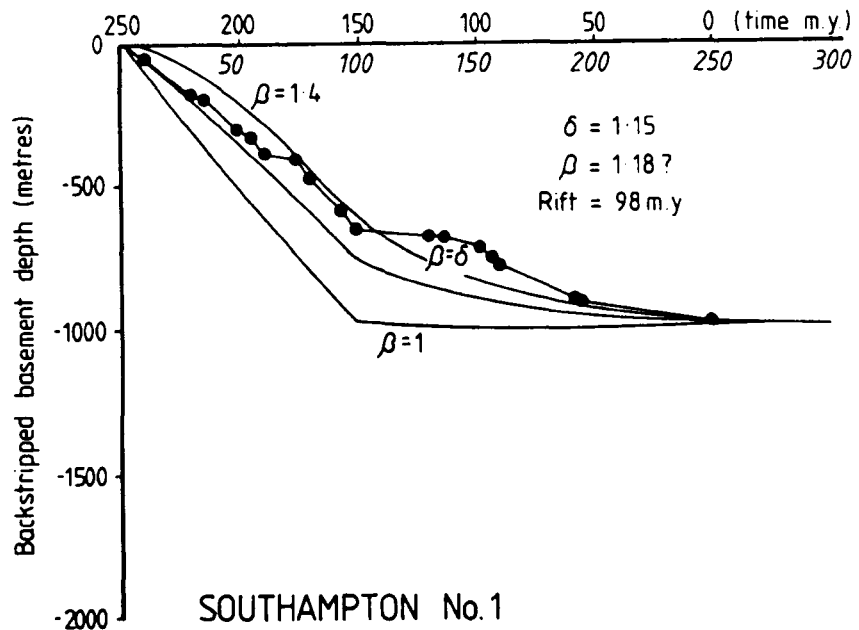
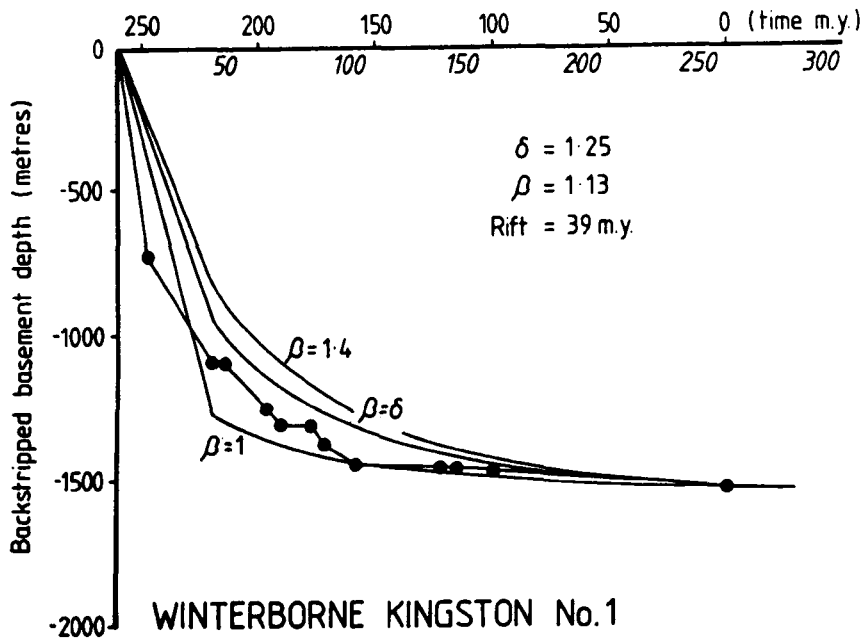


MECHANICAL

- 31.2 km
- 125 km
- Tectonic subsidence
- Sediment loading
- Unconformity
- Actual basement subsidence curve
- Decompacted correction
- Tectonic subsidence
- Time since rifting (my)
- My before present

porosity-depth relationship
 $\phi = 45\% \text{ EXP } (-z/a)$
 $a = 0.5665 \times 10^{-3}$
 $z = \text{depth (metres)}$

Fig. 2.25 Four selected wells including the effects of decollement extension relaying and finite rifting subsidence plots as a function of delta and beta (i.e. $\delta = \beta$). Delta was determined by the maximum backstripped subsidence. Three different types shown Beta = 1 (no lithospheric involvement) Beta = Delta (Delta and Beta) = 1.4



was used to estimate β across the Wessex Basin and summarised in Table 2.1. The resulting distribution of δ within the Wessex Basin shows an apparent increase towards the Channel with major but local variations occurring in close proximity to growth faults (and hence reactivated basement thrusts), with β being essentially constant, but significantly lower, across the entire basin. In particular, δ and β average 1.11 and 1.05 respectively. The strong correlation between δ and growth faults suggests that block rotation accompanying basement fault reactivation is primarily responsible for local basin subsidence and sediment accumulation. Observed fault offsets within the Wessex Basin are consistent with the low estimates of δ . Rift induced lithospheric failure is disqualified since δ/β which is also evident in the large variation in rifting times across the basin, even for closely spaced wells (e.g. Fig 2.16, nos. 44 and 35, separated by only 40 km). The Winterborne-Kingston well, while showing a negative exponential subsidence form (Fig. 2.24), suggests that $\delta > \beta$. Problems remain however, in that some wells continue to transect even the finite-rifting/cooling subsidence curves, with some estimates of β exceeding δ (e.g. Table 2.1; Southampton, Middleton, Bere Regis and Wytchfarm D5).

The extension models employed so far consider basin development as a two phase process; rifting (be it finite), followed by the passive recovery of the lithosphere. However, subsidence within the Wessex Basin is characterised by a general subsidence form punctuated by a number of rapid, but renewed finite subsidence events (Fig. 2.16 and 2.24). These rapid subsidence phases (which for convenience we will term mechanical), are correlatable in time and space across the basin (Table 2.2), suggesting that their synchronicity and regional extent may have a

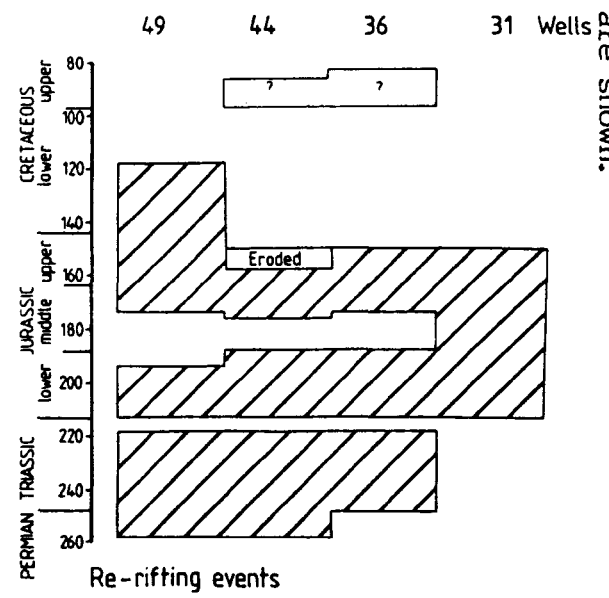
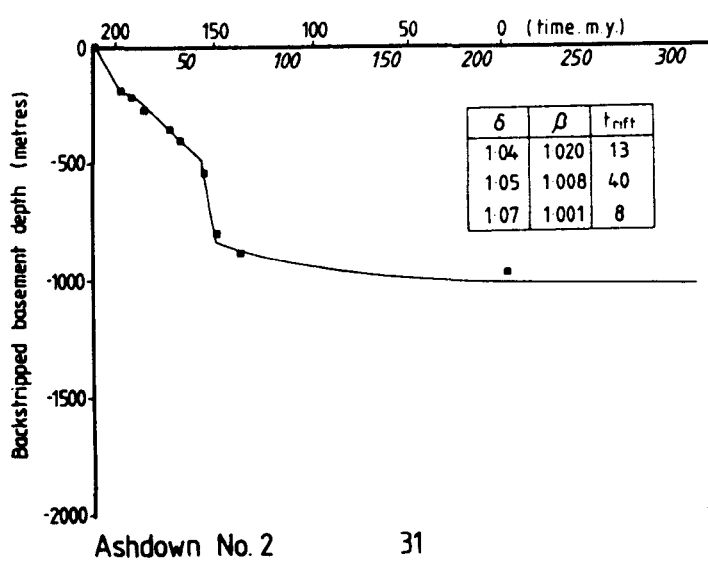
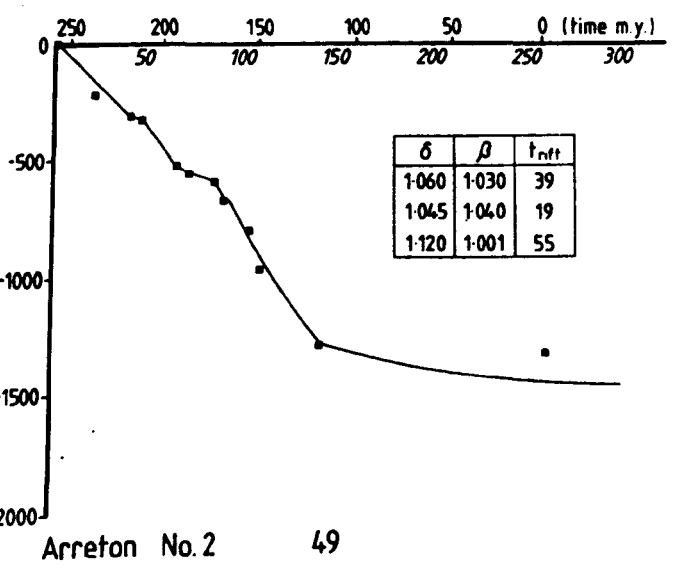
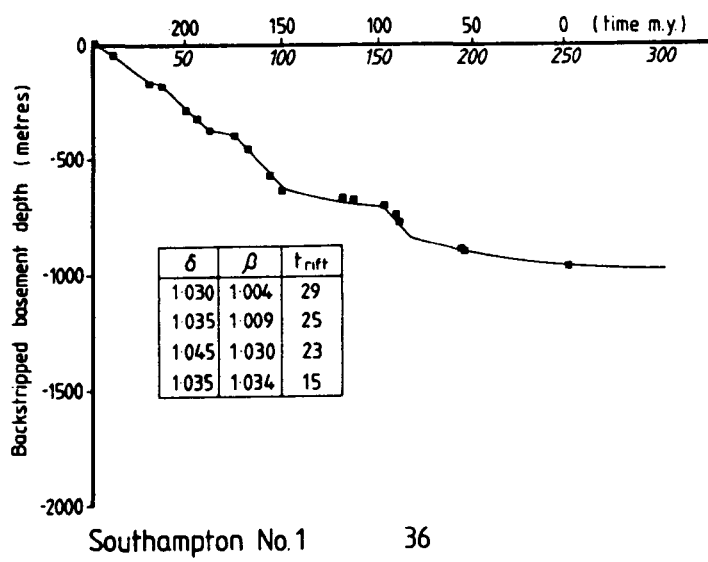
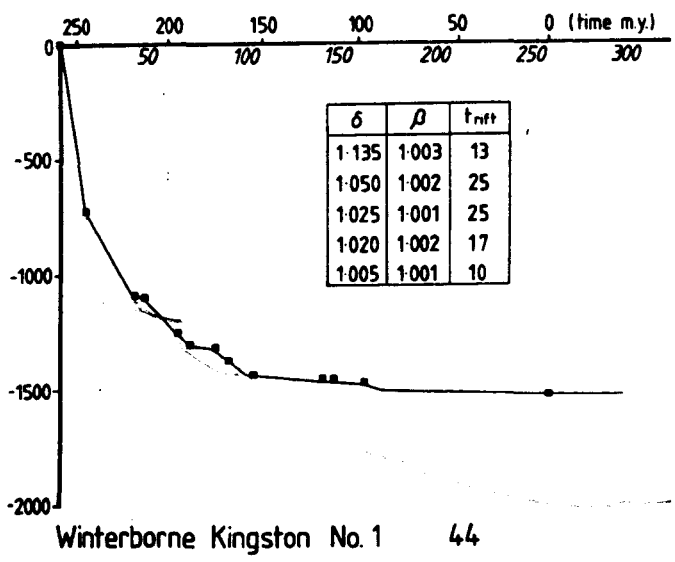
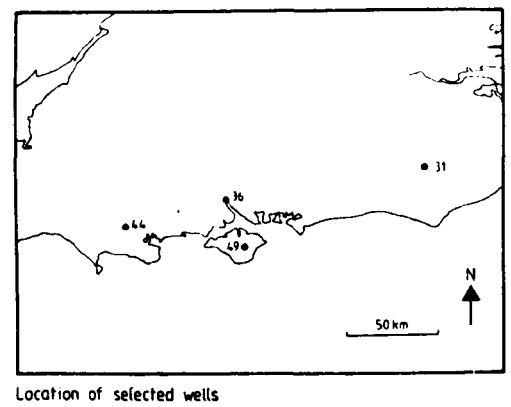
	BOREHOLE NAME	N.G.R	DEPTH TO BASEMENT (METRES)	BETA	DELTA	FINITE RIFTIN (M.Y)
1	FARINGDON 1	SU324 947	655	1.06	1.06	38
2	COOLES FARM 1	SU018 929	1205	1.05	1.12	79
3	HIGHWORTH 1	SU183 915	1065	1.00	1.09	74
4	WILLESSEN 1	TQ21 83	817	1.04	1.03	24.5
5	SONNINGEYE 1	SU742 759	413	1.05	1.03	91
6	CLIFFE 1	TQ74 76	324	1.05	1.03	30.5
7	HERNE 1	TR18 67	362	1.00	1.03	48
8	BOBBING 1	TQ89 65	384	1.00	1.03	50
9	KINGSCLERE 1	SU499 589	1873	1.05	1.14	130
10	ULSTER DEVIZES 1	ST960 570	946	1.05	1.07	55
11	WARLINGHAM 1	TQ348 572	1373	1.10	1.12	128
12	TATSFIELD 1	TQ41 57	1405	1.05	1.08	69
13	STRAT A1	SU948 528	963	1.05	1.07	148
14	HARMANSOLE 1	TR14 52	527	1.02	1.02	19
15	LYDDEN VALLEY 1	TR37 53	618	1.00?	1.01	6
16	BURTON ROW 1	ST336 521	1105+ (P)	1.00	1.04	58
17	SELWORTHY 1	SS924 462	60	1.01	1.01	25
18	SHALFORD 1	SU989 471	1641	1.02	1.15	50
19	BLETCHINGLY 1	TQ362 477	1910	1.05	1.15	75
20	COLLENDEAN FM 1	TQ248 443	1755	1.05	1.17	75
21	COWDEN 1	TQ467 428	1646 ?	1.05	1.14	81
22	ELHAM 1	TR18 44	487	1.05	1.04	25
23	WESTBURY 1	SU872 429	616+ (T)	1.05	1.11	19
24	SHREWTON 1	SU031 420	1601	1.10	1.15	108
25	PURITON 1	ST319 489	600+ (P)	1.04	1.05	55
26	BRABOURNE 1	TR100 308	627	1.00	1.05	62
27	FOLKESTONE 1	TR23 37	453	1.05	1.04	6
28	BRUTON 1	ST690 328	293	1.00	1.03	25
29	FARLEY SOUTH 1	SU236 285	1679	1.075	1.14	88
30	LOCKERLEY 1	SU307 259	2050 ?	1.10	1.17	93
★ 31	ASHDOWN 2	TQ512 295	1230+ (T)	1.03	1.17	75
32	BOLNEY 1	TQ280 243	2439	1.05	1.16	75
33	BRIGHTLING 1	TQ685 210	1322	1.05	1.11	63
34	HENFIELD 1	TQ182 151	1556	1.06	1.13	75
★ 35	FORDINGBRIDGE 1	SU188 118	1368+ (T)	1.02	1.12	167
★ 36	SOUTHAMPTON 1	SU416 120	1827	1.08	1.15	98
★ 37	MARCHWOOD 1	SU399 112	1725	1.08	1.15	92
38	CRANBOURNE 1	SU034 071	1663	1.075	1.12	87
39	PORTSDOWN 1	SU638 078	1998	1.17	1.18	98
40	WESTHAM 1	TQ610 054	887+ (P)	1.025	1.07	81
41	SEABOROUGH 1	ST435 062	1555	1.10	1.14	39
★ 42	MIDDLETON 1	SU973 015	1607 ?	1.06	1.14	108
43	MARSHWOOD 1	SY389 988	1339 ?	1.04	1.13	67
★ 44	WINTERBORNE KINGSTON 1	SY847 980	3043+ (P)	1.01	1.25	39
★ 45	BERE REGIS 1	SY864 956	1686+ (T)	1.12	1.25	20
★ 46	NETTLECOMBE 1	SY505 954	1910	1.00	1.17	39
★ 47	STOBOROUGH 1	SY913 870	1230+ (T)	1.04	1.24	39
★ 48	WYTFARM D5	SY996 855	2703	1.07	1.23	39
★ 49	ARRETON 1	SZ532 858	2423	1.07	1.24	139
50	BH 98/22-1	50° 14' 39" N 01° 39' 22" W	726+ (T)	1.04	1.07	79

Table 2.1 Resultant β (Beta) and δ (Delta) values for all the backstripped boreholes using finite rerifting plots.

tectonic control. Geologically, the rapid phases correspond with the development of a clay facies, whereas during the return to the slow, smooth subsidence (termed thermal) phase, a regressive facies is developed. As extension may feasibly occur as either a single event, or the cumulative effect of repeated events, we interpret Wessex Basin subsidence as the result of polyphase extension, the subsidence of which consists of a general "background" thermal subsidence, reflecting the extension of the sub-crustal lithosphere, punctuated by a rapid, rift-induced subsidence, reflecting extension of the crust.

The calculation of the rift (or mechanical) and thermal subsidence of the lithosphere due to its finite re-rifting is complicated, not only by the fact that the crust/lithosphere thickness ratio is constantly changing with time, but the residual temperature perturbation from the preceeding rifting event influences the next event. By extending the formulation by Cochran (1983), we have calculated the finite, re-rifting subsidence history for a number of Wessex Basin wells (in particular, those for which $\delta < \beta$, marked by stars in Table 2.1, and which incidentally represent the main depocentres) using the clay facies within the basin as an indicator of rift-onset and length (Table 2.1; Fig. 2.26). In all cases, the resultant β was significantly less than δ (e.g. Fig. 2.26; average δ and β for the starred wells of Table 2.1 is 1.19 and 1.05 respectively) suggesting that much of the subsidence within the Wessex Basin is occurring during prolonged periods of crustal rifting and within the depocentres. We have included the renewed subsidence event at 100 Ma even though the driving subsidence is probably independent of extension. The upper Cretaceous is characterised by inversion tectonics in which depocentres are inverted into structural highs while structural highs

Fig. 2.26 Four selected wells - polypphase finite rifting (i.e. $\partial/\partial t$)
Deltas and betas and finite rifting duration for each extension event are shown.



become depocentres. The Southampton (well no. 36, Fig. 2.26) region, in particular, has been involved in Laramide transpression along the Purbeck-Isle of Wight fault. The general variability between rift-length times and magnitude across the basin tends to confirm basin subsidence as being induced by brittle extension of the upper crust. Delta factors therefore, are a function of sediment accumulation following hanging wall collapse of the basement and characterise the total amount of stretching within the crust, while beta factors are indicative of the total amount of heat added to the sub-crustal lithosphere during polyphase rifting.

It would appear that the relaying of extension above and below the intracrustal detachment within the Wessex Basin has produced an apparent strain incompatibility since brittle failure (the average δ over the basin) is greater than the ductile extension (the average β over the basin). However, as suggested by Wernicke (1985), upper-crustal extension is balanced by lower crust/sub-crustal lithospheric extension, partly within, and partly external, to the region. To balance the measured lithospheric extension within the Wessex Basin requires a 5% extension of the sub-crustal lithosphere beneath the Armorican Massif, in turn inducing a cumulative 60m isostatic uplift over the past 100 m.y.

Watts et al., (1982) have demonstrated that the thermal, and hence the mechanical, recovery of rifted lithosphere predicts a stratigraphic basement onlap. Given that lithospheric stretching is minimal within the Wessex Basin (i.e. $\beta < 1.05$), the fact that major transgression has apparently occurred onto the London-Brabant platform from Permian to Cretaceous (Worssam and Ivimey-Cook, 1971; Anderton et al., 1979; Allsop et al., 1982; Dewey, 1982) is problematic. Further, a marine transgression also occurred during the Palaeogene (Arkell, 1947, pg.

216). To investigate the possible flexural control on Wessex Basin stratigraphy, (Fig. 2.27) and in particular, if the observed stretching history of the basin could account for the observed onlap patterns, we have forward modelled the late Palaeozoic-lower Mesozoic development of the Wessex Basin (i.e. excluding the inversion-induced subsidence) using the magnitude and distribution of stretching parameters summarised in Table 2.1. For comparison, we assembled a north-south cross-section across the Winterborne-Kingston Trough (Fig. 2.20), removing the complications introduced by inversion. By equating the depth to the 450°C isotherm (in space and time) with the effective elastic thickness of the lithosphere, it is possible to monitor the thermo-mechanical history of the lithosphere. When this history is linked to the theoretical equations for basin subsidence (e.g. McKenzie, 1978; Royden and Keen, 1980), the two-dimensional development history of the basin can be modelled as outlined by Watts et al., (1982). We have also included the eustatic sea-level curve of Pitman (1978) calibrated to a maximum variation of 150 metres. As can be seen from figure 2.28, no basement onlap occurs (the restriction of the modelled 10 m.y. old sediments is an artifact of assuming instantaneous rifting), consistent with the observed section in figure 2.28, and is a re-statement of Steckler (1983) and Kusznir and Karner (1985) that sub-crustal lithospheric heating, and hence rigidity resetting, is minimal until $\beta > 2$. The modelling suggests however, that the basin width should be 350-450 km wide and is a direct consequence of the large (essentially pre-rifting) flexural rigidity of the lithosphere ($T_e = 40$ km) and is consistent with the fact that the Wessex Basin was at its greatest extent in the upper Cretaceous. The reduced present-day distribution of the basin implies a large amount of

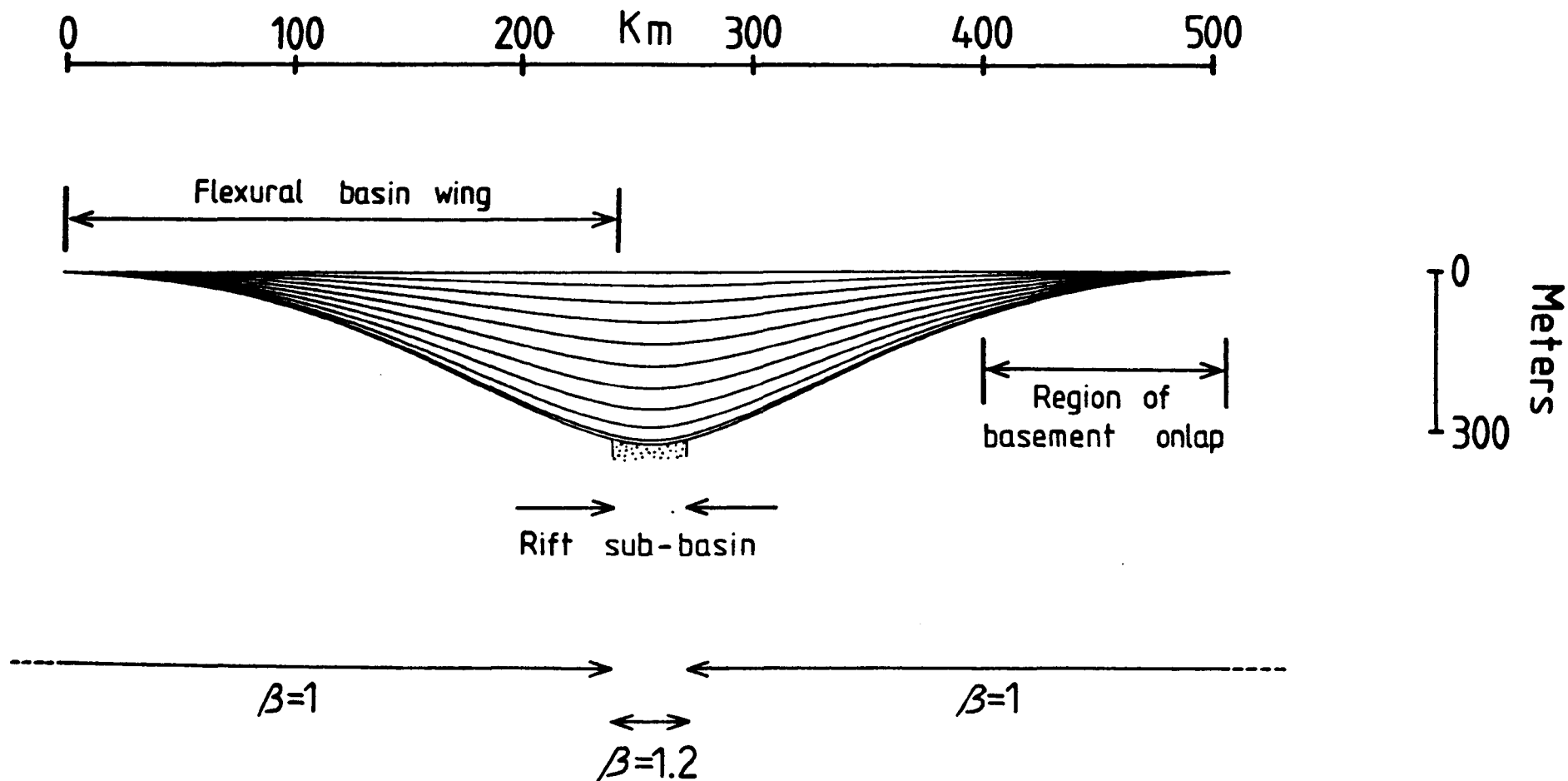
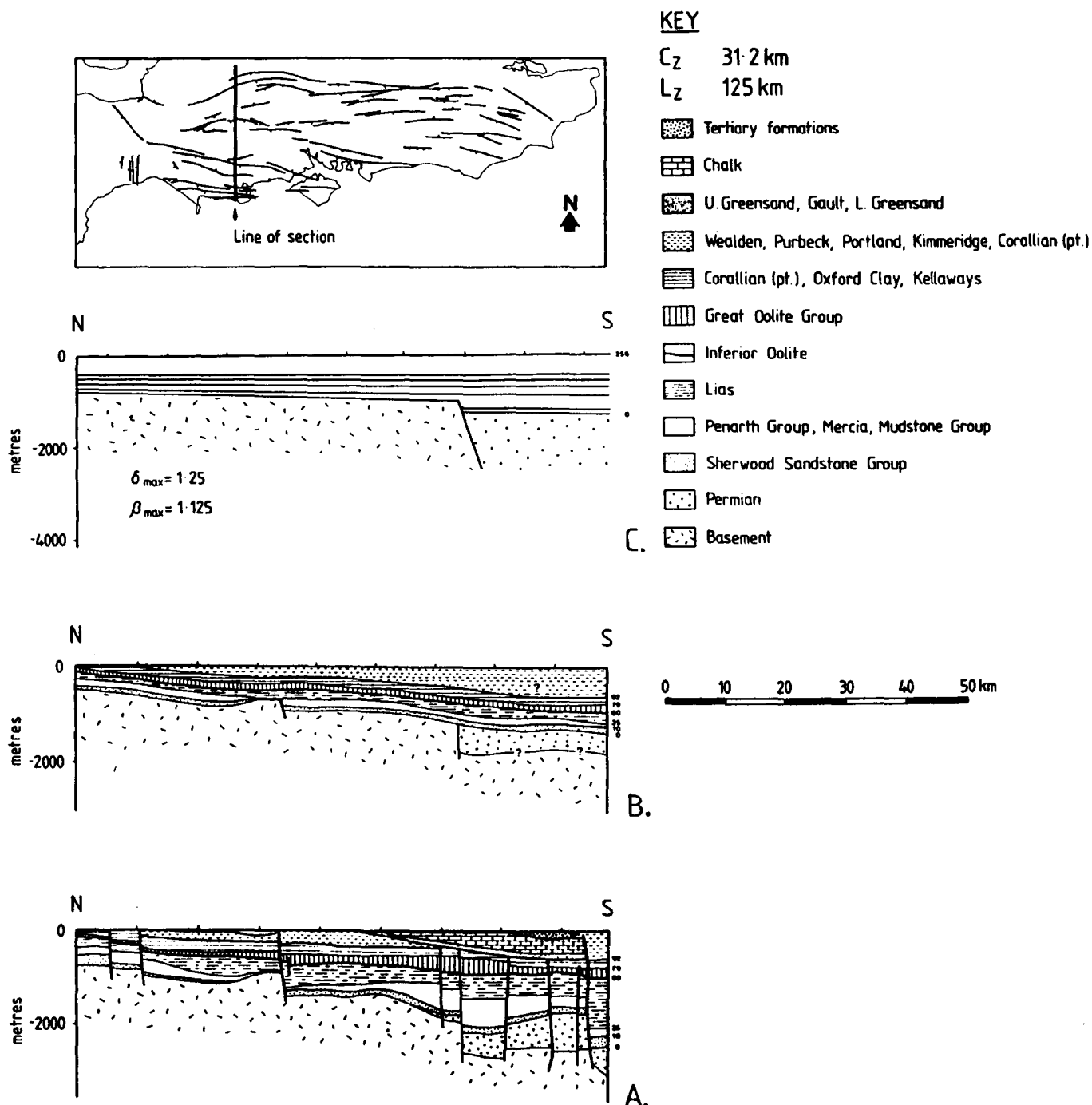


Fig. 2.27 Calculated flexural-phase stratigraphy of a theoretical sedimentary basin in which the thermal and mechanical properties of the lithosphere are integrated with the McKenzie stretching model. Maximum stretching is 20% and predicts a 300 metre deep basin, 400-500 km wide. Marginal onlap is a direct consequence of an increasing T_e (elastic thickness) with time since rifting. The rapid onlap in this model reflects the failure of β to appreciably reset the temperature structure of the lithosphere.

Fig. 2.28 North-south transect across the Wessex Basin using data from Whittaker (1985).

- Present-day observed structural configuration.
- Removal of inversion effects and thrust reactivation from section A to compare to forward modelled examples of the development.
- Forward modelling of the late Palaeozoic/lower Mesozoic development of the Wessex Basin using the magnetitude and distribution of stretching parameters on Table 2.1.



post-Cretaceous erosion. Further, much of the subsidence in the basin periphery appears to be flexurally induced by the driving subsidence and sediment loading in the main depocentres, thereby explaining the very low extension values ($\delta < 1.05$) observed on the London-Brabant Platform. Including a eustatic sea-level curve in the basin modelling produces a basin-wide transgression/regression between 92-256 m.y. after rifting (i.e. syn-post Jurassic). Though not explicitly modelled, it is possible that the Jurassic clay/sandstone/limestone cyclicity of the Wessex Basin may represent the interplay between the rates of change in sea-level (including sediment loading and supply) and the rift-induced mechanical subsidence. The next section analyses the cyclicity in more detail and is followed by a discussion on the Tertiary cyclicity in more detail.

1. Cyclicity

A. Introduction

The Late Palaeozoic to Cenozoic stratigraphic succession in the Wessex basin comprises a number of cycles. The nature of this repetition can be distinguished at a variety of scales. The most significant cycles have been recognised within the Jurassic (Arkell, 1933; Hallam, 1964; Hallam, 1978 etc.) whereby the succession is divisible into a number of major clay/silt/sand/limestone sequences reflecting general shallowing and regression. A detailed review of the recorded cyclicity within the basin is clearly beyond the scope of this thesis, however it is salient to draw attention to some major cyclic sequences, then outline their possible causes.

The Permo-Triassic sequence throughout the region is dominated by large scale clay/sandstone cyclicity (Fig. 2.29) in the order of 10-20 my. duration. Intermediate scale cyclicity has been identified by Jeans (1978) within the Mercia Mudstone Group, whilst Lott & Strong (1982) have recorded smaller fining upward fluvial cycles up to 3 metres thick within the Sherwood Sandstone Group in the Winterborne Kingston borehole.

The Liassic sequence at the base of the Jurassic is characterized by small scale, strikingly regular alternations of limestone and shale bands, with each cycle averaging less than 1m in thickness (see Hallam, 1964; Sellwood, 1970). Whilst some larger clay/sandstone/limestone cycles in the Middle Lias along the Dorset coast tend to amalgamate inland in the Ilchester area (N.G.R. ST 520 230) into one single sandstone unit. Knox et al., (1982) have recognized at least three major

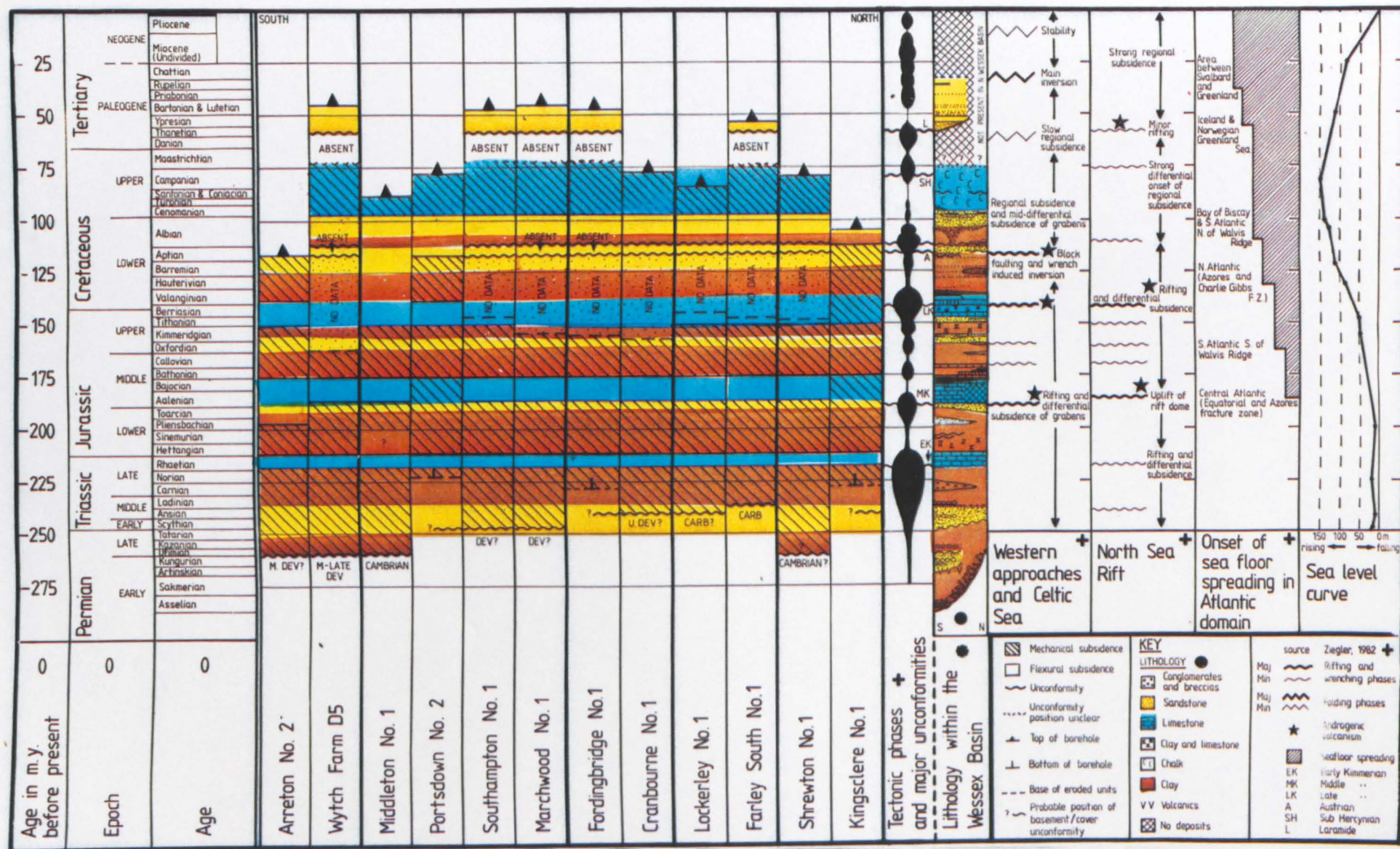


Fig. 2.29 The geologic correlation between polyphase extension events in a north-south transect across the Wessex Basin from borehole data to the large scale clay/sandstone/limestone cyclicity, and their correlation to tectonic events elsewhere.

coarsening upward cycles each terminating in a hiatus and overlain by the basal limestone unit of the following cycle within the Toarcian Bridport sands in the Winterborne borehole. Further up the succession Sellwood et al., (1985) have recognized cyclicity within the Great Oolite Limestone Formation from confidential borehole data in the Weald Basin. At least four major cycles are recorded within the Corallian Beds (Oxfordian) according to Talbot (1973) along the Dorset coast, whilst inland Wright (1981) has recognized possibly up to nine cycles in the same succession. The overlying Kimmeridge clay displays at least two differing small scale rhythms approximately 1 metre apart (Cox and Gallois, 1981). Townson (1975) identified two transgression and three regression cycles within an overall regression in the Portland group. Lake (1982) recognized at least three types of small scale rhythms within the Middle Purbeck sequence, some clearly equate with the faunicycles identified by Anderson & Bazley (1971) using ostracod faunas.

The succeeding Tertiary sequences are dominated by a series of cycles of variable duration (see Anderton et al., 1979; Plint, 1983). The causes for repetitive sedimentation can relate to at least one of four causes, or a mixture of them. These include sedimentary, climatic, tectonic and eustatic controls and the interaction between them.

B. Sedimentary Cyclicity

Cyclicity is a direct consequence of the depositional environment, cannot easily be distinguished from the other three types. In addition this type of cyclicity is usually applied to deltaic flood plain or turbiditic sequences. This type of cyclicity therefore may be developed within the Permo-Triassic or lower Cretaceous (Wealden) sequences but has

yet to be fully recognized.

C. Climatic Cyclicity

Climatic cyclicity may be the primary cause for many widely differing types of cycle (Hollingworth, 1962). Perhaps the most widely known type of climatic cyclicity is that associated with glaciations causing oscillations of sea level due to the advance and retreat of ice caps during alternating glacial and interglacial intervals (this is dealt with more appropriately in the section on eustatic control). More seasonal climatic variations are displayed in more lacustrine varve deposits or fossil tree-growth rings, the latter has been investigated by Francis (1984) in the Lower Purbecks of Dorset. Small scale layering is well exhibited within the Lias and Kimmeridge Clay although a seasonal cause has yet to be proved. Longer period cycles may also be invoked to explain microrhythms (House, 1985), although their periodic effect on sedimentation and climate has yet to be understood. Hays et al., (1976) first showed that spectral analysis of the climatic records observed in deep sea sediments revealed concentrations of variance at orbital frequencies and that orbital components such as precession, eccentricity, and tilt have variable controls on portions of the climatic system. Three major astronomical cycles have been identified, 100 kyr, 41 kyr and 23 kyr (Hays et al., 1976; Pisias and Shackleton, 1984). The first relates to changes in the eccentricity of the orbit (Hays et al., 1976) and the last is a precession effect. Attention, however, is drawn to the 41 kyr oscillation resulting from the obliquity of the ecliptic (Pisias & Shackleton, 1984). This has been shown by House (1985) to approximately coincide with sedimentary microrhythms observed within the Blue Lias and

the Kimmeridge Clay of Dorset (approximately 41 kyr). The characteristic limestone/clay cycles (Plate 2.1) within the Blue Lias have long attracted debate. A primary and secondary origin can be demonstrated throughout the sequence. Evidence for a primary origin is suggested by (1) variations in faunal content between the limestone and clay units; (2) burrows affecting both lithologies; (3) limestone units of great lateral extent and regularity; and (4) microlamina confined largely to shales and laminated limestones, in contrast to normal limestones. Evidence for a secondary origin is suggested by: (1) the fauna are better preserved in limestones in contrast to shales; (2) upper and lower limestone contacts are ²two irregular to be primary; (3) some limestones pass laterally into shales (not purely as a function of lateral facies variations); (4) local inverse of limestone cementation in the vicinity of large fossils; and (5) limestone units generally increase in thickness with an increase in Blue Lias thickness (c.f. Hallam, 1975). It is not clear whether House (1985) took these into account when he was relating the Lias cyclicity to orbited ^cforming mechanisms. Since ascribing the cyclicity to orbital forcing mechanisms must remove secondary induced cycles. This was shown by defining the duration of the Jurassic in Myr, subdividing the Jurassic into ammonite zones (assuming that zones or subzones are equal in duration, as a first order approximation), calculating the possible duration of each zone in Myr, determining the number of rhythms within each sequence length, and comparing the results with the cyclicity resulting from orbital forcing.

This technique was applied to the Bridport sands on the Dorset coast (N.G.R. SY 470 849). Dark grey siltstones are locally observed at the base of East Cliff these bear remarkable lithological similarities to the

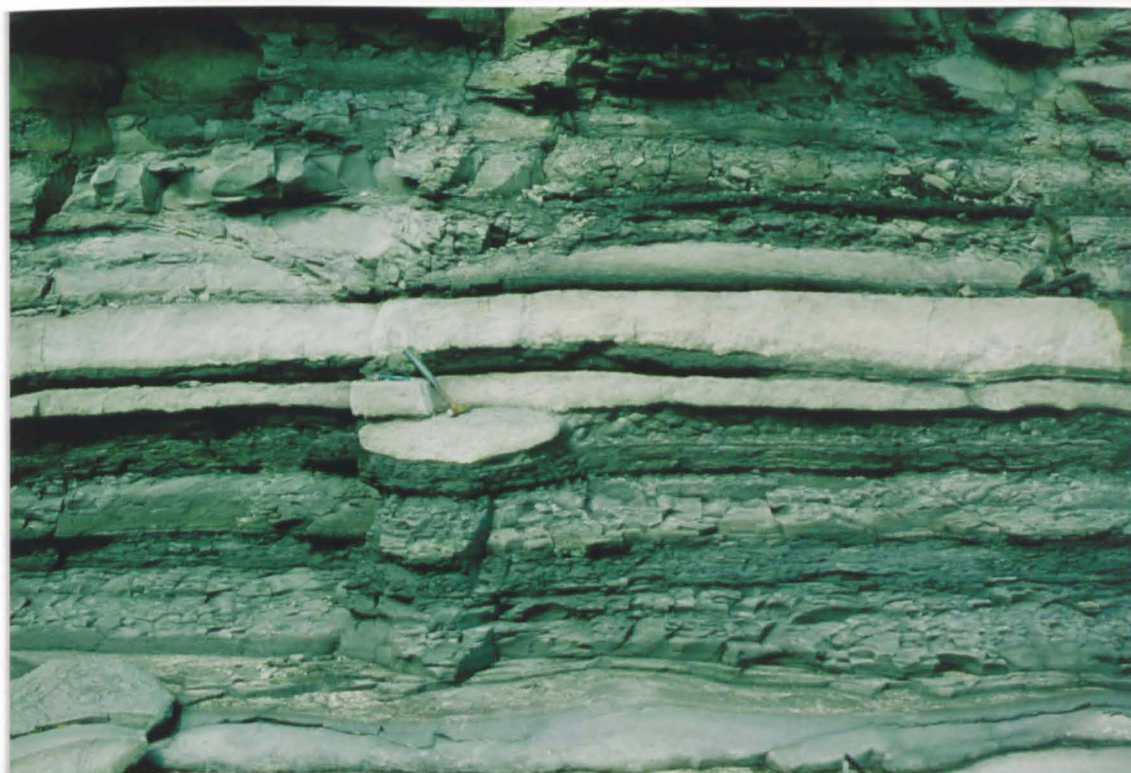


Plate 2.1 A view of the limestone/clay cyclicity at Lyme Regis (N.G.R. SY 328 909). The limestone nodule clearly is secondary in origin (post-compactional). These structures have been called by House (1985) 'Microrhythms', and are discussed more fully in Chapter 2. The microrhythms comprise laminated, dark, organic rich shale followed by lighter coloured calcareous shales and bioturbated limestone beds.

the underlying Down Cliff Clay. In addition the thickness of the outcropping Bridport Sands at East Cliff compares well with the total Bridport sand thickness measured by Cope et al., (1980), therefore the Bridport Sands succession is preserved at East Cliff is representative of the whole Bridport sand succession. Two subzones (Dumortieria Levesqui and moorei) comprise the whole Bridport Sands succession at Bridport (Davies, 1967), thus each subzone is approximately 0.25 my duration (0.5 my together). Figure II.5.5 displays the full Bridport Sand succession at East Cliff, where 24 cycles can be distinguished (excluding obvious secondary diagenetic units presumed to reflect post-depositional unmixing of CaCO_3 , which can in part be distinguished by their lateral discontinuity). Each rhythm approximates 21 kyr duration. Therefore perhaps the Bridport Sands succession displays evidence for the 23 kyr orbited precession cycle. The lateral extent of these small scale cycles (microrhythms) to subsurface borehole data within the basin cannot directly distinguish primary and secondary induced microrhythms without direct sampling and local three dimensional control to test their lateral extent.

Interestingly, Sandy (1985) has recently observed that the 39 faunacycles comprising alternating saline and freshwater tolerant ostracod assemblages identified originally by Anderson & Brazley (1971) within the Purbeck Beds may correlate with the 100 kyr cycle due to orbital forcing.

In conclusion microrhythms can be seen to correspond remarkably well to orbital forcing mechanisms. Such mechanisms are presumed to result in small climatic shifts at frequencies of 23 kyr, 41 kyr and 100 kyr (Pisias & Shackleton, 1984). However, assigning ^{cycle} dominated sequences to

orbited forcing is by no means unequivocal.

D. Tectonic and Eustatic Cyclicity

These are grouped together as it will be demonstrated that previously assumed eustatic control is related to tectonic causes. Tectonic control maybe demonstrated for example, within the Bridport Sands where 3 major cycles identified by Knox et al., (1982) in the Winterborne Kingston borehole cannot be identified a short distance away at Wytch Farm (see Colter & Havard, 1981). In the Corallian, Wright (1981) recognised up to 9 cycles inland compared to the 4 cycles within the sequence along the coast (Talbot, 1973). It is here suggested that such a rapid lateral variation in the sedimentary sequence reflects direct tectonic control. Sellwood et al., (1985) identified a series of cycles within the Great Oolite Limestone Formation prograding off the London-Brabant Platform. It is here suggested that the lateral extent of this carbonate ramp (almost confined solely to Weald and Vale of Pewsey Basins) and the progradation off a major Mesozoic high undoubtedly reflects a strong tectonic control although some of the cyclicity can be directly related to sea level fluctuation (see Chapter 2). Tectonic control of cyclicity can also be speculated for other times, for example Sinemurian & Pliensbachian (on the northern edge of the Mendips), Aalenian and Bajocian (Inferior Oolite), Tithonian (the Portland and Purbeck Beds), the Wealden (related to rejuvenated sourcelands) and the upper Cretaceous. The upper Cretaceous chalk facies is characterised by rhythmic bedding, lamination bedding, submarine erosion surfaces and current-piled banks, for example the rhythmic variation in the clay content in the chalk-marl facies of the Cenomanian (Hancock, 1975) may relate to orbital forcing mechanisms. However the detailed stratigraphy

of the Cenomanian and basal Turonian between Brancombe and Seaton in southeast Devon described by Jarvis & Woodroof (1984) have shown massive thickness variations across postulated active upper Cretaceous faults. It is suggested here that although some hardgrounds marking the top of individual formations are laterally extensive some hardgrounds thicken towards the faults and are only locally developed implying some tectonic control on the resulting observed cyclicity (c.f. Jarvis & Woodroof, 1984, their Figs 2 and 4).

Eustatic changes pertain to relative or absolute worldwide changes of sea level that affect all the oceans (Mitchum, 1977). Hays & Pitman (1973) were the first to demonstrate that the worldwide middle to upper Cretaceous sea level peak corresponded to a pulse of rapid spreading at mid-oceanic ridges.

Vail et al., (1977) in AAPG Memoir 26 recognised a series of cycles which they calibrated onto global sea level curve (Pitman, 1978) by measuring the duration and magnitudes of transgressions and regressions using seismic stratigraphy from different areas of the world. Three orders of cycles were recognized by Vail et al (1977). The first order cycle (durations of 200-300 Ma) was calibrated to the global sea level curve of Pitman (1978) ^{as} ~~is~~ determined by changes in mid-ocean ridge crest volumes. Second order cycles of 10-80 Ma in duration and third order cycles which span 1-10 Ma are of most interest because of their strong tectonic control outlined briefly in the following section. The second and third order cycles display slow increases in relative sea level followed by periods of rapid falls. The rate of fall has attracted considerable debate (e.g. Hallam, 1978, 1981) because Vail et al., (1977) erroneously equated relative changes of coastal onlap with relative

changes in sea level. It has since been shown that long term coastal onlap (50-100 my) observed along passive margins and intracratonic basins is a direct consequence of the heating of the lithosphere following rifting and subsequent cooling (Watts, 1982; Watts et al., 1982). Therefore although Vail et al., (1977) observed widespread patterns of onlap, the synchronous rifting at widely separated passive margins would incorrectly identify apparently corresponding eustatic events (Watts, 1982) consequently the second order cycles (supercycles) of Vail et al., (1977) are largely related to the cooling and hence mechanical recovery of the lithosphere following rifting (Karner, in prep.). The third order cycles span 1 to 10 My and represent one rise and fall in sea level. Such apparent sea level fluctuations on this scale and some supposed rapid falls on the second order scale cannot be adequately explained as a consequence of cooling and therefore mechanical recovery of the lithosphere following rifting (Watts, 1982). Such rapid rates of global sea level changes can only be attributed to glaciations such as the Eocene/Oligocene unconformity (Matthews, 1984) and those observed throughout the Quaternary. However, earlier rapid global fluctuations must be attributable to other causes. A tectonic mechanism has been proposed to explain those changes (Cloetingh et al., 1985; Karner, in prep.). These authors have shown that changes in intraplate lateral stress resulting from plate boundary reconfigurations (compressional and extensional settings) occur at geological time scales comparable to Vail's short term variations in relative sea level. Thus, for example, Karner (in press) has shown that compression will result in basin margin uplift thereby inducing a regressive cycle, the amplification of which is a function of basin subsidence and basin

wavelength.

In conclusion the short and long wavelength cycles determined by Vail et al., (1977), presumed to reflect eustatic changes of sea level, can be quantified and shown to be the result of changing mid oceanic ridge volume, the tectonic development of passive margins and intracratonic basins, and changes in intraplate lateral stress as a direct result of plate boundary reconfigurations. Therefore a re-evaluation of the observed Jurassic cyclicity outlined is applied to these recently developed models.

E. Discussion

It has already been briefly discussed that the Jurassic comprises a clay/sand/limestone cyclicity. Most of these cycles appear regressive (Sellwood, 1970; Talbot, 1973; Sellwood & Jenkyns, 1975), hence Hallam (1978) smoothed off the supposed rapid regressive events of Vail et al., (1977) in the Jurassic. Major regressive cyclicity is still observed whether one considers the limestones to mark the culmination (Sellwood & Jenkyns, 1975) or the base of each cycle (Talbot, 1973). Table 2.3 summarizes the transgressive and regressive events determined from the chrono lithostratigraphic chart on figure II.2.1 and compares them to regional events taken from Vail et al., (1977) global sea level curve. Clearly many of these larger cycles correlate to the previously presumed global eustatic sea level variations, such as the upper Jurassic regressive phase, and, as such, equate with Vail's second(?) and third order cycles (Table 2.3). Whilst the timing of events is synchronous with Vail et al's curves, one fundamental difference does occur, although no explanation can as yet be offered why; this difference is seen in the

ERA	SUB-ERA	EPOCH	AGE	M.A AGE	LITHOSTRATIGRAPHIC FORMATIONS	THIS THESES	HALLAM 1978	REGIONAL	SMALL CYCLES	
CENOZOIC	QUATERNARY									
	NEOGENE	PLIOCENE		2.0						
		MIOCENE		5.1					T	
	PALAEO- GENE	OLIGOCENE		24.6	Hamstead Beds	T			T	
		Eocene		38.0	Berbridge, Solent, Barton, Bracklesham Groups and London Clay	Tx6				PLINT (1983)
		PALAEOCENE		54.9	Reading Beds	T			R	
				65.0						
	UPPER CRETACEOUS	SENONIAN	Maastrichtian	73.0	Upper Chalk				T	HANCOCK (1975) BROMLEY & GALE (1982)
			Campanian	83.0						
			Santonian	87.5						
			Coniacian	88.5						
			Turonian	91.0	Middle Chalk					
			Cenomanian	97.5	Lower Chalk	T			T	
	LOWER CRETACEOUS		Albian	113.0	Upper Greensand and Gault	R				
			Aptian	119.0	Lower Greensand	T				
			Barremian	125.0	Wealden				T	
		Hauterivian	131.0	?						
		Valanginian	138.0				T			
		Berriasian	144.0							
JURASSIC	MALM	Tithonian	150.0	Purbeck Beds	many R	R		R	SANDY (1956) LAKE (1982) TOWNSON (1983) COX & GALE (1981)	
		Kimmeridgian	156.0	Portland Group Kimmeridge Clay	many T	T				
		Oxfordian	163.0	Corallian Beds Oxford Clay and Kellaways Beds	many T	many T		T		
		Callovian	169.0		T	T				
	DOGGER	Bathonian	175.0	Great Oolite Series	Rx3	Tx3		T		
		Bajocian	181.0	Inferior Oolite	T R	T R		T R		
		Aalenian	188.0							
		Toarcian	194.0	Upper Lias	T	T		T	KNOX et al. (1982)	
	LIAS	Piensbachian	200.0	Middle Lias	TRTR	TRTR				
		Sinemurian	206.0	Lower Lias	R T R	R T R			HOUSE (1985) HALLAM (1964)	
		Hettangian	213.0					T		
			219.0	Rhaetic	T			T		
	TRIASSIC	UPPER	Norian	225.0	Upper Keuper					
			Carnian	231.0						
			Ladinian	238.0	Lower Keuper (Keuper Marl, Waterstones) Upper Bunter (Bunter s/st, L. Keuper s/st)	T			T	
		MIDDLE	Anisian	243.0						
			SCYTHIAN	Spathian					?	
				Smithian						
				Dienerian		Lower and Middle Bunter (Budleigh Salterton Pebble Beds and Aylesbeare Group in part)	R			
Griesbachian										
PERMIAN	LATE	Tatarian	248.0	(Aylesbeare Group in part local sands, mudstones and breccias)				R		
		Kazanian	253.0							
		Ufimian	258.0							
		Kungurian	263.0							
		Artinskian	268.0							
		Sakmarian								
	EARLY	Asselian	286.0							
			BASEMENT			1	2	3	4	

Table 2.3 Wessex Basin cyclicity from the Permian-Present day compared to the regional cycles of Vail et al., (1977).
T = transgressions and R = regressions.

gradual transgressions and rapid regressions of the Vail curve, whereas the Wessex Basin is dominated by rapid transgressions and gradual regressions.

Detailed examination of the lithological and tectonic development of the Wessex Basin clearly shows that phases of rapid extension associated with rifting events correspond largely to clay and sandstone facies, whilst periods of tectonic quiescence correspond to the major limestone units. These tectonic events in turn clearly correlate with other synchronous rifting events, for example in the North Sea and Western Approaches Basins. Plint (1983) argued for a eustatic control in the Tertiary because of the synchronicity of five relatively major sedimentary cycles within the Hampshire Basin to those determined by Vail et al., (1977) (Table 2.3). Applying the arguments outlined above, such apparent eustatic variations are induced by regional plate reconfigurations and perhaps more local transgression and regressions reflect the pulsatory uplift of the inverting Channel Basin during the Tertiary (see Chapter 3).

In conclusion it can be shown that cycles at various scales can be distinguished. Seasonal rhythms may locally be distinguishable from varve preservation in the Lias and Kimmeridge Clay formation or in tree growth rings. Microrhythms of variable duration seemingly reflect orbital forcing phenomena resulting in a cyclicity of 23, 41 and or 100 kyr. These cycles are well displayed in the Lias and Kimmeridge clay (House, 1985), the Purbeck Beds (Sandy, 1985) and perhaps explain the observed microrhythms in the Bridport Sands. Tectonically induced rhythms are clearly displayed in the Corallian (Wright, 1981) whilst the tectonic component overprinted on the earlier assumed global eustatic sea level

curve of Vail et al., (1977) can be distinguished throughout the sedimentary sequence. The resulting tectonic development both within the basin and the surrounding area strongly influenced the lithological and facies development from the late Palaeozoic to Present day. First order cyclicity induced by changing mid oceanic ridge volumes cannot be ascertained except for the global peak in sea level which is coincident with the greatest areal extent of the Wessex Basin (upper Cretaceous) and peak palaeowater depth.

Finally, intergration of intrabasinal cyclicity with plate tectonic reconfigurations and stress prediction will undoubtedly become a valuable exploration tool in the future.

On the cessation of polyphase rifting in the lower Cretaceous (c.f. Table 2.4), the ensuing thermal subsidence will allow a check on the amount of residual heat dissipated from the sub-crustal lithosphere. If basin width continues to increase in the Tertiary, even during a major sea-level regression, it is most likely the result of continuing thermal subsidence and its associated flexural effects. The Tertiary outcrop of the Wessex Basin (Fig. 2.30) shows a general regressive sequence (and is not simply the result of erosion because each of the Tertiary units are in a proximal environment). Detailed analysis of the facies within these units has shown that they represent onlap and offlap patterns (Fig. 2.30), and correlate remarkably well with the timing of transgressive/regressive cycles of the Vail et al., (1977) curve (Fig. 2.30). It would appear therefore, that as the Tertiary stratigraphy is dominated by the second order effects in eustasy, thermal subsidence had been rendered negligible in approximately 35 m.y., consistent with the low B's estimated from the backstripped wells (c.f. Table 2.1).

Conclusions

From the thermal and mechanical development of the Wessex Basin outlined above, the following conclusions can be made:

- 1) The detailed structure of the Channel and Western Approaches Basins, Cherbourg and Hampshire-Dieppe Highs have been described. The geometry of the Channel Basin clearly reflects a pull apart origin along northwest-southeast trends.
- 2) East-west dipping reflectors in Lyme Bay imaged on seismic reflection data are interpreted as normally reactivated Variscan thrusts controlling the location and geometry of the subsequent

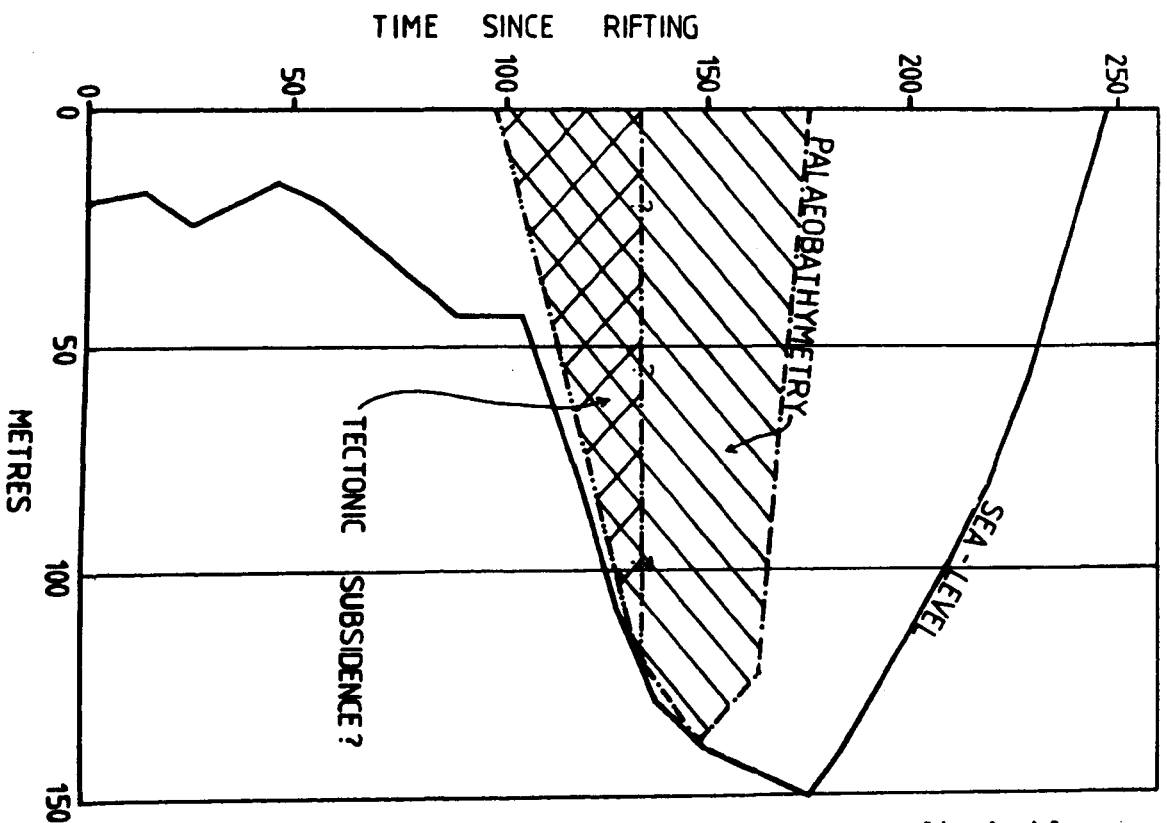
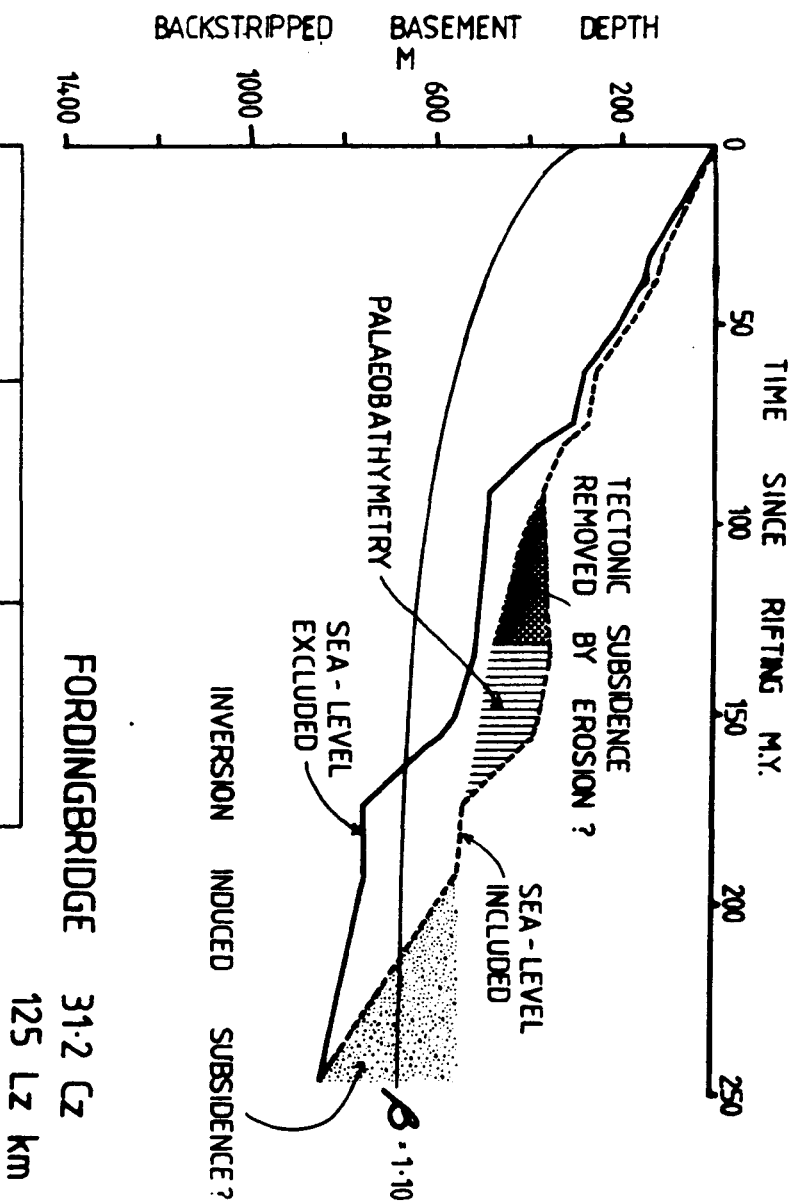
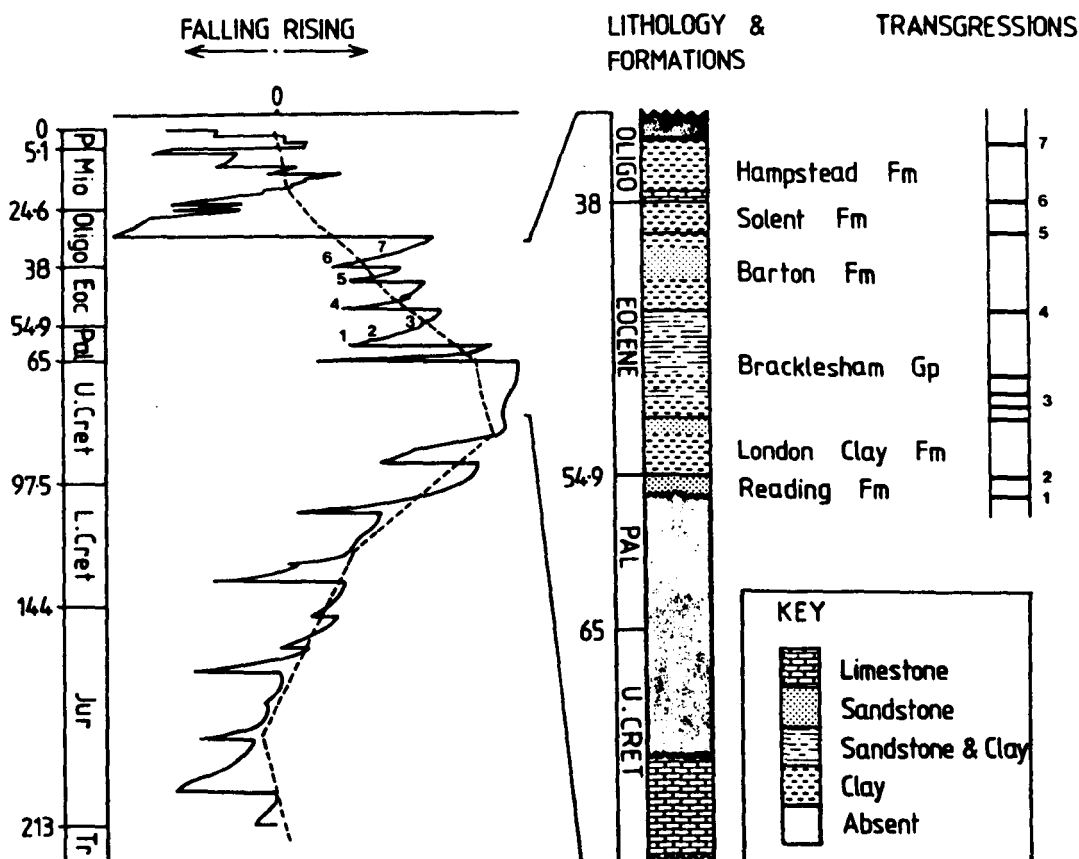


Table 2.4 Example sea-level correction for the Fordingbridge borehole. Removal of the apparent rift related subsidence (160-170 m.y. after rifting, upper Cretaceous) can be achieved with palaeobathymetry correction of Hancock (1975). Alternatively inversion induced subsidence may also account for both the upper Cretaceous and Tertiary rapid subsidence. (Sea level correction modified from Pitman, 1978 with a sea level maximum of 150 m). Tectonic subsidence assumed to account for the absent lower Cretaceous sedimentary section which was subsequently removed by the Aptian/Albian unconformity.





(b) Relative sea-level variations estimated by Vail et al., (1977), Solid and Pitman (1978), dotted, compared with the Tertiary onlap and offlap patterns of the Wessex Basin. Numbered transgressions observed in the Vail et al., (1977) curve can be directly compared with the observed transgressional phases in the basin. Transgressions from Anderton et al., (1979) and Plint (1983).

overlying depocentres, and represent the first documented example of such structures based on three dimensional seismic control.

- 3) The importance of both east-west and northwest-southeast reactivated Variscan structures on the structural configuration of the Wessex Basin is outlined.
- 4) The driving subsidence obtained from backstripped boreholes within the Wessex Basin was used to test the application of lithospheric stretching versus crustal extension for the post-Carboniferous development of southern England.
- 5) The fifty backstripped (to isolate the tectonic driving subsidence) boreholes clearly show a subsidence form not typically representative of a typical negative exponential subsidence predicted from the simple lithospheric stretching model.
- 6) Rifting migrates from west to the east from the Permian to the Jurassic.
- 7) The subsidence forms are more easily explained in terms of a polyphase rifting history with each renewed rifting event followed by little, if any, thermal subsidence (implying reduced heat input).
- 8) There is a lack of significant Moho topography between the basin and the surrounding massifs strongly suggesting that the upper and lower crusts are accommodating extension in a different way.
- 9) Areas of high sedimentation and therefore relatively high stretching is directly correlated with growth faults and hence regions of thrust fault reactivation. Therefore rift basin formation (or half graben generation) of varying geometry is controlled by structures within the underlying basement.

- 10) The degree of involvement of the sub-lithosphere during rifting is wavelength dependent and is necessarily regional (Karner & Dewey, 1986). Therefore crustal rifting may not be related to the extension of the sub-crustal lithosphere in a one to one fashion as required in the lithospheric stretching model.
- 11) The implication of the above arguments imply that whilst the estimation of δ (crustal stretching) represents the maximum observed subsidence, β is somewhat more problematical since it represents an estimate of the amount of heat introduced into the sub-crustal lithosphere during rifting. Finite rifting conductively removes lithospheric heat, accentuating the rift subsidence, whilst reducing the thermal subsidence and also relates more realistically to rift behaviour rather than the simple instantaneous rifting considered in the original McKenzie model.
- 12) Basement fault reactivation along a listric detachment is known to have played a fundamental role in basin development.
- 13) Therefore a more accurate determination of β was obtained by utilizing a lithospheric stretching model which included the effects of decollement relaying extension and finite rifting.
- 14) Depth dependent finite rifting predicted an essentially constant β across the basin significantly lower than the delta values obtained—previously, therefore lithospheric stretching does not apply to the Wessex Basin.
- 15) The resulting distribution of δ within the basin shows an apparent increase southwards towards the Channel sub-basin with local variations occurring in close proximity to growth faults (and hence mechanical basement thrusts), implying that block rotation



accompanying basement fault reactivation is primarily responsible for local basin subsidence.

- 16) However, much of the subsidence history within the basin as evidenced from backstripped wells is not simply a two phase process, rifting (finite or instantaneous), followed by the passive recovery of the lithosphere but indicates a general subsidence form punctuated by a number of rapid, but renewed finite subsidence events which are synchronous and basinwide superimposed on a general "background" thermal subsidence. These renewed extension events are characterized by major clay facies developments.
- 17) Where $\beta > \delta$ the ^ffinite rerifting subsidence histories were calculated and in all cases results in β being significantly less than δ , therefore implying reduced sub-crustal involvement. (average $\beta = 1.05$ $\delta = 1.19$).
- 18) The general variability in between rift length times and the magnitude across the basin tends to confirm the importance of upper crustal extension rather than wholesale lithospheric failure.
- 19) Delta factors characterise the total amount of crustal stretching and accord with the observed extension factors from fault geometries whilst the Beta factors characterise the total amount of heat added to the sub-crustal lithosphere during polyphase rifting.
- 20) The differing crustal and sub-crustal lithospheric involvement produced an apparent strain incompatibility, this is balanced by 5% sub-lithospheric extension beneath the Armorican Massif inducing a cumulative 60 m isostatic uplift over the past 100 my.
- 21) Forward modelling of the basin development in terms of $\delta > \beta$ suggests that no basement onlap occurs indicative of minimal sub-

crustal lithospheric heating and rigidity ^{derivation} resulting, with subsidence in the basin periphery being flexurally induced by the driving subsidence and sediment loading in the depocentres.

- 22) Sedimentary cyclicity has been recognised at all scales and ascribed to both climatic (orbital forcing phenomena) and tectonic causes. So called eustatic causes are re-evaluated in terms of an underlying tectonic control.
- 23) The direct relationship between Tertiary cyclicity and the timing of the second order effects in eustasy of Vail et al., (1977) implying that thermal subsidence and the associated flexural effects were negligible by that time.

CHAPTER 3

STRUCTURE, EVOLUTION AND INVERSION TECTONICS

3.1 Introduction

Basin studies are generally pre-occupied with only the initiating mechanism of sedimentary basins. Subsequent development is often considered only in terms of the passive thermal recovery of the rifted lithosphere. However, the development of many basins is often punctuated by either renewed subsidence or rapid uplift (i.e. inversion phases). Renewed subsidence owes its existence to rerifting or polyphase extension of the lithosphere while inversion transforms basin subsidence into uplift via intrabasinal thrusting/reverse faulting. Often, the rift-basin boundaries (the thermo-mechanical hinge zones of Watts and Steckler, 1981) act as the major ramps which allow the telescoping of the basin out and over its thermal basin.

Given the major role inversion can play in basin survival, little is known of the mechanism by which it occurs. For simplicity, we define inversion as the change in polarity of structural relief, from a basinal area into a structural high (positive inversion), or from a structural high into a depocentre (negative inversion). While transtension and transpression can result in local inversion, we will concentrate primarily on regional inversion, that is, the (semi) destruction of entire basin systems. The purpose of this paper is to investigate the causes and consequences of basin inversion by studying the structure and evolution of the Wessex Basin.

The Wessex Basin of southern England was first named and recognised as a major depocentre by Kent (1949), who constructed various isopachyte maps of the region based on hydrocarbon exploration data available at that time. More recently, increased exploration interest, and therefore

data, in the region has allowed a greater understanding of the configuration and formation of the basin and its sub-basins. The basin is typified by a moderately complete Permian to Cretaceous sequence, but with Tertiary inversion producing restricted sedimentation on former Mesozoic 'highs'.

This work utilizes the data from recent geophysical surveys, new maps released by the British Geological Survey, and borehole data to outline the structural development of the Wessex Basin via a series of palaeogeographic maps and structural cross-sections.

3.2 Structural Setting

The Wessex Basin originated as a series of fault controlled sub-basins in the northernmost part of the Hercynian fold belt, infilled with late Palaeozoic to Cenozoic sediments locally exceeding 3500 metres. The underlying basement largely comprises deformed Devonian/Carboniferous sediments although locally, inliers of lower Palaeozoic sediments have been encountered. The Wessex Basin is bounded by Hercynian highs; to the west the Cornubian massif, to the north and east by the London-Brabant Platform and to the south by the Armorican massif (Fig. 3.1).

Four sub-basins have been identified (Sellwood et al., 1985; Whitaker, 1985) on the basis of structural trends, basin fill, and the tectonic evolution of individual sub-basins (Fig. 3.1).

1. Channel Basin; predominantly a Mesozoic northerly dipping half graben developed almost entirely offshore in the present day English Channel.
2. Winterbourne Kingston Trough; a narrow west-northwest trending symmetric graben, largely infilled with Palaeozoic - Mesozoic sediments.

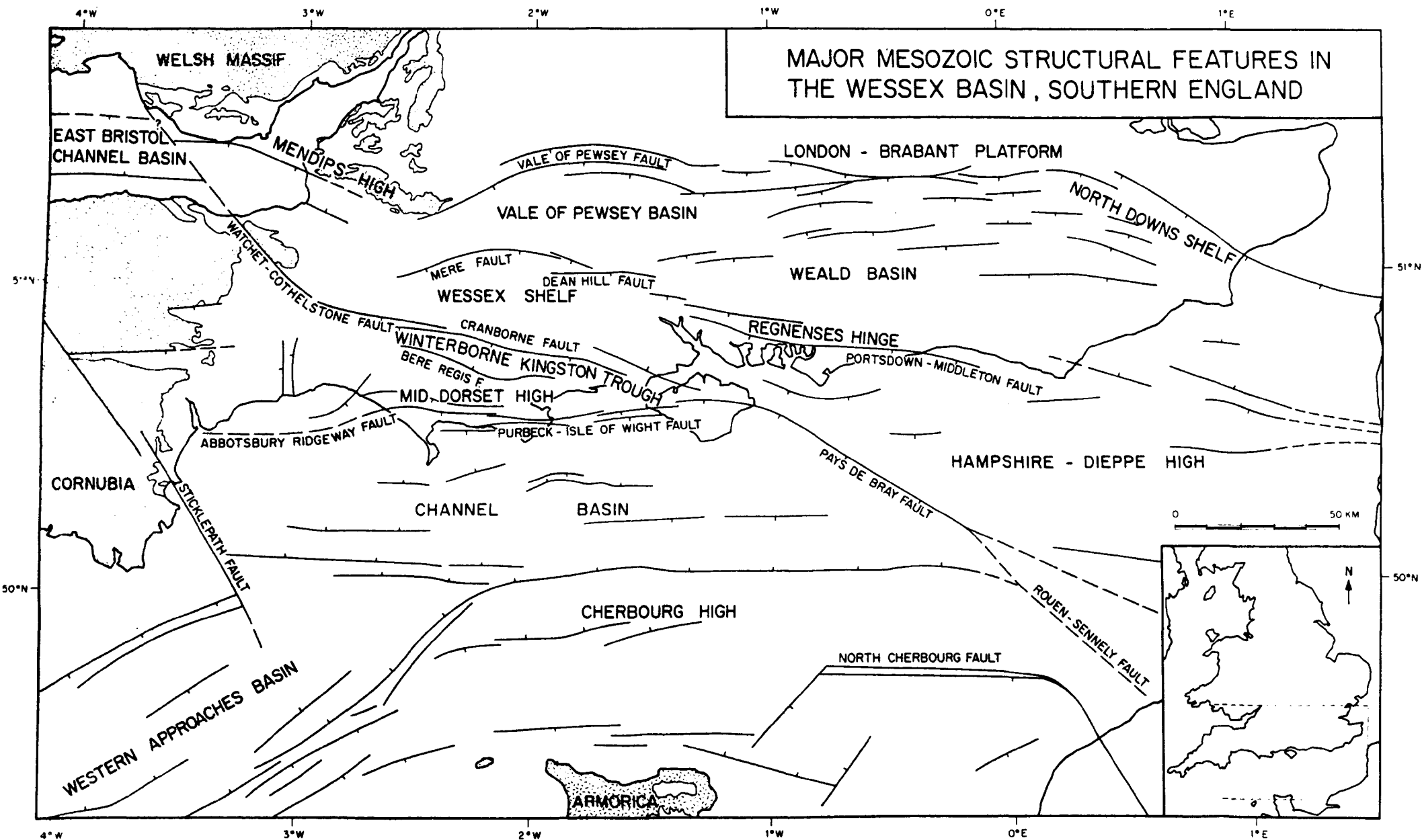


Fig. 3.1 Simplified regional tectonic map of the major Mesozoic structures in the Wessex Basin. Based on Whittaker (1985), Stoneley (1982), Sellwood et al., (1985), Kamerling (1979) and this thesis.

3. Vale of Pewsey Basin; predominantly a late Palaeozoic - Mesozoic northerly dipping half graben developed entirely onshore. The northern boundary of the basin approximately marks the limit of the Wessex Basin.
4. Weald Basin; a Mesozoic northerly dipping half graben becoming geometrically more symmetric eastwards.

All these sub-basins display two major structural trends, a predominant east-west trend intersected by a secondary northwest-southeast direction.

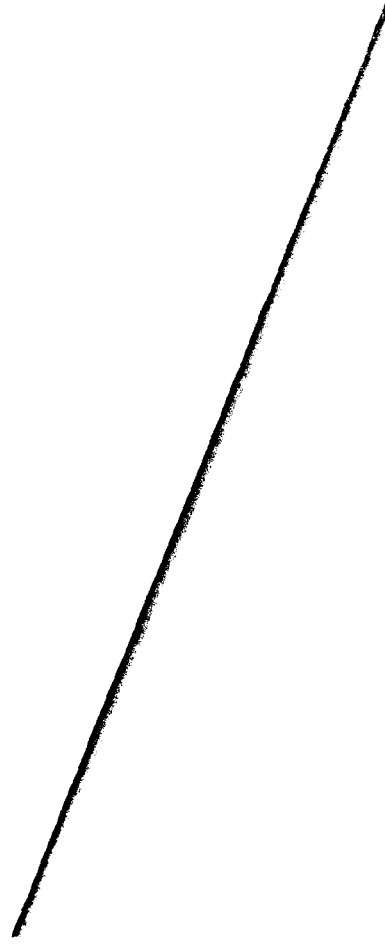
3.3 Crustal Configuration, Basement Structure and Basin Stratigraphy

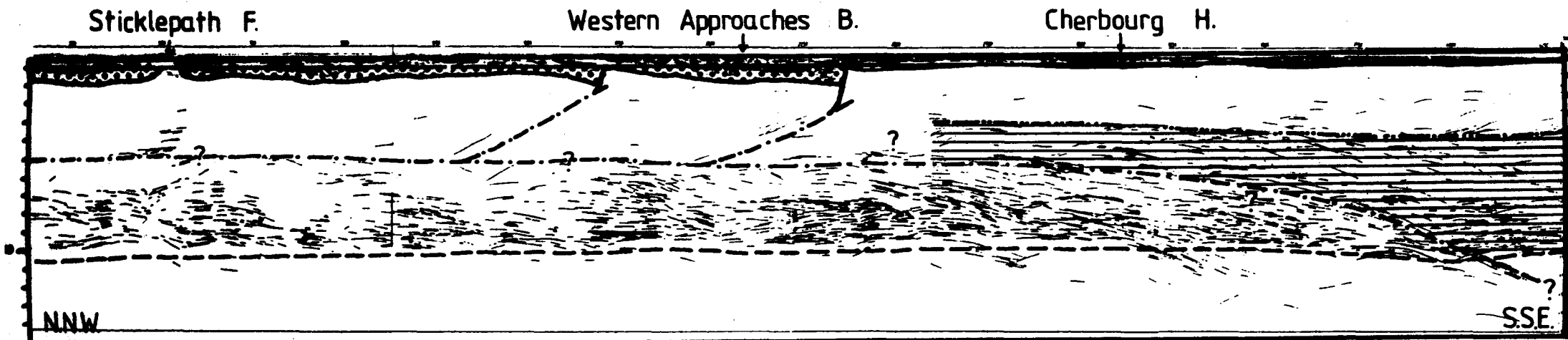
A number of studies have suggested that basement structure can strongly influence the form and orientation of subsequent sedimentary basin formation (e.g. Burchfiel and Royden, 1982; Brewer et al., 1983). It is necessary therefore, to outline the present-day structure and configuration of the crust (and hence basement) in southern England on which the Wessex Basin developed.

A. Pre-Basinal Phase

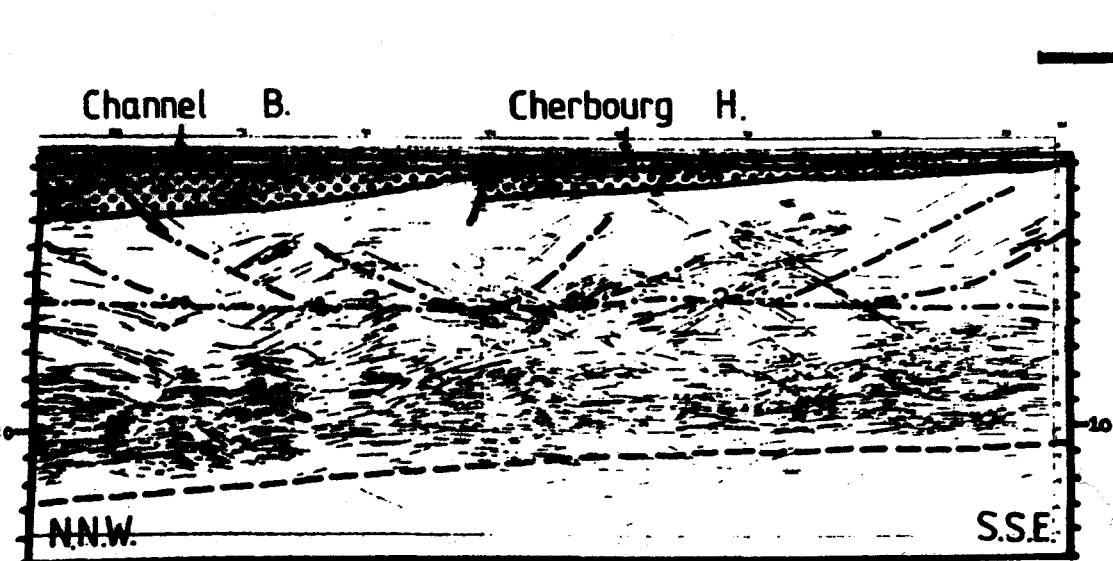
Information on the underlying pre-Permian (Variscan) basement structure is obtained from basement outcrops around the basin margins, borehole logs, and limited seismic reflection and refraction data. An interpretation of this data in terms of basement structure is presented in figure 3.2.

PULL
OUT



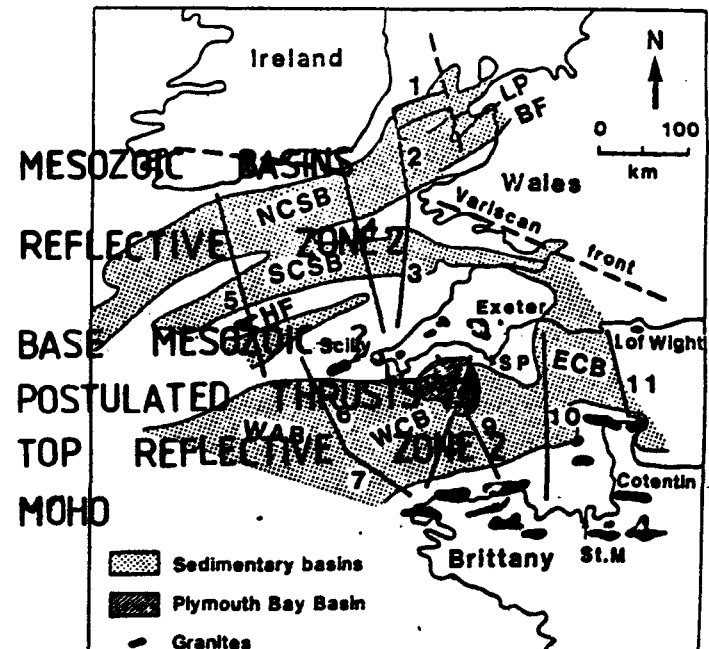
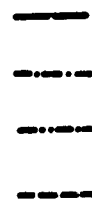


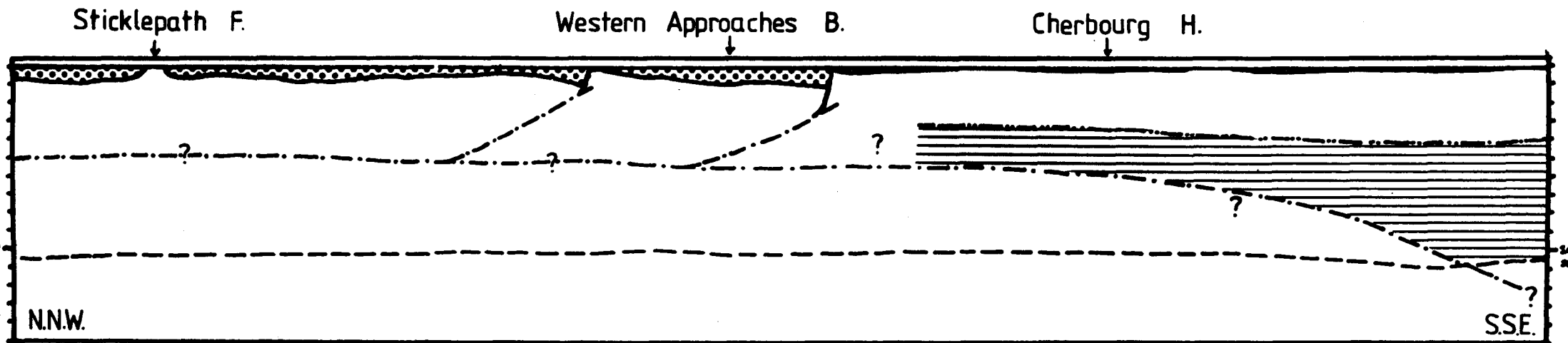
SWAT. 10



SWAT. 11 Interpretation 1 of SWAT lines 10 and 11. (Inset map from BIRPS/ECORS 1986).

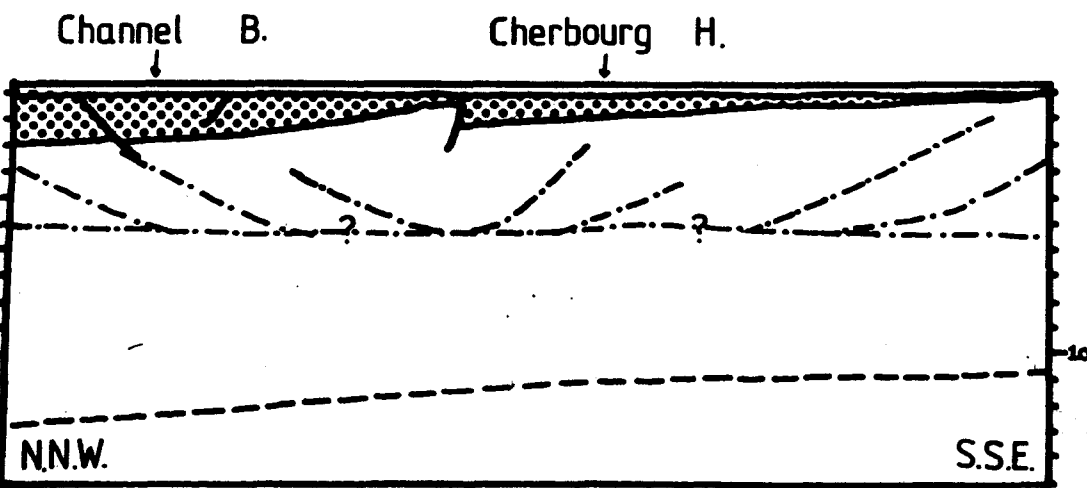
25 km











S.W.A.T. 10

25 km



S.W.A.T. 11

-  MESOZOIC BASINS
-  REFLECTIVE ZONE 2
-  BASE MESOZOIC ?
-  POSTULATED THRUSTS ?
-  TOP REFLECTIVE ZONE 2
-  MOHO

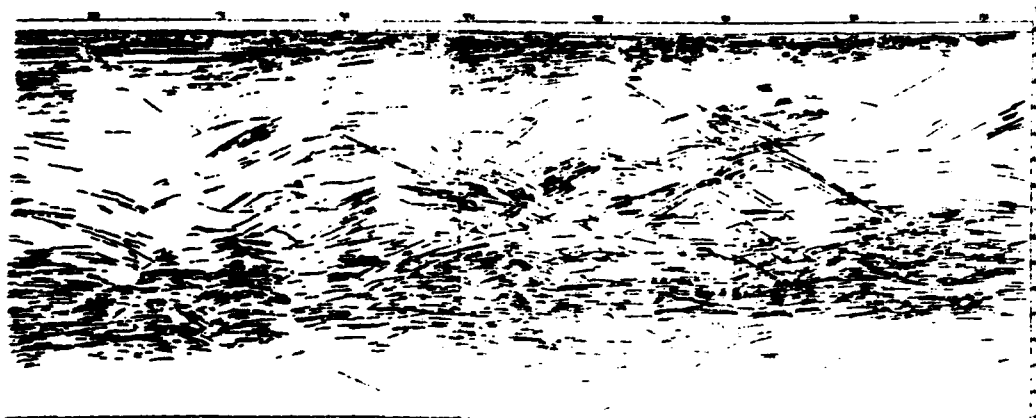
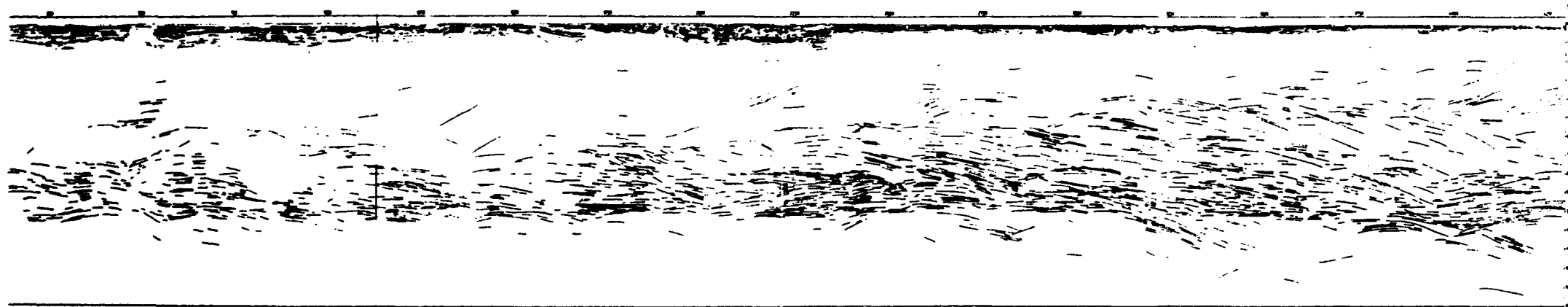
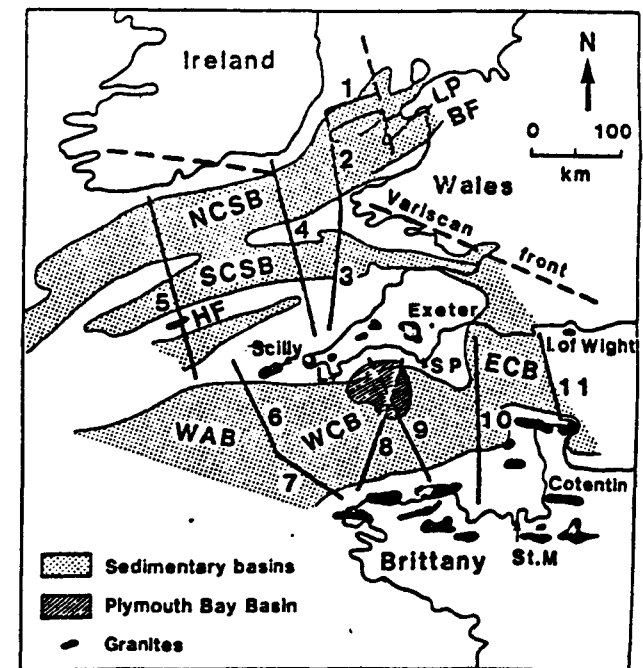
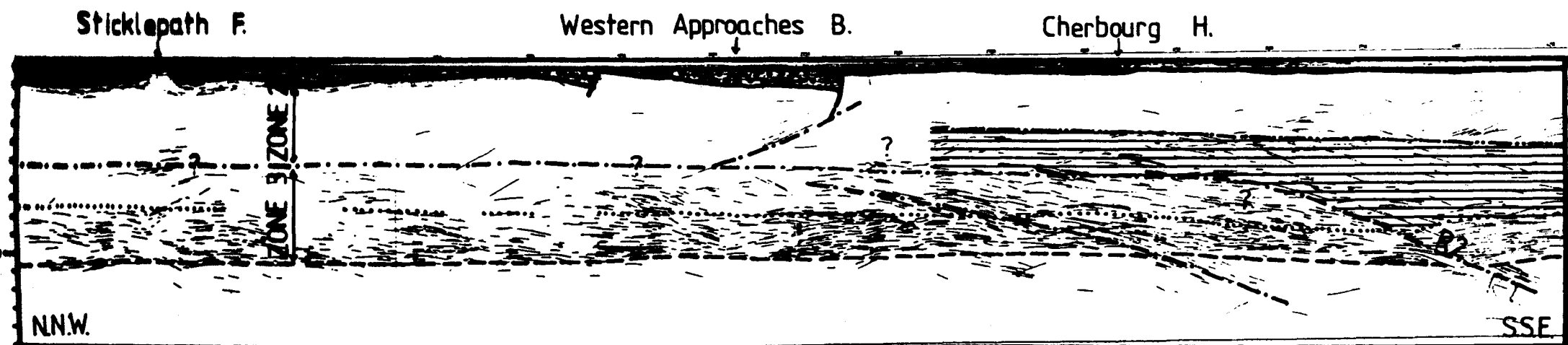


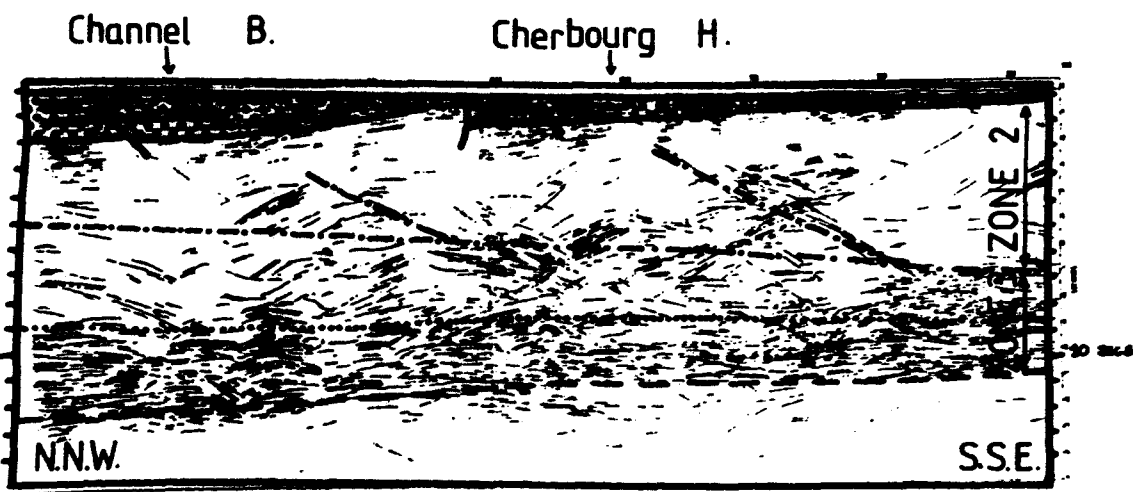
Fig. 3.3 Interpretation 1 of SWAT lines 10 and 11. (Inset map from BIRPS/ECORS 1986).





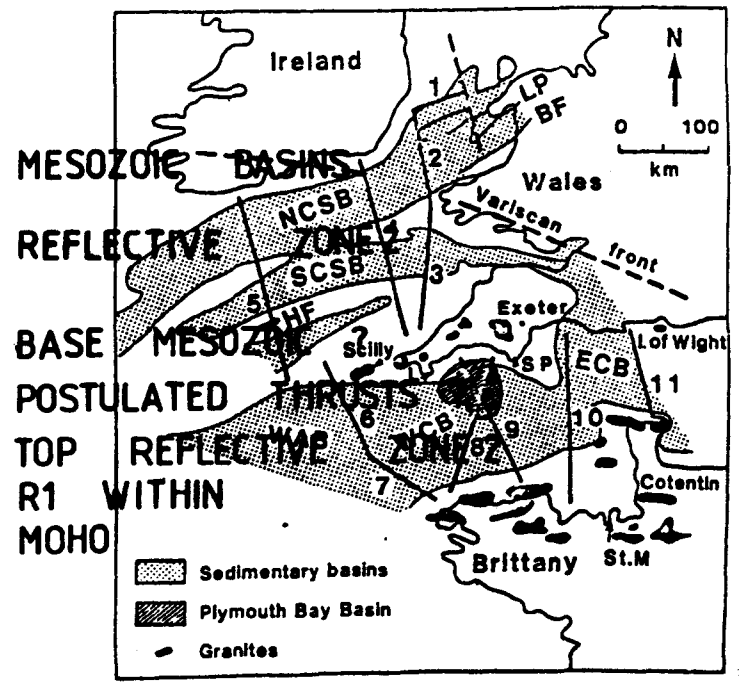
S.W.A.T. 10

25 km



S.W.A.T. 11

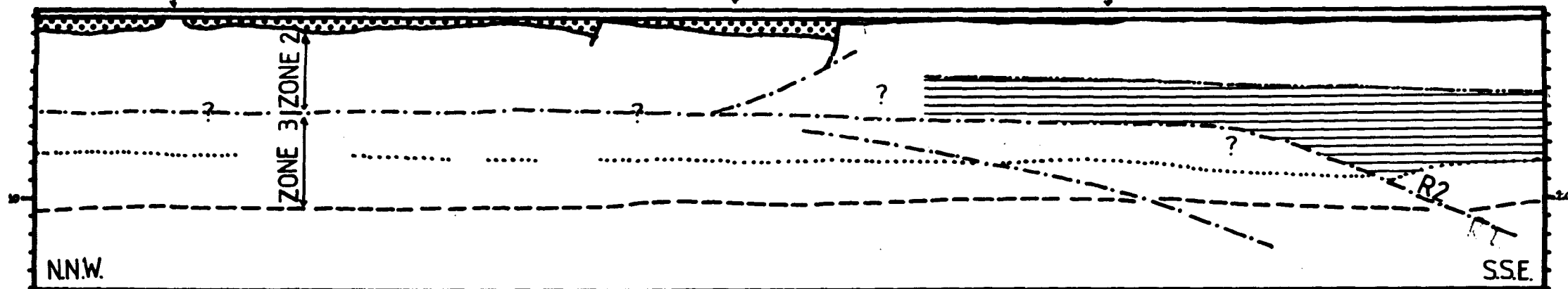
Interpretation 2 of SWAT lines 10 and 11. (Inset map from BIRPS/ECORS, 1986).



Sticklepath F.

Western Approaches B.

Cherbourg H.

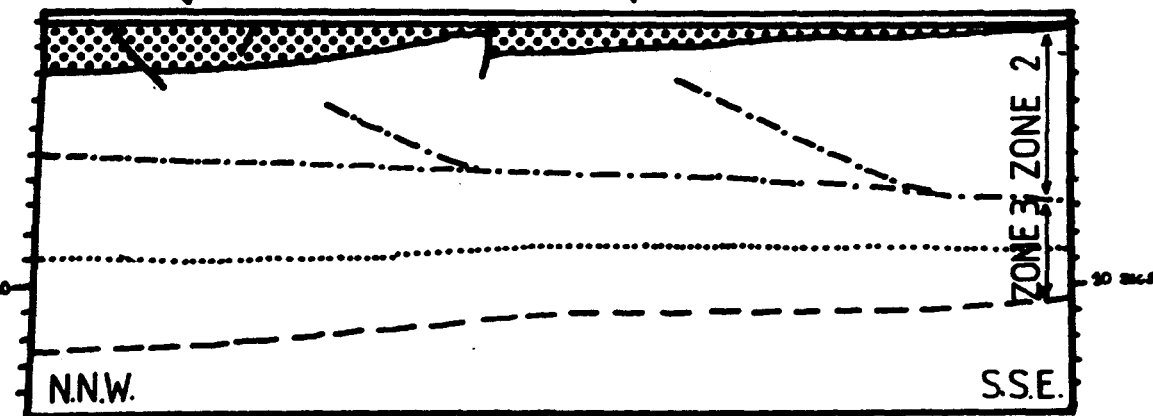


S.W.A.T. 10

25 km

Channel B.

Cherbourg H.



S.W.A.T. 11



MESOZOIC BASINS

REFLECTIVE ZONE 2

BASE MESOZOIC ?

POSTULATED THRUSTS ?

TOP REFLECTIVE ZONE 2

R1 WITHIN

MOHO

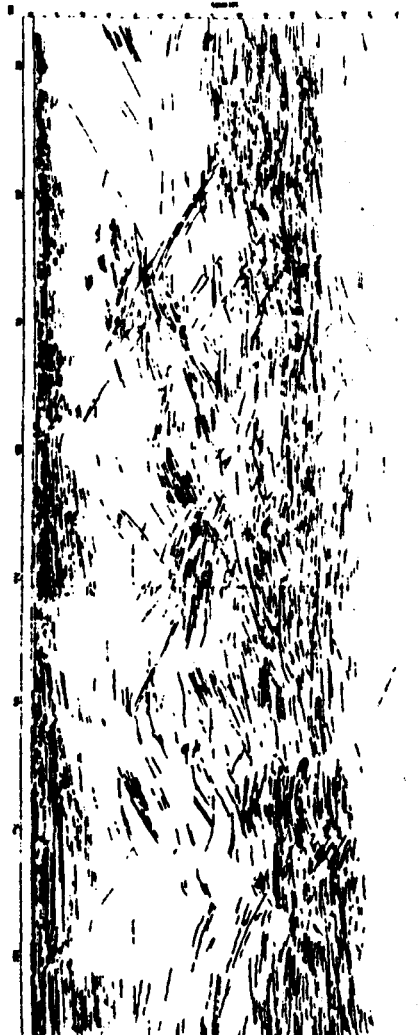
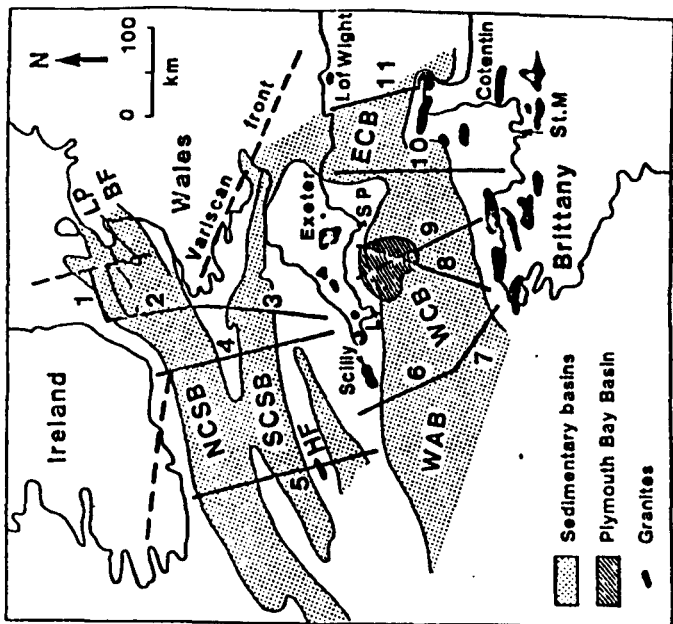
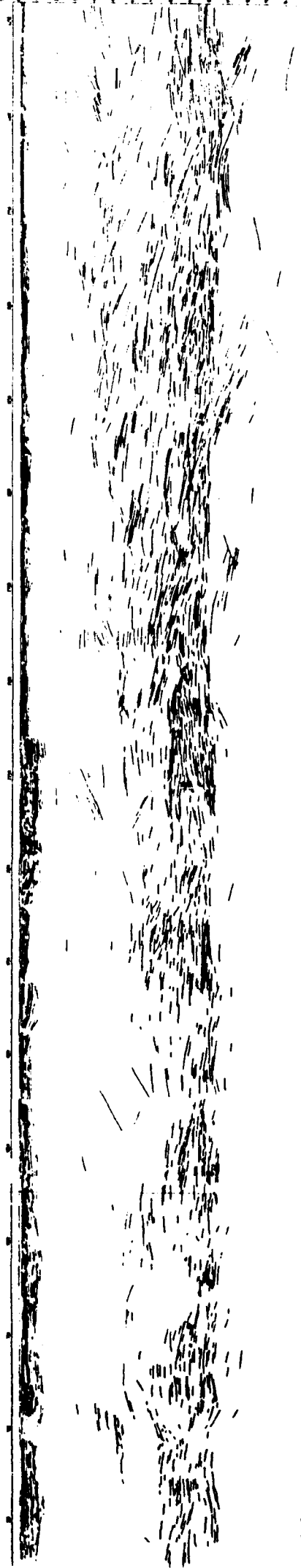


Fig. 3.4 Interpretation 2 of SWAT lines 10 and 11. (Inset map from BIRPS/ECORS, 1986).

subhorizontal reflection events which extend down to between 1 and 3 second (TWTT). They are interpreted as sedimentary reflectors within large sedimentary basins since these reflectors are frequently displaced by normal and reverse faults.

Zone 2 extends from the base of Zone 1 to a highly variable boundary between 3.5 seconds (TWTT) and 7 seconds (TWTT) which comprises discrete dipping reflections in a largely featureless zone. On the unmigrated profile 11 (Fig. 3.3), moderate to high-amplitude events show chaotic cross cutting relationships. The dipping reflection events have been interpreted as major thrusts, faults, shear zones or decollement surfaces (eq. Kenolty et al., 1981; Brewer & Smythe, 1984; Whittaker & Chadwick, 1984). The undoubted presence of an underlying Variscan foldbelt in Southern England, the preponderance of dipping events in comparison to the absence of similar events on the more stable English Midlands microcraton and from the discussion of the three dimensional geometry of those structures in Chapter 2 leads to the conclusion that the reflectors are more likely to be Variscan thrusts; some of which may have controlled to overlying basin geometry and evolution (see Chapters 2 and 3).

Zone 3 represents the lower crust and may extend to 13 second (TWTT), although on average 10 second (TWTT) corresponds to about 30 km depth (the Moho?). This zone is highly reflective and is characterized by strong continuous subhorizontal reflectors possibly and locally exceeding 10 km in length and generally increasing in intensity downwards towards the presumed Moho. In addition hyperbolic and dipping events can be clearly distinguished and may perhaps offset sub- horizontal reflectors. The high reflectivity essentially terminates downwards at around 10 seconds (TWTT) at the Moho as interpreted by Brewer & Smythe,

PULL

OUT

(1984.) Below the Moho only discrete dipping events can be distinguished. These are similar to those seen in zone 2 and have been interpreted as faults or shear zones within the upper Mantle (eq the Flannan thrust, Blundell et al., 1985).

The importance of the layered lower continental crust and the significance of the sub-horizontal events has attracted considerable debate. Blundell (oral comm) and Blundell & Reston (oral comm) believe that these events may be due to: reflections from underlying surfaces out of the plane of section; anastomosing shear zones; compositional banding; ductile fabrics; cumulate layering; lenses of partial melt; and water filled fissures. Although their interpretation still remains controversial, the final explanation of this feature needs to adequately explain both their lateral continuity and apparently widespread development elsewhere.

The geological interpretation of these zones on SWAT lines 10 and 11 are summarized on figures 3.3 and 3.4. Zone 1 clearly corresponds to the Mesozoic basins thus SWAT profile 10 displays in part the Channel Basin and Western Approaches basins and the surface expression of the Sticklepath fault zone; whilst SWAT profile 11 clearly shows the Channel basins, Mid-Channel fault and Cherbourg High. The topmost part of Zone 2 probably corresponds to the deformed Palaeozoic sequence within the Variscan fold belt. The southern half of SWAT profile 10 probably comprises shallow undifferentiated metamorphic basement and granite intrusions (Variscan or Caledonian in age), the latter outcropping onshore in France. Dipping events are locally distinguished and generally accord with the location of overlying Mesozoic basins and therefore presumed to control them. Jones & Warner (oral comm) examined

why the dipping reflectors are reflective in the Outer Hebrides region, and concluded that the events were fault zones where rock densities increased as a result of preferential removal of soluble quartz and feldspar from the zone. Geometrically they are similar to the dipping events recorded by Kenolty et al., 1981 and dipping events mapped in this study in Lyme Bay (see Chapter 2). Therefore dipping events with zone 2 are here postulated to represent Variscan age thrusts which extend to at least 6 seconds (TWTT). These steeply dipping events (approximately 30°) contrast strongly with the sub horizontal nappe structures identified along the Variscan strike; for example in the Rhenish Massif (Meissner et al., 1984). Brewer (1984) attributed this change as due to variations in the amount of overthrusting and the morphology of the continental margin. The presence of steeply inclined thrusts extending to 6 seconds (TWTT) is, here though to infer the presence of a deeper decollement surface. Onshore, in southern England, Williams & Brooks (1985) produced a valid balanced section based on Chadwick et al.,'s (1983) interpretation of the concealed Variscan structure from deep seismic reflection profiles. The restored decollement level lies at about 15 km and agrees with sub-horizontal reflection events imaged at that depth. Further west Brooks et al., (1984), using crustal refraction and wide angle reflection, identified a major reflector (R2) rising northwards from 15 to 10 km throughout southwest England, which they suggested may represent a major thrust of late Variscan age. This postulated level would approximately coincide with the boundary between zone 2 and 3 on SWAT lines 10 and 11. This has been taken into account in the interpretation on figures 3.3 and 3.4 which shows the sharply dipping events observed within zone 2 so sole cut along a postulated

decollement to the south. This interpretation would imply that the highly reflective horizons in zone 3 are a tectonic induced fabric (Butler pers Comm), consequently the resultant fabric should accompany the decollement updip to its eventual surface expression. Such a rise is clearly observed on SWAT profiles 2 and 3 where BIRPS/ECORS (1986) have recorded a strongly dipping event (interpreted as the Variscan front between the Bristol Channel and Cardigan Bay basins) which is here presumed to be the surface expression of the decollement plane. Associated with the rise of the postulated decollement is a decrease in the reflective properties of zone 3, which is presumed to indicate decreasing displacement towards the thrust front. Further south above the decollement level a similar rise of zone 3 along the Carrick, Lizard and Start thrust system on SWAT profiles 8 and 9 can be observed (c.f. BIRPS/ECORS 1986). This is coincident with the surface exposure of a basement metamorphic schists and granitoid gneisses) -cover contact. Fundamental problems still arise: firstly the high stress required to develop such a deep decollement for such long distances in the middle crust; and secondly the persistence of zone 3 in areas absent from known thrusting (c.f. SWAT profile 1).

Above the postulated decollement, dipping events are seen in both directions. Figures 3.3 and 3.4 delineate the two possible (end member) interpretations of these structures. Figure 3.3 displays two northerly dipping events presumed to be thrusts on SWAT profile 10, which control the development of two asymmetric Mesozoic half grabens; whereas SWAT profile 11 may portray two oppositely opposed dipping events. The northerly dipping events could be interpreted as backthrusts, which to some extent may influence Mesozoic basin development (eg the location of

the Mid-Channel fault). The geometry of those events observed on SWAT profile 11 show striking similarities to the deep structure postulated by Shackleton et al., (1982). Figure 3.4 differs in that it displays two southerly dipping events on SWAT profile 11 which seem to terminate on the postulated decollement level. Both interpretations appear equally viable. A previously unidentified event within zone 3 can be distinguished as a boundary between two zones of sub-horizontal reflectors of differing density; but the precise course and nature of this boundary is purely speculative. The southern portion of SWAT profile 10 displays both a higher elevation of sub-horizontal reflectors within zone 2 than is seen elsewhere together with major dipping events which cross cut zone 3 and extend down into the upper Mantle. The former reflective zone may be a tectonic induced fabric associated with a major thrust rising close to the surface just south of the section, alternatively and more feasibly they may correspond to the offshore continuation of the Brittany batholiths, since up to a 3 second (TWTT) rise in the reflection characteristic of the lower crust is observed under the Scilly Isle and Haiq Fras granites on SWAT profiles 5 and 6 (according to BIRPS/ECORS (1986)). Two major dipping events on SWAT profile 10 clearly extend down into the upper Mantle. Their hyperbolic form may suggest simple diffractions, alternatively the disturbance of the Moho reflector by R2 may imply a real phenomena cutting the Moho. Both figures show an interpretation of this reflector as a major thrust ramp, alternative explanations are equally feasible.

In conclusion interpretations of SWAT profiles 10 and 11 have been presented here in order to investigate Variscan structures in the Crust and upper Mantle. Three zones, based upon differing seismic character as

outlined by Whittaker & Chadwick (1984), are identified within the Crust. Onshore geological and geophysical data sets indicate a Variscan decollement rising northwards towards the supposed outcrop of the Variscan front. The analysis presented of SWAT profiles 10 and 11 are speculations on the offshore extent of this decollement with dipping reflectors immediately above the decollement interpreted as Variscan thrusts. The probable Moho is clearly imaged at approximately 30 km depth and appears fairly flat except in the northern portion of profile 11 where it is coincident with the deepening of the Channel Basin. However if the low seismic velocities in the overlying sedimentary sequence were taken into account the Moho will rise approximately to the same level as encountered elsewhere. The apparent increase in depth to the Moho under the Channel Basin would result if the Channel Basin is uncompensated. This conclusion is in broad agreement with the view of Warner (1985) that the elastic thickness of the lithosphere is very small (<5 km) around the UKCS. The lack of obvious crustal thinning (contrasting to that seen in the North Sea by Barton & Wood, 1984) is important when considering the thermo-mechanical and structural evolution of the basin.

The seismic reflection South West Approaches Traverse (SWAT) imaged the geometry of the overlying late Palaeozoic-Tertiary basins and underlying crust. The mid-crustal levels, though poorly reflective, show a series of shallow dipping events which have been interpreted as thrusts (Brewer et al., 1983; Whittaker & Chadwick, 1984; Brewer & Smythe, 1984). In addition, a single seismic refraction experiment, the Ridgeway line, represents a northnortheast-southsouthwest transect across the central onshore portion of the Wessex Basin and recorded an apparently flat Moho at 31-33 km and a prominent mid crustal reflector at ≈ 14 km (Hopkins, pers. comm. this reflector was also recorded further west in Corn^ubia by Brooks et al., 1984). The position of this mid-crustal reflector is consistent with a proposed crustal decollement at 15km based on structural balancing of a section across southern England by Williams and Brooks (1985). In France, the Etude de la Croute continentale et Oceanique par Reflexion et refraction seismique (ECORS) traverse imaged the Faille de Midi decollement at 10 km (offset vertically by the Pay-de-Bray fault) with Moho being recorded at approximately 40-45 km (Bois et al., 1985). Figure 3.5 presents an interpretation of the present crustal configuration across the Wessex Basin.

The basement consists of deformed Devonian/Carboniferous Molassic-type sediments which were originally deposited within the Variscan fore-deep and later deformed by the emplacement of thrust sheets during the Variscan Orogeny.

Various interpretations of the detailed structure of the basement has created considerable controversy. Some authors have explained basement evolution in terms of thick-skinned tectonics involving large-scale strike-slip motion (Arthaud and Matte, 1977; Autran and Cogne, 1980;

Badham, 1982; Sanderson, 1984) while others have invoked a thin-skinned origin (Isaac et al., 1982; Shackleton et al., 1982; Shackleton, 1984; Coward and Smallwood, 1984) involving shallow décollements and high amounts of shortening. Evidence exists for both hypotheses. Recent work by Coward and Smallwood (1984) has shown that thrust emplacement was generally north-northwest and that at least some northwest-southeast structures probably developed synchronously with thrust emplacement as lateral ramps. This same late Variscan trend may have played a major role in the structural evolution of western European basins. In particular, northwest-southeast transfer faulting has offset the east-west/northeast-southwest basin initiating faults of, for example, the Porcupine, Channel, Cardigan Bay, Kish-Bank, Irish Sea and Celtic Sea basins (see Chapter 4).

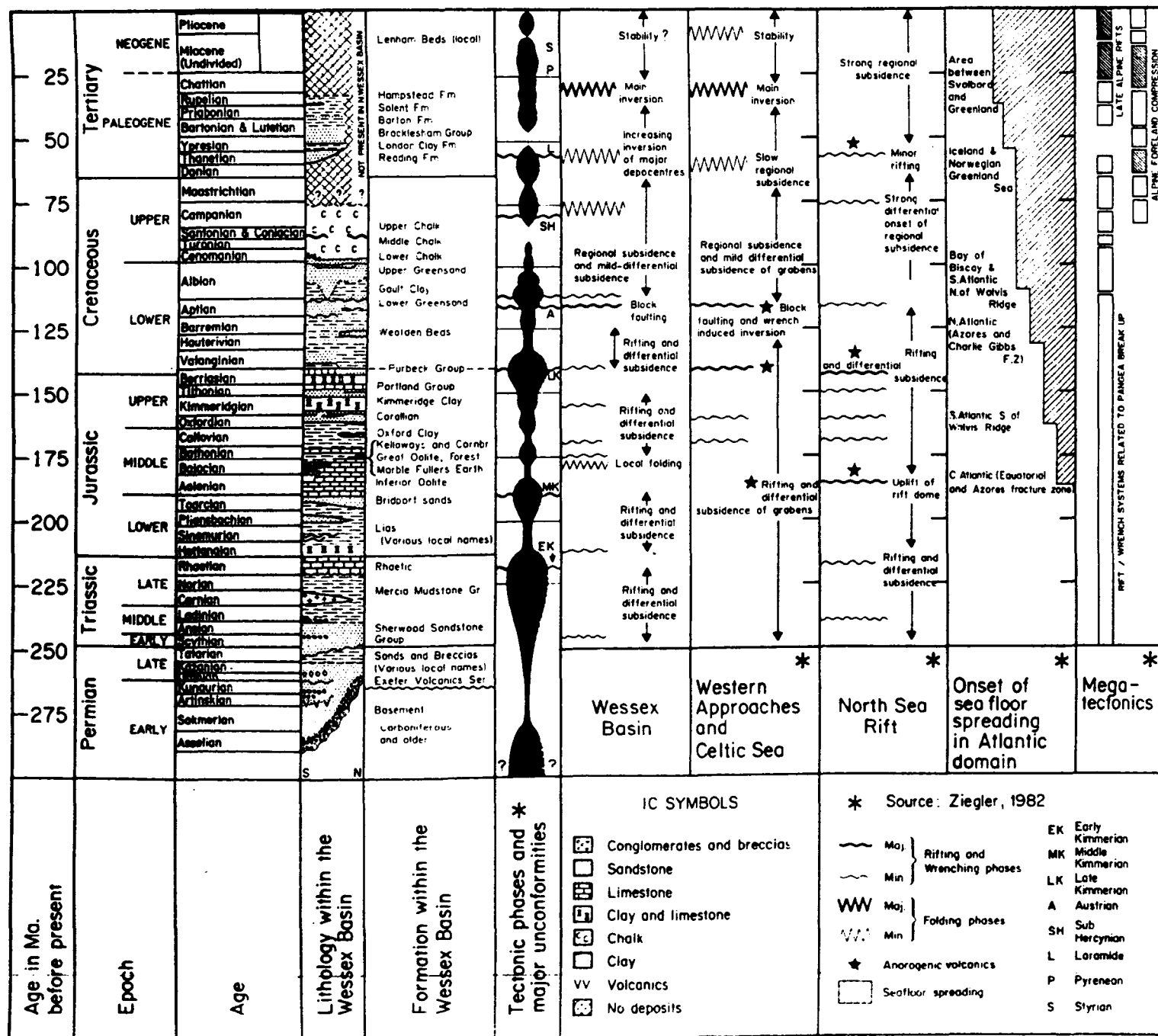
Following the normal reactivation of the basement thrusts, asymmetric grabens were produced by collapse of the hanging wall. Symmetric graben development, when it occurs, may represent antithetic faulting following hanging wall collapse or alternatively, the backthrusting of northward dipping Variscan basement faults (e.g. mid-Channel fault).

B. Basinal Phase

Unconformably lying on basement are Stephanian aged sands and conglomerates (Fig. 3.6). These sediments also represent the basal unit of the half-grabens and therefore date basin initiation. An upper Carboniferous age for basin formation is consistent with the radiometric ages of inter-digitated lavas and agglomerates (Edmonds et al., 1969).

Following basin initiation, erosion, locally severe (as in the Weald Basin) removed early Palaeozoic sedimentary sequences in an attempt to peneplain Variscan topography. Based on restored sedimentary thickness

Fig. 3.6 Generalized lithological sequence of the Wessex basin and correlation of tectonic events to nearby (Ziegler, 1982).



calculations by Williams and Brooks (1985), up to 10 km of sediment stripping may have occurred.

Sediment deposition within the newly formed half-grabens was strongly controlled by Variscan structure and topography. During the Permian, semi-arid/desert sedimentation was largely concentrated along the western margin of the Wessex Basin in a series of east-west trending cuvettes. Permian sedimentary structures indicate a dominant eastward drainage pattern with proximal alluvial fans prograding off active east-west fault scarps (Laming, 1982). Isopachyte data (Whittaker, 1985) clearly show progressive eastward sedimentary thinning with only minor isolated outliers present in the subsurface along the western margin of the Weald Basin. Sedimentation was thus largely absent in the Weald Basin and on the London-Brabant Platform.

Permian sediments are unconformably overlain by continental Triassic sands and silts (Colter and Harvard, 1981; Fig. 3.6). Local conglomerates in the western localities of the basin indicate a northerly directional drainage pattern (Audley-Charles, 1970). Detailed descriptions of Triassic sedimentology and palaeogeography are outlined by Audley Charles (1970), Warrington et al. (1980), Lott et al., (1982), Allen and Holloway (1984), and Whittaker (1985). As in the Permian, sedimentation was restricted to the west with the Weald Basin only becoming inundated from the south-west during the late Triassic (Rhaetian) marine transgression (e.g. Taitt and Kent, 1958). Following from this transgression, marine sedimentation continued during the lower Jurassic with progressive onlap onto Hercynian highs (e.g. such as the London-Brabant Platform). The complex onlap and offlap patterns observed on the major basement highs is probably best explained in terms of an

interference between the general Mesozoic eustatic sea-level rise with local tectonically-induced subsidence (Karner et al., 1986).

The middle Jurassic locally displays marked basinal variation in thickness and facies distribution as exemplified for example, by the Great Oolite Group (e.g. Sellwood et al., 1985). Bentonites were locally developed along the western extremities of the London-Brabant platform and have been attributed to volcanism in the North Sea and Western Approaches area (Hallam and Sellwood, 1968; Harrison, 1981). The upper Jurassic is marked by an upward shallowing marine sequence, indicative of an increasing proximity to the major source areas.

The lower Cretaceous was a period of major regional instability marked by basement fault reactivation which allowed the deposition of up to 1000 metres of non-marine brackish/freshwater sediments (Allen, 1981) and basin margin uplift. Most major depocentres were involved; viz., the Channel, Weald, and Vale of Pewsey Basins. The succeeding lower Greensand (Aptian) rests unconformably on earlier units and is, in turn, unconformably overlain by the Gault Clay (Albian; Fig. 3.6). Subsequent upper Cretaceous sedimentation essentially consisted of chalk. During this same period, the Weald Basin probably was at its greatest lateral extent as suggested by the distribution of flint gravels in Devon.

The basin-wide unconformity (Fig. 3.6) separating Tertiary and upper Cretaceous sediments documents the initiation of basin inversion in which late Palaeozoic/Mesozoic depocentres were uplifted to become source areas. Conversely, former Mesozoic highs became major Tertiary depocentres. Inversion occurred intermittently throughout the Eocene, culminating in the Oligocene/Miocene.

3.4 Structural Evolution of the Basin

In the previous section, we described the structure of the basement and the stratigraphic development of the basin. In this section, we describe the structural development of the basin itself through both the extensional and compressional (inversion) history of the basement.

Chadwick et al., (1983) noted a causal relationship between late Palaeozoic-Mesozoic growth faulting and normal reactivation of Variscan basement thrusts. More recently, data acquired by the British Institutions Reflector Profiling Syndicate (BIRPS) around the United Kingdom Continental Shelf (UKCS) show dipping reflectors at mid and lower crustal levels which may represent thrusts. Locally, some of these reflectors control Palaeozoic or Mesozoic basin development (e.g. Brewer and Smythe, 1984).

The Channel Basin appears to have developed as a consequence of the interaction between the Sticklepath Fault and Pay de Bray fault (Ziegler, 1982). By generalising this concept, we suggest that the interaction of the northwest-southeast strike-slip faults, with the major east-west thrust faults has controlled the opening of the entire Wessex Basin system. Northwest-southeast sinistral fault movement of only a few kilometres is sufficient to produce the observed distribution of basement half grabens. Sinistral motion is suspected because the northwest-southeast faults show no evidence of transpression or transtension (c.f. the development of the late Palaeozoic/Mesozoic Worcester graben, Chadwick 1985a).

Basin initiation appears to have migrated from the west (Winterborne Kingston sub-basin; Permian) to the east (Weald sub-basin; early Jurassic). However, if basin initiation is related to basement thrust react-

ivation, and the thrusts span from Ireland to Belgium, then this primary depocentre migration is somewhat puzzling. The absence of Permian sedimentation in the Weald Basin can be explained in one of a number of ways; (1) northwest-southeast sinistral transpression motion along the Pay de Bray fault resulted in the uplift of the Weald area to form a topographic high, (2) Weald Basin basement may have undergone a greater amount of Variscan shortening relative to western regions thereby requiring significant more extension to initiate basin sedimentation (i.e. again a topographic high), (3) Permian sediments may have been deposited but subsequently removed by pre-Jurassic erosion and (4), the Weald region, while topographically low, failed to receive sediments (i.e. sediment starved). Points (1) and (2) imply uplift and erosion. However, well data suggests that the Weald area was distal from the active source regions Allen & Holloway (1984). Point (3) requires firstly the deposition of terrigenous sediments followed by erosion. Again, no evidence exists for any re-worked Permian sediments. This leaves point (4) as the most likely, which in turn, suggests that basement extension (and hence rifting) had yet to occur in this region. We predict therefore, that extension migrates from the west (Permian-Triassic) to the east (Rhaetic). The postulated Permian palaeogeography of the Wessex Basin is outlined in figure 3.7.

Intra and interbasinal unconformities are produced by either (a) variations in eustatic sea-level, (b) local/regional tectonically induced uplift, or (c) by non-deposition and minor erosion followed by renewed sedimentation. Unconformities therefore, are an important constraint on understanding the structural and tectonic development of a sedimentary basin. The lower Triassic unconformity marked a period of basin subsi-

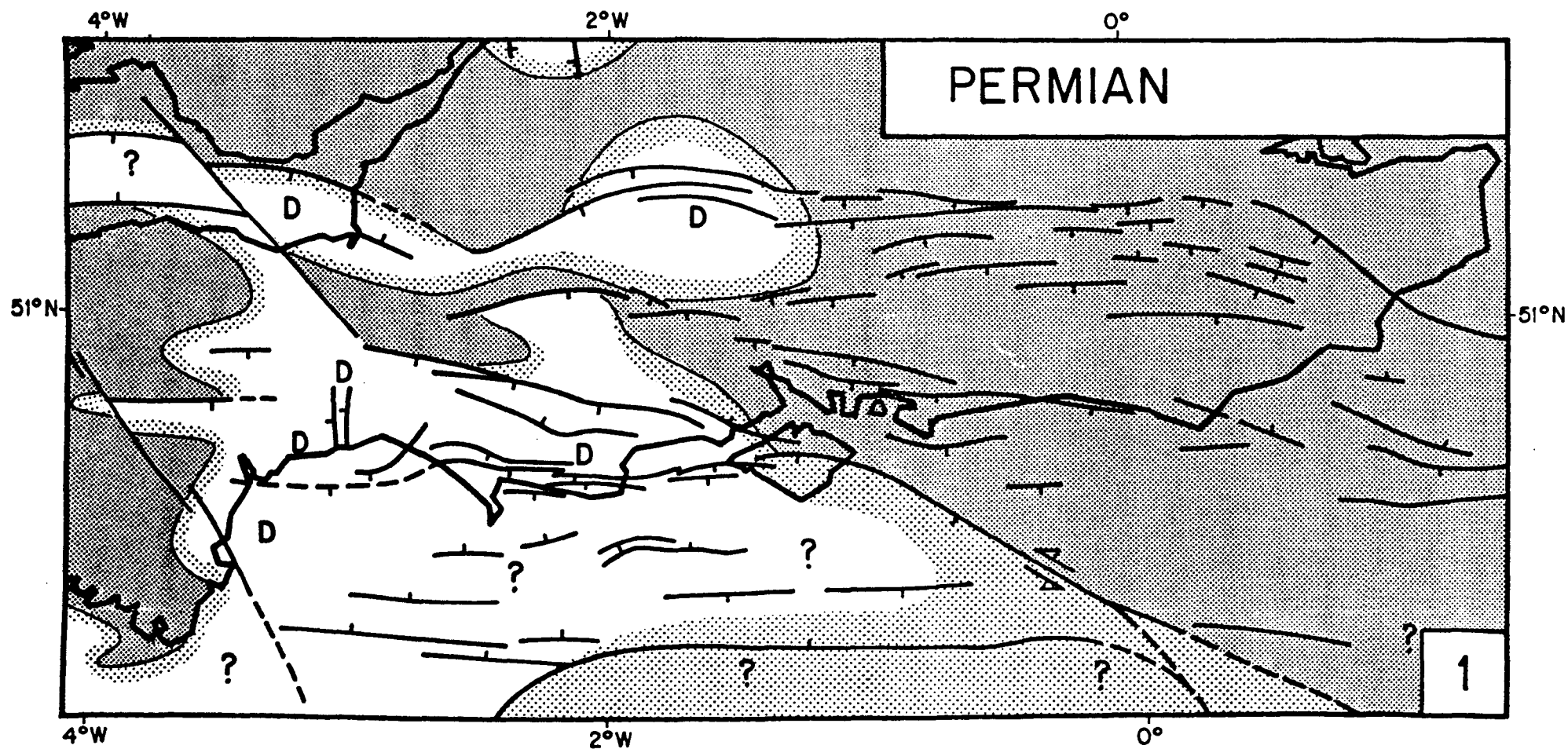


Fig. 3.7 Permian Palaeogeography. Based mainly on Ziegler (1981), Whittaker (1985), Rhys et al., (1982), Laming (1982), and Lloyd et al., (1973).

dence rejuvenation (following late Permian non-deposition) associated with renewed northwest-southeast sinistral extension (c.f. figures 3.7 and 3.8). In contrast, the Rhaetian unconformity formed at a time tectonic quiescence within the basin and correlates with the initiation of a world-wide transgressive eustatic event (e.g. Vail et al., 1977).

Polyphase crustal extension occurred throughout the Jurassic and is reflected in the sedimentary record by growth faulting. Extension was facilitated by the normal reactivation of basement listric faults as evidenced by the development of roll-over structures. Local sedimentary thinning and facies variations (Sellwood et al., 1985) along east-west and northwest-southeast trends, while possibly reflecting remnant Variscan topography, may also indicate fault reactivation and localized transpression associated with extension (Fig. 3.9-3.11). The upper Jurassic marked the initiation and rapid subsidence of the Weald and Channel basins. Regional subcrustal lithospheric readjustment to this local crustal extension resulted in peripheral uplift, as evidenced by reworked Jurassic material (e.g. West and Hooper, 1969), and hence the production of a major unconformity; the Kimmerian unconformity. The Kimmerian unconformity can only be demonstrated within the main sub-basins as it has subsequently been removed by Aptian/Albian erosion.

Unrelated to, but at the same time as, lower Cretaceous faulting within the Wessex Basin, the entire area was subjected to regional uplift (Figs 3.12 and II.3.1). This uplift was significantly more important in the west and south than the north and east, as evidenced by the increased erosion of pre-Aptian sediments within the Western Approaches Basin (Bennet et al., 1985) and Bristol Channel Basin (Kamerling, 1979). The resulting Aptian and Albian unconformities represent major stratigraphic

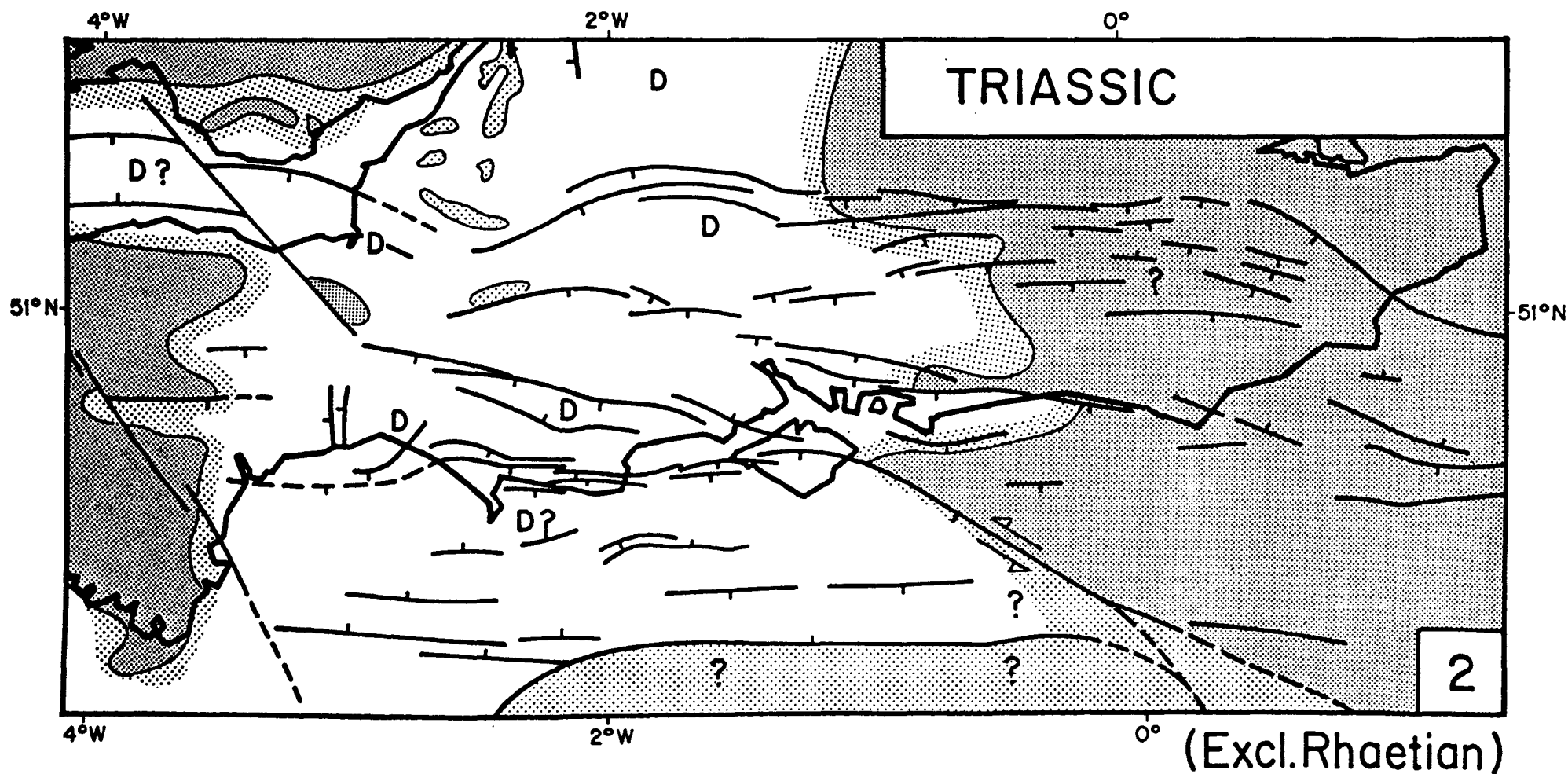


Fig. 3.8 Triassic Palaeogeography. Based mainly on Allen & Holl-
 oway (1984), Whittaker (1985), Lloyd et al., (1973),
 Cope (1984), and Holloway & Chadwick (1984).

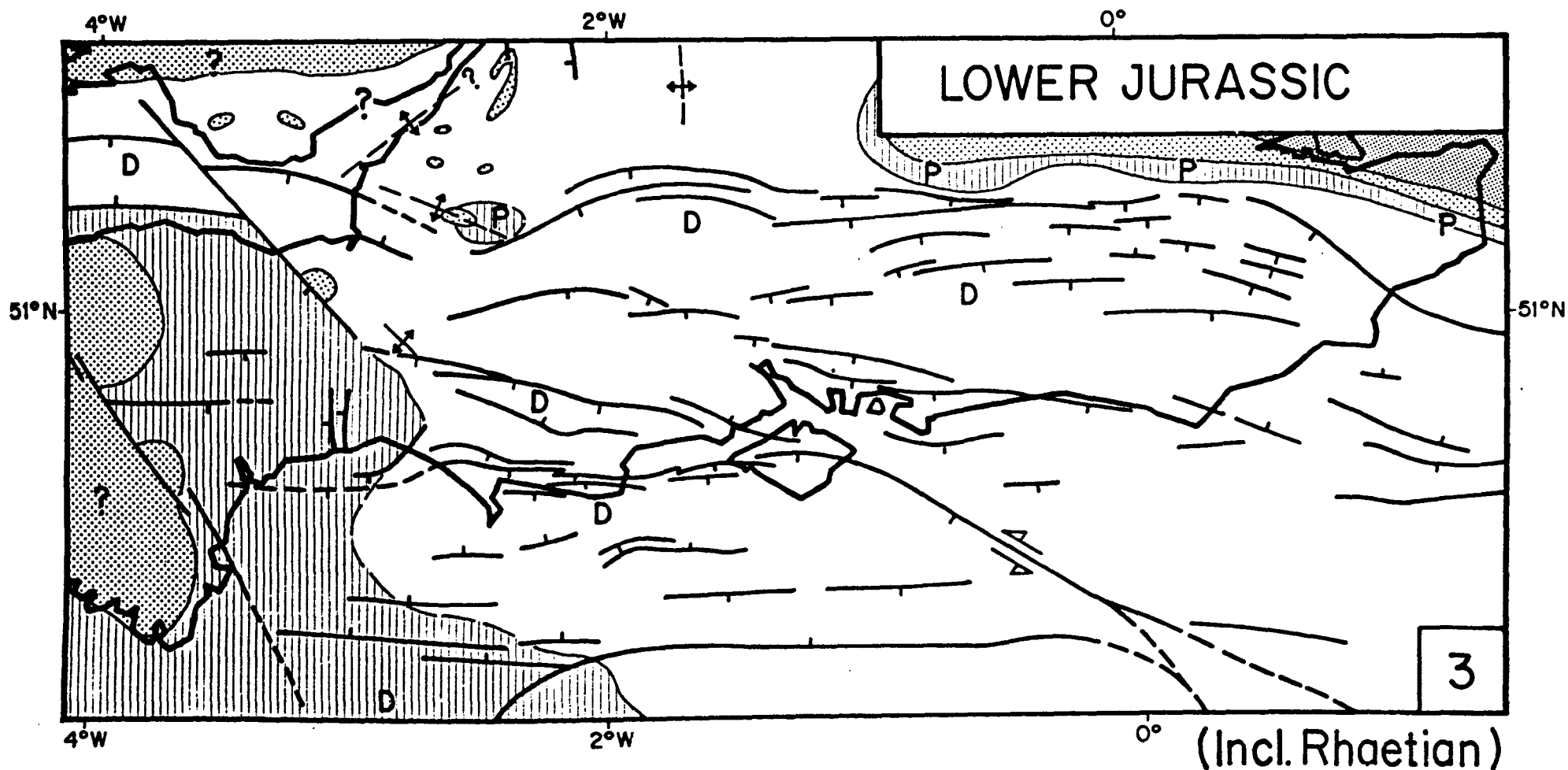


Fig. 3.9 Lower Jurassic Palaeogeography. Based mainly on Melville & Freshney (1982), Whittaker (1985), Sellwood & Sladen (1981), Kamerling (1979), Lloyd et al., (1973), Gallois & Edmonds (1965), Kellaway & Welch (1948), Cope (1984) and Worssam & Ivimey-Cook (1971).

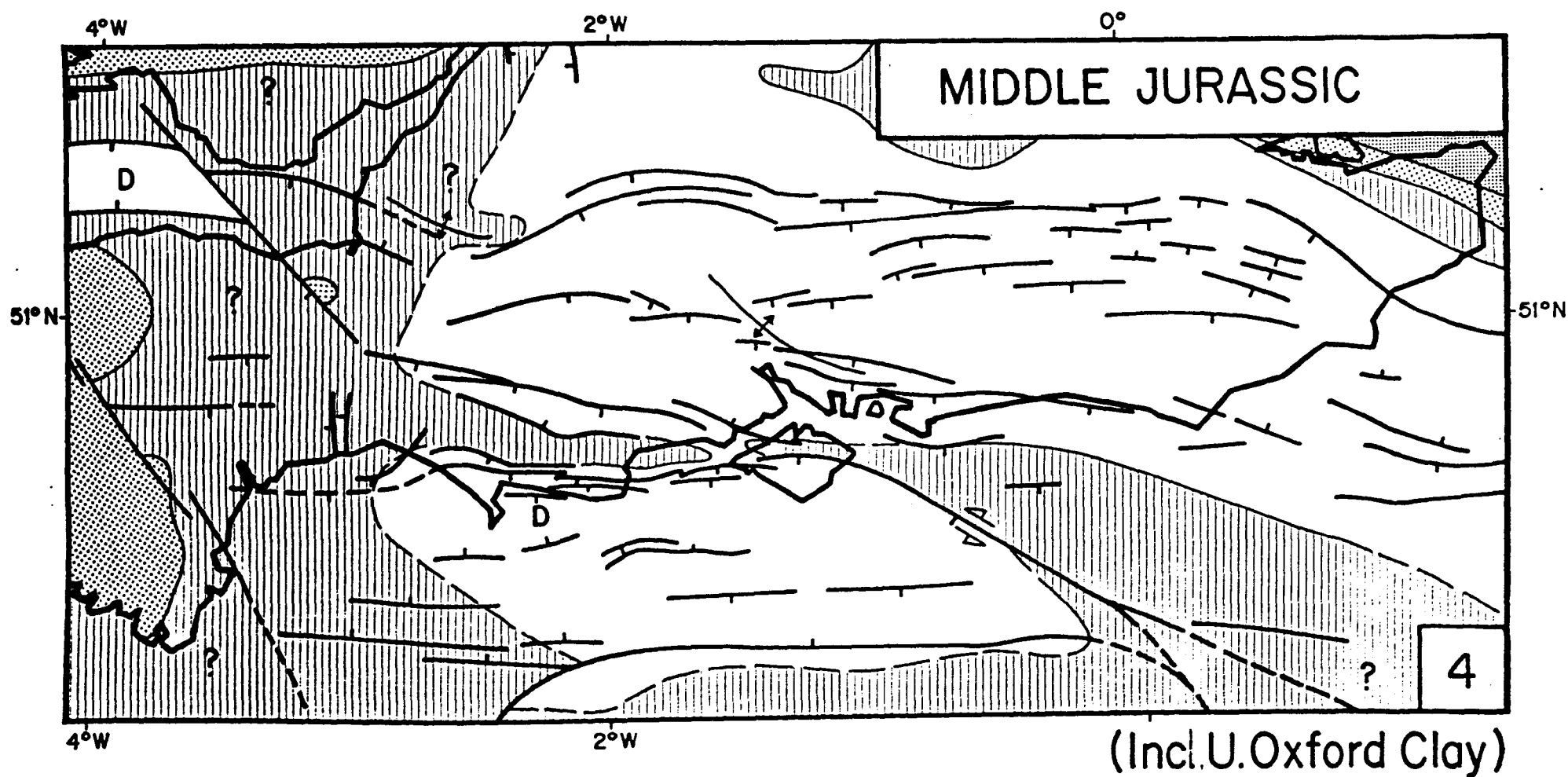


Fig. 3.10 Middle Jurassic Palaeogeography. Based mainly on Arkell (1933), Whitaker (1985), Melville & Freshney (1982), Sellwood et al., (1985), Penn (1982), Martin (1967), Sellwood & Sladen (1981) and Lloyd et al., (1973).

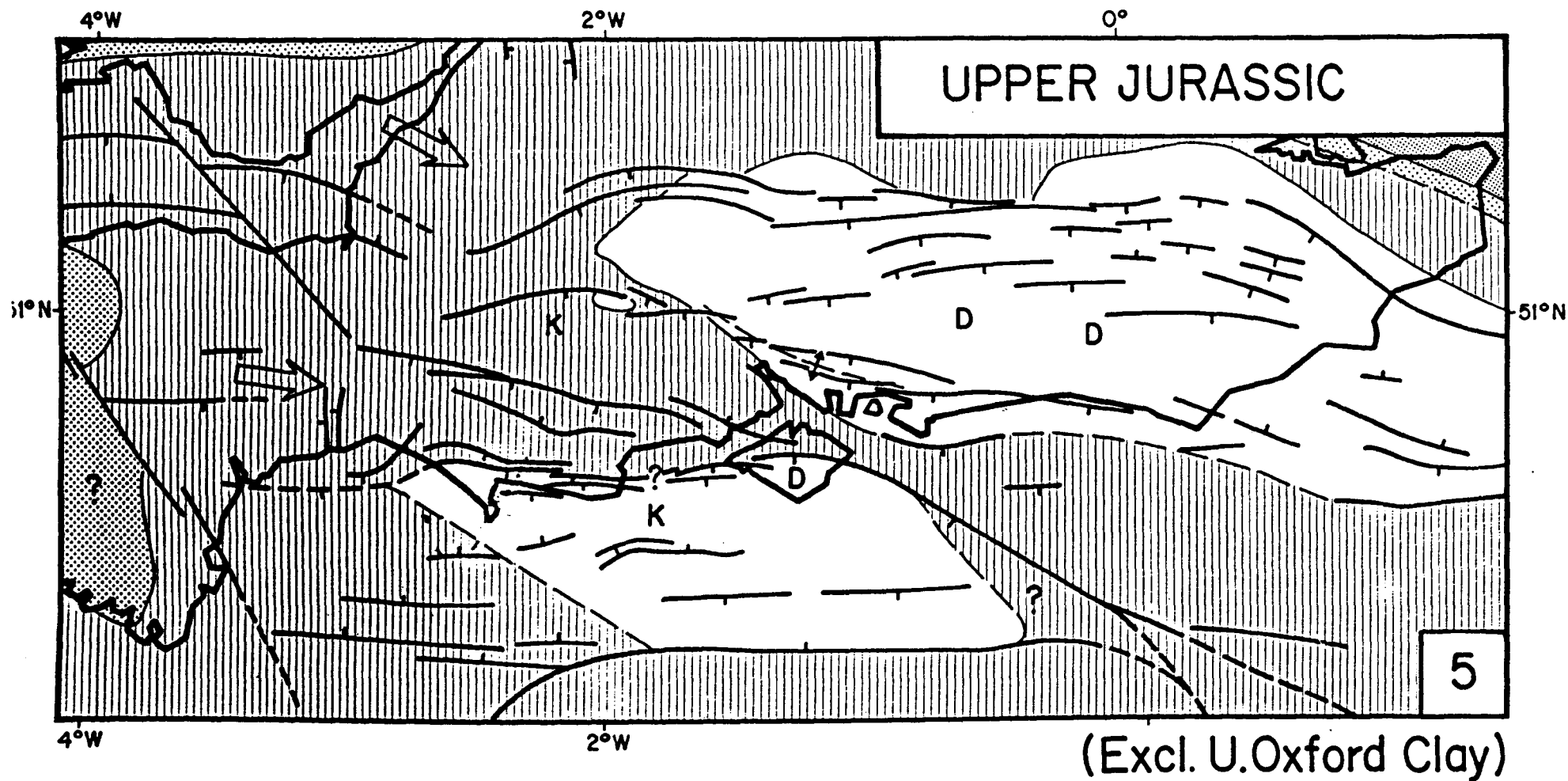


Fig. 3.11 Upper Jurassic Palaeogeography. Based mainly on Cox & Gallois (1981), Townson (1975), Whittaker (1985), Howitt (1964), Worssam & Ivimey-Cook (1971), Arkell (1947), Melville & Freshney (1982) and Lloyd et al., (1973).

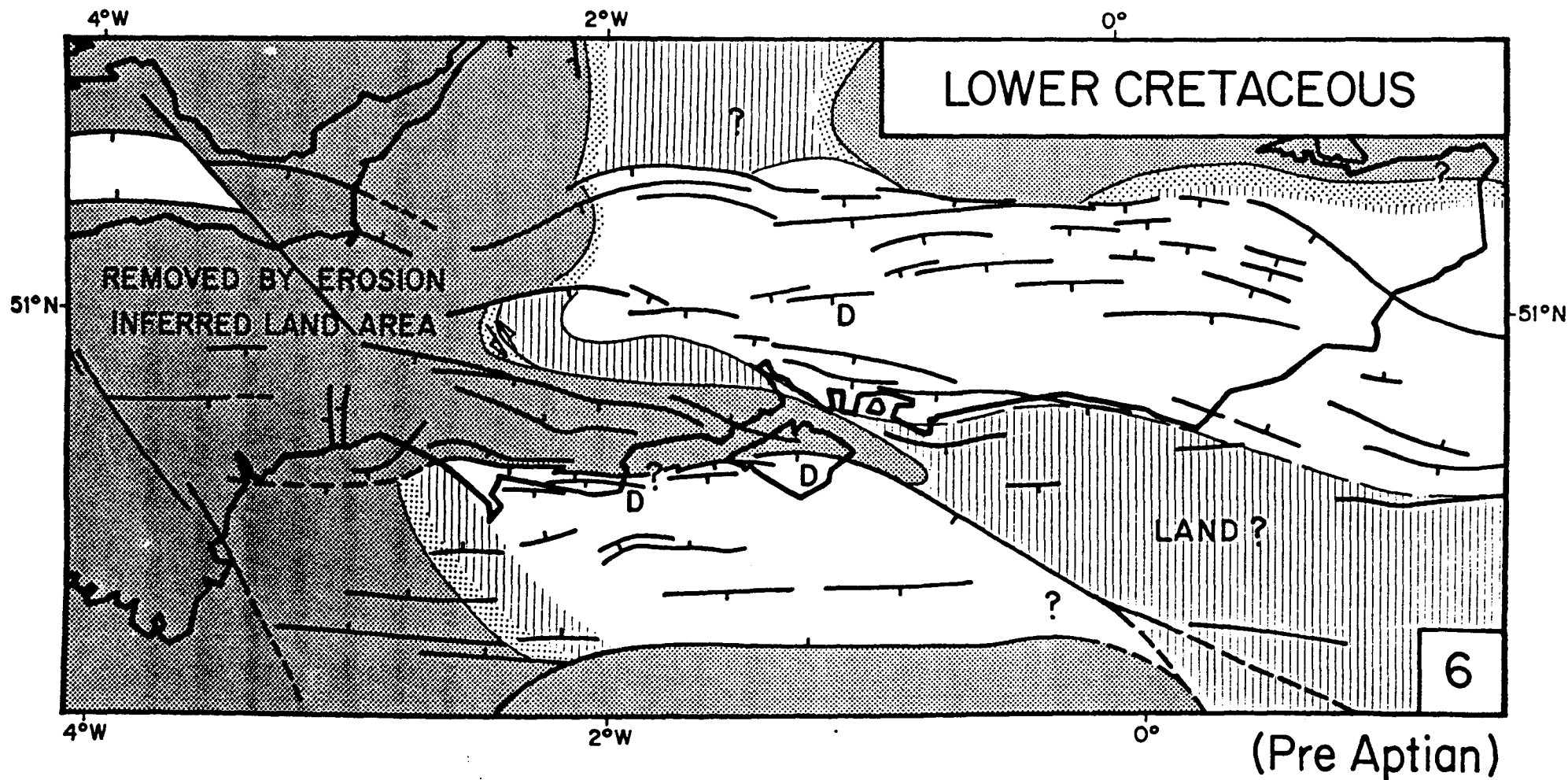


Fig. 3.12 Lower Cretaceous (Pre-Aptian). Based mainly on Allen (1981), Arkell (1947), Gallois & Edmonds (1965), Melville & Freshney (1982), Falcon & Kent (1960) and Worssam & Ivimey-Cook (1971).

breaks within all the basins of this region (c.f. Fig. 3.12 and 3.13). Their timing approximately coincides with the rift/drift transition within the Bay of Biscay and the North Atlantic (Soler et al., 1981; Talwani, 1978) respectively. We suggest that the increased sediment truncation towards the Bay of Biscay and Atlantic margins results from the rapid, but short-lived isostatic uplift of basement due to the thermal effects associated with continental rifting (c.f. the rift induced small-scale mantle convection of Steckler, 1985). The time difference between the Aptian/Albian unconformities possibly reflects the geographical setting of the Wessex Basin relative to each rifted margin (Bay of Biscay and Atlantic) and/or variations in rift-onset ages.

An alternative explanation of the Aptian/Albian unconformities, in terms of the isostatic rebound of the footwall following normal faulting within the Wessex Basin (e.g. Chadwick, 1985b) can hardly be expected to produce the observed distribution of the unconformities across north-west Europe. Neither can it explain the existence of the two discrete unconformities. For example, post-Aptian sedimentary units within the Wessex Basin progressively transgress the Aptian unconformity until they themselves are truncated in the Albian.

While continental rifting potentially explains the Aptian/Albian unconformities, it cannot explain the ubiquitous distribution of these unconformities within north-west Europe. Upper Jurassic-Neocomian continental rifting therefore, must be the response of a yet more fundamental tectonic process which affected all of western Europe. A useful kinematic explanation lies in the relative plate motion vectors between Africa and Europe recently defined by Livermore and Smith (1986; Fig. 3.14). From 173-119 Ma, the relative plate motion between Africa and

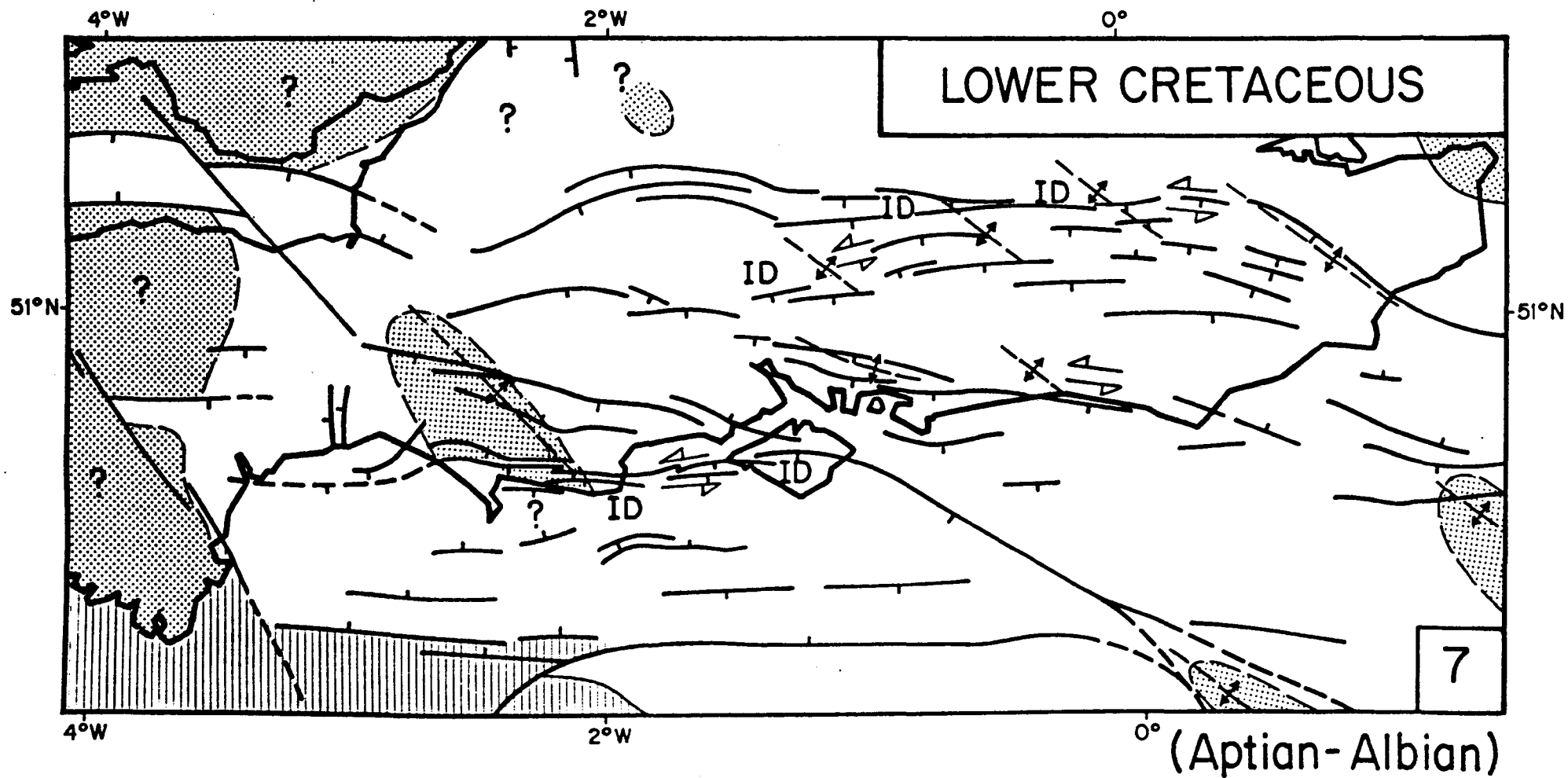


Fig. 3.13 Lower Cretaceous (Aptian-Albian). Based mainly on Drummond (1970), Owen (1975), Melville & Freshney (1982), Anderton et al. (1979) and Tresise (1961).

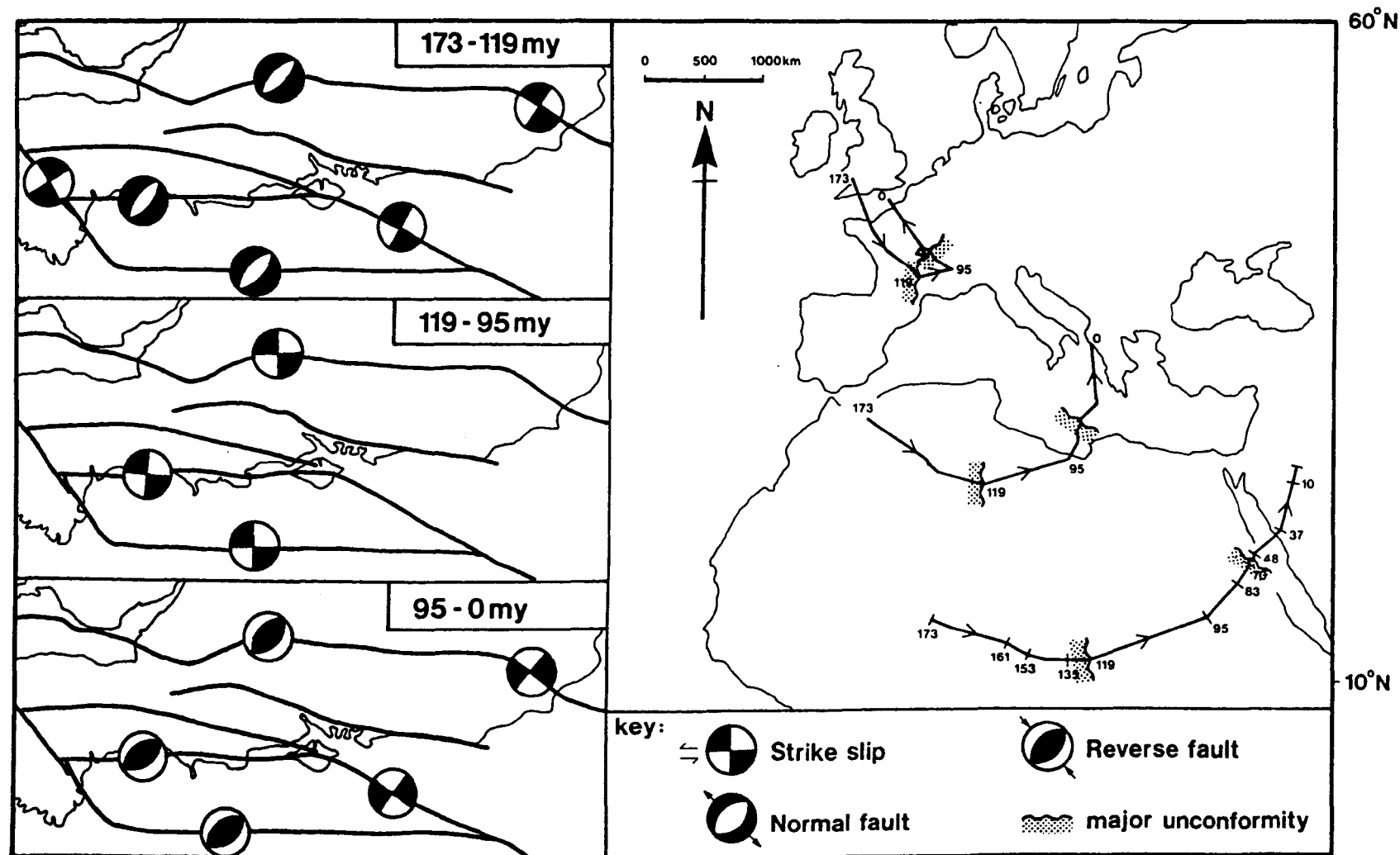


Fig. 3.14 Relative motions of Africa relative to Europe (after Livermore & Smith, 1986) compared to the main structural development of the Wessex Basin between 173 my and the present day. Schematic first-motion symbols (infilled, compressional quadrants; open dilatational quadrants) show the evolution in three main separate phases during the Mesozoic/Cenozoic.

Europe predicts a northwest-southeast sinistral motion within north-west Europe (Fig. 3.14). We believe that it is the resulting plate interactions implied in figure 7 which govern not only the rifting within the Bay of Biscay, but also the sinistral extension of northwest European basins in general (see Chapter 4).

Within the Wessex Basin, the lower Cretaceous (Aptian) is characterised by a major change in tectonic style (c.f. Figs 3.12 and 3.13) in which the northwest-southeast sinistral extension was replaced by east-west strike-slip movements (Fig. 3.13). Again, this transition in style correlates remarkably well with the observed relative change of motion between Africa and Europe at 119 Ma (Livermore and Smith, 1986; Fig. 3.14). East-west strike-slip motion is reflected as syn-sedimentary north-west trending swells above the basement faults (Figs 3.13 and 3.15). Similar upper Cretaceous syn-sedimentary folding indicative of east-west strike-slip motion, has been described by Drummond (1970) and Gale (1980).

East-west strike-slip motion continues to approximately 95 Ma, after which another major change occurs in the relative motion between Africa and Europe (Fig. 3.14). After that time, a general northwesterly convergence of the African continent with respect to Europe occurs until the present day (Fig. 3.14). We suggest therefore, that the initiation of inversion so characteristic of north-west Europe, may have started as early as 95 m.y. ago and is a direct consequence of the compression generated during the convergence between Africa and Europe (which of course, includes the Alpine/Pyrenean collisions).

3.5 Inversion

A. Timing of Inversion

As stated in the introduction, inversion implies a change in the polarity of structural relief, from a basinal area into a structural high (positive inversion) or a structural high into a basin (negative inversion). Positive inversion invariably relates to regionally induced compression but local inversion can also occur. For example, positive and negative inversion can be produced by transpression and transtension along strike slip faults respectively. Inversion of larger areas involving, for example, individual sub-basins, are more difficult to understand. In the Wessex Basin, both local and regional inversion has occurred.

As implied from figure 3.14, the initiation of regional inversion began in the upper Cretaceous (Laramide). All other inversion phases, such as the Styrian and Pyrenean phases of Ziegler (1982), are simply subsets of what can collectively be called "Laramide inversion".

B. Evidence for Laramide inversion

Since the upper Cretaceous, the relative motion between Africa and Europe predicts a northwest-southeast compression (Fig. 3.14). Dextral reactivation of favourably oriented strike-slip faults allowed the inversion of basins within north-west Europe. Evidence for the nature and timing of inversion is:

- 1) Marked erosion of the basin occurs between the upper Cretaceous and the lower Tertiary Wooldridge and Linton, 1938). Locally derived pebble (and hence proximal) suites eroded from the emerging basin were deposited on the former structural highs (c.f. Figs 3.15 and 3.16; Fig. 3.6) (Plint, 1982; 1983).

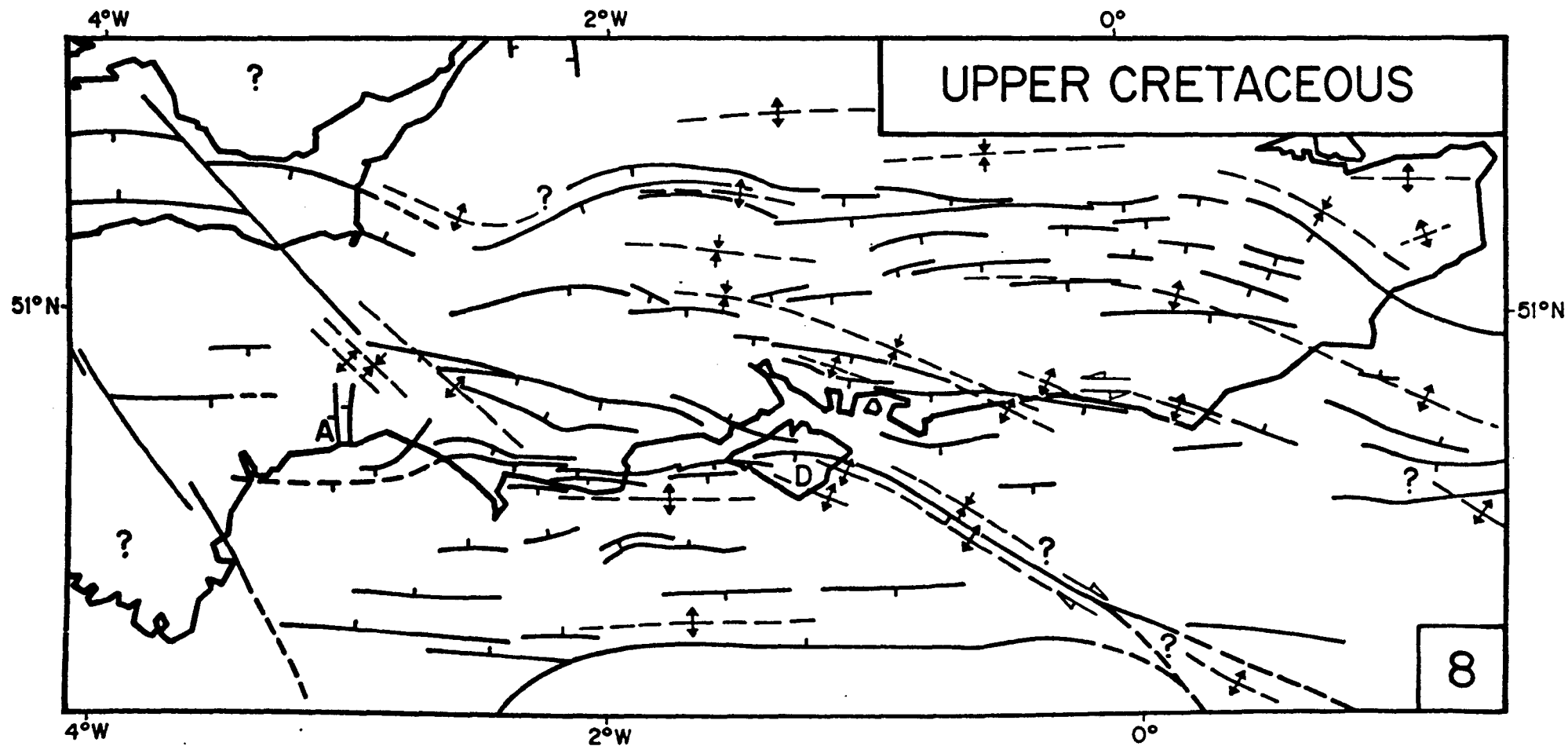


Fig. 3.15 Upper Cretaceous. Based mainly on Melville & Freshney (1982), Whittaker (1985), Drummond (1970), Gale (1980) and Anderton et al., (1979).

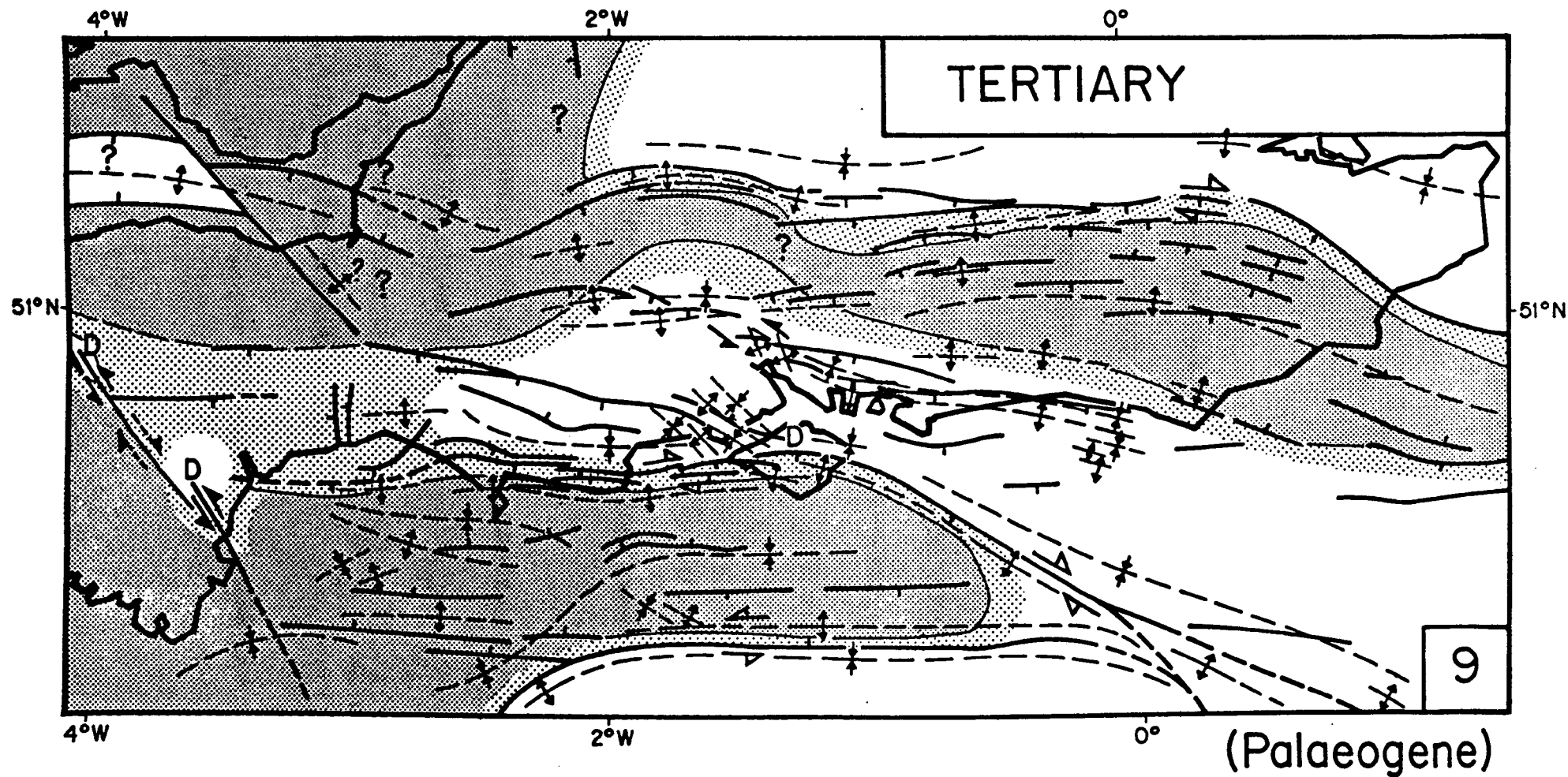


Fig. 3.16 Tertiary (Palaeogene). Based mainly on Flint (1982), Flint (1983), Curry et al., (1978), Laming (1982), Anderton et al., (1979) and Issac (1983).


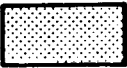

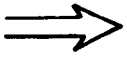
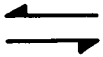
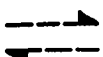
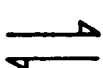
	Highs, areas of non - deposition and erosion
	< 50m Sediment
	Areas of Pre Aptian erosion (partly or total)
D	> 500m Sediment
ID	> 250m Sediment (Lower Cretaceous Aptian / Albian only)
K	Kimmerian erosion (outcrop or seismic)
P	Pre Upper Bajocian erosion
A	Upper Cretaceous active faulting
--†--	Intermittent active anticlinal fold axes
--‡--	Intermittent active synclinal fold axes
?	Unknown
	Encroaching land area (due to sea level fall and or uplift)
	Observed strike slip motion
	Observed later strike slip motion
	Inferred strike slip motion

Table 3.1 Summary of the symbols used in Figures 3.7 - 3.16.

- 2) There is a regional facies change across the basin from marine upper Cretaceous chalks to the non-marine late-Palaeocene fluvial sediments (Reading Formation, Fig. 3.6).
- 3) Major northwest-southeast chalk fissures along the Purbeck-Isle of Wight fault are infilled with Palaeocene terrigenous sediments.
- 4) East-west stylolites in the Purbeck Chalk (i.e. upper Cretaceous) date the onset of a compressional event (Jones et al., 1984).
- 5) The Palaeocene onlap pattern within the marine embayment north of the London Platform fault implies that the Weald Basin was topographically high during this period (see Bennison and Wright, 1969).
- 6) Local Eocene palaeosoils, developed on upper Cretaceous Chalk immediately south of the Purbeck-Isle of Wight fault, are in marked contrast to the marine sediments of the same age to the north of the fault (Plint, 1983).
- 7) Upper Cretaceous depocentre migration towards the northern and southern margins of the Weald basin (Mortimore, pers. comm.) reflect an uplift of the basin centre.
- 8) The Tertiary basins developed on former Mesozoic highs (c.f. Figs 3.1 and 3.16).
- 9) The timing of inversion within the Wessex Basin correlates with the inversion observed in adjacent basins (Ziegler, this volume).

Laramide inversion is generally manifested as monoclines around the basin margins. These monoclines are located along earlier Mesozoic growth faults (Stoneley, 1982). The amplitude of the monoclines have increased with time, culminating in the Oligocene/Miocene. The best

developed inversion structures within the Wessex Basin are those displayed across the Purbeck-Isle of Wight fault (Fig. 3.17). In effect, the inversion along this fault is primarily the result of Laramide transpression (east-west dextral strike-slip).

Reverse movements along earlier Mesozoic southward dipping growth faults resulted in northward facing monoclinal flexures. Although partial reversal was achieved along some of these faults (exceeding 200m), new lower angle reverse faults developed in the footwall (see Ridd, 1973) similar to the model studies outlined by Koopman (1986). In turn, reverse growth fault movement was the consequence of basement fault reactivation as thrusts. As an interesting aside, the stepping back of the lower angle faults has probably resulted in the breaching of hydrocarbon accumulations within the Wessex Basin immediately north of the major east-west growth faults. Therefore, major hydrocarbon plays are likely to be located a short distance behind the major growth faults. The degree of step-back will directly relate to the amount of inversion.

Whilst the northwest-southeast faults accommodated the bulk of the convergence between Africa and Europe, east-west faults allowed secondary accommodation by dextral oblique reverse slip (transpression, Fig. 3.17). In a more regional sense, the polyphase motion of the advancing Alpine nappe systems probably represented the ultimate cause for the intermittent uplift of basins in the deforming foreland. Major late Oligocene/Miocene uplift in the Wessex Basin coincided with the emplacement of the Helvetic nappes (1986).

The discussion so far has concentrated on basin depocentre inversion, the driving mechanism of which is related to the reactivation of basement thrust faults. However, Mesozoic structural highs also under-

PULL
OUT

went inversion to become Tertiary depocentres. Characteristically, these depocentres tend to deepen towards the major basement faults (in particular, the Purbeck-Isle of Wight fault) and suggests that transpression probably provides the driving subsidence for structural high inversion. By analogy to thrust sheet emplacement, reverse fault reactivation essentially emplaces a load onto the footwall side of the fault, the footwall basement flexing to produce a "mini" foreland basin. The degree of structural high inversion will depend on the amount of overthrusting, the wavelength of the overthrust block, and the flexural rigidity of the basement.

Following the culmination of inversion in the Oligocene/Miocene, sedimentation became severely restricted. Evidence for the former extent of Neogene sedimentation is confined to isolated outliers such as the infilled chalk solution pipes of the Pliocene Lenham Beds along the northern margin of the Weald Basin (Rasmussen, 1966). Major mesofractures observed throughout southern England also largely developed during this culmination and are concordant with present day in-situ stress directions (Schmitt, 1981; Batchelor, 1984). The fact that the observed mesofracturing has been produced almost entirely during the inversion phase is somewhat surprising. Polyphase rifting should induce a penetrative fabric within any pre-existing sediments, with internal deformation decreasing up-sequence (Dewey, 1982). However, as mesofracturing is primarily the result of Helvetic phase inversion, joint development appears to be independent of the earlier basin extensional phases, at least within the Wessex Basin (see Chapter 5).

The general convergence of Africa and Europe from 95-0 Ma adequately explains the in-plane compression and hence inversion of northwest Euro-

pean basins. While northwest-southeast fault reactivation is regionally demonstrable, small-scale inversion complexities also occur. We will illustrate some of these complexities by investigating the development of Tertiary pull-apart basins along the Sticklepath fault zone (Figs 3.18 and 3.19). The Sticklepath fault zone controlled the development of the western Wessex Basin and represents a reactivated Variscan basement wrench fault. In particular, sinistral motion throughout the late Palaeozoic and Mesozoic allowed development of the Channel sub-basin. During the Eocene-early Oligocene, small sinistral pull-apart basins (Bovey, Stanley-Bank and Petrockstow) formed between the main transform relays. Later dextral movement along this fault is indicated by the right-lateral offset of Variscan granites and intrabasinal thrusting and folding (Bristow and Hughes, 1971). As mid-Oligocene sediments are involved in the thrusting, the compression appears to correlate with the Oligocene/Miocene inversion culmination.

The formation (or modification) of Tertiary basins along the same northwest-southeast trend during apparent dextral motion is not limited to the Sticklepath fault (see Chapter 4). Other examples include the Bristol Channel, Kish Bank, Ulster Basins and Sea of Hebrides Trough. Another example of this sinistral motion (and apparent tension) during Tertiary inversion is the emplacement of the Eocene Lundy Granite Complex. This granite possibly reflects intracrustal intrusion during the opening of the crust between major left stepping faults. We have therefore, an apparent enigma in that during general basin inversion (Laramide), pull-apart basin and granite emplacement is also occurring.

Complexities of the convergence between Africa and Europe since the Cretaceous may offer an explanation for this enigma. While general

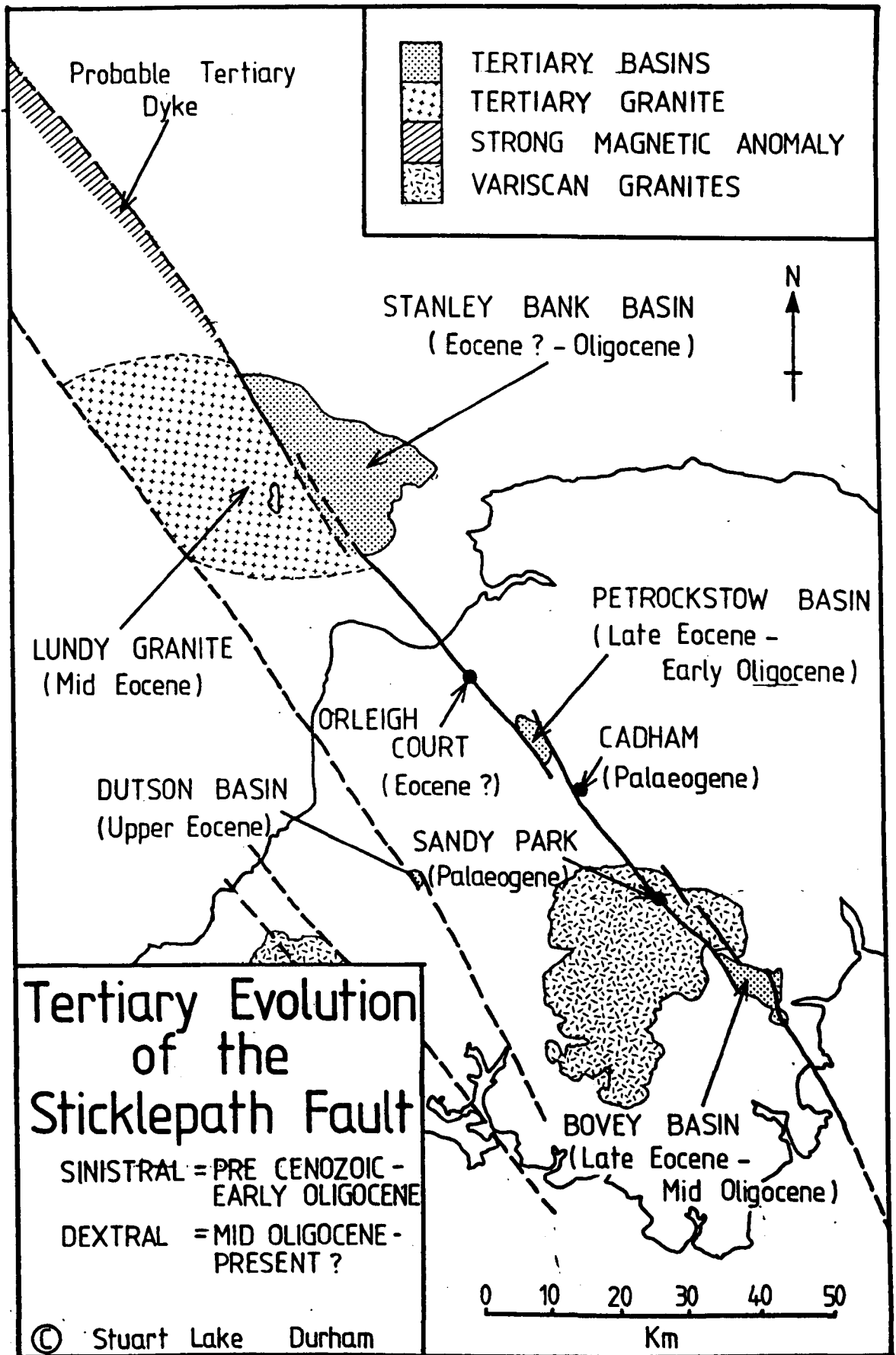


Fig. 3.18 Tertiary evolution of the Sticklepath fault zone. Sinistral pull-apart development of the Tertiary basins, other more local deposits developed along the same structure.

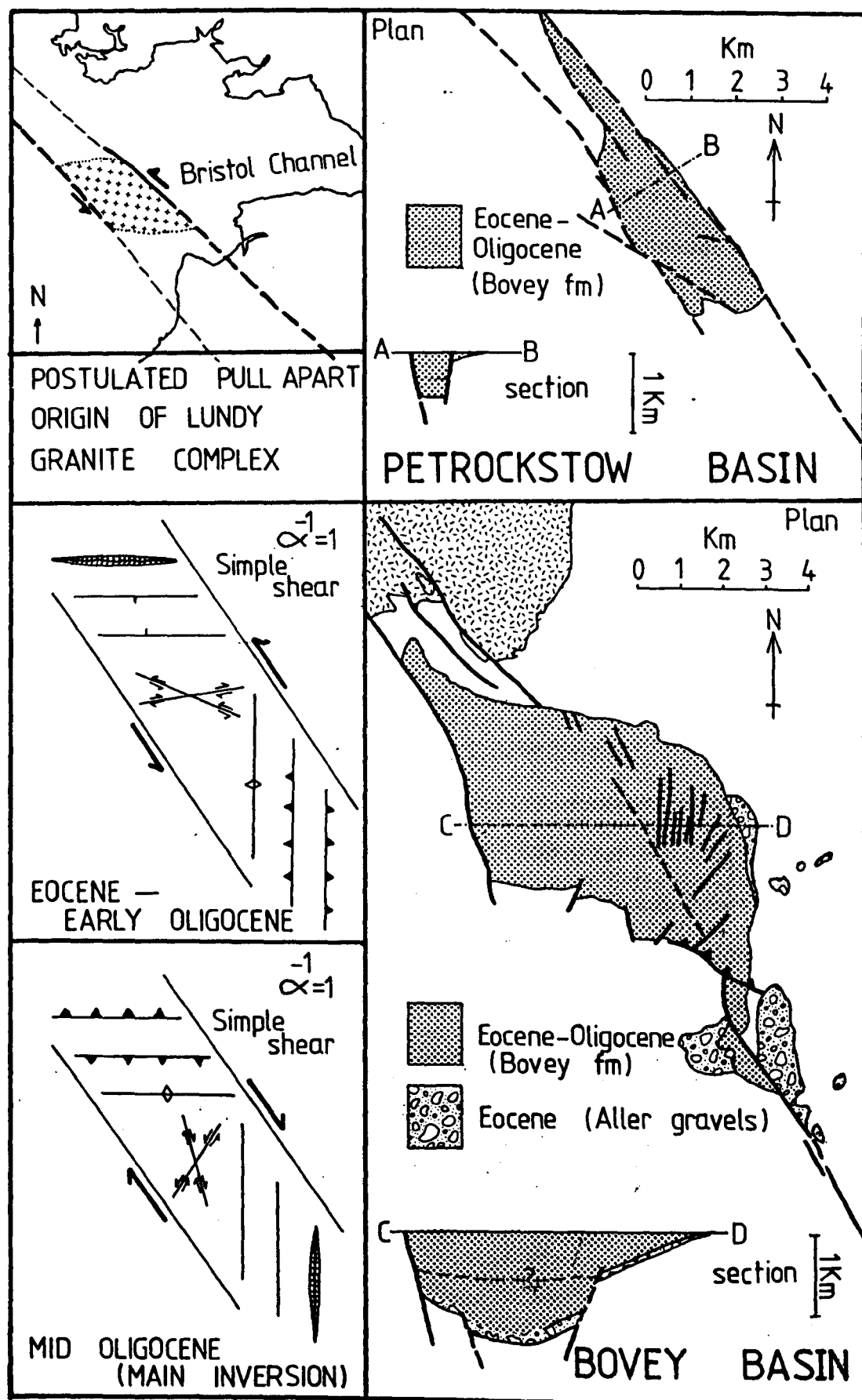


Fig. 3.19 Detailed structure of the main features developed along the Sticklepath fault zone. Plan and cross section views of the Bovey and Petrockstow basins are shown. Terminology summarized on Fig. 3.18.

convergence has occurred between Africa and Europe since the Cretaceous, small excursions occurred during the Maastrichtian-Oligocene period (Fig. 3.14). In particular, the motion digressed from northwest-southeast dextral shear to firstly a northeast-southwest shear, followed by increasing re-alignment towards the northwest-southeast trend. It was exactly within this time frame that the basins and granite were formed/emplaced along the Sticklepath fault. Basin formation ceased during the Oligocene as extension was replaced by regional compression. This same digression may help explain the northeast-southwest en-echelon folds north of the Purbeck-Isle of Wight fault (see Daley and Edwards, 1971; Plint, 1982) (Fig. 3.16).

Intracrustal decollements, while playing a major role in Wessex Basin inversion, may also have significant regional implications. The existence of intracrustal decollements within the European foreland (Fig. 3.5) facilitates not only the general development of small basins by hanging-wall collapse, but also the mobility of upper crustal blocks over considerable distances across a foreland. Evidence for the non-synchronicity of inversion across the European foreland is clearly displayed in the relative progression of basin inversion from the southeast towards the northwest. Shortening associated with Alpine compression inverted the Hunsruck-Taunus area in the upper Cretaceous (e.g. Ziegler, 1986; Meissner et al., 1984), migrated northwesterly to eventually invert the Channel Basin in the lower Tertiary, and finally the Bristol Channel and Celtic Sea Basins in the middle Tertiary (Ziegler, 1982).

3.6 Present Structural Style

The offshore stratigraphy of the Channel Basin is summarised in figure 3.17. Tertiary east-west monoclinial flexures and antiforms

identify the position of underlying Mesozoic growth faults and reveal the pattern of Mesozoic block boundary faults. Figure 3.17 follows a north-south transect across the Purbeck-Isle of Wight fault and clearly shows the characteristic signal of Wessex Basin inversion - the transpressional flower-structures and listric fault roll-over inversion to anticlines. The synchronous development of intrabasinal antithetic and synthetic faults accompanying hanging-wall basement collapse is clearly evident. While figure 3.17 shows the formation of monoclinal flexures across the Purbeck-Isle of Wight fault, along strike, local east-west periclines and synclines are produced due to growth fault reactivation as intrabasinal thrusts (indicating the development of complex ramp/flat geometries; along strike Vann, pers. comm.).

The present structural style of the Wessex Basin is clearly seen in the six north-south cross-sections of figures 3.20 and II.3.2. The cross-sections demonstrate the complexity and variability of both the inversion related structures and the earlier extensional features. Sections 1-3 show the inverted Weald Basin becoming increasingly asymmetric westwards towards the Vale of Pewsey Basin. Section 3 highlights the Tertiary depocentre developed above an attenuated Mesozoic sequence. Section 4 marks the transitional nature of the Wessex Basin from the Weald Basin to the Winterbourne Kingston Trough. Purbeck-Isle of Wight fault transpression, and its effects on controlling structural high inversion is particularly well-documented in section 5. Tertiary transpression has uplifted the Channel Basin and in so doing, has created an asymmetric 'foreland-type' basin. Major uplift has also occurred along the Mere fault which bounds the Wessex Shelf from the Vale of Pewsey Basin. Section 6 depicts the decreasing structural control on

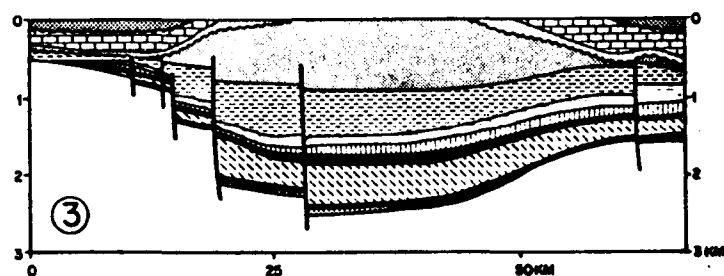
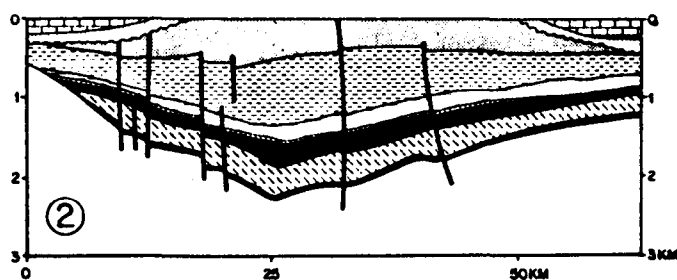
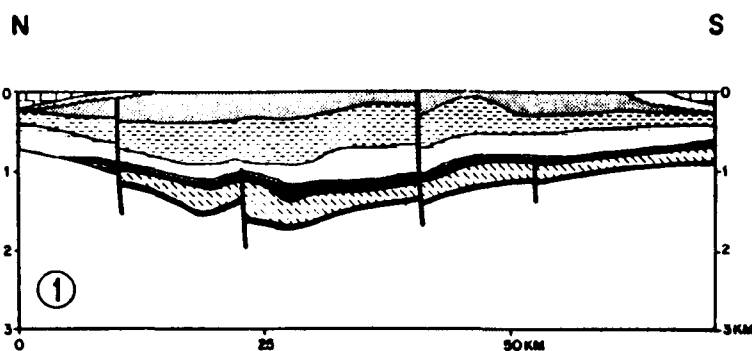
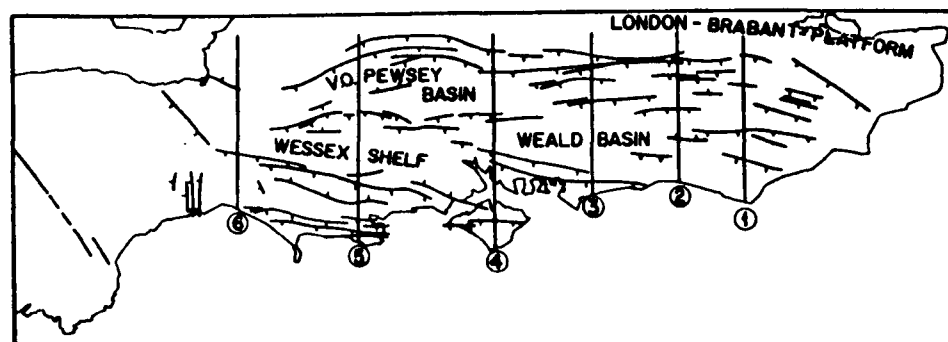


Fig. 3.20 Representative cross sections across the onshore portion of the Wessex Basin based on the isopachyte data of Whittaker (1985).

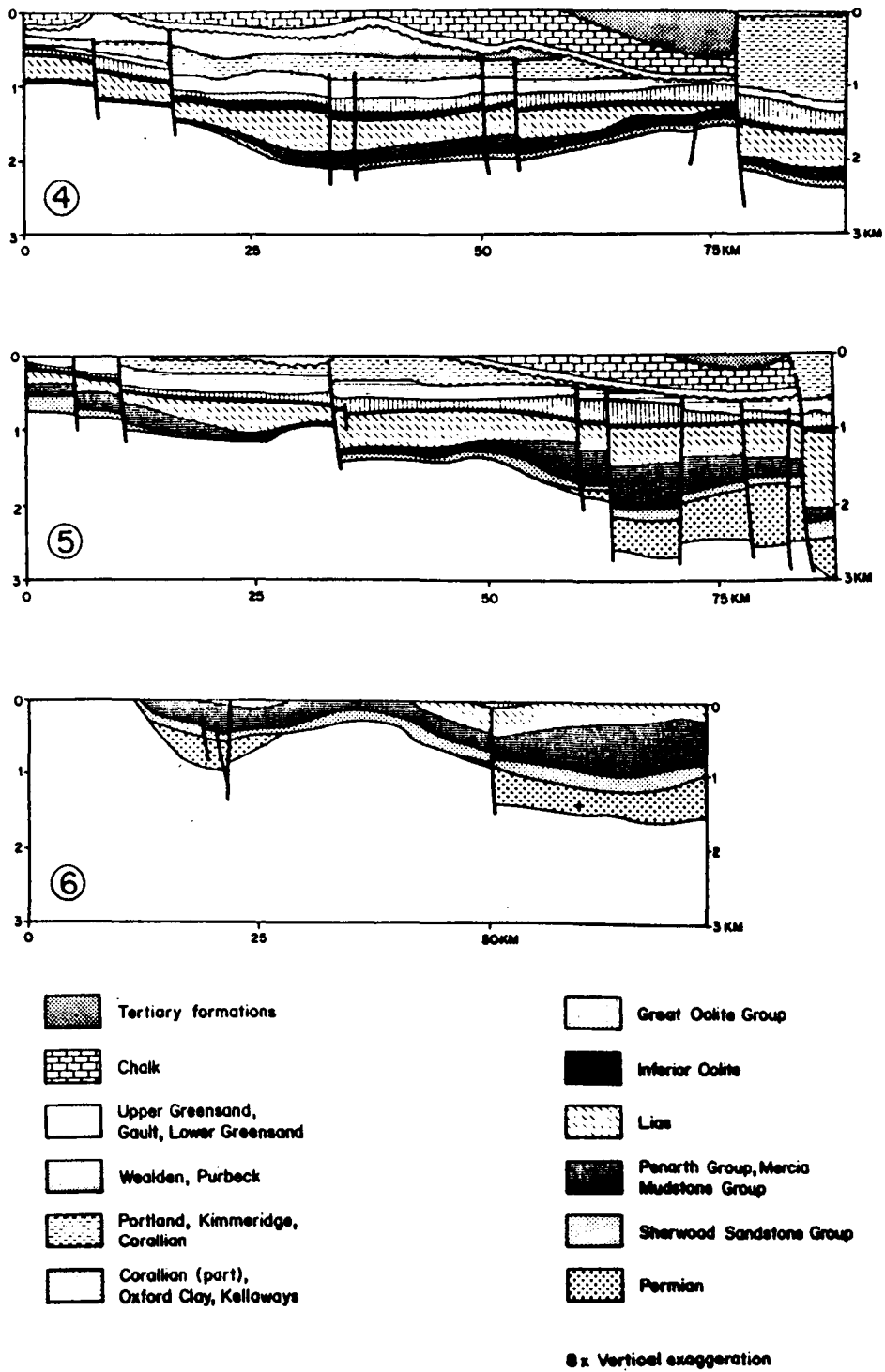


FIG. 3-20 contd....

peripheral basin development while showing the rift-type continuation of the Winterbourne Kingston Trough towards Cornubia.

While dextral motion of the northwest-southeast faults results in local pull-apart basin inversion, west-northwest faults (e.g. the Pay de Bray fault) display transpressional antiforms. Inversion induced thrusting generally occurs on the footwall side of the major east-west growth faults. Locally, particularly in the Isle of Wight region, complex three dimensional fault geometries (as seen in seismic reflection profiles) can be explained in terms of local oblique slip movement associated with uplift of the Channel Basin.

Present hydrocarbon exploration is largely targeted towards pre-Aptian tilted fault blocks developed on the footwall side of the major east-west growth faults, and away from inversion related structures which are likely to breach potential accumulations on the immediate footwall side (e.g. Wytch Farm oil field; c.f. Colter and Havard, 1981).

3.7 Conclusions

From the structural development and inversion history of the Wessex Basin outlined above, the following conclusions can be made:

- 1) The Wessex Basin is divisible into four sub-basins, each formed as a result of the normal reactivation of Variscan thrust and wrench faults which compartmentalised the basement.
- 2) Extension was essentially polyphase and initially restricted to the west, beginning in the Permian and Triassic but migrating to the east during the Jurassic and Lower Cretaceous.
- 3) The structural evolution of southern England is understandable in terms of major listric growth faults, detaching on reactivated

Variscan thrusts.

- 4) The Wessex Basin, and its rhomboidal shaped sub-basins, developed as a result of northwest-southeast sinistral strike-slip motion (with offsets of only a few kilometers). During inversion, these same faults underwent dextral motion, thereby significantly modifying the sub-basins.
- 5) Each major extension phase has an associated unconformity, viz., Permo-Triassic, Kimmerian, and Aptian-Albian unconformities respectively (Fig. II.3.3). The Kimmerian unconformity (Oxfordian-Kimmeridgian) owes its existence to the regional adjustment of the lithosphere during local crustal extension. This unconformity, therefore, was locally developed. In contrast the Aptian/Albian unconformity within the Wessex Basin owes its existence to the thermal effects (most probably small scale convection) associated with rifting in the Bay of Biscay and the North Atlantic.
- 6) The upper Cretaceous, formerly thought to be a period of relative stability, appears to be a time of local en-echelon periclinal formation resulting from east-west sinistral motion.
- 7) Major inversion took place initially in the upper Cretaceous (Laramide phase) and culminated in the Oligocene/Miocene (Helvetic phase) with the development of major monocline^{al} flexures above former Mesozoic growth faults. In particular, the same structures which facilitated basin initiation in the Permian-lower Cretaceous also induced intrabasinal compression (inversion) during the upper Cretaceous-early Tertiary. Syn and post inversion evolution of the Wessex Basin was dominated by mesofracture development throughout southern England.

- 8) Inversion was demonstrably intermittent, with former Mesozoic depocentres becoming structural highs and hence forming local source areas. The amount of uplift is greatest in the southern part of the Wessex Basin adjacent to the Purbeck/Isle of Wight fault.
- 9) Inversion related structures allowed the development of new, lower angle reverse faults in the footwall block.
- 10) Reverse oblique-slip motion along the major basin boundary faults during inversion resulted in complex three dimensional fault geometries. Significant hydrocarbon accumulations were probably breached at this time.
- 11) The Sticklepath fault zones displays a complex history. During the Tertiary, left lateral pull-apart basins developed synchronously with the Lundy Granite Complex. Both features developed between left lateral intracrustal relays.
- 12) The structural development of the Wessex Basin, both during extension (basin formation phase) and compression (inversion phase) (Tables 3.2 and 3.3), is dominated by the form of the plate tectonic convergence of Africa and Europe. In particular, the relative plate motions predicts a northwest-southeast sinistral motion until the Aptian, east-west sinistral motion from the Aptian to Cenomanian, and northwest-southeast dextral motion from the Cenomanian to the present day. Small digressions of the relative plate motions, especially during the lower Tertiary, help to explain complexities observed along the basin boundary faults.

PULL
OUT

PULL

OUT

CHAPTER 4

RELATIONSHIP OF THE WESSEX BASIN TO THE TECTONICS OF WESTERN EUROPE

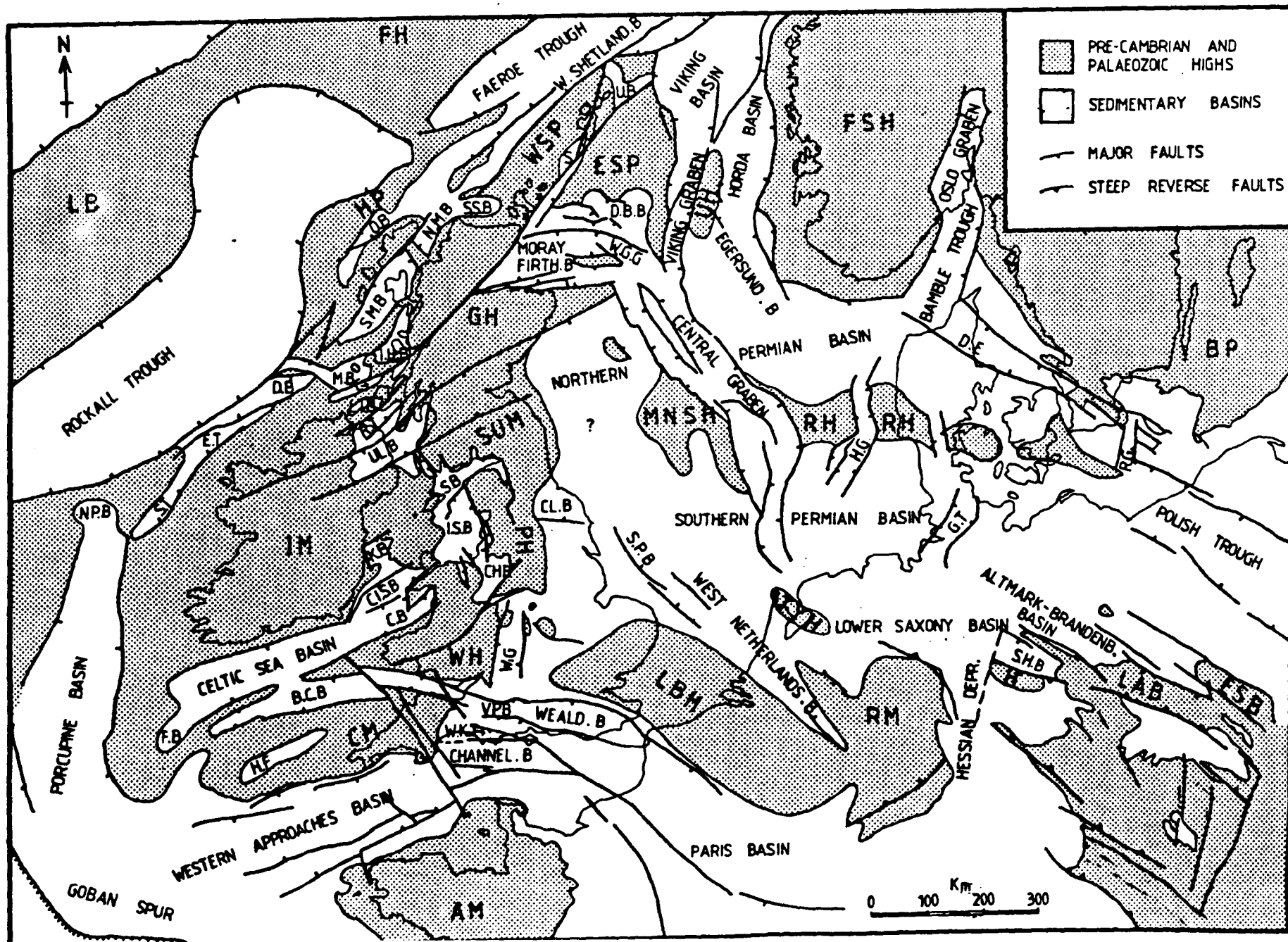
4.1 Introduction

The detailed structural evolution of the Wessex basin has already been outlined, however, it is important to consider this synthesis in a wider context and compare and contrast the basin evolution to the postulated evolution of the other Mesozoic basins, grabens and troughs of Western Europe.

Firstly it is important to consider the basement configuration following the Palaeozoic consolidation of Pangaea, and to what extent the structural controls influence subsequent basin evolution, in the subsequent dynamic tectonic framework. Secondly it is important to briefly summarize the main similarities and differences of the Wessex basin to other Mesozoic basins around Western Europe. These comparisons are clearly important when considering the subsequent Permo-Triassic instability and break up of the Pangean supercontinent and the role in which inherent crustal weaknesses from earlier deformations control the subsequent Mesozoic basin configuration. The dynamics of Mesozoic basin formation can be determined from the synthesis of a wide variety of geological data sources and is clearly important as an aid to developing future exploration strategies. Lastly and most importantly, consideration and integration of the synchronous Late Palaeozoic to Cenozoic plate tectonic evolution of the European area must be rationalized and its importance to predictability and testability outlined.

The basement configuration is well illustrated in a series of tectonic summary maps compiled by Ziegler (1982, 1983) (Fig. 4.1 and Table 4.1). With the exception of isolated outliers in northern England

Fig. 4.1 Late Palaeozoic/Mesozoic basin configuration of Western Europe (After Ziegler, 1982).



AM	ARMORICAN MASSIF
BP	BALTIC PLATFORM
CM	CORNUBIAN MASSIF
ESB	EAST SUDETIC BLOCK
ESP	EAST SHETLAND PLATFORM
FH	FAEROES HIGH
FSH	FENNO SCANDIAN HIGH
GH	GRAMPIAN HIGH
H	HARZ HIGH
HP	HEBRIDES PLATFORM
IM	IRISH MASSIF
LAB	LAUSITZ BLOCK
LB	LOUSY BANK
LBH	LONDON BRABANT HIGH
MNSH	MID NORTH SEA HIGH
PH	PENNINE HIGH
RH	RINGKOBING FYR HIGH
RM	RHENISH MASSIF
SUM	SOUTHERN UPLAND MASSIF
TYH	TEXEL YSSELM HIGH
UH	UTSIRA HIGH
WH	WELSH HIGHLANDS
WSP	WEST SHETLAND PLATFORM
BCB	BRISTOL CHANNEL BASIN
C	COLONSAY BASIN
CB	CARDIGAN BASIN
CHB	CHESHIRE BASIN
CISB	CENTRAL IRISH SEA BASIN
CL.B	CLEVELAND BASIN
DB	DONEGAL BASIN
DBB	DUTCH BANK BASIN
DE	DANISH EMBAYMENT
ET	ERRIS TROUGH
FB	FASNET BASIN
GT	GLUCKSTADT TROUGH
HF	HAIG FRAS DEPRESSION
HG	HORN GRABEN
IHB	INNER HEBRIDES BASIN
ISB	IRISH SEA BASIN
KB	KISH BANK BASIN
LIB	LOCH INDAAL BASIN
M	MALIN BASIN
NMB	NORTH MINCH BASIN
NPB	NORTH PORCUPINE BASIN
OB	OUTER HEBRIDES BASIN
RG	RHONE GRABEN
RT	RATHLIN TROUGH
S	SOUTH SHETLAND BASIN
SB	SOLWAY BASIN
SHB	SUBHERCYNIAN BASIN
SMB	SOUTH MINCH BASIN
SPB	SOLE PIT BASIN
SSB	SULE SGEIR BASIN
ST	SLYNE TROUGH
ULB	ULSTER BASIN
VPB	VALE OF PEWSEY BASIN
WG	WORCESTER GRABEN
WGG	WITCH GROUND GRABEN
WKT	WINTERBORNE KINGSTON TROUGH

Table 4.1 List of all the basins and structural highs shown figure 4.4

and the Midland Valley of Scotland, Carboniferous rocks mostly lie immediately south of the east-west mid North Sea high. To the north of the high the basement dominantly comprises lower Palaeozoic rocks deformed in the Caledonian Orogeny.

This orogeny followed late Pre-Cambrian continental rifting and separation, Iapetus subduction and late Silurian/Early Devonian Iapetus closure (Phillips et al., 1976) and terrane accretion (Bluck, 1984): these processes resulting in the formation of the Laurasian Super continent. The major faults in the system are northeast-southwest (eq. Great Glen Highland Boundary fault).

Less significant but still important are a series of northwest-southeast and east-west fracture sets, the former, at least in part, has a possible Pre Caledonian origin and may have accommodated stresses related to sinistral movement along the northeast-southwest fracture set (Watson, 1984). The later fracture set which may also be Caledonian (Watson, 1984), were significant in controlling of later basin configuration and structural development (see Threlfall, 1981).

Variscan deformation may have been the result of complex dextral megashear motion across Europe that joined the southern end of the Urals to the Alleghenides (Arthaud & Matte 1977; Badham, 1982). This dominantly overprinted the earlier Caledonian deformation particularly in the south. With the termination of Iapetus subduction in the early Devonian (Ziegler, 1984) significant extension, wrenching, back-arc rifting and associated volcanism occurred. Pre-existing Caledonian weaknesses were reactivated (eq Midland Valley, Great Glen fault) although postulated large scale sinistral motions (Kent & Opdyke 1979) are not now thought to have occurred (Kent & Opdyke, 1985). The Variscan

Orogeny probably resulted from the Early Carboniferous closure of palaeo-Tethys between Gondwana and Laurasia (Zieqler 1984). This resulted in northe^weasterly thrust propagation across the west central Europe. During the latest Westphalian/earliest Stephanian major east-west right lateral motion resulted in a complex pattern of northwest-southeast dextral strike slip faults (Arthaud & Matte 1977).

The dominant structural grain is therefore purely dependent upon the relative location of the study area with respect to earlier deformations. Thus south of the Variscan front, Caledonian or earlier structures are rarely expressed except where pre Variscan structures have propagated up through the thin-skinned Variscan decollement (see Shackleton, 1984). The dominant Caledonian grain north of the front locally displays clear Variscan overprint (e.g. Arthurton, 1984), such as in the Moray Firth and other parts of Scotland (see Threlfall, 1981; Watson, 1984).

Details on individual basins are more fully summarized in Illing & Hobson (1981) Naylor & Shannon (1982) and Zieqler (1982). However it is important here to consider the wider implications of their results, comparing and contrasting the major distinguishing features of the basins around the United Kingdom Continental Shelf (UKCS), with already outlined evolution of the Wessex basin. This is outlined below.

A. Western Approaches Basin

This basin trends east-northeast approximately parallel to Variscan aged structures in southwest England. The basin is a southward dipping half-graben (Fig. 2.9) comprising essentially a complete Permo-Triassic to Neogene sedimentary sequence. This was disturbed by the Aptian/Albian

unconformity which displays increasing truncation to the southwest, and Late Cretaceous/Tertiary inversion (see Chapter 3). Major east-northeast growth faults are probably offset by northwest-southeast transform faults e.g. Sticklepath fault which is displayed in part in the Western Approaches Basin as a positive topographic ridge (see Naylor & Shannon 1982 Fig. 3.2). Recently the BIRPS group have imaged a major depocentre, the Plymouth Bay Basin, with possibly up to 10 km of Permo-Triassic red bed infill (BIRPS/ECORS 1986). This is thought to be controlled by Variscan thrust reactivation and transfer movement along a northwest-southeast late Variscan wrench fault (geometrically similar to the Kish Bank Basin further north).

B. Bristol Channel Basin

The strong east-west trend changes westward to a more east-northeast trend parallel to the Celtic Sea and Western Approaches basins. Kamerling (1979) recognised essentially three sub-basins, which evolved from the Permo-Triassic stratigraphically the basin shows strong similarities to the Wessex basin with pre Aptian/Albian erosion and late Cretaceous/early Tertiary inversion. The east-west trending East Bristol Channel basin (Kamerling 1979) appears to be a northward dipping half graben, probably comparable to the Vale of Pewsey basin and Central Somerset Graben and thus probably the direct result of Mesozoic reactivation of the Variscan front. Local northwest-southeast transfer zones were the Colethstone and Sticklepath faults and others. The intermediate area comprises a southward dipping half graben (Kamerling 1979). Different dip geometry between these two sub-basins probably reflects the importance of the Sticklepath fault zone suggesting changing polarity of the underlying detachment zones. Other northwest-southeast

transfer zones, again probably reactivated along late Variscan dextral wrench faults, separate the intermediate basins from the main Bristol Channel Basin, itself a southward dipping half graben, geometrically similar to the Haiq Fras depression to the south west (cf. Ziegler 1982, Fig. 14).

C. Porcupine Basin, Slyne Trough, Erris Trough and Donegal Basins

The north-south Porcupine Basin which was initially rifted in the middle Jurassic (Lefort & Max, 1984) was controlled and cross cut by a series of northwest-southeast transform faults, here interpreted to be reactivated as dextral faults. The Slyne Trough, Erris Trough and Donegal Basins, although similar in age, appear to be en-echelon northeast-southwest southeastward dipping half grabens. These may be separated by northwest-southeast transfer zone. An undated northeast-southwest dyke swarm in the Slyne Trough (Naylor & Shannon 1982) may reflect NW-SE extension. There is no evidence for significant crustal thinning in these troughs and basins in contrast to the observed lithospheric involvement displayed in the Porcupine Basin (Naylor & Shannon 1982).

D. Fasnet basin

This basin initiated in the Permo-Triassic. Reactivated Caledonoid faults are offset by secondary northwest-southeast strike slip faults which display sinistral motion. These latter faults controlled the development of the Fasnet pull-apart basin (Robinson et al., 1981), here postulated to be parallel to the sinistral opening of the Wessex basin. Late Bajocian volcanism controlled by the northwest-southeast faults appears to be synchronous with rifting and doming in the North Sea. This

'tectonic' event resulted in local uplift and non-sequences within the Wessex basin and around other basin margins, (see Ziegler 1982, encl.4) (i.e. the Vesulivian transgression in southern England.)

E. Celtic Sea and Cardigan Bay basins

The Celtic Sea Basin developed as a northward dipping half graben (Naylor & Shannon 1982) with up to 9 km of sediment infill (BIRPS/ECORS, 1986). The basin appears to be strongly controlled by reactivation of the postulated Variscan front which displays a complex ramp/flat geometry (BIRPS/ECORS, 1986). Assuming the 'front' crosses obliquely across southern Ireland (e.g. Cooper et al., 1984), the hanging wall geometry of the Celtic Sea Basin becomes more symmetric along strike to the southwest, similar to the change in geometry of the asymmetric Vale of Pewsey Basin of along strike (following the subsurface trace of the postulated Variscan front) to the symmetric eastern end of the Weald Basin. The westward change in geometry of the Bristol Channel sub-basins may also in part reflect this, although transfer zones could explain the sudden change in geometry along their strike. Similar rapid fault controlled rift subsidence occurred from the Permo-Triassic (Fig. 4.2) and continued throughout the Jurassic again comparable to the Vale of Pewsey and Weald basins in southern England. Northwest-southeast transfer zones reactivated along older northwest-southeast Variscan dextral strike-slip faults may account for the separation of the Fasnet and Celtic Sea Basins as well as the south dipping and thus oppositely directed (Caledonian?) detachment (the Bala fault) associated with the Cardigan Bay Basin. Thus the postulated northwesterly continuation of the Sticklepath fault zone essentially transfers the differing rotation

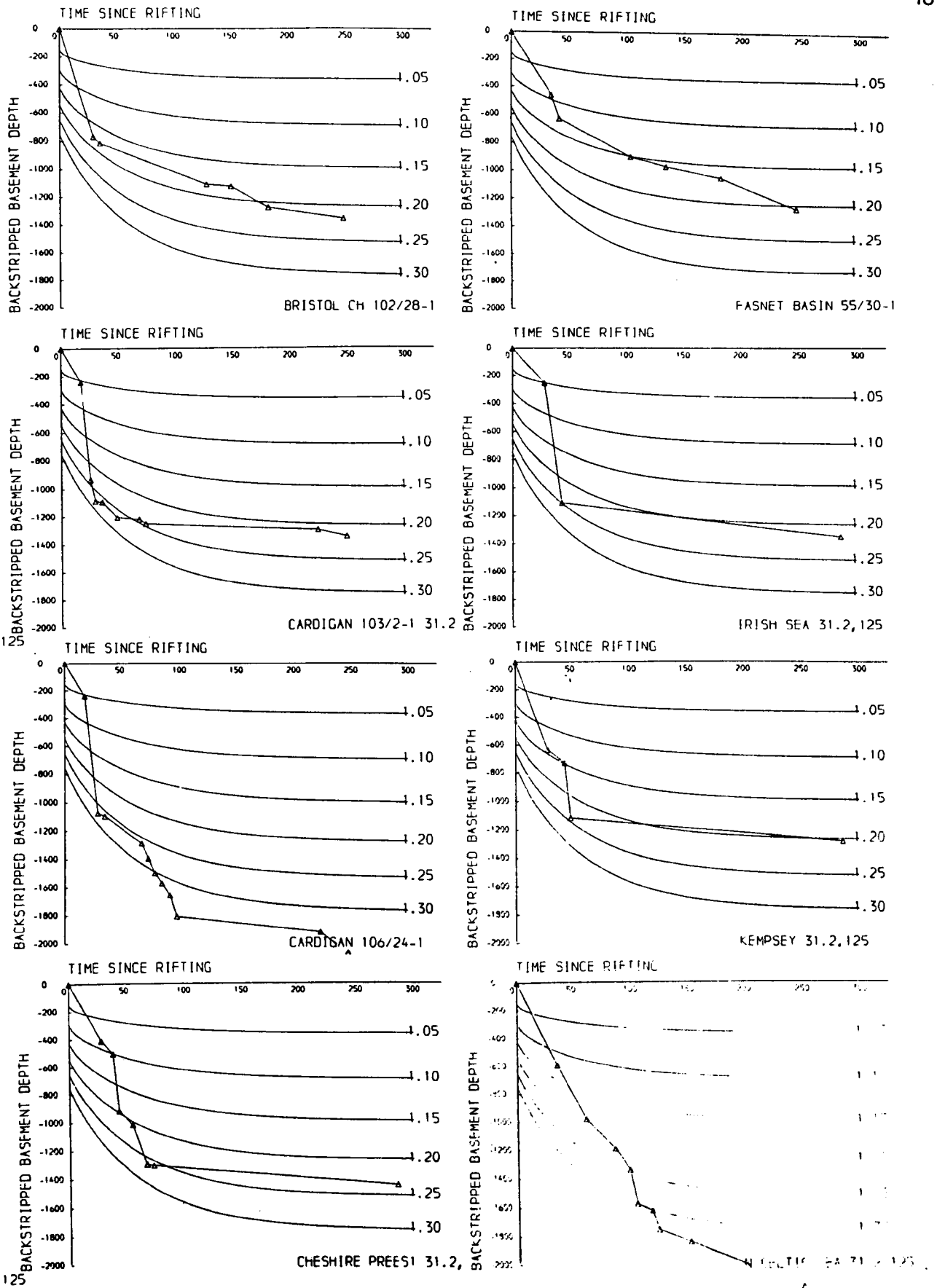


Fig. 4.2 Backstripped tectonic subsidence curves from selected basins in north-west Europe. (Bristol Channel - North Celtic Sea basins).

between the two basins and may reflect an original large scale dextral offset of the Variscan front off the Pembroke coast.

F. Kish Bank Basin

This northward dipping half graben which probably initiated in the Upper ^CCarboniferous (Jenner 1981), is transected by a major northwest-southeast dextral strike slip fault, similar to the Plymouth Bay Basin. Thus it bears strong structural similarity to the Wessex Basin in terms of evolution.

G. Cheshire, Irish Sea, Solway, Ulster, Rathlin Trough, Loch Indaal Basins

All these basins developed as half grabens. The Solway and Irish Sea Basins developed largely as southwest and north easterly dipping half grabens respectively. Excluding the northeast dipping Loch Indaal Basin, all the other basins essentially dip southeastwards. Again, all these basins seemingly reflect reactivated Caledonian basement trends, many were inverted between the upper Cretaceous and the Miocene, and many are directly underlain by Carboniferous half grabens although the precise timing of inversion is not known. Major flower structures in the Irish Sea follow a northwest-southeast trend which is important when considering the postulated late Variscan control discussed later.

H. West Scottish Basins and Shetland Basins

These basins again reflect half graben reactivation along Caledonian or older structures. Some, such as the South and North Minch basins possibly reflect normal reactivation of Caledonian thrusts such as is the case with the Outer Isles thrust (see Brewer et al., 1983, Brewer & Smythe, 1984).

I. Moray Firth Basin

This ^bBasin is strongly controlled by the Caledonian Great Glen Fault which essentially bounds this northwest dipping half graben. McQuillin et al., (1982) postulated synchronous dextral motion with basin development along this fault. This would result in the observed synchronous sinistral motions along the northwest-southeast orientated conjugate fractures around the UKCS.

J. North Sea Basin

Permian volcanism in this basin occurred synchronously with volcanism in the Wessex Basin (Dixon et al., 1981, Knill 1982). The postulated asymmetric Permo-Triassic rifting may have been controlled by reactivation of a westward dipping Caledonian thrust (Barton & Mathews 1984), although full scale lithospheric extension probably initiated in the Middle Jurassic. This may in part explain the differences in Beta estimates between present day observed crustal thicknesses and backstripped well data. Lithospheric extension in the middle Jurassic resulted in uplift, volcanism and local widespread subsidence outside the area of demonstratable crustal thinning (Leeder 1983). Perhaps much of this uplift can now be attributed to secondary convection mechanisms associated with renewed extension, similar to the Gulf of Suez (see Steckler 1985).

K. Sole Pit and Cleveland Basins

The Sole Pit Basin has been related to pull-apart motion along the Dowsing fault zone (Glennie & Boegner, 1981) with dextral opening between the Permian and early Cretaceous and sinistral shortening during

early/upper Cretaceous (Sub Hercynian) inversion. The Cleveland Basin probably displays a similar history to the Sole Pit Basin since it develops on the western side of the Dowsing fault zone. Backstripped subsidence curves (Fig. 4.3) clearly show a similar subsidence form to the Winterborne Kingston Trough within the Wessex basin, whereas the Sole Pit Basin clearly display continued rapid subsidence throughout the Mesozoic (Fig. 4.3) similar to the Weald basin. The East Midlands shelf area in the Lincolnshire area probably developed as a flexural wing to the North Sea.

L. Worcester Basin

This westward dipping half graben appears to be reactivated along a Caledonian transtensional and Variscan transpressional fault zone (Chadwick, oral comm). Permian and Triassic extension has been identified (Chadwick 1985a) similar to the Wessex Basin with fault geometries and extension values indicating oblique slip with northwest-southeast extension to allow for synchronous extension in the nearby Wessex Basin.

M. Paris Basin

This basin clearly displays a series of separate depocentres seemingly developed along the northwest-southeast Pay de Bray disturbance. Perrodon & Cornellis (Oral comm) have identified clockwise rotation of the rift subsidence, thus it is here speculated that this reflects sinistral strike-slip motion along the Pay de Bray Fault from Permian times. Thus Permo-Triassic depocentres delineated by Meqnién (1980) are here interpreted as local pull-aparts developed along the Pay de Bray and the Rouen - Sennely fault systems. These fault zones

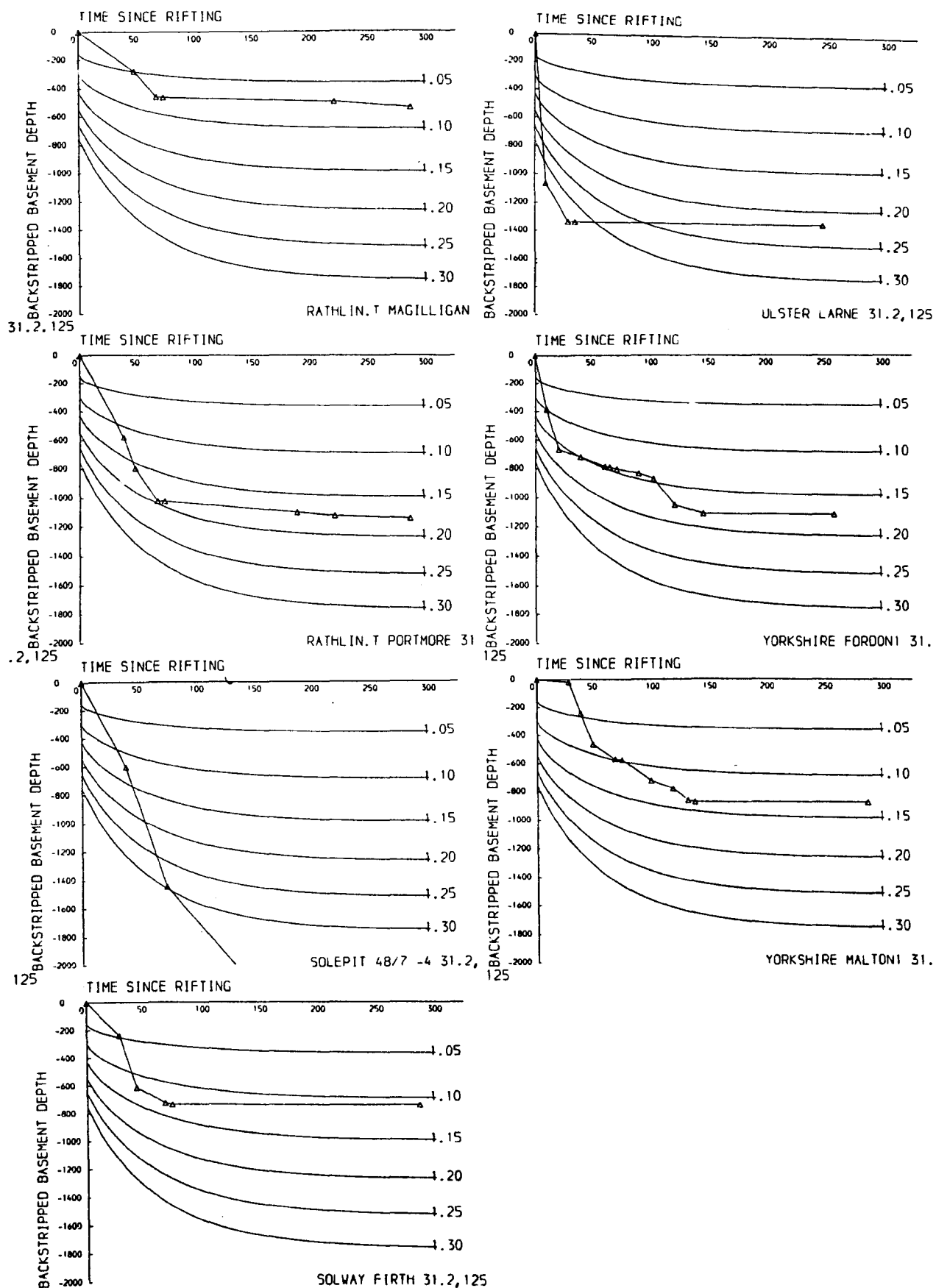


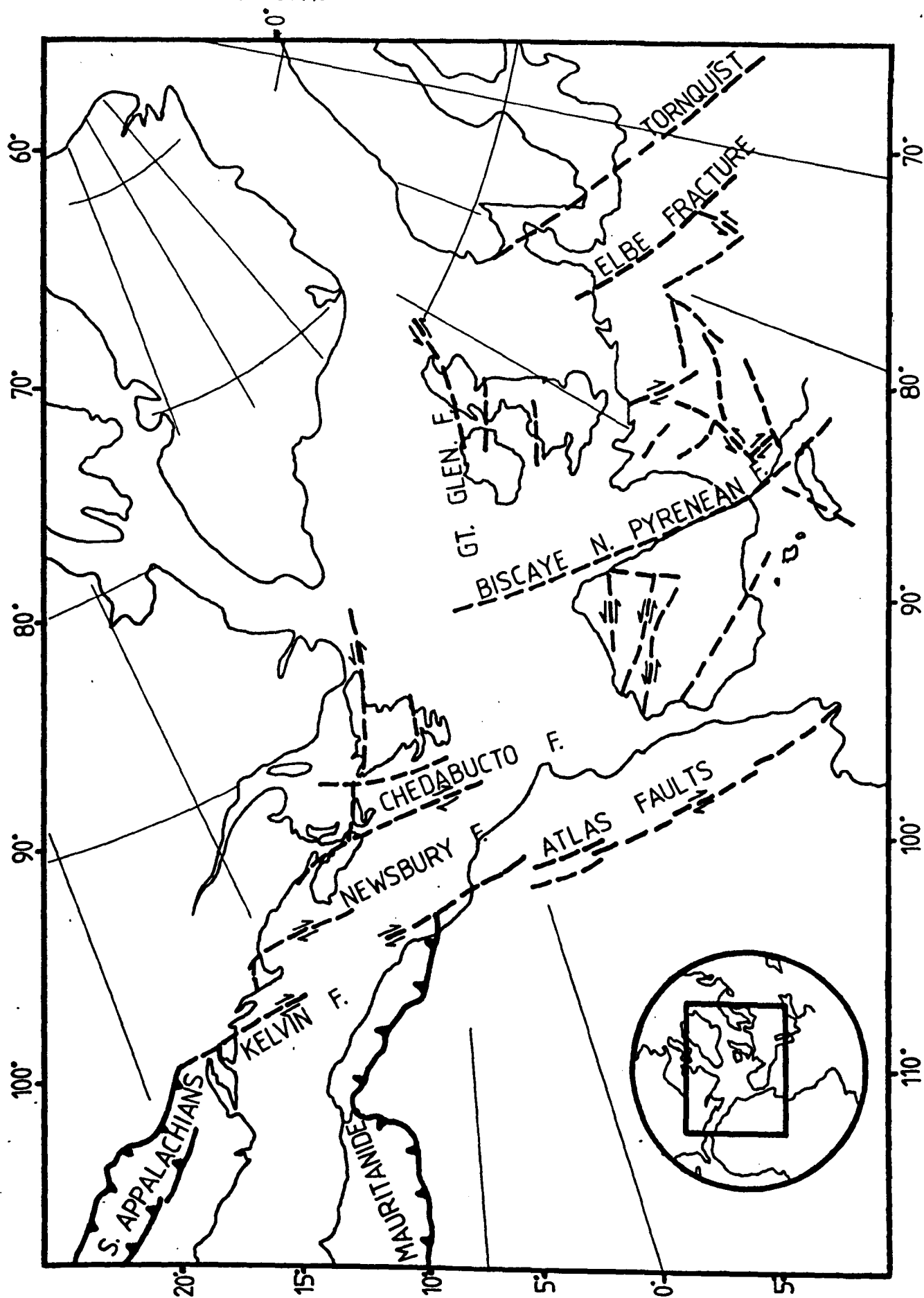
Fig. 4.3 Backstripped tectonic subsidence curves from selected basins in north-west Europe. (Rathlin Trough - Yorkshire (Cleveland) Basin).

synchronously controlled the development of the Wessex basin.

4.2 Discussions

Therefore most of the basins around the UKCS are seemingly controlled by northwest-southeast transforms, transfers and strike slip faults, largely interpreted as reactivated earlier Variscan or Caledonian structures. Figure 4.4 shows the location of the major Mesozoic/Tertiary basins throughout Western Europe. Excluding the obvious northeast-southwest Caledonian trend to the north and west of Britain another probably more significant trend is here recognised following a northwest-southeast trend. These postulated fractures are probably of similar age and generation to the major late Variscan dextral strike slip faults (see Arthaud & Matte 1977) (Fig. 4.5). For example line 1 on Fig. 4.4 probably is the site of the Torquist line and controlled the subsidence of the Polish Trough. Line 2 (the Elbe line?) speculatively controlled the orientation of the Central Graben and possible Witch Ground Graben/Moray Firth Basin boundary. Line 3 coincides with the northwest-southeast Dowsing fault zone and the Broad Fourteens Basin (Lutz et al., 1975) and major flower structures in the West Netherlands Basin (Bodenhause and Ott 1981). The most significant feature is line 4 which lines up with the Cheshire, Irish Sea and northeast offshore Irish Basins and offsets the Rockall Trough further north. Further south a strong magnetic signature is depicted on magnetic anomaly maps across the London-Brabant high and coincides with a postulated Variscan lateral ramp between the high and the Paris Basin along the French Belgium frontier. The implication is that although many of the basins are clearly related to reactivated Caledonian fault trends, the overprint of this late Variscan fracture set clearly indicates no

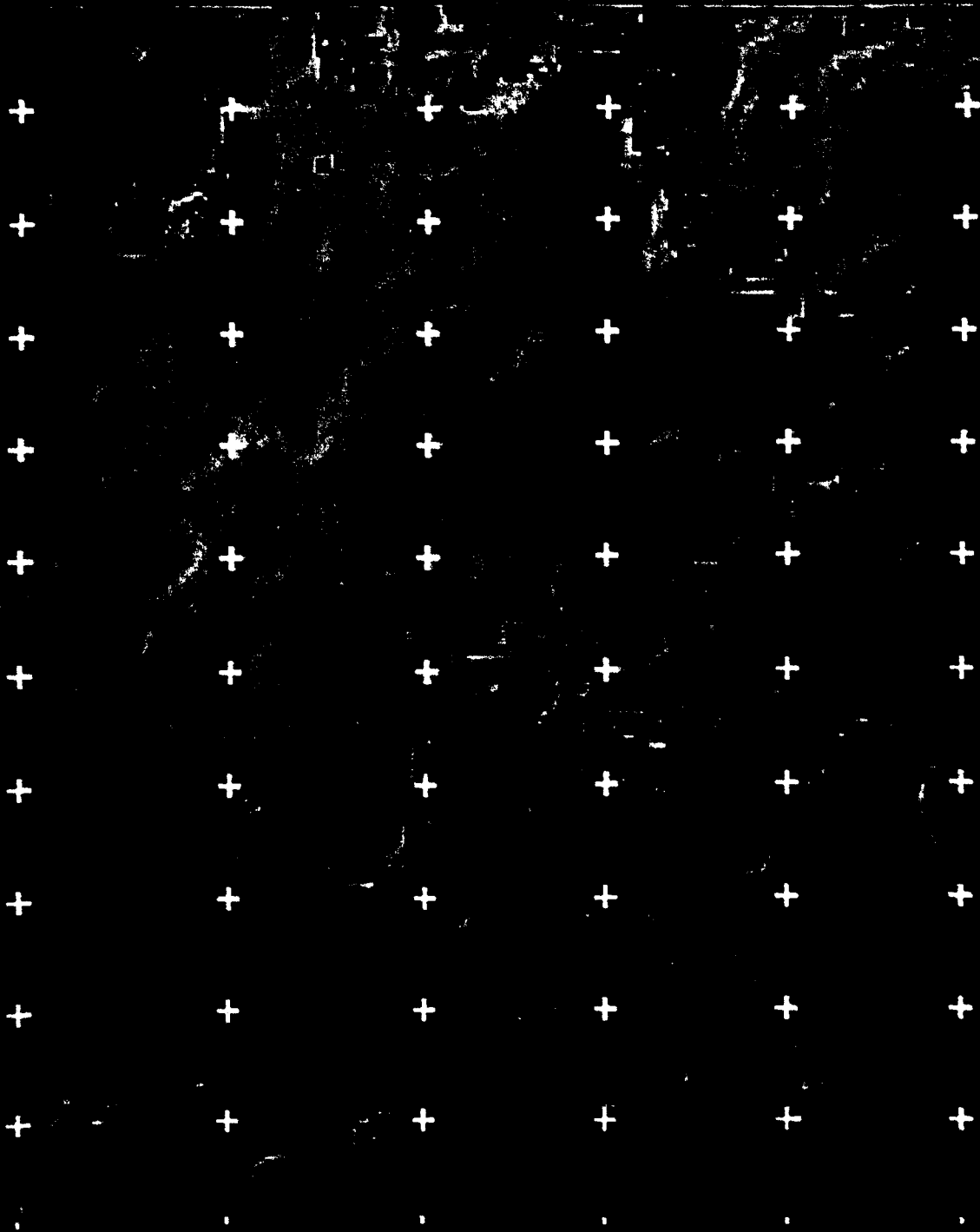
Fig. 4.5 Structural map of the late Variscan structure, from the Urals to the southern Appalachians. Heavy continuous and dashed lines represent the observed and inferred main fractures. Fit of continents after Le Pichon et al., (1977), Europe fixed. (Modified from Arthaud & Matte, 1977).



significant lateral motion could have occurred along northeast-southwest trends at least since the late Palaeozoic. Line 5 may reflect a larger scale northwest-southeast late Variscan strike slip fault dividing the Wessex Basin in two. This explains the northwest-southeast deflection of the Portsdown fault and its correspondence to the Pay de Bray fault. Further north it coincides with the northwest-southeast Codling fault across the Kish Bank Basin. The Sticklepath fault zone represents the surface expression of line 6, which has already been shown to control the Wessex, Bristol Channel Celtic Sea and Cardigan Bay Basins: all reflect changing opposite-directed half graben systems. Lines 7-9 are postulated as basin boundary faults, and transfer zones, and in the Porcupine Basin as transform zones, coinciding with strong northwest-southeast orientated magnetic signatures. Thus this postulated northwest-southeast late Variscan or older fault system, extends well into the Variscan foreland north of the Variscan 'Front': partly or totally controlling the half graben geometry, location and basin evolution of the subsequent late Palaeozoic - Cenozoic rifts in northwest Europe. Such structures are particularly well imaged on the recently processed gravity data (Fig. 4.6).

Backstripped subsidence curves and stratigraphic details indicate that extension events were largely synchronous throughout northwest Europe. Much of this extension resulted in strike-slip and oblique-slip motion along northwest-southeast late Variscan structures from the Permian. This postulated sinistral movement is recognisable primarily in the Wessex, Paris and Fasnét Basins along northwest-southeast trends although other basins probably demonstrate a similar history. Most basins in the UKCS seemingly developed on rigid crust as reflected by

Fig. 4.6 Composite Bouguer Gravity image of north-west Europe. Preferential illumination from the northeast to the southwest to enhance the postulated northwest-southeast Variscan fractures. Figure 4.6 kindly supplied by G.D. Karner).



insufficient rise of the Moho to compensate the overlying basin geometry. The results of the BIRPS deep seismic reflection lines (Brewer et al., 1983; Brewer & Smythe 1984, BIRPS/ECORS 1986) clearly image a flat Moho, although consideration of the effect of density in the overlying basin fill on velocity structure may actually cause velocity pull-^{down}~~ups~~ affecting the Moho. This is particularly well evidenced by the BIRPS group in the Plymouth Bay Basin where the postulated 10 km post Carboniferous sediment infill lies uncompensated above a flat Moho, and may imply no extension or sublithospheric involvement and perhaps this is further evidence of crustal rather than wholesale lithospheric failure (see Chapter 2). However, more detailed studies using gravity and refraction work, particularly in the Porcupine Basin and in the North Sea (Barton & Wood 1984), have shown obvious subcrustal involvement more closely comparable with the McKenzie model (1978). Lastly all the basins in the UKCS, excluding the post mid-Jurassic evolution of the North Sea Basin, essentially developed as asymmetric rifts, with geometric complexities similar to those described by Bosworth (1985).

Obvious dissimilarities such as differing fault trends reflect the underlying basement grain. In particular many Caledonian trending basins probably reactivated above Caledonian strike-slip faults, whereas basins south of the Variscan front largely seem to be controlled by underlying Variscan thrust geometry (Fig. 3.3 and 3.4) (depending on the level of pre-Permian erosion and the depth to detachment.) The importance of these earlier structural weaknesses utilized by later basin development has been emphasized by many authors (eg Johnson & Dingwall 1981; Naylor & Shannon 1982; Chadwick et al., 1983, Brewer & Smythe 1984). Also although general rapid fault controlled subsidence was fast throughout

the Permo-Triassic and Kimmeridgian (and in part the Neocomian), individual basins may reflect slight variations in the subsidence form. For example, rapid fault controlled subsidence of the Sole Pit Basin throughout the Jurassic is reflected largely by exponential (thermal?) subsidence in the Cleveland Basin (Fig. 4.3).

Stratigraphic details including unconformities etc. vary locally from basin to basin. The reasons for this may be directly related to sea level variations (see Chapter 2), the orientation and geometry of basins with respect to plate boundary reconfiguration, uplift of rift shoulders (which may be due to secondary convection in the underlying low velocity zone (see Steckler 1985)), uplift of a peripheral bulge associated with loading, differing erosion rates, differing [↗]ridgities and varying subcrustal involvement. These all may play a role on basin edge stratigraphy. The association of rift initiation and separation in relation to basin stratigraphy is particularly well exemplified by early Tertiary volcanism (Plateau basalts and intrusives) associated with North Atlantic sea floor spreading. Comparison of the Campanian/Turonian to Palaeocene/Eocene palaeogeography in that region (see Ziegler 1982, encl 23, 24) clearly displays how this uplift associated with spreading caused marked rapid variations in paleogeography.

Locally, such as the Sole Pit Basin area; dextral strike-slip motion is observed along northwest-southeast trends (Glennie & Boegner 1981). In addition the complex subsequent inversion history (both Sub-Hercynian and Laramide) undoubtedly reflects the complex nature of the fault zone, with local transpressional uplift and transtensional depocentres perhaps in part controlling the Cleveland Basin.

In summary, the evolution of Western Europe throughout the late

Palaeozoic to present day can be envisaged to be the direct result of instability of the Pangean supercontinent and eventual break-up. Regional extension resulted in discrete depocentres developing along earlier crustal weaknesses. The dominant crustal weaknesses generally follow Variscan or Caledonian trends although in late Variscan northwest-southeast fractures are particularly important as they appear in the overprint whole European lithosphere.

Many basins reflect a similar tectonic history to that described in the Wessex Basin, in particular they may have developed as discrete pull-apart basins in response to regional extension of the northwest European lithosphere. It is postulated that many basins including, for example, the Bristol Channel and Celtic Sea opened substantially along northwest-southeast trends which are interpreted as late Variscan wrench faults extending a considerable distance into the foreland from the Variscan deformation front. Much of this extension can be explained in terms of crustal but not necessary equal lithospheric extension (see Chapter 2) balanced by partial but more regional lithospheric involvement during the Permo-Triassic throughout western Europe. The extension was essentially polyphase largely terminating by the end of the Cretaceous. Subsequent northeasterly convergence of Africa relative to Europe initiated during this time resulted in progressive Alpine deformation and inversion of many basins in northwest Europe. Therefore it can be predicted that many basins throughout Western Europe probably display northwest-southeast sinistral motion at least from the lower Jurassic until the Aptian where upon changing plate reconfiguration resulted in east-west translation of Africa relative to Europe (see Livermore & Smith, in press) as probably expressed by a period of east-west sinistral strike-slip motion from the

Aptian to Cenomanian. This was followed by general directed plate convergence, deformation and inversion reflected by decreasing uplift northwestwards across the foreland of northwest Europe. Local inversion further north than non-inverted basins undoubtedly reflects the orientation of the basin and the importance of the underlying basement configuration with respect to the northwest-southeast compression.

CHAPTER 5

LOCAL STRUCTURES AND BRITTLE MICROTECTONICS

5.1 Local Structures

A. Introduction

The purpose of this chapter is to detail the mesoscale structures observed in the field and their possible interpretations with respect to the basin kinematics. In particular do these mesoscale features reveal any further information on the complicated extensional history? The term mesoscale is here inferred to be related to structures observable in one continuous exposure. The structures outlined include folds, faults, shear zones, vein arrays, fissures, kink bands, stylolites, superficial structures and joints, thus they generally reflect structures which have received little attention, with the exception of the work by Phillips (1964), Mimran (1975), Bevan (1985a and 1985b) along the Dorset coast. The following detailed descriptions refer to individual localities, the sequences present at these outcrops and their locations are summarized in Appendix A. The angular unconformity at the base of the Aptian marks a significant change in tectonic style between sequences below and those above, hence the subsequent section sub-divides the deformations into those developed prior to the Aptian and those developed after.

B. Folding

1. Introduction

Folding is rarely evident at mesoscales although on the larger scale it may provide important kinematic information on the evolution of the area (see Chapter 3). The following section deals with those observed at mesoscales.

2. Pre-Aptian

Pre-Aptian fold structures can be demonstrated immediately below the unconformity, such as those seen at Holworth House (locality 264) where the sub-horizontal Gault Clay truncates the Portland Sand which dips 17°N . Although Arkell (1947) discussed the nature of this folding and mapped similar structures in the nearby area, recent structural analyses would suggest that the folds are undoubtedly related to hanging wall anticlines and synclines which developed throughout the Jurassic along the Abbotsbury-Ridgeway fault zone. Synsedimentary slumps presumed to be triggered by earthquakes have been recognised in the Rhaetic and Purbeck Beds by Hallam (1960) and Ensom (1984) respectively and these undoubtedly reflect the polyphase and continued tectonic activity.

3. Post-Aptian

Gale (1980) recorded synsedimentary Campanian folding in the Portsdown area (N.G.R. SY 602 066) whilst Bevan (1985a) considered a symmetric upright fold at Colwell Bay (N.G.R. SZ 330 888) to be northerly directed and post upper Eocene in age. Both are local indicators of the complicated inversion of the area. Detailed fold structures, particularly evidenced within the Purbeck Beds (Broken Bed unit) are clearly associated with inversion (see Appendix E). Further folds have been described in detail by Arkell (1947) and Phillips (1964) along the Dorset coast and are comparable in age to those described previously. Localities 75 and 76 display mesoscale low amplitude east-west fold axes presumably related to the nearby northwest-southeast Colethstone fault and reflect simple shear motion. Locality 180 displays a north-south trending synuous fold in the Blue Lias of unknown age, but presumably related to those on a larger scale in Lyme Bay (see Darton et al., 1981).

Most folds are presumably inversion related, but their general limited extent and poor exposure make accurate dating largely impossible.

C. Faulting

1. Introduction

Faulting at the mesoscale has proved very informative in elucidating the deformational development of the area. In particular, synsedimentary movement can be demonstrated along some structures, whilst other age determinations can be obtained by offsetting relationships, and their lateral continuity either by 1) following one individual mapped fault trace or 2) by attributing other nearby faulting of the same orientation to the same kinematic deformation.

2. Pre-Aptian

Synsedimentary movement can be demonstrated at Budleigh Salterton (N.G.R. SY 070 819) within the Triassic (Stoneley pers comm) and the Toarcian at Watton Cliff (N.G.R. SY 452 909) by Jenkyns & Senior (1977). Two new localities have been recognised, 1) in Fullers Earth at Herbury (N.G.R. SY 612 811) and 2) within the Tithonian at Durlston Head (N.G.R. ST 036 773) (see Appendix F for further details).

Contractional mesofaults have been identified at Kimmeridge (N.G.R. SY 908 792). These are displayed in the Flats Stone Band (see Arkell, 1947 for terminology) where a 'polygonal' network of low angle ramp/flat thrusts are exposed (Fig. 5.1 and Plates 51, 52). Bellamy (1977) proposed that their formation was related to the diagenetic growth of dolomite which characterises the horizon. The elongate polygonal development can be demonstrated to increase in intensity towards the Kimmeridge anticline suggesting some tectonic control. The lack of erosion of the structures

Fig. 5.1 Contractional mesofaults. Examples (1) Kimmeridge Bay (N.G.R. SY 908 792), Kimmeridge Clay; (2) Ridgeway (N.G.R. SY 671 852), Purbeck Beds and (3) Horbarrow Bay 2 (N.G.R. SY 896 791) Kimmeridge Clay.

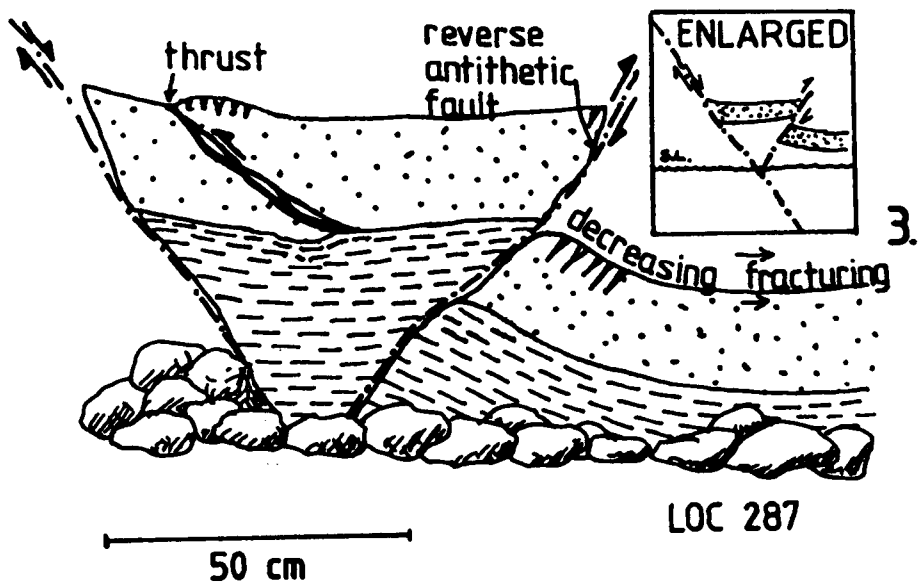
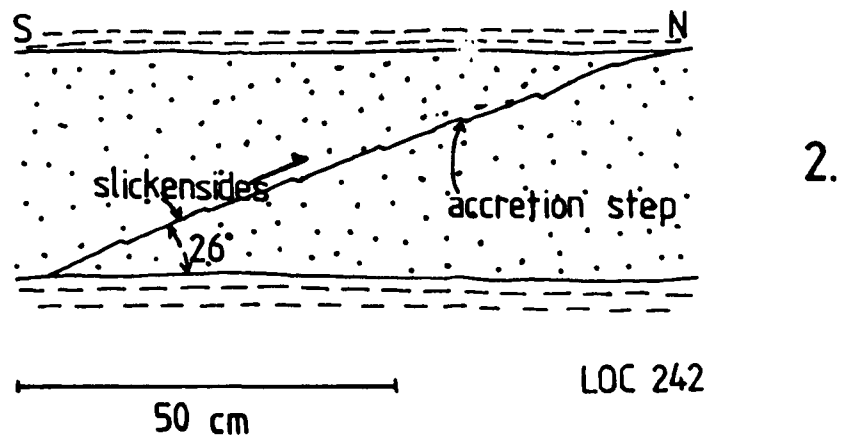
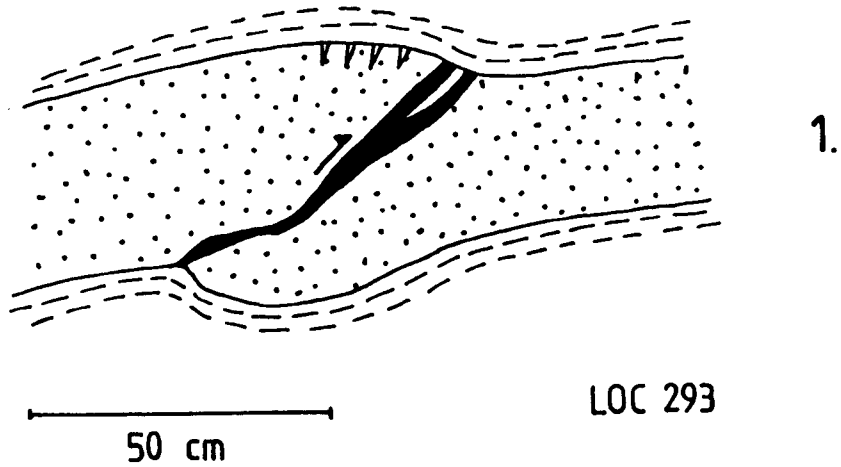




Plate 5.1 A side view of a contractional mesofault (thrust) within the 'Flat Stone Band' at Horbarrow Bay (N.G.R. SY 896 790). A duplex is evident in the footwall, while the hanging wall displays a local backthrust.



Plate 5.2 An oblique view of the 'Flat Stone Band' at Kimmeridge Bay (N.G.R. SY 898 788), showing thrust surface in plan. The hanging wall has been removed by erosion.

and the disruption of the overlying sequence suggests they have a subsurface origin. However the absence of thrusting in other similar cementstone units along the anticlinal crest suggests some sedimentological control too. The Kimmeridge anticline is pre-Albian in age according to Arkell (1947), thus thrusting is presumably similar in age.

3. Post-Aptian

Two compressional mesofaults shown on figure 5.1. are undated, however the southward dipping mesofracture on figure 5.1 is presumably inversion related due to its close proximity to the Abbotsbury-Ridgeway fault, whilst the local antithetic reversal shown on figure 5.1 and on plate 5.3 is probably of the same date (c.f. Donovan & Stride, 1961).

Extensional mesofaults shown on figures 5.2 and 5.3 and plate 5.4 clearly relate to layer parallel extension resulting from monoclinial flexuring (c.f. Bevan, 1985b) when using layering as datum rather than the horizontal. Bevan (1985b) recently reclassified the microfaults originally identified by Arkell (1938) and Phillips (1964) into two sets of conjugate extension faults related to the same phenomena just described.

Conjugate shear faults on figure 5.4 clearly postdate inversion related folding and indicate a north-south σ_1 . This probably occurred synchronously with conjugate shear fracture development discussed in the following section.

D. Conclusions

Mesoscale structures have provided a smaller scale understanding of the kinematic development of the basin. These results have been

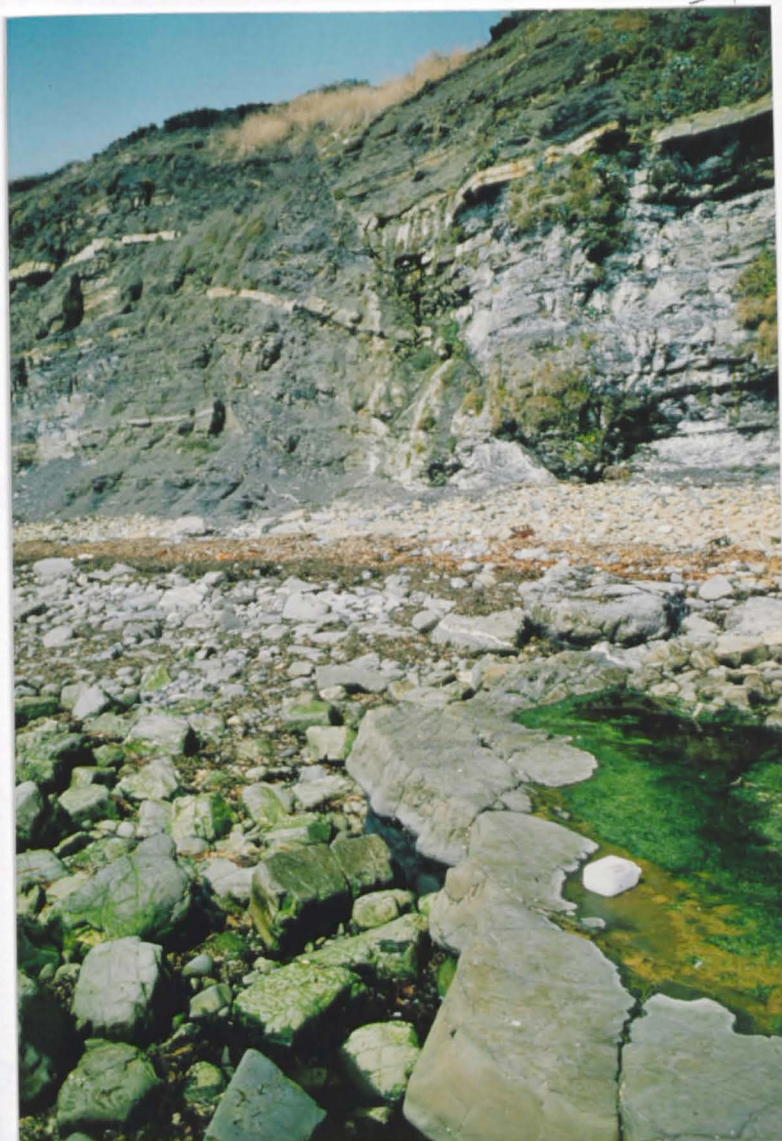


Plate 5.3 An oblique view of two normal faults within the Kimmeridge Clay at Horbarrow Bay (N.G.R. SY 896 790). Local reverse antithetic faulting is displayed in the middle ground and discussed in more detail on Figure 5.1. Normal drag of the 'Flats Shone Band' in the foreground is clearly seen.

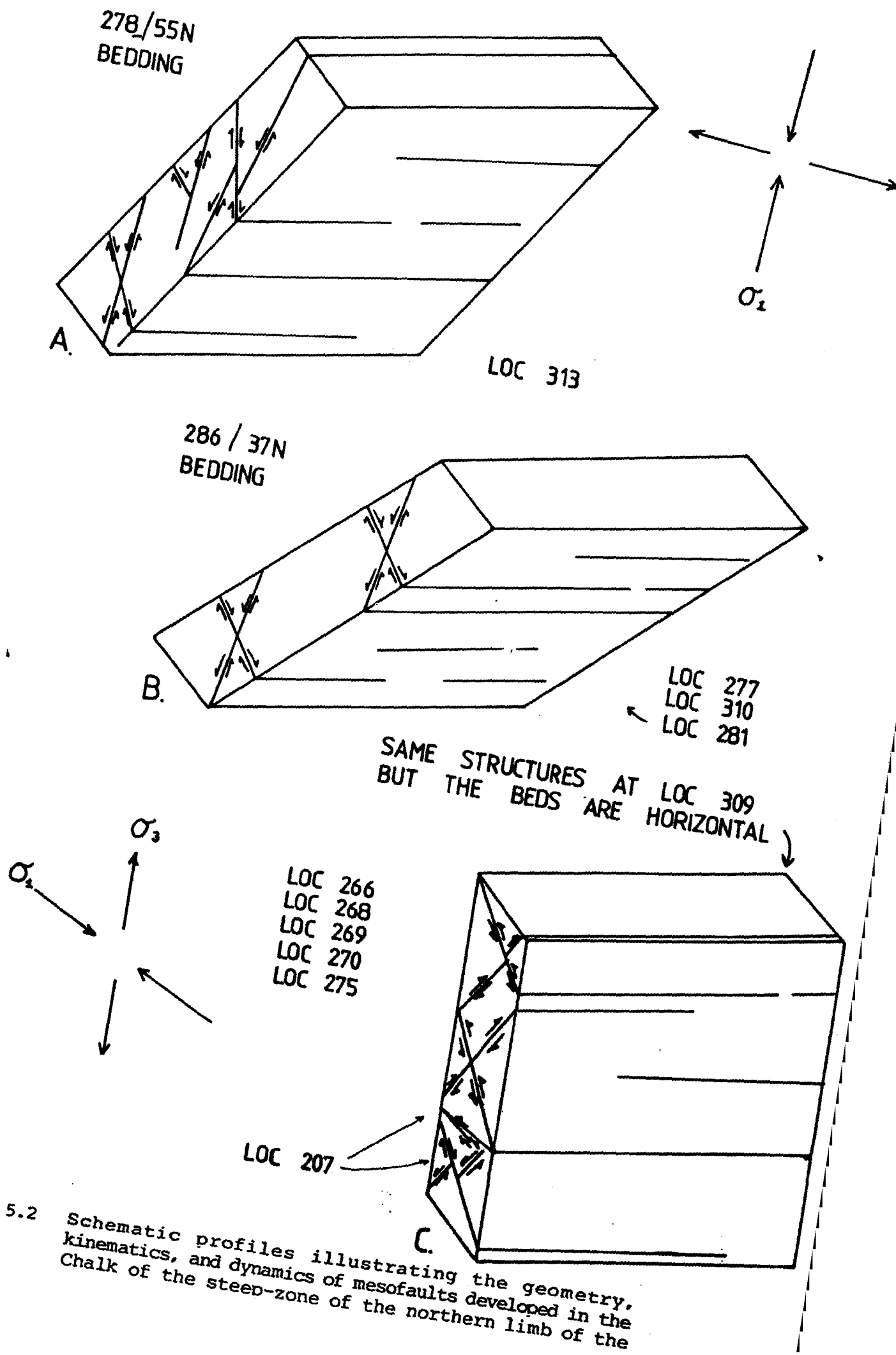
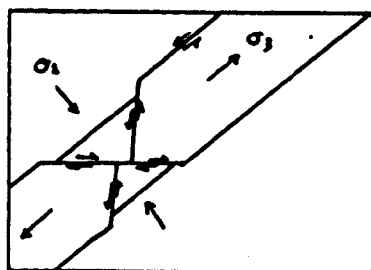
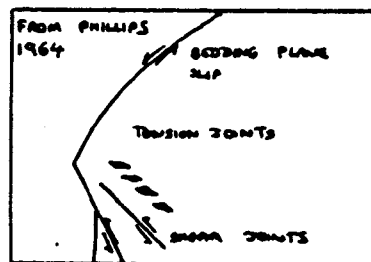


Fig. 5.2 Schematic profiles illustrating the geometry, kinematics, and dynamics of mesofaults developed in the Chalk of the steep-zone of the northern limb of the



- ① LITTLE DIRT BED.
- ② GREAT DIRT BED.
- ③ BRONZE BEDS.

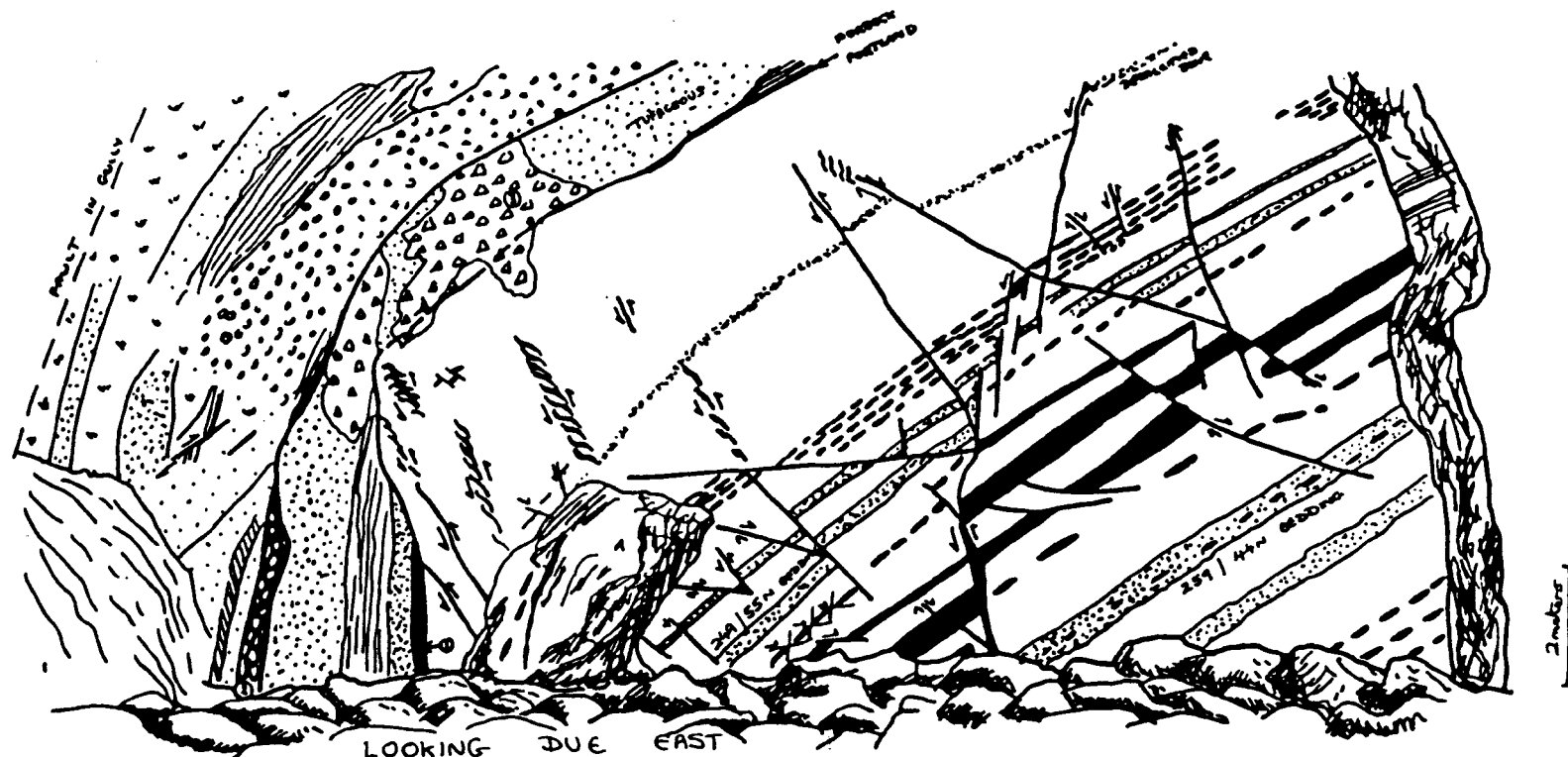


Fig. 5.3 A field sketch of the observed conjugate mesofaults within the Portland Beds at Dungy Head (N.G.R. SY 815 800) interpreted as indicative of layer-parallel extension.



Plate 5.4 Looking due east at a series of conjugate extension fractures in the Portland Beds at Dungeness Head (N.G.R. SY 823 798) reflecting layer-parallel extension in the northern limb of the Weymouth anticline. The undulating basal contact of the Purbeck Beds clearly displays bedding plane slip. The detailed interpretation of these structures are described on Figure 5.3.

intergrated into the previous chapters on the structural development of the region. The next section deals specifically with other kinematic indicators and attempts to integrate the results with the development of the basin.

5.2 Brittle Microtectonics

A. Introduction.

The term brittle microtectonics is applied to the application of mesofracture analysis to the solution of tectonic problems (Hancock, 1985). Mesofractures refer to joints, shear zones, en-echelon cracks, kink bands, fissures and veins which can be observed in a single continuous exposure. Mesofaults which also encompass this term were dealt with in the previous section. The use of mesofractures in determining regionally significant palaeostress trajectories has been demonstrated by many authors, for example Hancock et al., (1984) and Engelder (1985). The principles of inferring stress and strain trajectories are beyond the scope of this thesis, however they are adequately summarized by Price (1966) and Hancock (1985). The purpose of this chapter is to outline the brittle microtectonics of the Wessex Basin from an analysis of 350 localities in an attempt to relate extension rates and directions as recorded by fracture and fabric studies to basin geometry, sedimentary wedge patterns and sedimentation/compaction rates and integrate the results to the tectonic development of the basin.

B. Data collection and analysis

Data collection was largely confined to the Jurassic sedimentary successions because the sequence displayed rapid lateral and vertical facies variations, the sequence could be accurately dated using ammonite

zones (1 m.y.) the succession displays a complex multiple stretching and thermal recovery history. This work was carried out concurrently with another similar project at Bristol University by Tim Bevan, who analysed Cretaceous (post-Aptian) to present day sequences within the basin.

Within the basin over 800 Jurassic localities were visited (Figures 5.5 and 5.6, II.5.1 and II.5.2) of these only 350 localities were proved suitable for mesofracture analysis. All the important stratigraphical horizons were sampled and logs completed at a large number of locations. The number of measurements recorded was in excess of 30,000 (an average of about 85 per locality). The localities varied from foreshore rock platforms and cliff sections to inland road cuttings, quarries and natural exposures. At each locality a note of the orientation of the structural planes, the lineations, the horizon lithology and the thickness of the beds, joint frequencies and dimensions, surface markings, mineral infillings and cross cutting relationships were taken. Restoration of bedding to horizontal was completed on the shear fractures, however the resulting nature and timing of brittle microtectonic structures, showed clearly that further restoration of other mesofracture features were unnecessary.

C. Kinematic indicators

This section describes the main mesostructures and how they provide unambiguous kinematic information about directions of shortening, dilation or shear.

1. Bedding

Bedding dips average $2-3^{\circ}$ throughout the basin, locally beds maybe overturned for example along the northern limb of the Weymouth anticline.

Fig. 5.5 Locality location map (Grid references in Appendix A).

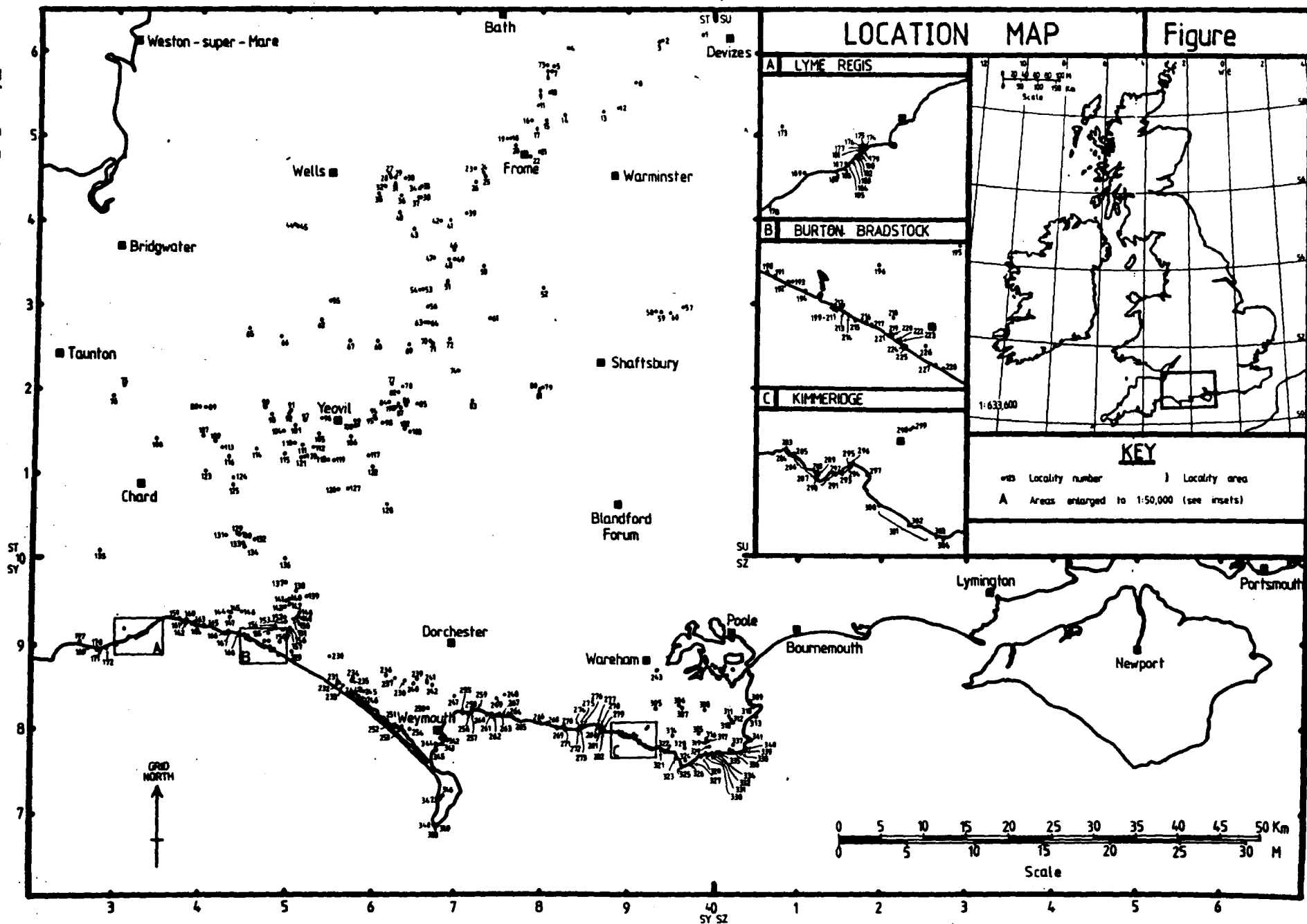
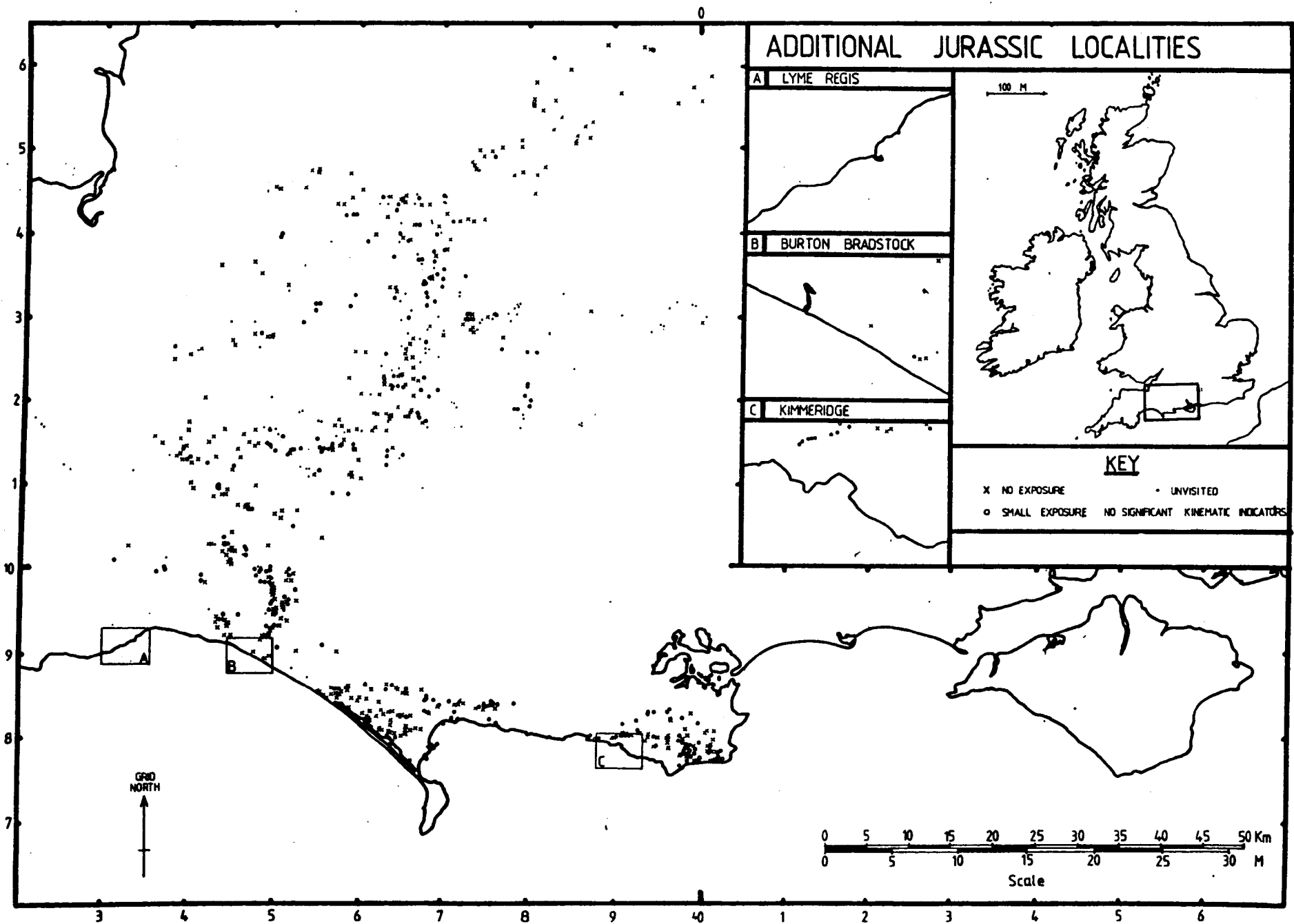


Fig. 5.6 Additional Jurassic localities also visited during the research. (where no significant kinematic indicators were observed)



Dips in excess of 3° are generally located in the vicinity of faults and reflect inversion of earlier structures.

2. Shear Zones

Mesozoic shear zones within the basin are characteristically displayed as en-echelon vein arrays facing against the direction of shear and local en-echelon folding facing in the direction of shear. All these structures may display a polyphase history demonstrated by multiple vein and fissure infillings or are overprinted by similar structures. Although different types of vein array can be distinguished, their classification has long attracted debate (see Hancock 1985, p.443). The interpretation preferred here is based on Hancock (1972) is that arrays which develop between $10-20^{\circ}$ to the shear direction are reidal shears, arrays between $20-40^{\circ}$ are interpreted as hybrid fractures whilst dips greater than 40° are interpreted as extensional fractures. This classification is here applied to conjugate shear fractures which display obvious displacements either seen by offsets or by the development of lineations and steps on the fracture surface. Most of the recorded shear fractures display congruous steps with the development of accretion steps and growth fibres, however shear fractures within the upper Cretaceous chalk have generally incongruous steps with oblique stylolites (slick - olites) developed along the fracture surface reflecting an opposite sense of movement (Fig. 5.7). These features generally follow a northwest-southeast and northeast-southwest trends, the former generally indicating dextral motion whilst the latter is sinistral. A summary of differing mesoscopic shear indicators observed at different localities within the basin are shown diagrammatically on figures 5.7, 5.8, 5.9, 5.10, 5.11, and

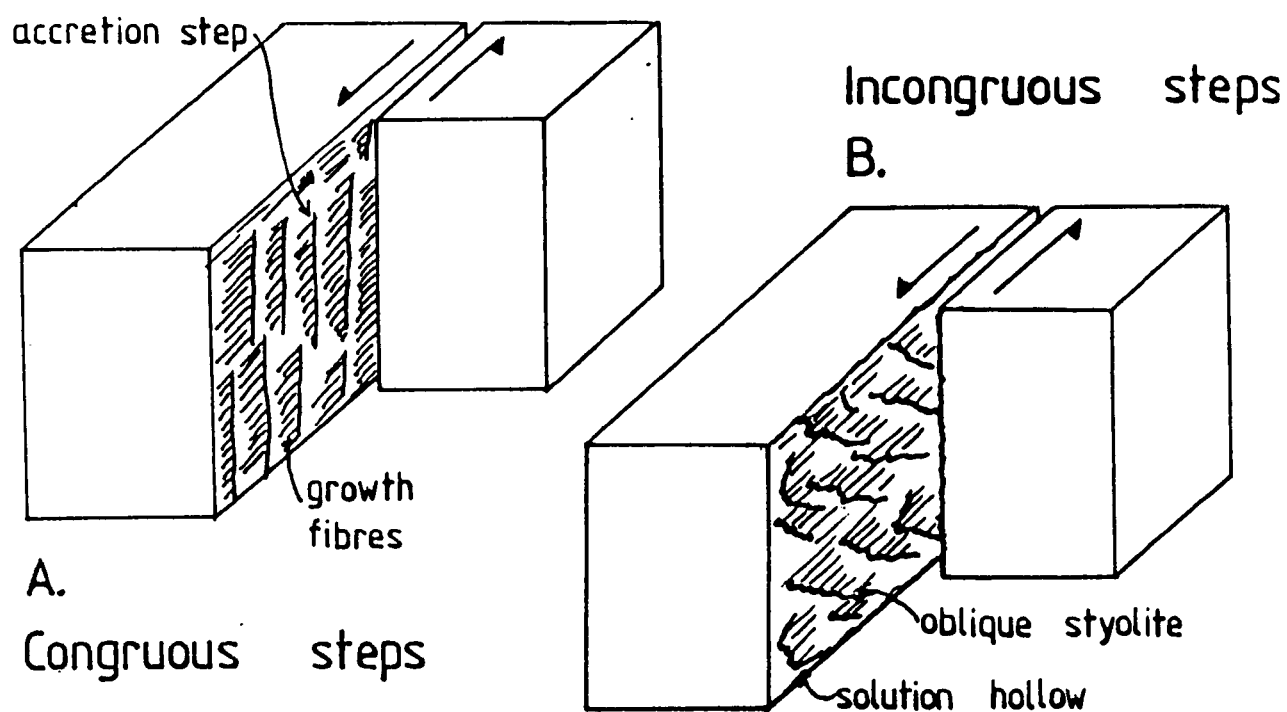


Fig. 5.7 Types of lineations and steps on mesofault surfaces. (a) Accretionary growth of crystal fibres (frictional type not shown) (B) Oblique pressure solution. (Redrawn from Hancock, 1985).

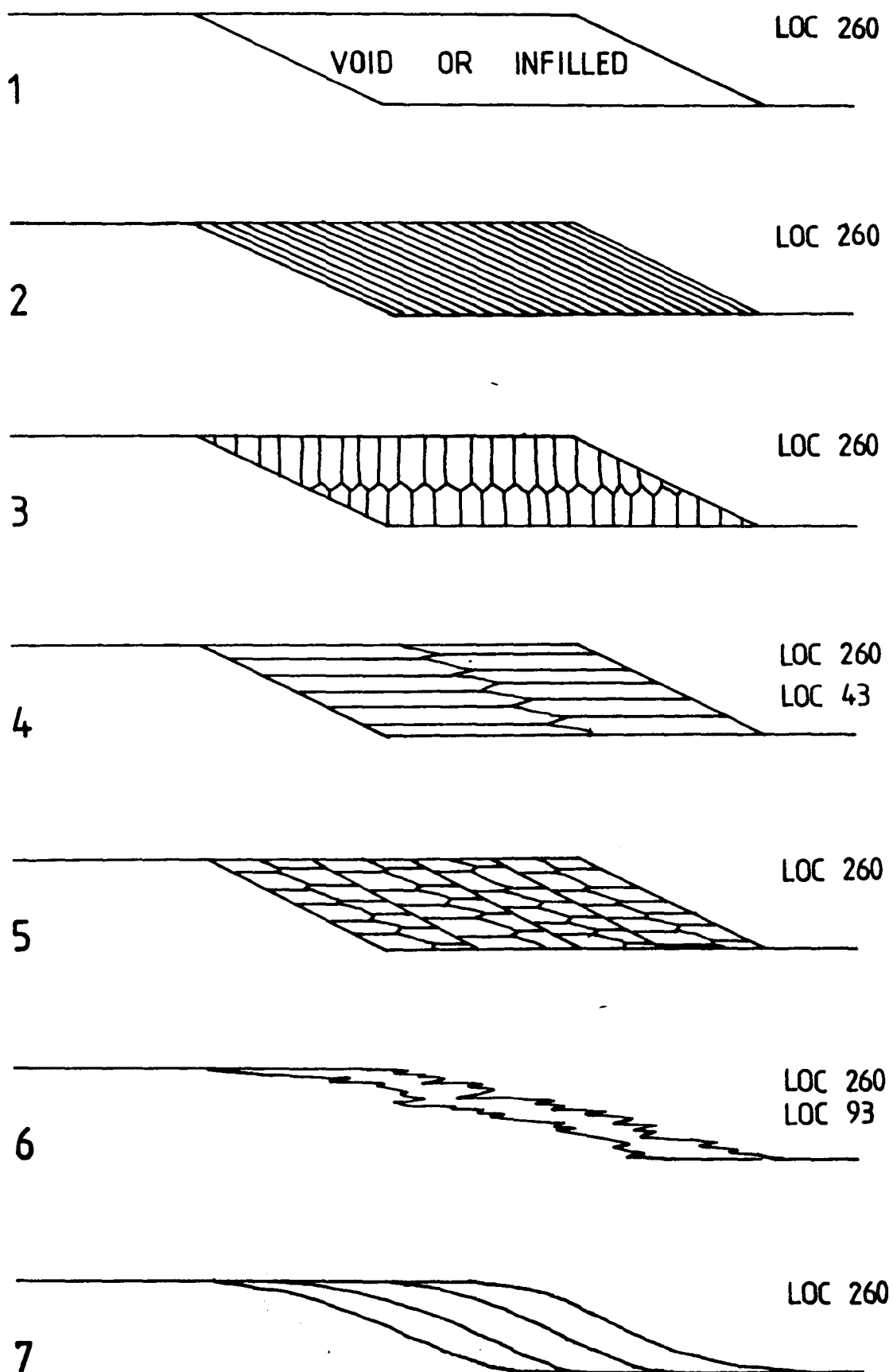


Fig. 5.8 Shear indicators (all examples are sinistral). Complex infillings also discussed. Infilling displays polyphase movement or one single incremental movement.

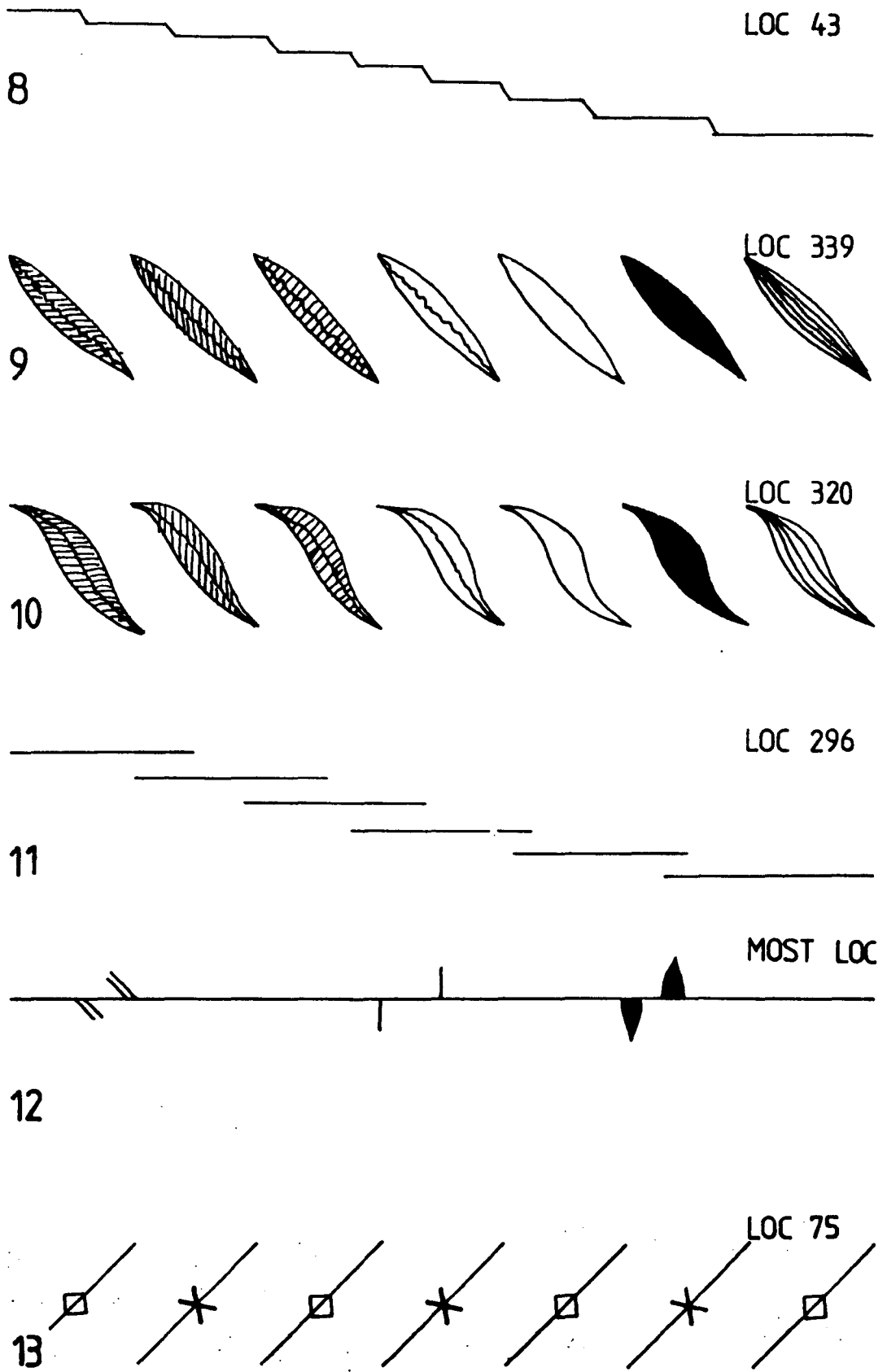


Fig. 5.9 Shear indicators continued, from Fig. 5.8.

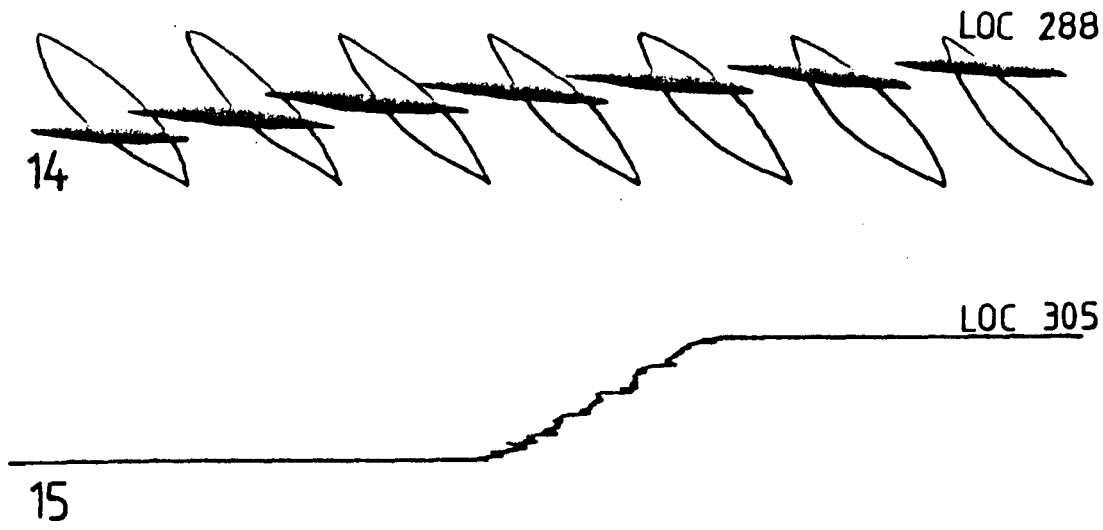
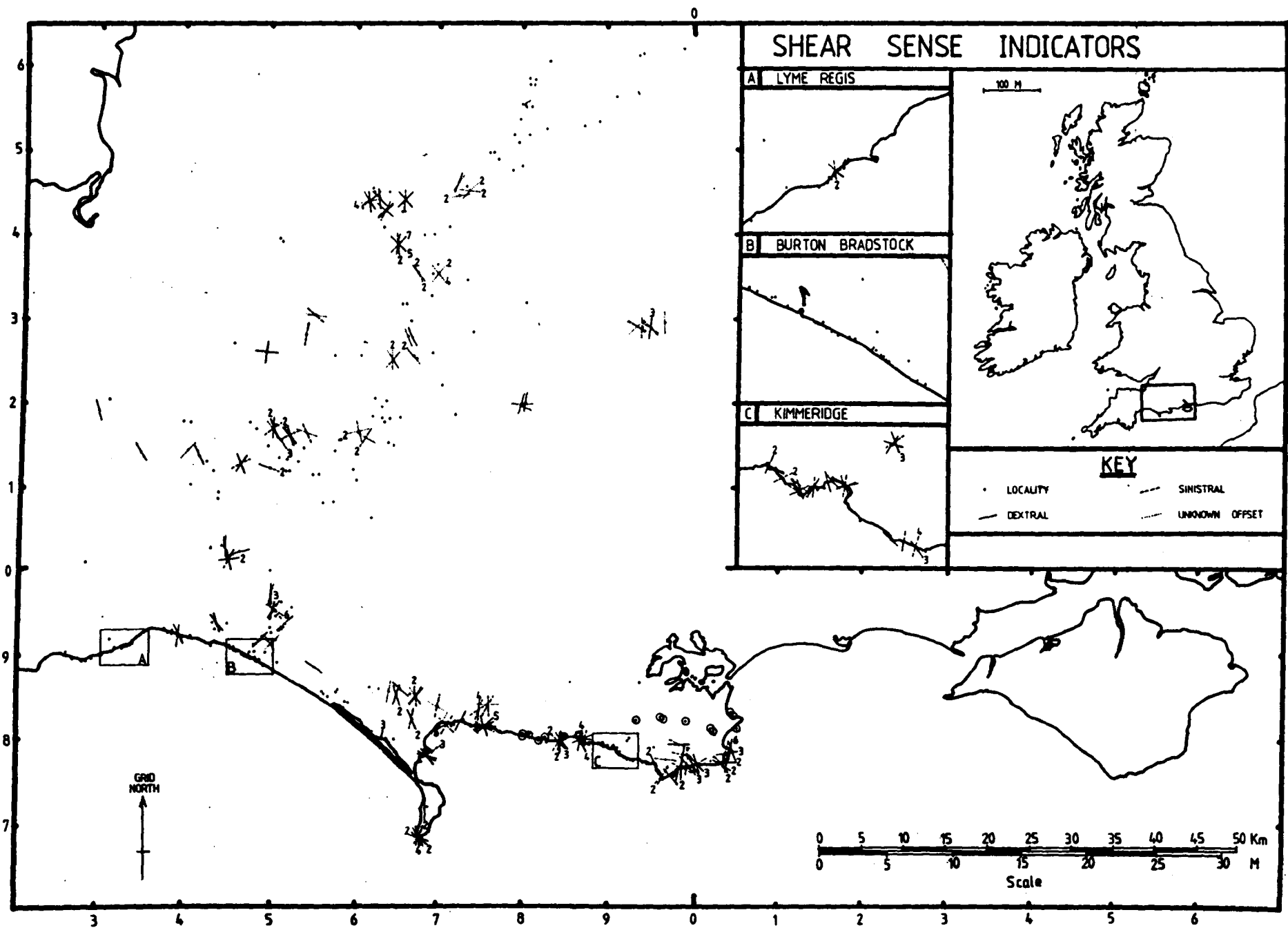


Fig. 5.10 Shear indicators continued. (Number 16 = stylolitic margin still representing sinistral motion).

Fig. 5.11 Shear sense indicators spatially summarized (western Wessex Basin).



II.5.3. The lateral distribution and orientation of these structures is shown on figure 5.11. Most of these structures were best developed in sandstone and limestone lithologies (in particular the Blue Lias, Junction Bed, Ham Hill stone, Inferior Oolite, Corallian and Portland Beds). The majority of these structures indicate northwest-southeast dextral and northeast south-west sinistral motion, presumed to reflect a general north-south compression. They are here assumed to reflect Tertiary north-south compression evidenced by their cross cutting relationships. Furthermore, they may relate directly to Bevan's (1985a) group G mesofractures because of their orientation with respect to σ_1 and thus were formed during the early stages of inversion and monoclinial flexuring (Eocene/Oligocene) rather than later when the monocline level rotated more than 45° and entered the stretching field resulting in layer parallel extension. Such a north-south compression could result at anytime during northwest-southeast dextral strike-slip fault movement.

3. Kink Bands

Kink bands have only been recorded at locality 76 within the Blue Lias clay sequence, reflecting the good mechanical anisotropy of the unit. Kink bands have been classified by Dewey (1965) into normal and reverse kink bands. At locality 76 the kink bands are clearly reverse and are located immediately above the limb of a east-west trending low amplitude fold. Cobbold et al., (1971) have shown that reverse kink bands form when the principle compression is parallel or at a low angle to the fabric in the rock. Therefore their deformation within the basin can either be attributed to Tertiary inversion causing the development of the nearby fold or they may relate to northwest-southeast dextral strike slip movements because of their close proximity to the northwest-

southeast Colethestone fault.

4. Styolites

Styolites have been recorded in many of the Jurassic and Cretaceous limestone sequences. In particular attention is drawn to horizontal east-west styolites present within the chalk at locality 305, where Jones et al., (1984) have demonstrated that they immediately postdate chalk consolidation and developed prior to inversion related monoclinial development along the Purbeck-Isle of Wight fault during the early Tertiary. Styolites elsewhere postdate vein development and are undoubtedly inversion related.

5. Veins

Vein orientation, widths and infills were recorded at most localities in order to identify amounts and directions of extension and relate them to the kinematic development of the basin. The majority of veins are infilled with calcite, however locally pyrite veining is recorded. The veins may be totally infilled or may have subsequently opened either as a result of movement or weathering. Locality 151 unusually displayed late haematitic infilling (identified by XRD) subsequent to calcite infill. Some infillings clearly show syntaxial or antitaxial growth fibres or composites of the two which may record some later or synchronous movement history (Plate 5.5). The orientation of individual fibres reveals the direction of dilation. Fibrous calcite veins ('Beef') are well developed parallel to bedding within the Blue Lias and may have formed as a consequence of overpressuring (Stoneley, 1983). Some veins may exhibit a selenite covering, this generally occurs in areas where superficial movement has taken place. Plate 5.6 clearly



Plate 5.5 Dextral calcite vein segments in the Kimmeridge Clay at Horbarrow ledges (N.G.R. SY 897 790). These displacement shears represent some lateral movement associated with fault zone. The fault breccia in the bottom left hand corner of the exposure corresponds to the same fault zone on Plate 5.13 and Figure 5.1.

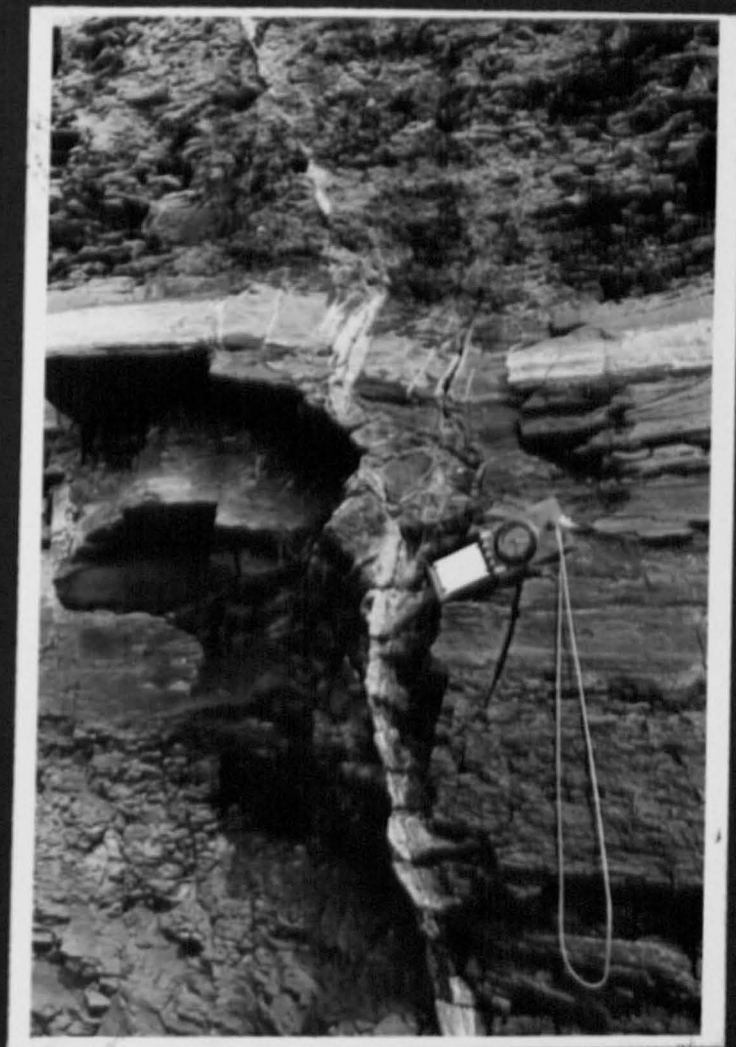


Plate 5.6 A north-south normal fault zone and flexure in the Kimmeridge Clay at Cuddle, Kimmeridge (N.G.R. SY 912 782). Outer arc extension is well displayed.

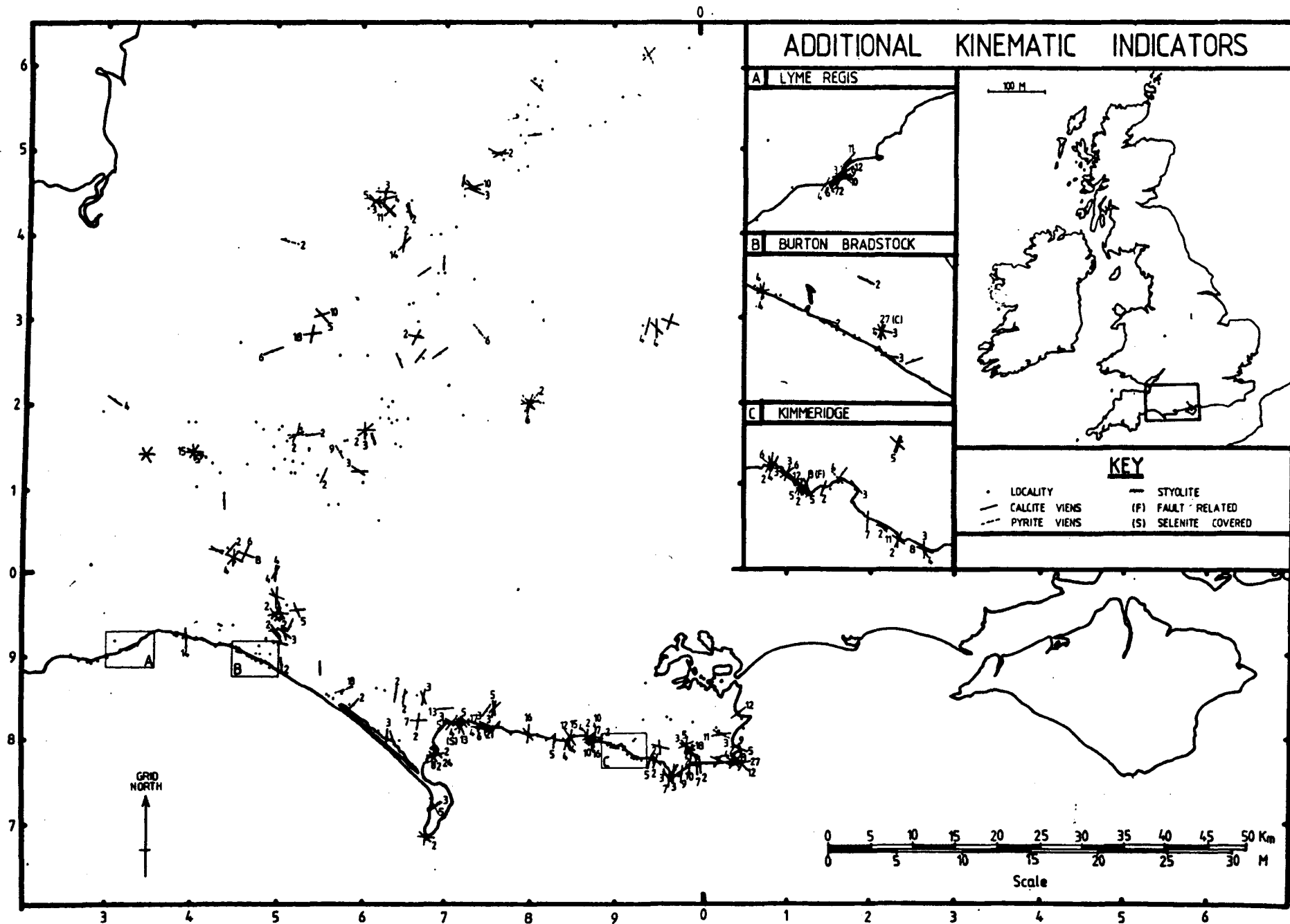
displays calcite veining associated with outer arc extension of a flexure resulting from post Kimmeridgian fault movement. Elsewhere similar fault related calcite veining can be demonstrated. The resulting orientations and frequencies of vein development are summarized on figures 5.12 and II.5.4. Although veins are generally, presumed to predate mesofracture development and perhaps reflect a complex extensional history. This is shown later to be incorrect and that most veins are Tertiary in age. Evidence for pre-Tertiary vein development can only be demonstrated at Durlston Head (locality 339) where east-west veins are related to parallel Tithonian growth faulting (see Appendix F). Pyrite veins generally predate calcite vein development but show no preferred orientation as such they are difficult to date. Calcitic slickensides reflect directions of shear with the slickenstep terminations facing the direction of motion (see earlier). The predominance of north-south veining (Figs 5.12 and II.5.4) in the vicinity of the Purbeck-Isle of Wight fault may imply that they are inversion related and general reflect north-south early Tertiary compression. There is no evidence that any veining can be directly related to the pre-Tertiary kinematic development of the basin.

6. Fissures

Fissure development is divisible into two types: (1) Synsedimentary fissures and (2) superficial fissures.

Although many types of fissure can be recognised (see Robinson, 1957) it is pertinent to consider only three types here: (1) synsedimentary fissures, (2) Neptunian fissures and (3) superficial fissures. Point (3) is more appropriately discussed later.

Fig. 5.12 Additional kinematic indicators spatially summarized (western Wessex Basin).



Synsedimentary fissures occurred synchronously with sedimentation and are largely tectonically induced. The term Neptunian fissures is here applied to fissure infillings that postdate the rock formation in which they are present, these may be submarine or terrestrial in origin and may display a polyphase history of infilling.

Synsedimentary fissures have been identified within the Junction Bed at Watton Cliff, fault Corner (locality 191) (Jenkyns & Senior, 1977) and in the Purbeck Beds (Ensom, 1985). During the course of this study, other fissures have been recognised within the Junction Bed inland (localities 47, 92, 96, 97, and 108) and in the Inferior oolite (localities 95, and 151) and similar structures probably occur in the other limestone units (especially the Cornbrash, Corallian Beds and Portland Beds). Some apparent fissure infillings clearly are infilled burrows e.g. the Rhaetic Bone Bed at locality 178 (see Sellwood et al., 1970).

Neptunian fissures have been clearly identified in the Mendip region (see Robinson, 1957). Most of these fissures were developed in the late Carboniferous along major joint and fault planes which may be subsequently widened into a cavern system. Fissure infills range from Rhaetic to Inferior Oolite in age. The fissures may have been open at the time of deposition or reopened later. Most of these fissures trend east-west and may have opened due to sedimentary loading of the basins further north and south during the Permian-Jurassic (i.e. the Mendip region may have behaved as a peripheral bulge). Locality 26 best displays multiple fissure infillings with semi or total lithification between each infill (these infills in turn range from Rhaetic to Inferior Oolite in age and contain the only recorded Junction Bed aged fissures

in the whole region).

Many joint planes described later have been infilled with clay south of the Purbeck-Isle of Wight fault and are probably post inversion to recent aged phenomena. In conclusion, synsedimentary fissures display a multiple infill history, these periods are only exemplified in limestone and sandstone lithologies, and are not displayed in the clay facies even though such facies occurred at periods of greater extension (see Chapter 2). Neptunian fissures in the Mendip region may display complex polyphase history perhaps reflecting period of major extension and loading in the nearby basins, reactivating along an earlier (late Carboniferous) fractures system (c.f. Roberts, 1974).

7. Sediment filled mesofractures

Although some sediment filled mesofractures were described in the previous section, this passage deals with a previously undescribed phenomena discovered in the Toarcian sands. At East Cliff, Bridport (e.g. Loc 199) major northeast-southwest trending (220°) tabular zones up to 1 metre in width contain poorly cemented angular quartz fragments. These zones are developed parallel to the major but secondary (see later) jointing in the area. They extend at least 70 metres through the rhythmic Bridport Sands succession, cross cutting and in part offsetting earlier primary and secondary cemented units (Plate 5.7). The fractures trend parallel to the valley sides and could be, in part misinterpreted as a cambering phenomena, however they are very extensive and are even well developed away from recent cambering processes; in addition, inland they can be seen to be oblique if not at right angles to local valley sides. Thin section analysis reveals that the infill varies in detail



Plate 5.7 A detailed view of extensional tilted fault block structures within the Bridport Sands under East Cliff, Bridport (N.G.R. SY 453 909).

from the surrounding rock, for example the quartz fragments within the zone are more angular than those external to the zone, and the cement has been largely removed within the zone emphasizing its original fluid nature. These structures are termed fracture solution pipes (see figure II.5.5). Late Pleistocene infills (partly resulting from cambering) at the top of figure II.5.5 do not extent to great depths and emphasise the importance of these pipes as previous lines of weakness. Some well cemented blocks within the pipes imply that fluidized sandstone was injected from below, while other blocks have clearly subsided into the matrix. Some of these pipes appear to be truncated by the Inferior Oolite at East Cliff, Bridport (localities 199-217) although the inaccessibility of the section makes this difficult to verify. Because these structures are extensive they cannot be related to the nearby Mangerton Tear fault. They do however, parallel joint orientations (see later) and presumably date from the same time. Clarke (pers comm) believes that the fluidization is not the result of dewatering from the underlying downcliff clay, but is caused by hydrocarbon escape presumably hydraulically injected. If this is so then the gas probably escaped towards the end of inversion from earlier pre inversion gas traps, since no burial could have occurred following the Upper Cretaceous/Tertiary initiation of inversion (see Chapter 3).

8. Superficial structures

Superficial structures here include gulls, Valley bulge and differing forms of cambering and landslip. A brief resume of examples of these structures will be shown.

Gulls are fissures which taper downwards as a result of cambering and are generally infilled. Gulls are well developed at Ham Hill

(locality 93) (Fig. 5.13) where they lie parallel to the valley sides. The fracture solution pipes within the Toarcian sands have been subsequently opened close to the valley sides, for example figure displays Pliocene rubble infilling such structures at Bridport.

Valley Bulge occurs where the incompetent material is forced up into a valley by the weight of the hill masses on either side, two important examples were encountered at (1) Charmouth (N.G.R. SY 365 930) discussed in detail by Lang (1933) and (2) Liberty farm (locality 126) where the Forest Marble has been intensely deformed. This phenomenon could be mistaken for tectonic induced deformation.

Cambering and landslip has occurred along much of the coast, some of which has been described by Arber (1973).

This phenomenon must be taken into account especially where anomalous dips are encountered.

9. Jointing

The kinematic indicators previously described were measured to derive the stress trajectories. Joint system architecture can also be used to a lesser extent if other indicators are absent, in order to determine stress orientations.

Joints are cracks and fractures in rock along which there has been little or no movement (Price, 1966). If they display any mineral fill, then the feature is termed a vein (Hancock, 1985). Fractures displaying slickensides or other signs of obvious movement are classed as faults or shear fractures and were summarized earlier. The description of joint system architecture are adequately summarized by Price (1959), Price (1966), Roberts (1966), Hancock (1968) and Hancock (1985). It is

PULL

OUT

however, important to briefly outline the classification used in this study. Planar and parallel joints are termed systematic while irregular ones are termed non-systematic, the latter forms have proved to be useless in defining the stress trajectory because of the varying orientations along strike. At the majority of the localities visited, one set of joints is often more dominant, being larger or more frequent than other joint sets. Joint sets of decreasing frequency and width are termed Secondary and Tertiary systematic joints respectively. Although more recently other classifications have been developed (eg. Hancock et al., 1984; Bevan, 1985a and Hancock, 1985), these are not available prior to the completion of fieldwork and as will be shown later, may add unnecessary complications. Joint plane morphology in particular roughness of the joint, surface plumose structures (feather joints), cross cutting relationships, frequency, lithology and mineralization were also examined. The resulting orientations from some nine months fieldwork are summarized on figures 5.14, 5.15, 5.16, II.5.6, II.5.7 and II.5.8. Primary systematic joints (Figs 5.14, and II.5.5) trend northwest-southeast (320 degrees) whereas secondary joints trend 240 degrees (Figs 5.15, and II.5.7). Tertiary joints seem to follow no preferred orientation (Figs 5.15, and II.5.7). All these joint sets follow the same trend whatever the lithology or age of the sequence, also these joint systems were not restored to horizontal (because dips rarely exceed 3° degrees), and even in areas where dips exceed 45 degrees, the joint orientations remain constant. Some localities displayed joint sets that could not be morphologically separated, these are summarized on figures 5.16 and II.5.8. The majority of these clearly follow trends parallel to the three class joint systems described earlier, thus they

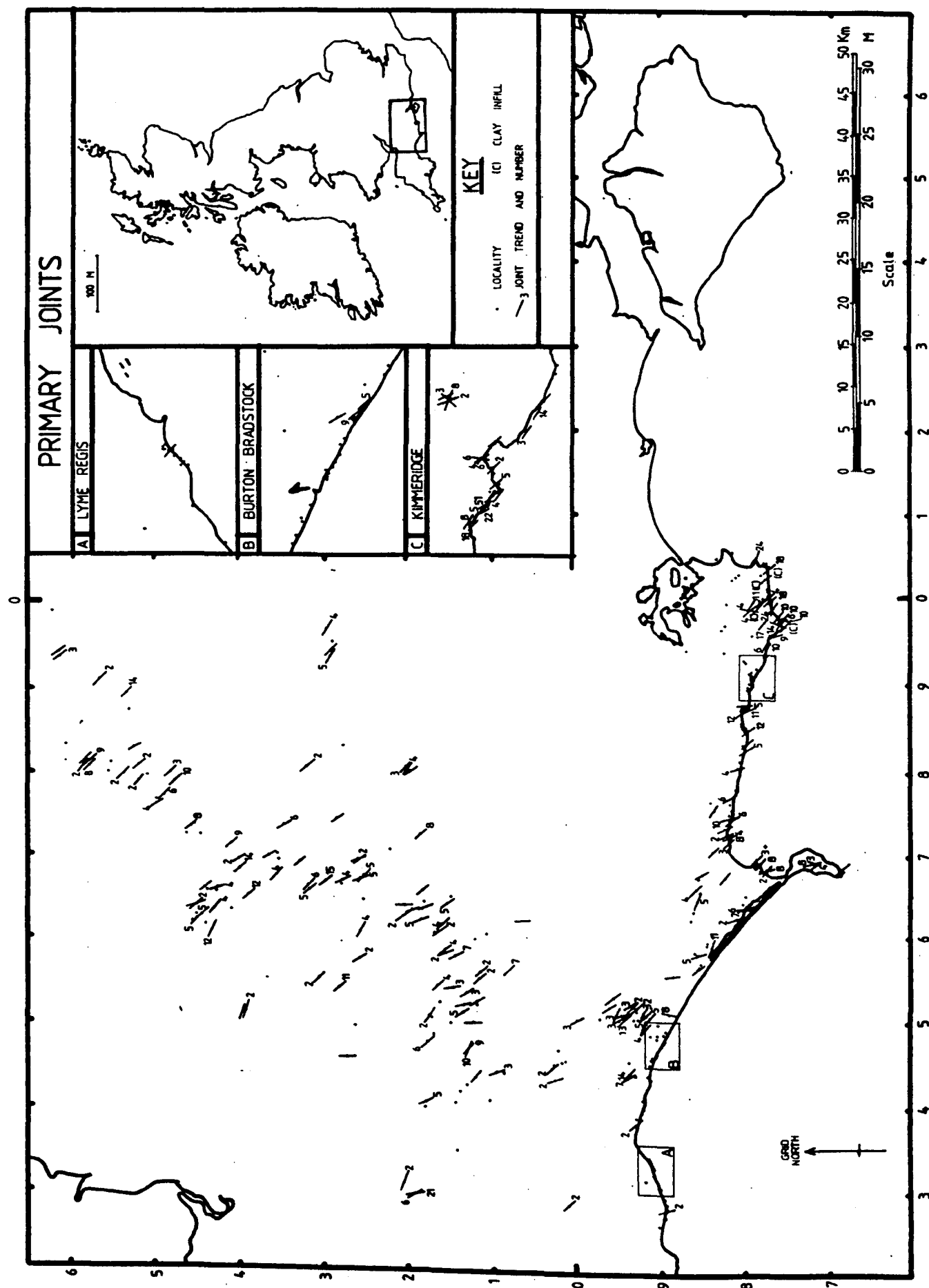


Fig. 5.14 Primary Joint summary map (western Wessex Basin).

Fig. 5.15 Secondary and Tertiary Joint summary map (western Wessex Basin).

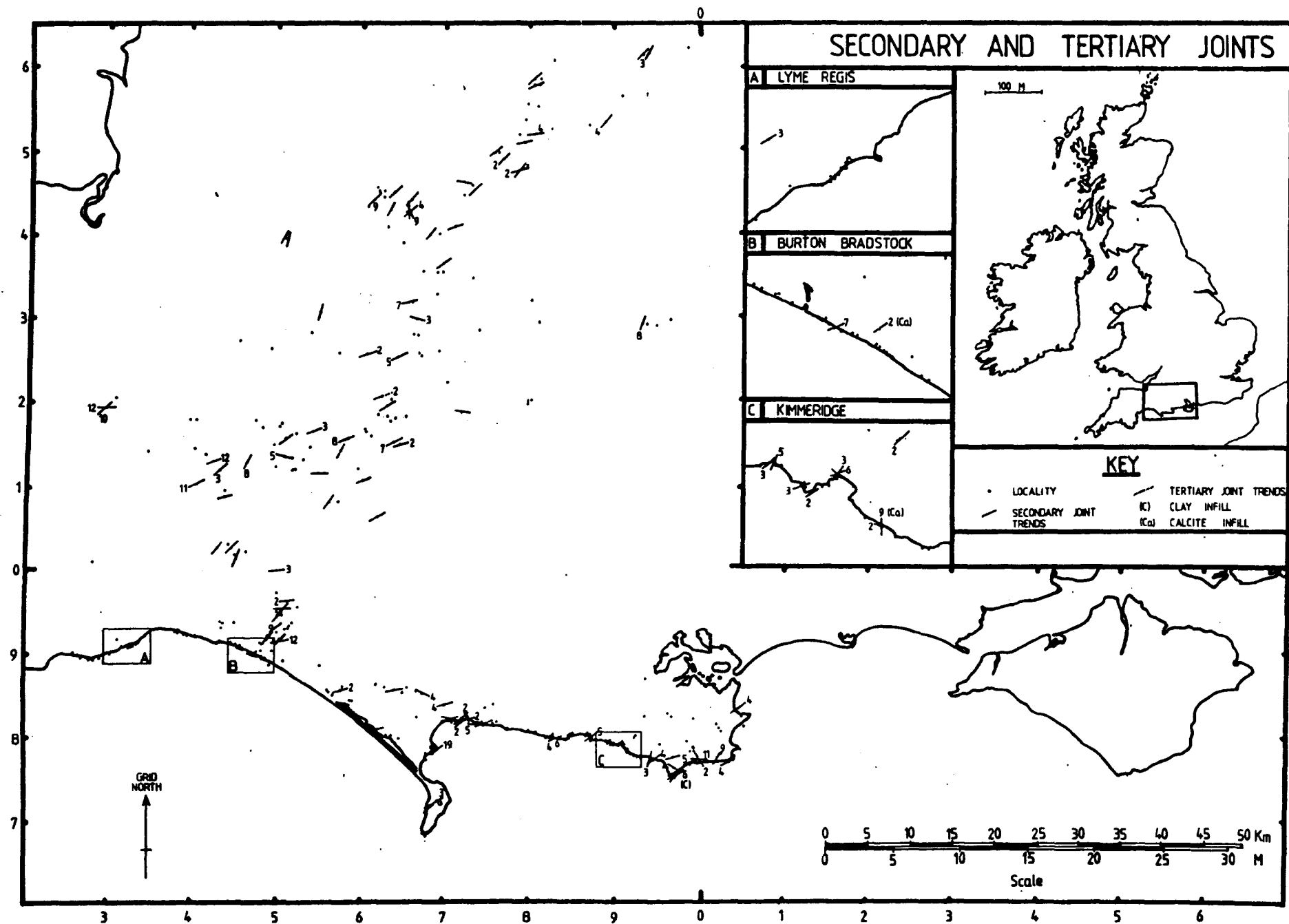
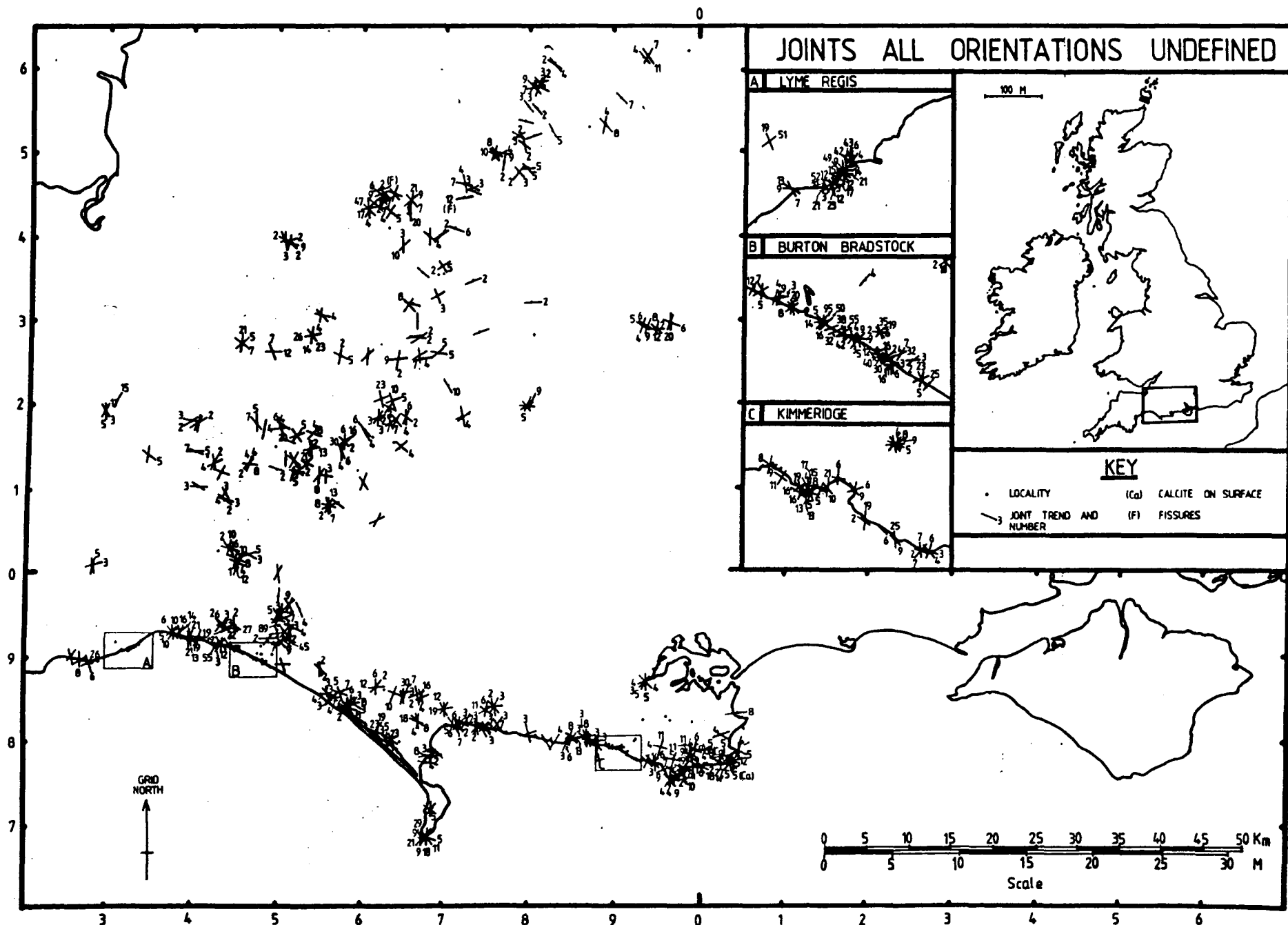
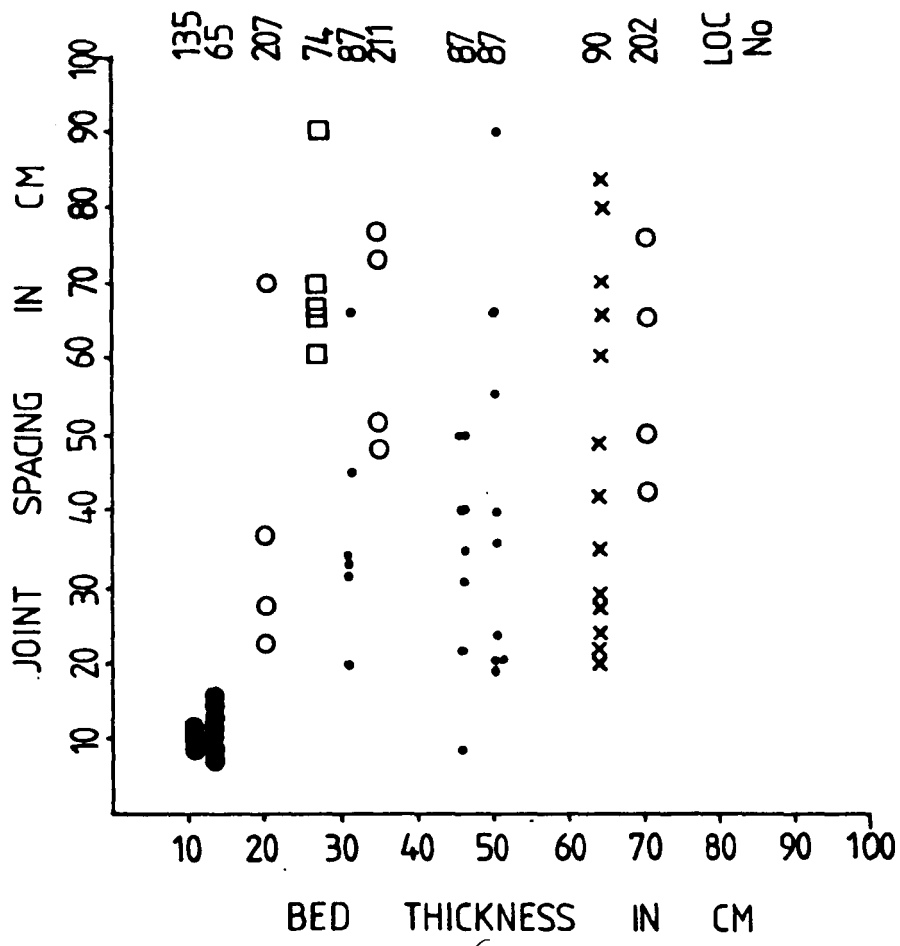


Fig. 5.16 Joints, all orientations which are undefined. Summary map.



represent smaller joint sets which parallel the larger structures and may therefore be of the same generation. Many closely spaced joints define a joint zone (e.g. localities 77, 100 and 146). These zones again parallel major joint orientations although some may relate to recent fault movement. Major extensive joint zones may be identified using remote sensing techniques, as lineaments, which clearly do not relate to any deep structural features. Since joints uncommonly dip less than 90 degrees (i.e. normal to bedding) joint dip as such need not be considered. Where dips were less than 90 degrees, they are generally related to refraction of jointing due to contrasting lithologies, implying that σ_2 was not perpendicular to bedding to layering during failure. This is particularly evident in the Blue Lias (localities 174-189).

Joint frequency although a much greater order of magnitude than fault frequency, is highly variable between localities. The former may be a function of lithology, bed thickness and tectonic deformation, whilst the latter presumably reflects the differing age and movement. Joint frequencies related to lithological variations are summarized on Table 5.1, where it can be clearly seen that there is no direct relationship between the two. Average joint spacing approximates between 30 and 60 cm apart, whilst sequences such as the Kimmeridge Clay display a significant joint frequency range (Table 5.2). A relationship between joint spacing and bed thickness has been noted by many elsewhere (eg Harris et al., 1960) however, there may only be a correlation between small spacing and small bed thickness (i.e. where Bed thickness = joint spacing in the Blue Lias) whilst other sequences clearly show no correlation (Table 5.1).



KEY

- FOREST MARBLE
- INFERIOR OOLITE
- BRIDPORT SANDS
- × JUNCTION BED
- BLUE LIAS

Table 5.1 Joint frequency versus bed thickness for differing aged units and lithologies.

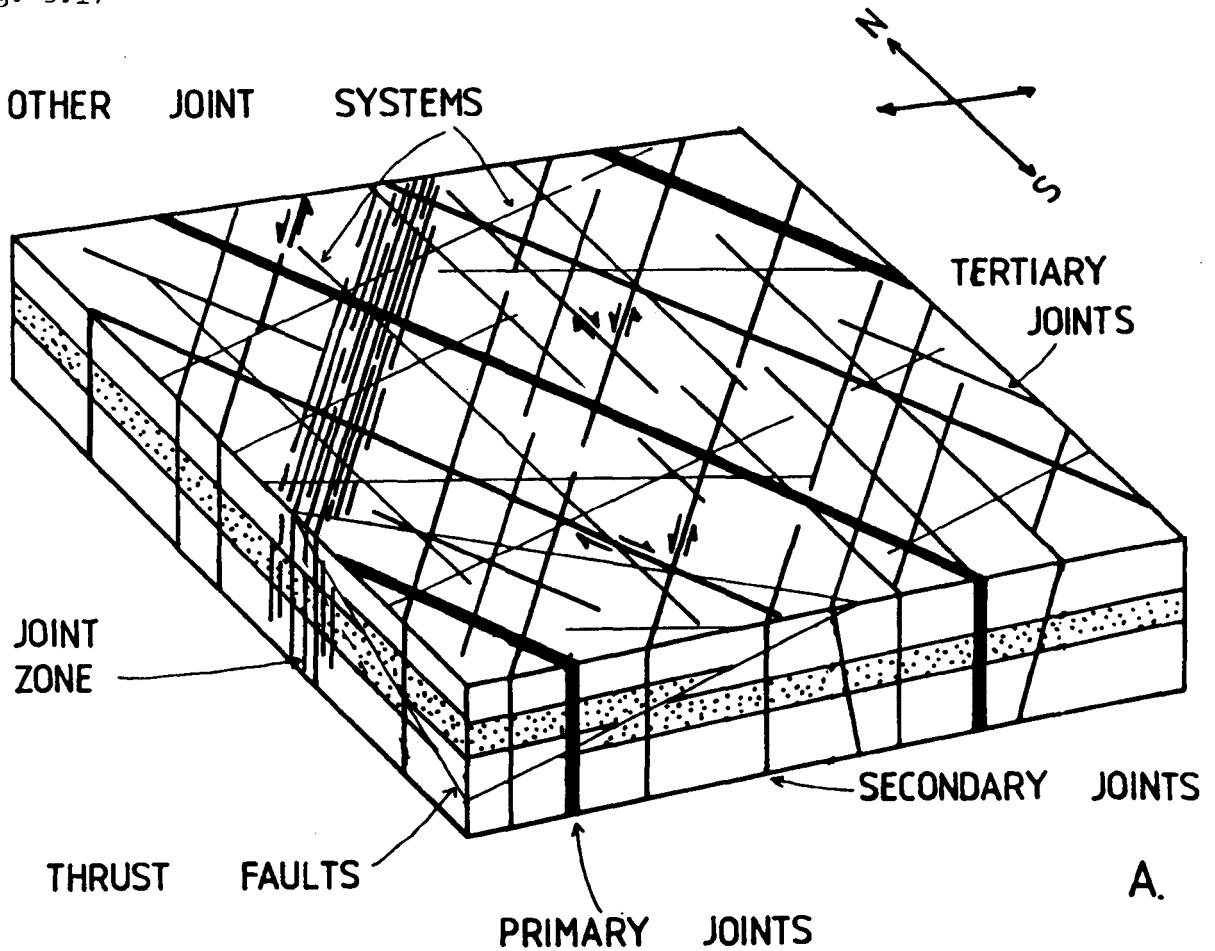
Table 5.2 Joint spacing for differing aged units and lithologies. (Numbers denote frequency at individual localities). Spacings greater than 3 m summarized.

	10	20	30	40	50	60	70	80	90	100	110	120	130	140	150	160	170	180	190	200	210	220	230	240	250	260	270	280	290	300			
TERTIARY				7								3																					
LOWER GREENSAND			6																														
WEALDEN			8																														
PURBECK			5	4	5	4	3	9				3	2		2																		
PORTLAND			5	7	5	3	3	11					10	2		7										3		4				3-28 (8) 2-8 (7) 3-0 (14) 2-85 (6)	
KIMMERIDGE	19 13	31 3	7 3	35 7	9 7	4 2	9 10	6 3	6 4	7 9	6 6	4 11	4 9	2 2	2 3	2 2	4 2	2 5	8 8	2 2	5 5						3 3						
CORALLIAN			.	10 10	. 26	3 2	13 2		6 6			6 14				.										4 4		2 2					
CORNBRASH		6				30																											
FOREST MARBLE				7	.		.					2		.																			
INFERIOR OOLITE	31 31		.	11 8	7 7	.	.	33 33	6 5	5 4		33 33	5 5	.			3 3									13 13							4-37 (13)
BRIDPORT SANDS			.	11 14	14 2		.	4 4		10 10		14 14		14 14													15 15						5-73.
HAM HILL STONE		5 4																															
JUNCTION BED							.			.																							
EYPE CLAY				24 24	47 47																												
GREEN AMMONITE B.																					20 20		18 18					14 14					
BLUE LIAS	21 21	9 9	6 6	7 7			11 11	4 4		13 13		4 4															2 2						LARGER JOINT SPACING

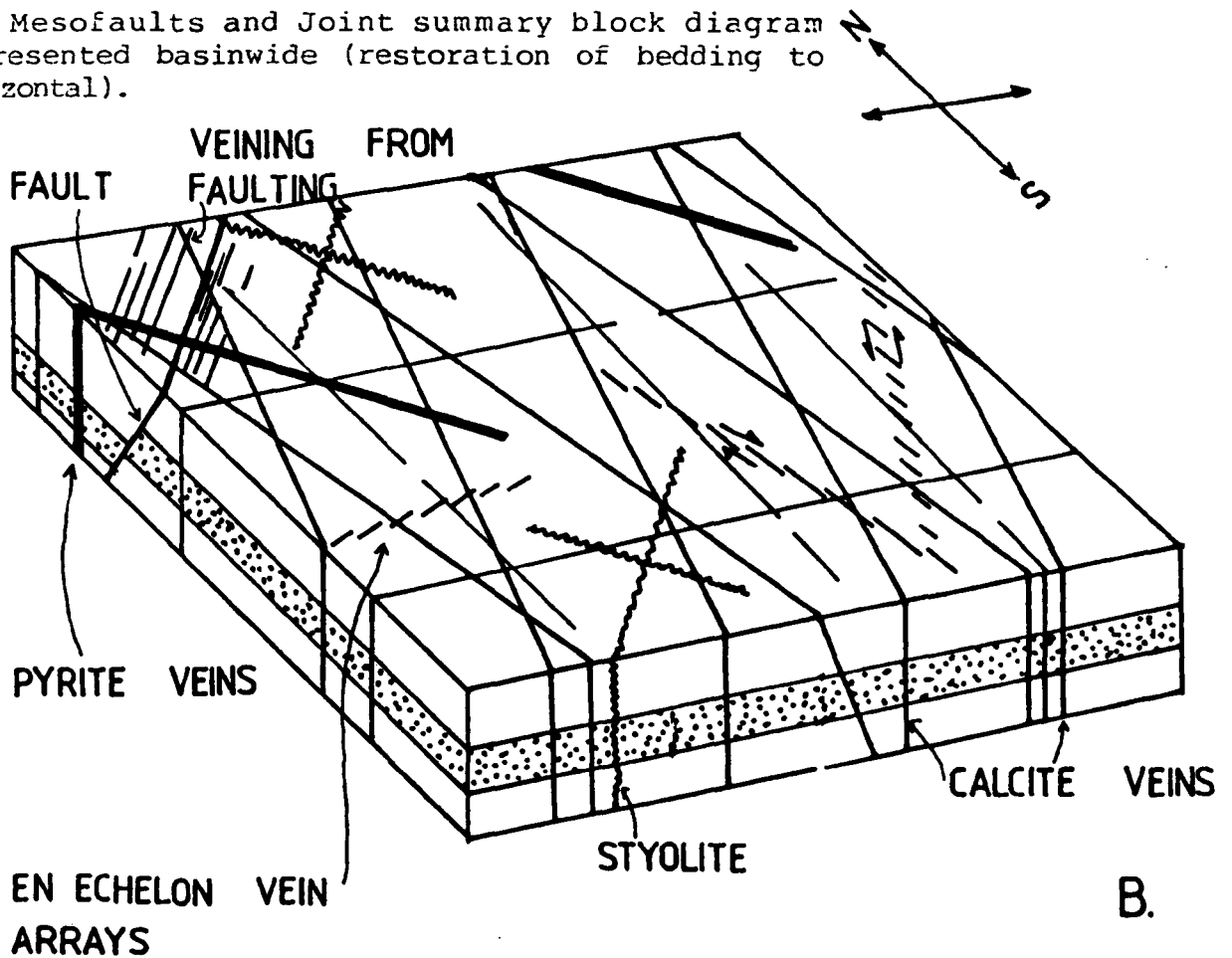
Cross cutting relationships are generally not helpful in describing the evolution of joint sets. For example, locality 331 displays both primary and secondary joint sets offsetting each other whilst other localities clearly display primary joints truncating other joint sets (e.g. locality 304). Plumose or feather joints were clearly developed at some localities (e.g. locality 293) such structures trend northwest-southeast (primary) or north-south. They may be formed during extensional or compressional failure (c.f. Hancock, 1985 for discussion), but nevertheless developed synchronously with other joint systems. Mineralized joint sets are here viewed as veins and were dealt with in the previous sections. One locality 327, however displays chert infill along the primary joint systems. Portland Chert has been shown to develop soon after cementation, as evidence by reworked Portland Chert in the Purbeck Beds (West & Hooper, 1969), the orientation of this joint set, cross cutting obvious Tertiary inversion related structures, suggests remobilization of the original chert and subsequent fracture infill. Therefore the mineralization of such joint sets is by no means a conclusive phenomena for dating joint development.

The timing of jointing with respect to tectonics has proved relatively complex, most joint sets described clearly postdate inversion culmination (Oligocene-Miocene) and may result from residual stresses from one single phase of compression and uplift. This can clearly be seen from comparing figure 5.17 which summarizes all the major, kinematic indicators and their respective orientation to Price's (1966) postulated model of fractures (his figure 46) resulting from one complete tectonic cycle. The similarity between the geometry proposed by Price (1966, Fig. 46) and the geometry of the Cotswold joint and fault pattern was noted by

Fig. 5.17



A. Mesofaults and Joint summary block diagram represented basinwide (restoration of bedding to horizontal).



B. Additional kinematic indicator summary block diagram represented basinwide restoration of bedding to horizontal. Compare both diagrams with Price (1966, Fig. 46).

Hancock (1969). The model could therefore be applicable to most post Mesozoic joint systems throughout the British Isles. In particular, Bevan & Hancock (in press) noted the major development of northwest-southeast extensional fracture sets across south eastern England in Cretaceous and Tertiary strata. Similar joint sets were recorded in Mesozoic strata in the Vale of Glamorgan by Roberts (1974, 430,200,280⁰ respectively). The shear fractures discussed earlier appear to postdate jointing (e.g. locality 328) while some, particularly en-echelon vein arrays associated with faulting (e.g. Plates 5.8 and 5.9), pre-date joint development. The primary system joint set trends northwest-southeast and is well developed at most localities, these joints appear to be related to a northeast-southwest minimum principle stress axis. The lack of significant offset along these fractures compared to the northwest-southeast shear fractures would imply the former developed in part earlier. Bevan & Hancock (in press) found that normal mesofaults and steep hybrid or small shear fractures were initiated when the maximum stress was vertical and probably developed synchronously with the northwest-southeast vertical extension joints. These authors also believe that they decrease in intensity westwards, a view not altogether inconsistent with the observations here, furthermore they suggested that resultant mesofractures developed synchronously with the generation of normal faulting in the upper Rhinegraben and were therefore associated with Alpine northwesterly convergence. It is therefore clear that the primary joints developed after the inversion (Mid Miocene, of Dewey, 1982) and that they were formed as a result of northwesterly Alpine convergence. Whilst this is true the Alpine deformation is the result and not the cause. The cause is more likely related to the northwesterly

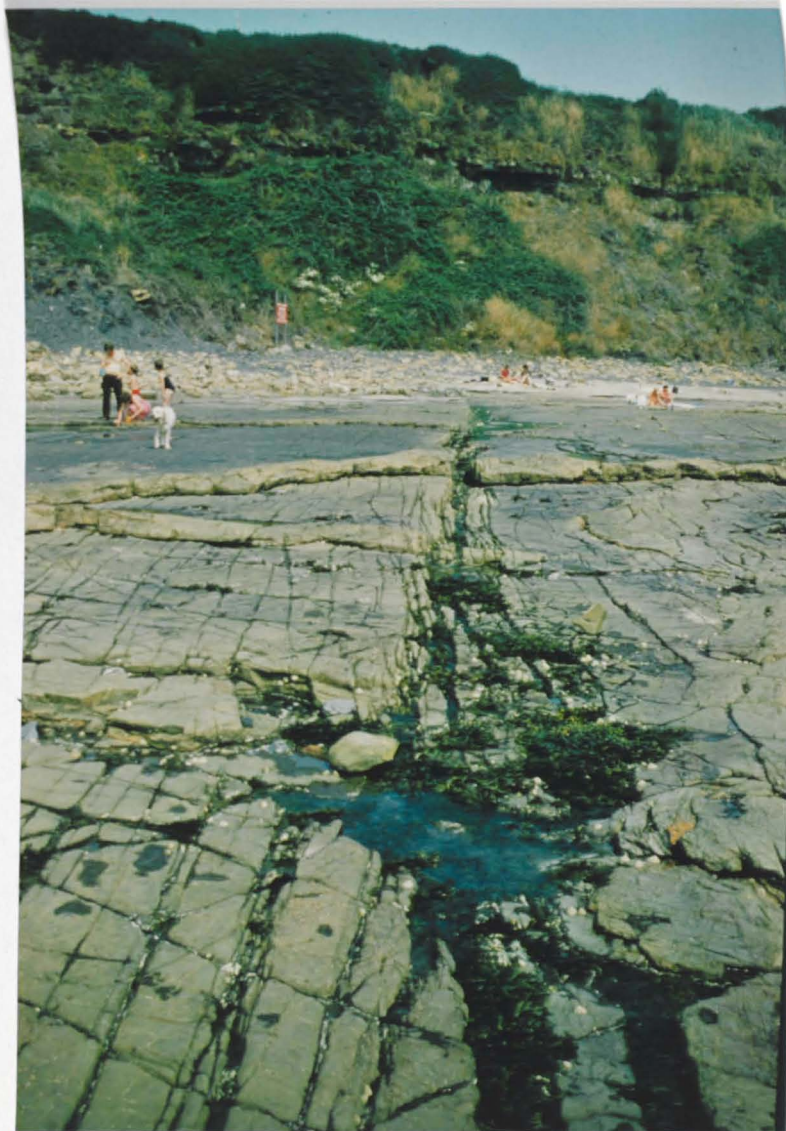


Plate 5.8 Looking along a north-south fault plane at Kimmeridge Bay (N.G.R. SY 908 792) which transects and offsets the hanging wall anticlines (displayed clearly as ridges) of the overlapping contractional mesofaults (thrusts) in the 'Flats Stone Band'.

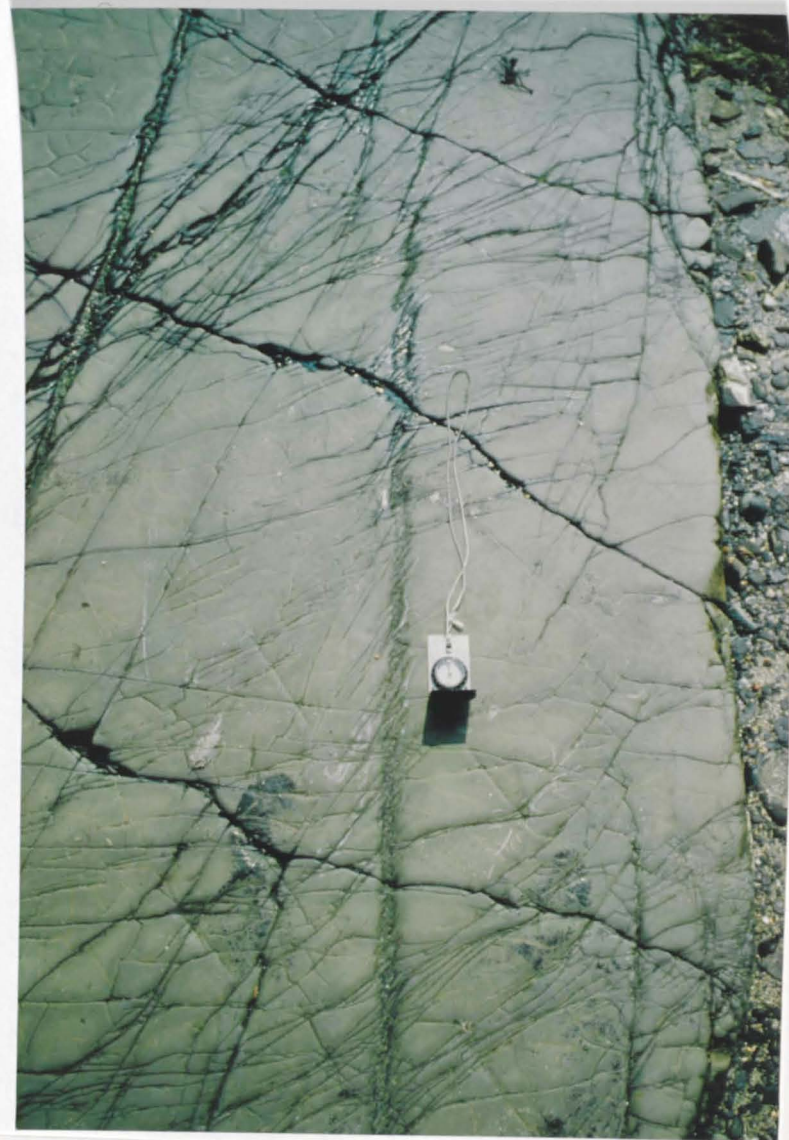


Plate 5.9 North-south dextral en-echelon hybrid fractures within the 'Flats Stone Band', at Kimmeridge Bay (N.G.R. SY 904 792). These are developed parallel to the fault plane displayed clearly in plate 5.8.

relative plate motion of Africa relative to Europe. The relationship between this joint set and other sets imply that other joint sets formed at the same time. The conjugate northwest-southeast dextral and northeast-southwest sinistral extension fractures imply east-west extension (σ_3) which are presumed to initiate during inversion (see Bevan, 1985a), (stylolites and vein arrays reflect the same phenomena), and generally postdate joint development as clearly displayed by later dextral and sinistral movement along northwest-southeast and northeast-southwest trends respectively. (e.g. localities 289, 328, and 331). These later movements are also concordant with conjugate fault development described earlier. Between the development of the jointing shown to postdate inversion, (pre-late Pliocene according to Bevan & Hancock, in press) reflecting a northeast-southwest (σ_3) minimum stress trajectory and the present day northeast-southwest σ_1 stress trajectory (see Schmitt, 1981; Batchelor, 1984), the minimum stress trajectory must have been orientated east-west (i.e. between the late Pliocene and present day these stress trajectories undoubtedly formed most of the lineament orientations and developments discussed earlier and more fully outlined in Appendix D. The joint systems are therefore not related to variations in extension rates and directions but relate to the final phase of basin development which in this case largely postdate the Oligocene/Miocene inversion, and this section seriously raises doubt whether more complex forms of brittle microtectonic classification such as those outlined by Hancock (1985) are really required, since a simple system of classification seems to achieve the similar result.

D. Conclusions

Mesoscale faults and folds are generally useful kinematic indicators, which have been shown to enhance the evolutionary sequence of the basin in greater detail. Most structures are presumed to have developed during inversion but some are demonstratably earlier as evidenced by synsedimentary growth faulting. Brittle microtectonic structures can be variably dated as late Cretaceous to Quaternary reflecting the complex inversion history of the area discussed more fully in Chapter 3. The fissure infills in the region formed synchronously with basin development but show no preferential opening history. Jointing developed during the post inversion stage when the principle stress lay northwest-southeast parallel to the relative plate motion convergence of Fig. 3.14. A later north-south compression cannot be directly correlated with plate motions and is assumed to reflect stress diffraction during general northwest-southeast compression.

CHAPTER 6

HYDROCARBON OCCURENCES

6.1 Introduction

Since the need arose for indigenous petroleum sources the Wessex Basin has attracted considerable exploration interest over the past 50 years. The discovery of oil seepages, impregnated sandstones and conglomerates along the Dorset coast (Lees & Cox, 1937) and the nearby large anticlines of comparable geometry to those encountered by the Anglo-Persian Oil Company geologists in the Middle East (around Fars and Khuzistan), (Kent, 1985) provided an impetus to exploration in the area and led to the discovery of Kimmeridge oilfield in 1959. This was subsequently followed by the successful exploration programs of Amoco, British Gas, British Petroleum, Carless Petroleum, Conoco and Shell. Currently the Wessex Basin has the three largest onshore oilfields in the United Kingdom; Wytch Farm, Horndean and Humbly Grove (Figs 6.1 and II.6.1).

An outline of the potential source and reservoirs rocks as well as proven and prospective hydrocarbon plays are discussed in this section. For a more detailed account, attention is drawn to Lees & Cox (1937), Colter & Havard (1981), Cornford (1984) and Ebukanson (1984).

6.2 Source Rocks

Major source rocks are essentially divisible into Palaeozoic sources in the basement (pre-basin) and Mesozoic sources principally within the Jurassic (syn-basin). In terms of pre-basin sources most of the basin is underlain by Devonian/Carboniferous sediments, (gas prone sources) although the Shrewton borehole recorded weak gas shows in Tremadoc mudstones (Whittaker, 1980). Devonian/Carboniferous sources were largely lost during uplift and erosion following the Variscan orogeny. In

PULL

OUT

addition many upper Carboniferous sources along the 'Variscan front' have exceeded vitrinite reflectance (V.R) values of 2%, e.g. the south Wales anthracites. These high values were also probably reached during the Variscan orogeny, since there has been insufficient subsequent burial of the London-Brabant platform. Devonian/Carboniferous sources may have been partly preserved in local pockets under the Wessex Basin, however the nature of the Variscan deformation severely limits delineation of the potential source area available for maturation.

Triassic (syn-basin) sources are probably only significant north of latitude 65°N where marginal marine shales have been encountered (Cornford, 1984). In southern England the Triassic offers no source potential because of the lack of organic components.

Jurassic petroleum sources are largely confined to the Lias. Oxford and Kimmeridge clays.

The Lower Lias clays (Hettangian-Pliensbachian) are rich in Kerogen facies type II-IV (Ebukanson, 1984) with laminated shales and limestones offering the best potential. Historically oil shales were extracted in north Somerset around Kilve, whilst around the Lyme Regis area the high sulphurous content of these rocks combined with the high bituminous content frequently ignited the Lias cliffs due to the heat generated by the decomposing pyrite (Edmonds et al., 1975).

Vitrinite reflectance data confirms Lias maturity up to 0.90% in Arreton No2, with slightly lower values in Winterborne Kingston, Marchwood, Winchester, Warlingham and Henfield (Ebukanson, 1984), however some relatively positive areas e.g. Wytch farm (Colter & Havard, 1981) are immature. C. Cornford (oral comm) ^{cor'd} recorded low V.R. values around Lyme Regis (0.36%), compared with values of around 0.46% in North

Somerset and even higher values in South Wales (0.51%). He attributed this to increasing northward burial (1.5 Km to 2.9 Km respectively). The structural analysis of the Lyme Regis area confirms its relative positive nature although the close proximity of the Bristol Channel graben and the geological complexity along the Bristol Channel margins, emphasises that other processes (involving increased heat flow) may have severely affected his results.

The Liassic mature source areas are summarized on figure 6.1 and II.6.1, in which it can be seen that the major source areas are located on the downthrown hanging wall side of the growth faults (Colter & Havard, 1981) and in the central depocentre of the Weald basin. The latter may have reached sufficient burial depths for gas migration during the Tertiary (Dolan Personal comm), because the Lias is rich in oil and gas prone matter. In addition to this a Palaeozoic source could be responsible for recent gas discoveries in this area.

The Oxford clay offers the next source rock of greatest potential, particularly in the shales of the Lower Oxford clay and the mudstone in the Upper Oxford clay where kerogen facies were comparable to the Lower Lias (Ebukanson, 1984). In the North Sea the Oxford clay facies comprises fair to rich gas prone rocks (Barnard & Cooper, 1981) and also has local oil potential.

The Kimmeridge clay has a rich source potential although it is not comparable to the North Sea where large fairways have reached maturity. Colter & Havard (1981) observed that the Kimmeridge clay is close to maturity in the Arreton No2, however at outcrop in the Kimmeridge area Farrimond et al., (1984) observed V.R values around 0.36% which indicates from a secondary input of mature hydrocarbons. Other potential

hydrocarbon sources include the Fullers Earth (Bathonian) in the Weald (Dolan, oral comm) and the Gault clay, the latter undoubtedly never having reached maturity due, undoubtedly to insufficient burial.

In conclusion the Lias offers the best source potential, covering by far the largest area of maturity. The Oxford and Kimmeridge clays also offer some potential, although present day oil seepages from these seem to be secondary, except in the deepest portions of the basin.

6.3 Maturation and Migration

During burial, kerogenic material undergoes physical and chemical changes due largely to temperature increases with depth. Present day geothermal gradients about $28^{\circ}\text{C}/\text{Km}$ (Fig. 6.2) do not relate to past temperature distributions (Andrews-Speed et al., 1984) and in addition direct comparison of thermo-mechanical models of basin formation such as the McKenzie model of lithospheric stretching would indicate that such a gradient would only be preserved if the present day lithospheric thickness is 42 km (assuming an original 125 km thickness, see Sclater & Christie, 1980; Dewey, 1982). Moreover vitrinite reflectance data is strongly time dependant (Hood et al., 1975; Waples, 1980). Therefore the present day temperature does not relate to the palaeotemperature structure, therefore maturity predictions cannot be accurate.

Palaeotemperature information can be partly inferred from the presence of Saddle dolomite, which is usually indicative of temperatures exceeding 60°C (Radke & Mathis, 1980), (the oil window is 60°C - 150°C). However, Gregg & Sibley (1984) from an examination of dolomite fabrics considered that Saddle dolomites may be formed at slightly lower temperatures (greater than 50°C). Sellwood et al., (1985) have recorded

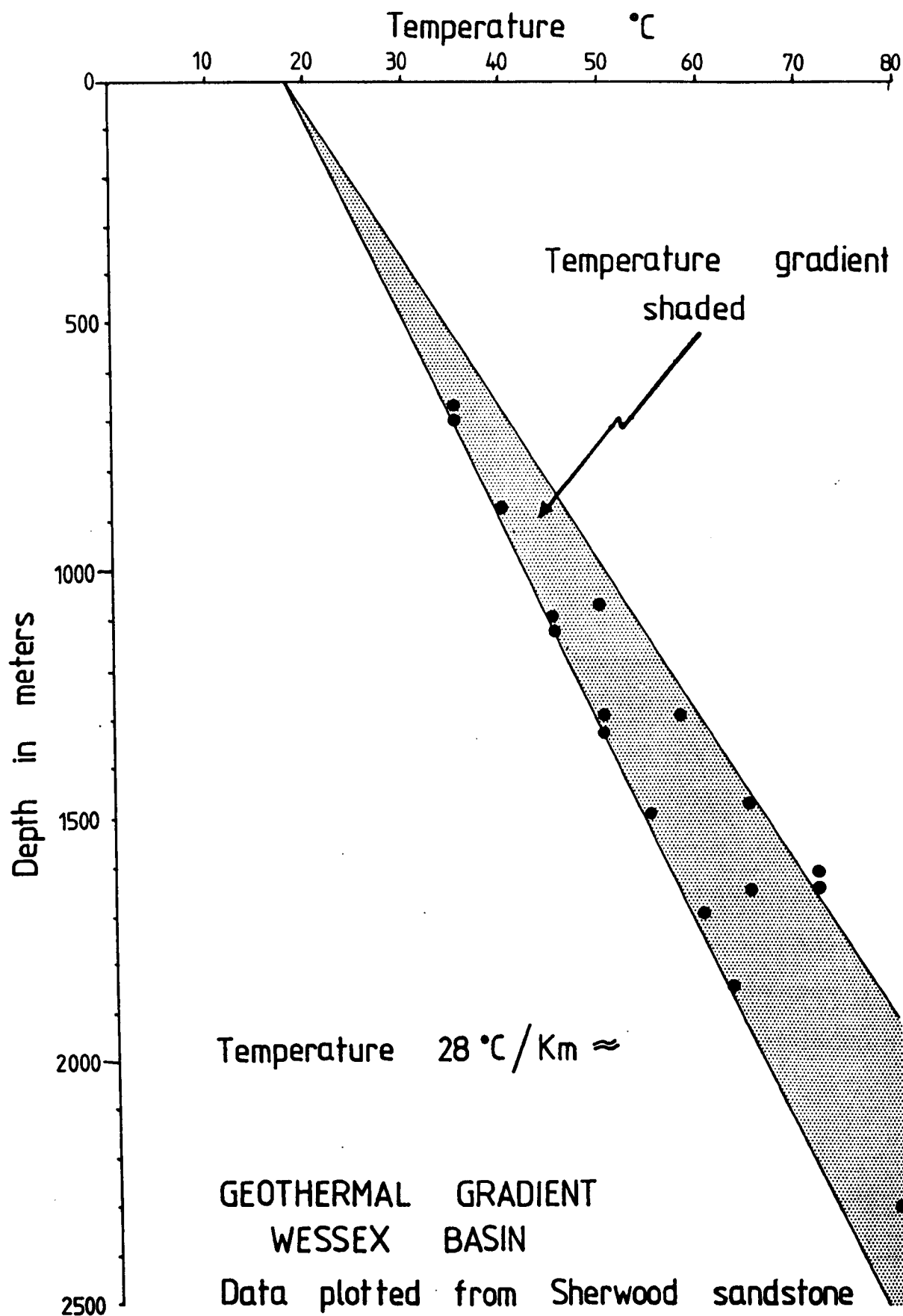


Fig. 6.2 Geothermal gradient of the Wessex Basin plotted from the Sherwood Sandstone. Based on temperature structure mapped by Allen & Holloway (1984).

the presence of saddle dolomite in the Humbly Grove area and at outcrop in the Forest Marble along the Fleet shore in south Dorset, and thought these indicative of temperatures exceeding 50°C and burial depths greater than 2 Km. Information concerning expulsion efficiencies, source rock volumetrics and migration paths are beyond the scope of this thesis.

Major oil 'kitchens' are located in the Channel and Weald basins. Maturation and migration was largely achieved prior to the late Cretaceous inversion when the maximum burial depths were achieved. Dead oil conglomerates in the Wealden along the Dorset coast indicate that some migration occurred in the lower Cretaceous.

Migration may have been slightly controlled by fracture permeability e.g. the Bridport Sand fracture solution pipes, although the evidence outlined earlier clearly indicated that most of the mesofractures developed during the late Tertiary. Colter & Havard (1981) demonstrated that major oil migration paths cut obliquely across the major east-west growth faults. Complication may result if later gas generation and migration displaces earlier oil traps or if inversion causes secondary migration to new reservoirs and traps. Inversion related structures also tend to break previous seals, which has led to problems in interpreting structures in the Weald and Channel basins.

6.4 Reservoirs

The main reservoirs are the Sherwood Sandstone, Bridport sands and Great Oolite Limestone Formation (Figs 6.1 and 6.3). The first two reservoirs are only developed in the western portion of the Wessex Basin, whilst the latter is confined almost solely to the Weald basin (Fig. 6.1).

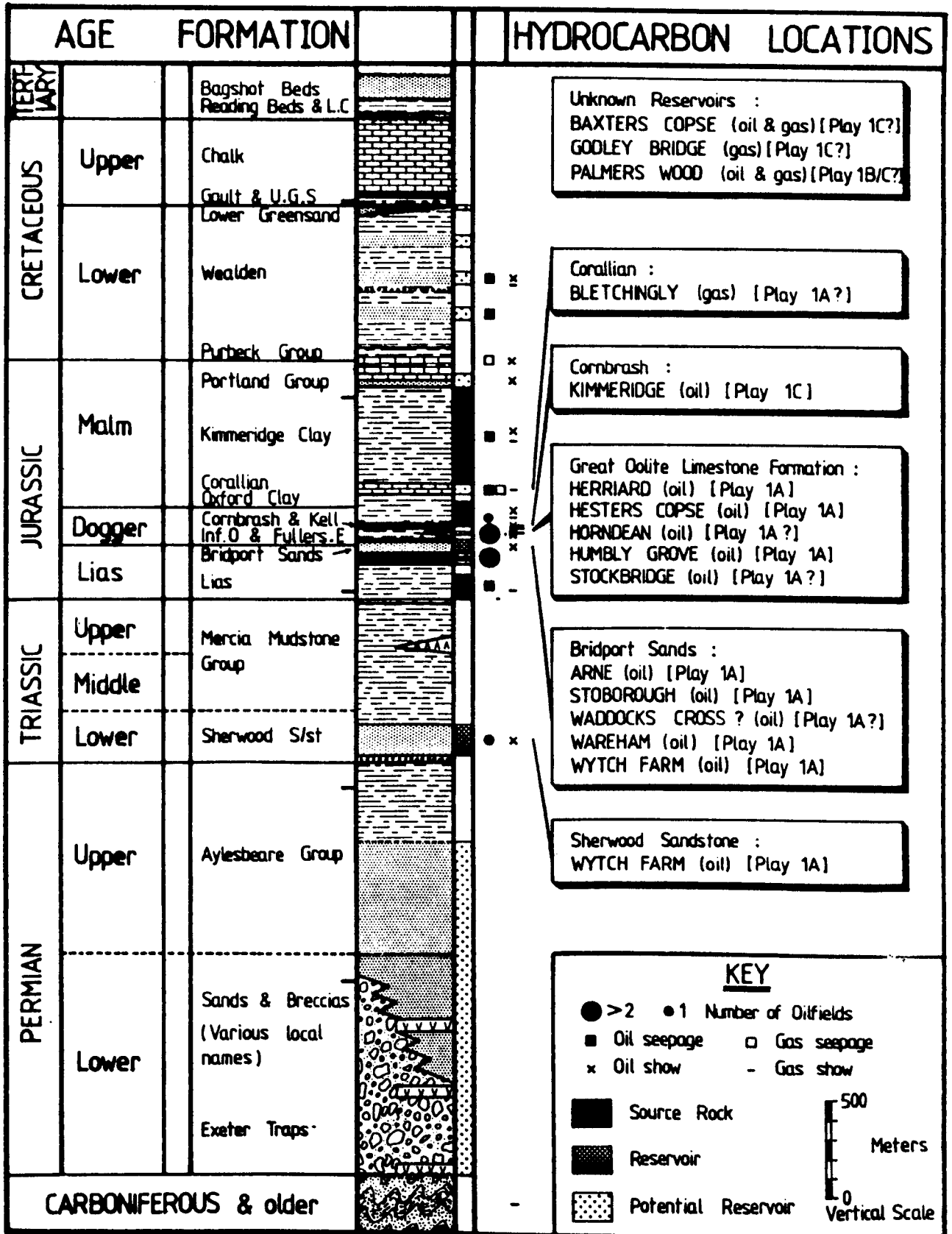


Fig. 6.3 Simplified stratigraphic column of the Wessex Basin to scale. Source, Reservoir units are shown. Main hydrocarbon funds are summarized and the possible play type they are associated with.

The Sherwood Sandstone group is characterised by high porosities (22%) and permeabilities (20-110mD), (Burgess, 1982). In the Wytch Farm oilfield, porosities vary from 4-29%, with permeabilities around .01-7D (Colter & Havard, 1981). The Bridport sands have porosities less than 10% in the cemented bands to 32% in the friable sandstones. Problems with predicting its reservoir quality are compounded by decreasing grain size with depth and highly variable permeabilities (0-300 mD). The Great Oolite Limestone Formation reservoir comprises variable dolomitic grainstones and packstones and has been recently discussed in detail by Sellwood et al., (1985). Other reservoir plays are summarized on figure 6.3, the most important being the lower Corallian and the Portland sands which are well developed in the Weald, although suitable cap rocks for example the upper Portland limestone are generally absent.

6.5 Hydrocarbon Plays

1. Introduction

A hydrocarbon play is a set of geological circumstances which combine to create the conditions necessary for hydrocarbon accumulation (Parsley, 1984). Four major plays with proven hydrocarbon success have been distinguished. At least two secondary plays are defined which have yet to be tested.

2. Primary Plays

A. Play 1A Pre Aptian/Albian Tilted Fault Blocks

These are developed immediately north of major east-west listric normal growth faults. This is the most prolific hydrocarbon play in southern England and the best documented example (it contains the Wytch Farm oilfield, Hinde (1980), Colter & Havard (1981), Stoneley (1982)) and

has proven tilt block growth faulting both in the lower Fullers Earth and Bridport sands. However, growth faulting may have initiated in the Late Carboniferous/early Permian. These plays were developed prior to and during migration. Mature to marginally mature source rocks are located immediately south of the growth faults e.g. Purbeck-Isle of Wight fault. The tilted fault blocks are best developed some 4-7 Km to the north of major southward dipping growth faults, which are located beyond the inversion effects (see Chapter 3). Where these structures are developed some distance away from the major faults prospects have proved dry. The reservoirs and the locations of this type of play are summarized on figure 6.3.

B. Play 1B Stratigraphic Pinch Outs

Stratigraphic pinch outs result either from onlap onto a basement high, sea level variations, or local tectonics such as syndepositional rotation of the hanging wall block above a listric detachment. These pinchouts may reflect original topography; palaeogeographic reconstructions can help predict their location and facies (see Chapter 3). The best recorded stratigraphic pinchouts occur around the London-Brabant platform (c.f. Donovan et al., 1979; Allsop et al., 1982) where progressive Rhaetic/Lias onlap and upper Sinemurian to Great Oolite overstep is observed. The platform was probably finally submerged in the Cretaceous. Shallow water neretic facies on the low relief palaeo landsurface has not yet been recorded in the Lias, although Donovan et al., (1979), have documented arenaceous/rudaceous "Rhaetic" sediments which may be of this type along the northwestern margin of the London Platform. Sedimentary pinchouts have also been recorded in the Great Oolite Limestone Formation from subsurface data by Sellwood et al.,

(1985) northeastwards towards the London Brabant platform. Other highs such as the Regneses hinge may also prove prospective.

Local intrabasinal pinchouts resulting from epeirogenic and sea level fluctuations (see Chapter 2) may also prove prospective in the future. Such as the wedge outs associated with the Birdport Sands in the Winterborne Kingston Trough compared with the same sequence preserved at Wytch Farm (Colter & Havard, 1981).

Synsedimentary rotation of the hanging wall block above a listric detachment can also predict stratigraphic traps in the hanging wall block caused by wedge-outs. Beach (1984) related episodic extensional movements in the Wytch Ground graben in the North Sea to such structures. This form of trap may prove prospective in the central Channel area. Lateral changes in facies may also result in wedge-outs. Again inversion tectonics may destroy such traps or cause secondary migration into the resulting inversion structures.

C. Play 1C Roll Overs, Hanging Wall Drapes, Monoclinial Flexures and Folds

These are associated with large scale structural inversion. The Kimmeridge oilfield is an example of a roll-over: perhaps complicated by oblique-slip motion along the nearby Purbeck/Isle of Wight fault. Roll-overs can be further complicated by thinning in the hanging wall (sedimentary and tectonic), synthetic and antithetic faults, shallow counter fans, riders, secondary detachments (see Gibbs, 1984 for terminology). If the detachment has ramp/flat geometry, hanging wall anticlines and hanging wall synclines will develop e.g. Poxwell anticline. Hanging wall drapes associated with downfaulted horsts and major graben fault zone antithetic faulting may further complicate the

trap form. Monoclinial flexures and folds associated with the main Miocene inversion have largely proved dry due to breaking of seals or secondary migration, although hydrocarbon traces are common; major oil migration predates many of these structures.

D. Play 1D Strike Slip Related Structures

Strike-slip induced structures dominate along northwest-southeast trends although some evidence for minor east-west strike slip has been found. Geometrically the resulting structures will be similar to those outlined by Harding (1984), in particular on en-echelon periclinal subparallel to the strike-slip trend and transfer directions. In this situation displacements may control but are generally insufficient to displace facies (e.g. Great Oolite). In addition small amounts of offset are generally sufficient to preserve small periclinal structures. Inversion controlled by these northwest-southeast trends such as the Pays de Bray fault may break oil seals in the periclinal structures or again result in secondary migration.

There may be evidence of some wrench control on the Arreton and Kimmeridge structures (see Chapter 5), en-echelon enclosures following the Portsdown fault along a west-northwest trend in the Southampton area (Marinex report) may be the result of such minor strike slip motions.

3. Secondary Plays

Secondary plays are postulated in the light of the structural evolutionary model outlined in Chapter 3.

A. Play 2A Horsts

Horst structures, either involving basement or intrabasinal, are inferred from gravimetric and seismic reflection surveys. Such

structures may be further complicated by compaction induced drapes.

If basement is involved, impermeable shales may drape over Devonian/Carboniferous sediments, for example the footwall side of the Mere fault (Allen & Holloway, 1984; Holloway & Chadwick, 1984) where Mercia Mudstone drapes over Carboniferous limestone. Horst uplift may be associated with wrenching such as in the Compton Valence dome (c.f. Melville & Freshney, 1982). Intrabasinal highs are more localised and may be fault bounded or simple swell areas associated with differential basin subsidence or strike-slip motions.

B. Play 2B Buried Fans

Buried fan plays, located along the major Permo-Triassic fault scarps or non-faulted basement highs may prove prospective. These structures have been described in detail by Tucker (1977) in South Wales and by Laming (1982) in South Devon in the Permo-Triassic. Farther east Allen & Holloway (1984) have postulated buried fans along the Mere-Portsdown fault. Other plays, including various kinds of subtle trap and salt diapirs with drapes are not regarded as important exploration targets. The later structures previously emphasized by Falcon & Kent (1960) are now considered in the light of extensive seismic acquisition to be non-existent (Melville & Freshney, 1982).

4. Wytch Farm Oilfield: Example

The Wytch Farm oilfield is located immediately north of the Purbeck-Isle of Wight fault (Figs 6.1 and II.6.1). The Sherwood Sandstone and Bridport Sands provide the major oil reservoirs although significant shows have been encountered in the Cornbrash. The major source area is located immediately south of the Purbeck-Isle of Wight fault as Colter &

Havard (1981) have recorded Liassic, Oxford and Kimmeridge clays close to or at maturity in the Arreton No2 borehole. Clearly some source rocks are younger than the reservoirs. Structural reconstructions, removing the inversion effects clearly show that the Lias was structurally lower than the Sherwood Sandstone Group during the major migration phase. Some oil may have migrated from the Winterborne Kingston Trough southwards into the Pre-Aptian tilted fault blocks of the Wytch Farm oilfield.

Present production is around 4000 barrels per day from the Bridport Sandstone reservoir, with an expected recovery rate around 32%. Future plans by British Petroleum to exploit the underlying Sherwood Sandstone reservoir expect production to increase to around 36,000 barrels per day with a 38% recovery rate (B.P. report). Current reserve estimation is around 175 million barrels (Financial Times 11.7.84), although the full eastward extent of the Sherwood Sandstone reservoir has not yet been established.

6.6 Future Exploration

Many plays have yet to be drilled, and attention will be largely focused on planned drilling operations around Charlton Marshall near Blandford Forum (Dorset Evening Echo, 10.4.84), Mappowder, Kingston Barn (near Corfe Castle) and Studland and Fitzworth farm on the south side of Poole Harbour.

6.7 Conclusions

The Wessex Basin has been shown to be an area of significant hydrocarbon discoveries and future prospects. Although many dry holes have been encountered (Figs 6.1 and 11.6.1) the discovery success rate

has been high. Dry holes have been encountered for a variety of reasons. Many have encountered hydrocarbon shows e.g. Shrewton and Portsdown No2, and frequently were drilled prior to recently developed testing such as swabbing, fracturing and acidising. Many early wells were drilled on the mappable Miocene antiforms along the Dorset coast, and have subsequently been shown to be heavily fractured superficial structures. Other holes along the basin margins were located some distance from mature source rocks and the migration paths, and some were drilled prior to the major discoveries and therefore never reached proven reservoirs. In some circumstances migration may not have crossed major faults, but instead used them as conduits. Lastly the major inversion structures can compound exploration success, for example heavy fracturing through to the surface (e.g. Weymouth Bay, Donovan & Stride, 1961) or breaking of fault seals, or secondary migration. Many of these problems can now be resolved in the light of current exploration techniques.

Recent hydrocarbon discoveries, future improvements in seismic acquisition and the reexamination of previous seismic, well data clearly indicate that the Wessex Basin still remains a prospective exploration area.

REFERENCES

References

- Allen, D.J. and Holloway, S., 1984. The Wessex Basin. Invest. geotherm. potent. U.K. Inst. Geol. Sci. 80 pp.
- Allen, P., 1975. Wealden of the Weald: a new model. Proc. Geol. Assoc. London, 86: 389-437.
- Allen, P., 1981. Pursuit of Wealden models. J. geol. Soc. London., 138: 375-405.
- Allsop, J.M., Holloway, D.W., Jones, C.M., Kenolty, N., Kirkby, G.A., Kubala, M. and Sobey, R.A., 1982. Palaeogeological maps of the floors beneath two major unconformities in the Oxford-Newbury-Reading area. Rep. Inst. Geol. Sci., 82/1: 48-51.
- Anderson, F.W., and Bazley, R.A.B., 1971. The Purbeck Beds of the Weald (England). Bull. Geol. Surv. G.B., 34: 174pp.
- Anderton, R., Bridges, P.H., Leeder, M.R. and Sellwood, B.W., 1979. A dynamic stratigraphy of the British Isles. George Allen and Unwin Ltd., London. 301pp.
- Andrews-Speed, C.P., Oxburgh, E.R. and Cooper, B.A., 1984. Temperatures and Depth-Dependent Heat Flow in Western North Sea. Am. Assoc. Petrol. Geol., 68: 1764-1781.
- Arber, M.A., 1973. Landslips near Lyme Regis. Proc. Geol. Assoc. London, 84: 121-133.
- Arkell, W.J., 1933. The Jurassic System in Great Britain. Clarendon Press, Oxford. 681pp.
- Arkell, W.J., 1938. Three Tectonic Problems of the Lulworth District: Structures in the Middle Limb of the Purbeck fold. Q. J. geol. Soc. London., 94: 1-54.
- Arkell, W.J., 1947. The geology of the country around Weymouth, Swanage, Corfe and Lulworth. Mem. geol. Surv. U.K., 386 pp.
- Artemjev, M.E., and Artyushkov, E.V., 1971. Structure and isostasy of the Baikal rift and the mechanism of rifting. J. Geophys. Res., 76: 1179-1211.
- Arthaud, F. and Matte, P., 1977. Late Palaeozoic strike-slip faulting in southern Europe and northern Africa: Result of a right-lateral shear zone between the Appalachians and the Urals. Bull. geol. Soc. Am., 88: 1305-20.
- Arthurton, R.S., 1984. The Ribblesdale fold belt, NW England - a Dinantian-early Nanurian dextral shear zone. In: D.H.W. Hutton and D.J. Sanderson, (Editors), Variscan Tectonics of the North Atlantic

- Region. Geol. Soc. Spec. publ. Blackwell. 14: 131-138.
- Audley-Charles, M.G., 1970. Stratigraphical correlation of the Triassic rocks of the British Isles. Q. J. geol. Soc. London., 126: 19-47.
- Autran, A. and Cogne, J., 1980. La Zone intene de l'orogene Varisque dans l'Quest de la France et sa place dans le developement de la Chaîne Hercynienne. Cont. 20 Gr'pe Francaise Project 27 'Orogene Caledonien de Regions nord atlantiques'. P.I.C.G. 91-109.
- Badham, J.P.N., 1982. Strike-slip orogens - an explanation for the Hercynides. J. geol. Soc. London., 139: 493-504.
- Barnard, P.C. and Cooper, B.S., 1981. Oils and source rocks of the North Sea area. In: L.V. Illing and G.D. Hobson (Editors), Petroleum Geology of the Continental Shelf of North-West Europe. Heyden and Son Ltd: 169-175.
- Barr, K.W., Colter, V.S. and Young, R., 1981. The geology of the Cardigan Bay - St. George's Channel Basin. In: L.V. Illing and G.D. Hobson (Editors), Petroleum Geology of the Continental Shelf of North-West Europe. Heyden and Son Ltd: 432-443.
- Barton, P.J. and Wood, R., 1984. Tectonic evolution of the North Sea Basin: crustal stretching and subsidence. Geophy. J. R. astr. Soc. 79: 987-1022.
- Barton, P.J. and Matthews, D.H., 1984. Deep structure and geology of the North Sea region interpreted from a seismic refraction profile. Annales Geophysicae. 2: 663-668.
- Batchelor, A.S., 1984. Hot dry rock Geothermal Exploitation in the United Kingdom. Modern Geology., 9: 1-42.
- Beach, A., 1984. Structural evolution of the Witch Ground Graben. J. geol. Soc. London. 141: 621-628.
- Bellamy, J., 1977. Subsurface expansion megapolygons in upper Jurassic dolostone (Kimmeridge, UK). J. Sed. Pet. 47: 973-978.
- Bennet, G., Copestake, P. and Hooker, N.P., 1985. Stratigraphy of the Britoil 72/10-1A Well, Western Approaches. Proc. Geol. Assoc. London., 96: 255-261.
- Bennison, G.M., and Wright, A.E., 1969. The Geological History of the British Isles. Edward Arnold Ltd., London. 406pp.
- Bevan, T.G., 1985a. Tectonic evolution of the Isle of Wight: a Cenozoic stress history based on mesofractures. Proc. Geol. Assoc. London. 96: 227-235.
- Bevan, T.G., 1985b. A reinterpretation of fault systems in the Upper Cretaceous rocks of the Dorset Coast. Proc. Geol. Assoc. London., 96: 337-342.

- Bevan, T.G. and Hancock, P.L., in press. Late Cenozoic fractures in southern England and northern France: their relationship to the neotectonics of NW Europe. *J. geol. Soc. London*. 000:000-000.
- B.I.R.P.S. and E.C.O.R.S., 1986. Deep seismic reflection profiling between England, France and Ireland. *J. Geol. Soc. London*. Thematic set on the Variscan.
- Bloomer, J.R., 1980. Methods of geothermal exploration with application to the Hampshire Basin. Ph.D. thesis, University of Oxford (Unpubl.).
- Bluck, B.J., 1984. Pre-Carboniferous history of the Midland Valley of Scotland. *Trans. Roy. Soc. Edinburgh. Earth Sci.* 75: 275-295.
- Blundell, D.J., 1957. A palaeomagnetic investigation of the Lundy dyke swarm. *Geol. Mag.* 94: 187-193.
- Blundell, D.J., Hurich, C.A. and Smithson, S.B., 1985. A model for the MOIST seismic reflection profile, N. Scotland. *J. geol. Soc. London*. 142: 245-258.
- Boccaletti, M., Coli, M. and Napoleone, G., 1980. Landsat lineation pattern in the Apennine and its geodynamic significance. *Modern Geology*. 7: 95-103.
- Bodenhause, J.W.A. and Ott, W.F., 1981. Habitat of the Rijswijk Oil Province, onshore, The Netherlands. In: L.V. Illing and G.D. Hobson (Editors), *Petroleum Geology of the Continental Shelf of North-West Europe*. Heyden and Son Ltd: 301-309.
- Bois, C., Cazes, M., Damotte, B., Galdeano, A., Hirn, A., Mascle, A., Mathe, Ph., Van Ngoy, P., Raoult, J.F. and Toreilles, G. 1985. The Hercynian crust in Northern France: First results from the ECORS - Nord de la France deep seismic profile. Abstract. The Evolution of the European lithosphere 4th Meeting of European Geological Societies. Edinburgh 9-12 April.
- Bond, G.C. and Kominz, M.A., 1984. Construction of tectonic subsidence curves for the early Palaeozoic Miogeocline, southern Canadian Rocky mountains: Implications for subsidence mechanisms, age of breakup, and crustal thinning. *Bull. geol. Soc. Am.* 95: 155-173.
- Bosworth, W., 1985. Geometry of propagating continental rifts. *Nature*, 316: 625-627.
- Bott, M.H.P., 1971. Evolution of young continental margins and formation of shelf basins. *Tectonophysics*, 11: 319-327.
- B.P. report, 1984. A consultative document. The Proposed Overall Development scheme for Wytch Farm Oilfield. 26pp.
- Brewer, J.A., 1984. Clues to the deep structure of the European

- Variscides from crustal seismic profiling in North America. In: D.H.W. Hutton and D.J. Sanderson, (Editors), *Variscan Tectonics of the North Atlantic Region*. Geol. Soc. Spec. publ. Blackwell. 14: 253-264.
- Brewer, J.A., Matthews, D.H., Warner, M.R., Hall, J., Smythe, D.K., and Whittington, R.J., 1983. BIRPS deep seismic reflection studies of the British Caledonides. *Nature*, 305: 206-210.
- Brewer, J.A. and Smythe, D.K., 1984. MOIST and the continuity of crustal reflection geometry along the Caledonian-Appalachian orogen. *J. geol. Soc. London*, 141: 105-120.
- Bristow, C.M. and Hughes, D.E., 1971. A Tertiary thrust fault on the southern margin of the Bovey Basin. *Geol. Mag.*, 108(1): 61-68.
- Brooks, M., Doody, J.J. and Al-Rawi, F.R.J., 1984. Major crustal reflectors beneath SW England. *J. geol. Soc. London*, 141: 97-104.
- Burchfiel, B.C. and Royden, L., 1982. Carpathian foreland fold and thrust belt and its relation to the Pannonian and other basins. *Am. Assoc. Petrol. Geol.*, 66: 1179-1195.
- Burgess, W.G., 1982. Hydraulic characteristics of the Triassic Sherwood Sandstone and the Lower Jurassic Bridport Sands intervals, as derived from drill stem tests, geophysical logs and laboratory tests. In: G.H. Rhys., G.K. Lott and Calver, M.S. (Editors). *The Winterborne Kingston borehole, Dorset, England*. Rep. Inst. Geol. Sci. 81/3. 164-175.
- Canich, D.W. and Gold, D.P., 1976. A study of fractures in Tyrone-Mount Union lineament. *Proc. 2nd Int. Conf. on Basement Tectonics*. Newark, Delaware. 141. Abstract.
- Casey, R., 1963. The dawn of the Cretaceous Period in Britain. *Bull. S.E. Union Sci. Soc.*, 117.
- Chadwick, R.A., Kenolty, N. and Whittaker, A., 1983. Crustal structure beneath southern England from deep seismic reflection profiles. *J. geol. Soc. London*, 140: 893-912.
- Chadwick, R.A., 1985(a). Seismic reflection investigations into the stratigraphy and structural evolution of the Worcester Basin. *J. geol. Soc. London*, 142: 187-202.
- Chadwick, R.A., 1985(b). End Jurassic - early Cretaceous sedimentation and subsidence (late Portlandian to Barremian) and the late-Cimmerian unconformity. In Whittaker, A. (Editor) *Atlas of Onshore Sedimentary Basins in England and Wales: Post-Carboniferous Tectonics and Stratigraphy*. Blackie, Glasgow.
- Chadwick, R.A. and Kirby, G.A., 1982. The geology beneath the Lower Greensand/Gault surface in the Vale of Wardour area. *Rep. Inst. Geol. Sci.*, No. 82/1: 15-18.

- Chauval, J.J., Robardet, M. and Lefort, J.P., 1980. Massif Armorican. In: C. Lorenz (Editor) *Geologie des pays europeens*. Dunod, France.
- Christie, P.A.F. and Sclater, J.G., 1980. An extensional origin for the Buchan and Witchground Graben in the North Sea. *Nature*, 238: 729-732.
- Christie-Blick, N. and Biddle, K.T., 1986. Deformation and basin formation along strike-slip fault. In: K.T.B. Biddle and N. Christie-Blick (Editors) *Strike-Slip Deformation, Basin formation, and sedimentation*- Society of Economic Palaeontologists and Mineralogists, Spec. publ. No. 37: 000-000.
- Cloetingh, S., McQueen, H. and Lambeck, K., 1985. On a tectonic mechanism for regional sea level variations. *Earth Planet. Sci. Lett.*, 75: 157-166.
- Cobbold, P.R., Cosgrove, J.W. and Summer, J.M., 1971. Development of internal structures in deformed anisotropic rocks. *Tectonophysics*, 12: 23-53.
- Cochran, J.R., 1983. Effects of finite rifting times on the development of sedimentary basins. *Earth. Planet. Sci. Lett.*, 66: 289-302.
- Colter, V.S. and Barr, K.W., 1975. Recent developments in the geology of the Irish Sea and Cheshire Basins. In: A.W. Woodland (Editor) *Petroleum and the Continental Shelf of North-West Europe*. vol. 1, Geology Applied Science Publ., London: 61-75.
- Colter, V.S. and Havard, D.J., 1981. The Wytch Farm oil field, Dorset. In: L.V. Illing, and G.D. Hobson, (Editors), *Petroleum Geology of the Continental Shelf of north-west Europe*. Heyden and Son Ltd: 494-503.
- Cooper, M.A., Collins, D., Ford, M., Murphy, F.X. and Trayner, P.M., 1984. Structural style, shortening estimates and the thrust front of the Irish Variscides. In: D.H.W. Hutton and Sanderson, D.J. (Editors), *Variscan Tectonics of the North Atlantic Region*. Geol. Soc. Spec. publ. Blackwell. 14: 167-176.
- Cope, J.C.W., 1984. The Mesozoic history of Wales. *Proc. Geol. Assoc.*, London. 95(4): 373-385.
- Cope, J.C.W., Duff, K.L., Parsons, C.F., Torrens, H.S., Wimbledon, W.A. and Wright, J.K., 1980. A correlation of Jurassic rocks in the British Isles Part Two: Middle and Upper Jurassic. *Geol. Soc. London. Spec. Rep.*, 15: 109pp.
- Cornford, C., 1984. Source Rocks and Hydrocarbons of the North Sea. In: K.W. Glennie (Editor). *Introduction to the Petroleum Geology of the North Sea*. Blackwell, London. 171-204.
- Cosgrove, M.E., 1972. The geochemistry of the potassium-rich Permian

- volcanic rocks of Devonshire, England. *Contr. Mineral. Petrol.* 36: 155-170.
- Coward, M.P. and Smallwood, S., 1984. An interpretation of the Variscan tectonics of SW Britain. In: D.H.W. Hutton and D.J. Sanderson, (Editors), *Variscan Tectonics of the North Atlantic Region*. *Geol. Soc. Spec. publ.* Blackwell. 14: p. 89-102.
- Cox, B.M. and Gallois, R.W., 1981. The stratigraphy of the Kimmeridge Clay of the Dorset type area and its correlation with some other Kimmeridgian sequences. *Rep. Inst. Geol. Sci.*, No. 80/4: 43 pp.
- Curry, D., Adams, C.G., Boulter, M.C., Dilley, F.C., Eames, F.E., Funnell, B.M. and Wells, M.K., 1978. A correlation of Tertiary rocks in the British Isles. *Geol. Soc. London. Spec. Report no.* 12, 72 pp.
- Daley, D. and Edwards, N., 1971. Palaeogene warping in the Isle of Wight. *Geol. Mag.*, 108: 399-405.
- Darton, D.M., Dingwell, R.G. and McCann, D.M., 1981. Geological and geophysical investigations in Lyme Bay. *Rep. Inst. Geol. Sci.*, No. 79/10. 24pp.
- Davey, J.C., 1981. Geophysical studies across the Permian outcrop in central and east Devonshire. *Proc. Ussher. Soc.*, 5: 194-199.
- Davies, D.K., 1967. Origin of friable sandstone-Calcareous sandstone rhythms in the Upper Lias of England. *J. Sed. Pet.* 37: 1179-1188.
- Day, G.A., in press. The Hercynian evolution of the South West British Continental Margin. In: *Deep structure of the continental crust*. *Am. Geophys. Union. Geodynamics Series.*, Washington D.C., U.S.A.
- Day, G.A. and Edwards, J.W.F., 1983. Variscan thrusting in the Basement of the English Channel and SW Approaches. *Proc. Ussher. Soc.*, 5: 432-436.
- Dewey, J.F., 1965. Nature and origin of kink bands. *Tectonophysics*, 1: 459-94.
- Dewey, J.F., 1982. Plate tectonics and the evolution of the British Isles. *J. geol. Soc. London.* 139: 371-414.
- Dixon, D.G., Munday, T.J. and Lake, S.D., 1985. Structural and lithological mapping in the Wessex Basin of southern England using Seasat SAR, Landsat MSS and TM data. *Fourth Thematic Conference: "Remote Sensing for Exploration Geology"*, San Francisco, California, April 1-4, 1985.
- Dixon, J.E., Fitton, J.G. and Frost, R.T.C. 1981. The tectonic significance of post- Carboniferous igneous activity in the North Sea Basin. In: L.V. Illing and G.D. Hobson (Editors). *Petroleum geology of the Continental Shelf of North-West Europe*. Heyden and

Son Ltd: 121-137.

- Donovan, D.T. and Stride, A.H., 1961. An acoustic survey of the sea floor south of Dorset and its geological interpretation. *Phil. Trans. Roy. Soc., A.*, 244: 299-325.
- Donovan, D.T., Horton, A. and Ivimey-Cook, H.C., 1979. The transgression of the Lower Lias over the northern flank of the London Platform. *J. geol. Soc. London.*, 136: 165-173.
- Drummond, P.V.O., 1970. The Mid-Dorset Swell. Evidence of Albian-Cenomanian movements in Wessex. *Proc. Geol. Assoc. London.*, 81: 679-714.
- Drummond, P.V.O., 1982. Discussion In: Stoneley, R. The structural development of the Wessex Basin. *J. geol. Soc. London.*, 139: 553-554.
- Ebukanson, E.J., 1984. An Investigation of some potential Jurassic hydrocarbon source rocks of southern England. Ph.D. thesis, University of London (Unpubl.).
- Edmonds, E.A., McKeown, M.C. and Williams, M., 1975. British Regional Geology: South-west England. H.M.S.O., London., 133 pp.
- Edmunds, F.H. and Burley, S.D., 1977. Catalogue of Geothermal data for the land area of the United Kingdom. Department of Energy Report, London.
- Engelder, T., 1985. Loading paths to joint propagation during a tectonic cycle: an example from the Appalachian Plateau, U.S.A. *J. Struct. Geol.*, 7: 459-476.
- Ensom, P.C., 1984. Geology in 1983. *Proc. Dorset Nat. Hist. and Arch. Soc.*, 105: 165-169.
- Ensom, P.C., 1985. Tectonic Fissures in the Marly Freshwater Member, Purbeck Limestone Formation, Worbarrow Tout, Dorset. *Proc. Dorset Nat. Hist. and Arch. Soc.*, 106: 165-166.
- Falcon, N.L. and Kent, P.E., 1950. Chalk Rock of Dorset - more evidence of salt? *Geol. Mag.*, 87: 302-303.
- Falcon, N.L. and Tarrant, L.H., 1951. The gravitational and magnetic exploration of parts of the Mesozoic-covered areas of South-Central England. *Q. J. geol. Soc. London.*, 106: 141-170.
- Falcon, N.L. and Kent, P.E., 1960. Geological results of petroleum exploration in Britain, 1945-1947. *Mem. geol. Soc. London.*, 2: 56 pp.
- Farrimond, P., Comet, P., Edlington, G., Evershed, R.P., Hall, M.A., Park, D.W. and Wardroper, A.M.K., 1984. Organic geochemical study of the Upper Kimmeridge Clay of the Dorset type area. *Marine and Petrol.*

Geol., 1: 340-354.

- Francis, J.E., 1984. The seasonal environment of the Purbeck (upper Jurassic) Fossil Forests. *Palaeog. Palaeoclim. Palaeoecol.*, 48: 285-307.
- Falvey, D.A., 1974. The development of continental margins in plate tectonic theory. *Aust. Petro. Explo. Assoc. Jour.*, 14: 95-106.
- Gale, A.S., 1980. Penecontemporaneous folding, sedimentation and erosion in Campanian chalk near Portsmouth, England. *Sedimentology.*, 27: 137-51.
- Gallois, R.W. and Edmonds, F.H., 1965. *British Regional Geology: The Wealden District*, H.M.S.O. London., 101 pp.
- Gardiner, P.R.R. and Sheridan, D.J.R., 1981. Tectonic framework of the Celtic Sea and adjacent areas with special reference to the location of the Variscan Front. *J. Struct. Geol.* 3: 317-331.
- Gibbs, A.D., 1984. Structural evolution of extensional basin margins. *J. geol. Soc. London.*, 141: 609-620.
- Glennie, K.W. and Boegner, P.L.E., 1981. Sole Pit inversion tectonics. In: L.V. Illing and G.D. Hobson (Editors) *Petroleum geology of the Continental Shelf of North-West Europe*. Heyden and Son Ltd: 110-120.
- Goetz, A.F.H. and Rowan, L.C., 1981. Geologic remote sensing. *Science.*, 211: 781-791.
- Goetz, A.F.H., Rock, B.N. and Rowan, L.C., 1983. Remote sensing for exploration: an overview. *Econ. Geol.* 78: 573-590.
- Gregg, J.M. and Sibley, D.F., 1984. Epigenetic dolomitization and the origin of xenotopic dolomite texture. *J. Sed. Pet.*, 54: 908-931.
- Hallam, A., 1960. The White Lias of the Devon Coast. *Proc. Geol. Assoc. London.*, 71: 47-60.
- Hallam, A., 1964. Origin of the limestone-shale rhythm in the blue Lias of England: a composite theory. *J. Geol.*, 72: 157-169.
- Hallam, A., and Sellwood, B.W., 1968. Origin of Fuller's Earth in the Mesozoic of Southern England. *Nature.*, 220: 1193-1195.
- Hallam, A., 1975. *Jurassic Environments*. Cambridge University Press, Cambridge. 269pp.
- Hallam, A., 1978. Eustatic cycles in the Jurassic. *Palaeog. Palaeoclim. Palaeoecol.*, 23: 1-32.
- Hallam, A., 1981. A revised sea-level curve for the early Jurassic. *J. geol. Soc. London.*, 138: 735-743.

- Hancock, J.M., 1975. The petrology of the Chalk. *Proc. Geol. Assoc. London.*, 86: 499-535.
- Hancock, P.L., 1968. Joints and Faults: the Morphological Aspects of their Origins. *Proc. Geol. Assoc. London.*, 79: 141-151.
- Hancock, P.L., 1969. Jointing in the Jurassic Limestones of the Cotswold Hills. *Proc. Geol. Assoc. London.*, 80: 219-241.
- Hancock, P.L., 1972. The analysis of en-echelon veins. *Geol. Mag.*, 109: 269-276.
- Hancock, P.L., 1985. Brittle microtectonic: principles and practice. *J. Struct. Geol.*, 7: 437-457.
- Hancock, P.L., Al Kadhi, A. and Sha'at, N.A., 1984. Regional joint sets in the Arabian platform as indicators of intraplate processes. *Tectonics.*, 3: 27-43.
- Harding, T.P., 1984. Graben hydrocarbon occurrences and structural style. *Am. Assoc. Petrol. Geol.*, 68: 333-362.
- Harland, W.B., Cox, A.V., Llewellyn, P.G., Pickton, C.A.G., Smith, A.G. and Walters, R., 1982. A geological time scale. Cambridge University Press: 131 pp.
- Harris, J.F., Taylor, G.L. and Walper, J.L., 1960. Relation of deformational fractures in sedimentary rocks to regional and local structures. *Am. Assoc. petrol. Geol.*, 44: 1853-1859.
- Harrison, R.K., 1981. Mesozoic magmatism in the British Isles and adjacent areas. In: D.S. Sutherland, (Editor). *Igneous rocks of the British Isles*: 333-344.
- Hawkins, H.L., 1942. Some episodes in the geological history of the South of England. *Q. J. geol. Soc. London.*, 98: 1-19.
- Haxby, W.F., Turcotte, D.L. and Bird, J.M., 1976. Thermal and mechanical evolution of the Michigan Basin. *Tectonophysics.*, 36: 57-75.
- Hays, J.D. and Pitman, W.C., 1973. Lithospheric plate motion, sea level changes and climatic and ecological consequences. *Nature*, 246: 18-22.
- Hellinger, S.J. and Sclater, J.G., 1983. Some comments on two-layer extensional models for the evolution of sedimentary basins. *J. Geophys. Res.*, 88: 8251-8269.
- Hill, M.N. and Vine, F.J., 1965. A preliminary magnetic survey of the Western Approaches to the English Channel. *Q. J. geol. Soc. London.*, 121: 463-475.
- Hinde, P., 1980. The Development of the Wytch Farm Oilfield.

Communication 1133. Inst. Gas Engineers, London.

- Hobson, D.M. and Sanderson, D.J., 1983. Variscan deformation in southwest England. In: Hancock, P.L. (Editor). The Variscan Fold Belt in the British Isles. Hilger. Bristol: 108-129.
- Holder, A.P. and Bott, M.H.P., 1971. Crustal structures in the vicinity of southwest England. *Geophys. J. R. astron. Soc.*, 23: 465-489.
- Hollingworth, S.E., 1962. The climatic factor in the geological record. *Q. J. geol. Soc. London.*, 118: 1-21.
- Holloway, S. and Chadwick, R.A., 1984. The I.G.S. Bruton Borehole (Somerset, England) and its regional structural significance. *Proc. Geol. Assoc. London.*, 95: 165-174.
- Hood, A., Gutjahr, C.C.M. and Heacock, R.L., 1975. Organic metamorphism and the generation of petroleum. *Am. Assoc. Petrol. Geol.*, 59: 986-996.
- House, M.R., 1985. A new approach to an absolute timescale from measurements of orbital cycles and sedimentary microrhythms. *Nature.*, 315: 721-725.
- Howitt, F., 1964. Stratigraphy and structure of the Purbeck inliers of Sussex (England). *Q. J. geol. Soc. London.*, 120: 77-113.
- Illing, L.V. and Hobson, G.D., 1981 (Editors) *Petroleum Geology of the Continental Shelf of North-West Europe.*, Heyden and Son Ltd. 521pp.
- Issac, K.P., 1983. Discussion on Eocene sedimentation and tectonics in the Hampshire Basin: reply by Plint, A.G. *J. geol. Soc. London.*, 140: 319-320.
- Issac, K.P., Turner, P.J. and Stewart, I.J., 1982. The evolution of the Hercynides of central SW England. *J. geol. Soc. London.*, 139: 523-534.
- Jarvis, I. and Woodroof, P.B., 1984. Stratigraphy of the Cenomanian and basal Turonian (Upper Cretaceous) between Branscombe and Seaton. S.E. Devon, England. *Proc. Geol. Assoc.*, 95: 193-215.
- Jones, C.V., 1978. The Origin of the Triassic Clay assemblages of Europe with special reference to the Keuper Marl and Rhaetic of parts of England. *Phil. Trans. Roy. Soc. London., Ser. A.*, 289: 549-639.
- Jenkyns, H.C. and Senior, J.R., 1977. A Liassic palaeofault from Dorset. *Geol. Mag.*, 114: 47-52.
- Jenner, J.K., 1981. The Structure and stratigraphy of the Kish Bank Basin. In: L.V. Illing and G.D. Hobson (Editors) *Petroleum Geology of the Continental Shelf of North-West Europe.* Heyden and Son Ltd: 426-431.

- Johnson, R.J. and Dingwall, R.G., 1981. The Caledonides: their influence of the stratigraphy of the North-West European Continental Shelf. In: L.V. Illing and G.D. Hobson (Editors) *Petroleum Geology of the Continental Shelf of North-West Europe*. Heyden and Son Ltd: 85-97.
- Jones, M.E., Bedford, J., and Clayton, C., 1984. On natural deformation mechanisms in the Chalk. *J. geol. Soc. London.*, 141: 675-684.
- Kamerling, P., 1979. The geology and hydrocarbon habitat of the Bristol Channel Basin. *J. Petrol. Geol.*, 2: 75-93.
- Karner, G.D., 1984. Continental tectonics - a quantitative view of the thermal and mechanical properties of the continental lithosphere in compressional and extensional stress regimes. Centre National d'Etudes Spatiales, Summer School of Space Physics, Toulouse, France. 53pp.
- Karner, G.D., in press. The effects of lithospheric pre-stress on sedimentary basin stratigraphy.
- Karner, G.D. and Watts, A.B., 1982. On isostasy at Atlantic-type continental margins. *J. Geophys. Res.*, 87: 2923-2948.
- Karner, G.D., Steckler, M.S. and Thorne, J.A., 1983. Long-term thermo-mechanical properties of the continental lithosphere. *Nature*, 304: 250-253.
- Karner, G.D. and Dewey, J.F., 1986. Rifting: Lithospheric versus crustal extension as applied to the Ridge Basin of southern California. *Am. Assoc. Petrol. Geol.*
- Karner, G.D., Lake, S.D. and Dewey, J.F., 1986. The thermo and mechanical development of the Wessex Basin, southern England. *Spec. publ. Continental Shelf tectonics J. geol. Soc. London.*
- Kellaway, G.A. and Hancock, P.L., 1983. Structure of the Bristol District, the Forest of Dean and the Malvern Fault Zone. In: Hancock, P.L. (Editor). *The Variscan Fold Belt in the British Isles*, Hilger, Bristol: 83-106.
- Kellaway, G.A., and Welch, F.B.A., 1948. *British Regional Geology. Bristol and Gloucester District*. H.M.S.O. 88 pp.
- Kenolty, N., Chadwick, R.A., Blundell, D.J. and Bacon, M., 1981. Deep seismic reflection survey across the Variscan front of southern England. *Nature*, 293: 451-453.
- Kent, P.E., 1949. A structure-contour map of the surface of the buried pre-Permian rocks in England and Wales. *Proc. Geol. Assoc. London.*, 60: 87-104.
- Kent, P.E., 1985. UK onshore oil exploration, 1930-1964. *Marine and Petrol. Geol.*, 2: 56-64.

- Kent, D.V. and Opdyke, N.D., 1979. The early Carboniferous palaeomagnetic field of North America and its bearing on tectonics of the northern Appalachians. *Earth. Planet. Sci. lett.*, 44: 365-372.
- Kent, D.V. and Opdyke, N.D. 1985. Multicomponent magnetizations from the Mississippian Mauch Chunk Formation of the central Appalachians and their tectonics implications. *J. geophys. Res.*, 90: 5371-5383.
- Knill, D.C., 1969. The Permian igneous rocks of Devon. *Bull. geol. Surv. Gr. Br.*, 29: 115-138.
- Knill, D.C., 1982. Permian volcanism in south-western England. In: D.S. Sutherland (Editor) *Igneous Rocks of the British Isles*. John Wiley and Sons Ltd: 329-332.
- Knox, R.W. O'B., Morton, A.C. and Lott, G.K., 1982. Petrology of the Bridport Sands in the Winterborne Kingston borehole, Dorset. In: Rhys, G.H., Lott, G.K. and Calver, M.A. (Editors). *The Winterborne Kingston borehole, Dorset, England*. Rep. Inst. Geol. Sci., No. 81/3: 107-121.
- Koopman, A., 1986. Model studies on Inversion Tectonics. *Tectonophysics*. 000:000-000.
- Kusznir, N. and Karner, G.D., 1985. Dependence of the flexural rigidity of the continental lithosphere on rheology and temperature. *Nature.*, 316: 138-142.
- Lake, S.D., 1982. The stratigraphy of the Purbeck Group in Dorset. B.Sc. thesis. U.C.W. Aberystwyth. (Unpubl).
- Lake, S.D., 1985. The structure and evolution of the Wessex Basin in southern England. Unpubl. Ph.D. thesis, University of Durham.
- Lake, S.D., Munday, T.J. and Dewey, J.F., 1984. Lineament Mapping and analysis in the Wessex Basin of southern England: A Comparison between MSS and TM data. *Proc. Anniv. Int. Conf. Satellite Remote Sensing*, Reading, U.K: 361-375.
- Lake, S.D. and Karner, G.D., 1986. The structure and evolution of the Wessex Basin, southern England: An example of inversion tectonics. *Tectonophysics*. 000.000-000.
- Laming, D.J.C., 1982. The New Red Sandstone. In: E.M. Durrance, and D.J.C. Laming, (Editors). *The Geology of Devon*. Univ. of Exeter: 148-178.
- Lamplugh, G.W., Kitchin, F.L. and Pringle, J., 1923. The concealed Mesozoic Rocks in Kent. *Mem. Geol. Surv. E and W*.
- Lang, W.D., 1933. The geology seen at the Golden Cap meeting. *Proc. Dorset Nat. Hist. and Arch. Soc.*, 54: 145-172.

- Larson, B.S., 1982. Examination of some factors in selecting landsat imagery for lineament interpretation. Proc. Int. Symp. Remote Sensing of Env. 2nd Thematic Conf. 'Remote Sensing for Exploration Geology'. Fort Worth, Texas. 293-302.
- Leeder, M.R., 1983. Lithospheric stretching and North Sea Jurassic clastic sourcelands. *Nature*, 305: 510-514.
- Lees, G.M. and Cox, P.T., 1937. The geological basis of the present search for oil in Great Britain by the D'Arcy exploration Company Limited. *Q. J. geol. Soc.*, 93: 156-189.
- Lefort, J.P. and Max, M.D., 1984. Development of the Porcupine Seabight: use of magnetic data to show the direct relationships between early oceanic and continental structures. *J. geol. Soc. London.*, 141: 663-674.
- Lefort, J.P. and Segoufin, J., 1978. Etude comparee des structures profondes et des anomalies magnetique allongee reconnues en manche occidentale et en bari d'Andierne: Existence possible d'une suture crustique au nord-ouest du massif Armorica (France). *Tectonophysics.*, 46: 65-76.
- Le Pichon, X., Sibuet, J.C. and Francheteau, J., 1977. The fit of the continents around the North Atlantic Ocean. *Tectonophysics.*, 38: 169-209.
- Leutiwein, F., Sonet, J. and Zimmermann, J.L., 1972. Dyke basiques du Massif Armorica Septentrional, contribution a leur etude geochronologique. *C. R. Acad. Sci. Ser. D.*, 275: 1327-1329.
- Leveridge, B.E., Holder, M.T. and Day, G.A., 1984. Thrust nappe tectonics in the Devonian of south Cornwall and the western English Channel. In: D.H.W. Hutton and D.J. Sanderson (Editors). *Variscan Tectonics of the North Atlantic Region*. Geol. Soc. London, Spec. publ., Blackwell., 14: 103-112.
- Livermore, R.A. and Smith, A.G., 1986. Some boundary conditions for the evolution of the Mediterranean region. In: D.J. Stanley and F.C. Wezel (Editors). *Geological Evolution of the Mediterranean Basin: Raimondo Selli Commemorative Volume*. Springer-Verlag, Berlin.
- Lloyd, A.J., Savage, R.J.G., Stride, A.H., and Donovan, D.T., 1973. The geology of the Bristol Channel floor. *Phil. Trans. Roy. Soc. A.*, 274: 595-626.
- Lott, G.K., Sobey, R.A., Warrington, G. and Whittaker, A., 1982. The Mercia Mudstone Group (Triassic) in the western Wessex Basin. *Proc. Ussher. Soc.*, 5: 340-346.
- Lott, G.K. and Strong, G.E., 1982. The petrology and petrography of the Sherwood Sandstone (? Middle Triassic) of the Winterborne Kingstone borehole, Dorset. In: Rhys, G.H., Lott, G.K. and Calver, M.A.

- (Editors). The Winterborne Kingston borehole, Dorset, England. Rep. inst. Geol. Sci., No. 81/3: 135-142.
- Lutz, M., Kaaschieter, J.P.H. and van Wijhe, D.H., 1975. Geological factors controlling Rotliegend gas accumulations in the Mid-European basin. Proc. 9th Wld. Pet. Cong. (Tokyo)., 2: 93-103.
- Martin, A.J., 1967. Bathonian sedimentation in southern England. Proc. geol. Assoc. London., 78: 473-488.
- Matthews, R.K., 1984. Oxygen-Isotope Record of Ice-Volume History: 100 Million Year of Glacio-Eustatic Sea-level Fluctuation. In: Schlee, J.S. (Editor) Interregional unconformities and hydrocarbon accumulation. Am. Assoc. Petrol. Geol. Mem. 36.
- McKenzie, D., 1981. The variation of temperature with time and hydrocarbon maturation in sedimentary basins formed by extension. Earth. Planet. Sci. lett. 55: 87-98.
- McQuillin, R., Donato, J.A. and Tulstrip, J., 1982. Development of basins in the Inner Moray Firth and the North Sea by crustal extension and dextral displacement of the Great Glen fault. Earth Planet. Sci. lett. 60: 127-139.
- Meissner, R., Springer, M. and Fluh, E., 1984. Tectonics of the Variscides in north-western Germany based on seismic reflection measurements. In: D.H.W. Hutton and D.J. Sanderson (Editors). Variscan Tectonics of the North Atlantic Region. Geol. Soc. London. Spec. Publ. Blackwell, 14: 23-32.
- Melville, R.V., and Freshney, E.C., 1982. The Hampshire Basin and adjoining areas. British Regional Geology. The Hampshire Basin and adjoining areas. H.M.S.O. 146 pp.
- Megnien, C., 1980. Synthèse Géologique du bassin de Paris. Vol. II. Atlas. Memoir B.R.G.M. 102.
- Miller, J.A. and Fitch, F.T., 1962. Age of the Lundy granites. Nature, 195: 553-555.
- Mimran, Y., 1975. Fabric deformation induced in Cretaceous chalks by tectonic processes. Tectonophysics, 26: 309-316.
- Mitchum, R.M., 1977. Glossary of Terms Used in Seismic Stratigraphy. In: C.E. Payton (Editor) Seismic Stratigraphy - applications to hydrocarbon exploration. Am. Assoc. petrol. Geol., Mem. 26: 205-212.
- Naylor, D. and Shannon, P., 1982. Geology of offshore Ireland and West Britain. Graham and Tortman. 161pp.
- O'leary, D.W., Friedman, J.D. and Pohn, H.A., 1976. Lineament, liner, lineation: some proposal new standards of old terms. Geol. Soc. Am. Bull., 87: 1463-1469.

- Owen, H.G., 1975. The Stratigraphy of the Gault and Upper Greensand of the Weald. *Proc. Geol. Assoc. London*, 86: 475-498.
- Parsley, A.J., 1984. North Sea Hydrocarbon Plays. In: K.W. Glennie (Editor) *Introduction to the Petroleum Geology of the North Sea*. Blackwell: 205-230.
- Parsons, B. and Sclater, J.G., 1977. An analysis of the variation of ocean floor bathymetry and heat flow with age. *J. Geophys. Res.*, 82: 803-827.
- Penn, I.E., 1982. Middle Jurassic stratigraphy and correlation of the Winterborne Kingston borehole, Dorset. In: G.H. Rhys, G.K. Lott and M.A. Calver (Editors). *The Winterborne Kingston borehole, Dorset, England*. *Rep. Inst. Geol. Sci.*, No. 81/3: 53-76.
- Phillips, W.J., 1964. The structures in the Jurassic and Cretaceous rocks on the Dorset coast between White Nothe and Mupe Bay. *Proc. Geol. Assoc. London.*, 75: 373-406.
- Pisias, N.G. and Shackleton, N.J., 1984. Modelling the global climatic response to orbital forcing and atmospheric carbon dioxide changes. *Nature*, 310: 757-759.
- Pitman, III, W.C., 1978. The relationship between eustasy and stratigraphic sequences of passive margins. *Bull. Geol. Soc. Am.*, 89: 1389-1403.
- Plint, A.G., 1982. Eocene sedimentation and tectonics in the Hampshire Basin. *J. geol. Soc. London.*, 139: 249-254.
- Plint, A.G., 1983. Facies, environments and sedimentary cycles in the Middle Eocene, Bracklesham Formation of the Hampshire Basin: evidence for global sea-level changes? *Sedimentology.*, 30: 625-653.
- Price, N.J., 1959. Mechanics of jointing in rocks. *Geol. Mag.*, 96: 149-157.
- Price, N.J., 1966. *Fault and Joint development in Brittle and Semi-brittle Rock*. Pergamon Press: 176pp.
- Pringle, J., 1922. On a Boring for Coal at Westbury, Wiltshire. *Sum. Prog. Geol Surv. for 1921*. 146-53.
- Radke, B.M. and Mathis, R.L., 1980. On the formation and occurrence of saddle dolomite. *J. Sed. Petrol.* 50: 1149-1168.
- Rasmussen, L.B., 1966. Molluscan faunas and biostratigraphy of the marine Young Miocene Formations in Denmark. *Danm. geol. Unders.* (2)., 88: 358pp.
- Rawson, P.F., Curry, D., Dilley, F.C., Hancock, J.M., Kennedy, W.J., Neale, J.W., Wood, C.J. and Worssam, B.C., 1978. A correlation of

- Cretaceous rocks in the British Isles. Geol. Soc. Spec. Rep. No. 9. 73pp.
- Rhys, G.H., Lott, G.K. and Calver, M.A. (Editors). The Winterborne Kingston borehole, Dorset, England. Rep. Inst. Geol. Sci., No. 81/3: 196 pp.
- Richardson, L., 1928. Wells and Springs of Somerset. Mem. Geol. Surv. G.B: 78pp.
- Ridd, M.F., 1973. The Sutton Poyntz, Poxwell and Chaldon Herring Anticlines, Southern England: a reinterpretation. Proc. Geol. Assoc. London: 84: 1-8.
- Robbie, J.a., 1950. The Chalk rock at Winterborne Abbas, Dorset. Geol. Mag., 87: 209-213.
- Roberts, J.C., 1966. A study of the relation between jointing and structural evolution. Geol. J., 5: 157-172.
- Roberts, J.C., 1947. Jointing and minor tectonics of the Vale of Glamorgan between Ogmore-by-Sea and Lavernock Point, South Wales. Geol. J., 9: 97-114.
- Robinson, P.L., 1957. The Mesozoic fissure of the Bristol Channel area and their vertebrate faunas. J. Linnean. Soc. London., 43: 260-282.
- Robinson, K.W., Shannon, P.M. and Young, D.G.G., 1981. The Fasnet Basin; an integrated analysis. In: L.V. illing and G.D. Hobson (Editors) Petroleum Geology of the Continental Shelf of North-West Europe. Heyden and Son Ltd: 444-454.
- Royden, L. and Keen, C.E., 1980. Rifting processes and thermal evolution of the continental margin of eastern Canada determined from subsidence curves. Earth Planet. Sci. lett., 51: 343-361.
- Royden, L., Sclater, J.G., von Herzen, R.P., 1980. Continental margin subsidence and heat flow: important parameters in formation of petroleum hydrocarbons. Am. Assoc. petrol. Geol., 64: 173-187.
- Royden, L., Horvath, F., Nagymarosy, A. and Stegena, L., 1983. Evolution of the Pannonian Basin system 2. Subsidence and thermal history. Tectonics., 2: 91-137.
- Sanderson, D.J., 1984. Structural variation across the northern margin of the Variscides in N.W. Europe. In: D.H.W. Hutton and D.J. Sanderson (Editors). Variscan Tectonics of the North Atlantic Region. Geol. Soc. London. spec. publ., Blackwell, 14: 149-166.
- Sandy, M.R., 1985. Sedimentary microrhythms: Matters Arising. Nature., 318: 81.
- Saunders, D.F. and Hicks, D.E., 1976. Regional geomorphic lineaments on satellite imagery - their origin and applications. Proc. 2nd Int.

- Conf. on basement Tectonics. Newark, Delaware. 326-352.
- Schmitt, T.J., 1981. The West European Stress Field: new data and interpretation. *J. Struct. Geol.*, 3: 309-15.
- Sclater, J.G. and Christie, P.A.F., 1980. Continental stretching: an explanation of the post-mid-Cretaceous subsidence of the Central North Sea Basin. *J. geophys. Res.*, 85: 3711-3739.
- Sellwood, B.W., 1978. Shallow-water Carbonate Environments. In: Reading, H.G. (Editor) *Sedimentary Environments and Facies*. Blackwell: 259-313.
- Sellwood, B.W., Durkin, M.K. and Kennedy, W.J., 1970. Field meeting on the Jurassic and Cretaceous rocks of Wessex. *Proc. Geol. Assoc. London.*, 81: 715-732.
- Sellwood, B.W. and Jenkyns, H.C., 1975. Basins and swells and the evolutions of an epeiric sea. (Pleinsbachian-Bajocian of Great Britain). *Q. J. geol. Soc.*, 131: 373-388.
- Sellwood, B.W. and Sladen, C.P., 1981. Mesozoic and Tertiary argillaceous units: distribution and composition. *Q. J. eng. Geol. London.*, 14: 263-275.
- Sellwood, B.W., Scott, J., Mikkelsen, P. and Arkroyd, P., 1985. Stratigraphy and sedimentology of the Great Oolite Group in the Humbly Grove Oilfield, Hampshire. *Marine and Petrol. Geol.*, 2: 44-55.
- Shackleton, R.M., Ries, A.C. and Coward, M.P., 1982. An interpretation of the Variscan structures in SW England. *J. geol. Soc. London.*, 139: 535-544.
- Shackleton, R.M., 1984. Thin-skinned tectonics, basement control and the Variscan Front. In: D.H.W. Hutton and D.J. Sanderson (Editors). *Variscan Tectonics of the North Atlantic Region*. Geol. Soc. London, spec. publ. Blackwell, 14: 125-130.
- Sleep, N.H., 1971. Thermal effects of the formation of Atlantic continental margins by continental breakup. *Geophys. J. R. astr. Soc.*, 325-350.
- Smalley, S. Westbrook, G.K., 1982. Geophysical evidence concerning the southern boundary of the London Platform beneath the Hog's Back, Surrey. *J. geol. Soc. London.*, 139: 139-146.
- Smith, W.E., 1957. Summer field meeting in south Devon and Dorset. *Proc. Geol. Assoc. London.*, 68: 136-152.
- Smith, A.J. and Curry, D., 1975. The structure and geological evolution of the English Channel. *Phil. Trans. R. Soc. London*, A279: 3-20.
- Soler, R., Lopez Vichez, J. and Riaza, C., 1981. Petroleum geology of

- the Bay of Biscay. In: L.V. Illing, and G.D. Hobson, (Editors) *Petroleum Geology of the Continental Shelf of North-West Europe*. Heyden and Son Ltd.: 474-482.
- Spohn, T. and Neugebauer, H.J., 1978. Metastable phase transition models and their bearing on the development of Atlantic-type geosynclines. *tectonophysics.*, 50: 387-412.
- Steckler, M.S., 1981. The thermal and mechanical evolution of Atlantic type continental margins. Ph.d. thesis, Columbia University, New York.
- Steckler, M.S., 1985. Uplift and extension at the Gulf of Suez: indications of induced mantle convection. *Nature.*, 317: 135-139.
- Steckler, M.S. and Watts, A.B., 1978. Subsidence of the Atlantic-type continental margin off New York. *Earth Planet. Sci. Lett.*, 41: 1-13.
- Stoneley, R., 1982. The structural development of the Wessex Basin. *J. geol. Soc. London.*, 139: p. 543-554.
- Stoneley, R., 1983. Fibrous calcite veins, overpressures and primary oil migration. *Am. Assoc. Petrol. geol.*, 67: 1427-1428.
- Strahan, A., 1898. The Geology of the Isle of Purbeck and Weymouth. *Mem. geol. Surv. U.K.*
- Strahan, A., Holme, T.V., Dewey, H., Cunningham, C.H., Simmons, W.C., King, W.B.R. and Wray, D.A., 1916. Thickness of strata in the counties of England and Wales exclusive of rocks older than Permian. *Mem. Geol. Surv. G.B.*
- Taitt, A.H. and Kent, P.E., 1958. Deep Boreholes at Portsdown (Hants) and Henfield (Sussex). B.P. Technical publ. British Petroleum, London.
- Talbot, M.R., 1973. Major sedimentary cycles in the Corallian beds (Oxfordian) of Southern England. *Palaeog. Palaeoclim. Palaeocol.*, 14: 293-317.
- Talwani, M., 1978. Distribution of basement under the eastern North Atlantic Ocean and the Norwegian Sea. In: D.R. Bowes and B.E. Leake (Editors). *Crustal evolution in northwestern Britain and adjacent regions*. Geol. Soc. London, Spec. Publ. Blackwell. 10: 348-375.
- Terris, A.P. and Bullerwell, W., 1965. Investigation into the underground structure of Southern England. *Advanc. Sci.* August: 232-252.
- Threlfall, W.F., 1981. Structural framework of the central and northern North Sea. In: L.V. Illing and G.D. Hobson (Editors). *Petroleum Geology of the Continental Shelf of North-West Europe*. Heyden and

Son Ltd: 98-103.

- Townson, W.G., 1975. Lithostratigraphy and deposition of the type Portlandian. *J. geol. Soc. London.*, 131: 619-638.
- Tresise, G.R., 1961. The Nature and Origin of Chert in the Upper Greensand of Wessex. *Proc. Geol. Assoc. London.*, 72: 333-356.
- Tucker, M.E., 1977. The marginal Triassic deposits of South Wales: continental facies and Palaeogeography. *Geol. J.*, 12: 169-188.
- Vail, P.R., Mitchum, Jr, R.M. and Thompson, III, S., 1977. Seismic stratigraphy and global changes of sea level, Part 3: Relative changes of sea level from coastal onlap. In: C.E. Payton (Editor) *Seismic stratigraphy - applications to hydrocarbon exploration*. Am. Assoc. Petrol. Geol. Mem. 26: 63-81.
- Wallace, P., 1983. The Subsurface Variscides of Southern England and their Continuation into Continental Europe. In: P.L. Hancock (Editor) *The Variscan Fold Belt of the British Isles*. Adam Hilger Ltd., Bristol.
- Waples, D., 1980. Time and temperature in petroleum formation; application of Lopatin's method to petroleum exploration. *Am. Assoc. Petrol. Geol.*, 64: 916-926.
- Warrington, G., Audley-Charles, M.G., Elliott, R.E., Evans, W.B., Ivimey-Cook, H.C., Kent, Robinson, P.L., Shotton, F.W. and Taylor, F.M., 1980. A correlation of Triassic rocks in the British Isles. *Geol. Soc. London, Spec. Report No. 13*: 78pp.
- Watson, J.V., 1984. The ending of the Caledonian orogeny in Scotland. *J. geol. Soc. London.*, 141: 193-214.
- Watts, A.B., 1982. Tectonic subsidence, flexure and Global changes of sea level. *Nature*, 297: 469-474.
- Watts, A.B. and Ryan, W.B.F., 1976. Flexure of the lithosphere and continental margin basins. *Tectonophysics.*, 36: 25-44.
- Watts, A., and Steckler, M.S., 1981. Subsidence and tectonics of Atlantic type continental margins. *Oceanologica Acta.*, No. SP., Colloque C3, *Geologie des Marges Continentales.*, 26 eme, C.G.I: 143-154.
- Watts, A.B., Karner, G.D. and Steckler, M.S., 1982. Lithospheric flexure and the evolution of sedimentary basin formation. In: *The evolution of sedimentary basins*. *Phil. Trans. Roy. Soc.*, A305: 249-281.
- Watts, A.B. and Thorne, J., 1984. Tectonics, Global changes in sea-level and their relationship to stratigraphic sequences at the U.S. Atlantic continental margin. *Marine. Petrol. Geol.* 1: 319-339.

- Wernicke, B. and Burchfiel, B.C., 1982. Modes of extensional tectonics. *J. Struct. Geol.*, 4: 105-115.
- Wernicke, B., 1988. Uniform-sense normal simple shear of the continental lithosphere. *Can. J. Earth. Sci.*, 22: 108-125.
- West, I.M., 1975. Evaporites and associated sediments of the basal Purbeck formation (Upper Jurassic) of Dorset. *Proc. Geol. Assoc. London.*, 86: 205-225.
- West, I.M. and Hooper, M.J., 1969. Detrital Portland chert and limestone in the Upper Purbeck Beds at Friar Waddon, Dorset. *Geol. Mag.*, 106: 277-280.
- White, P.H.N., 1949. Gravity data obtained in Great Britain by the Anglo-American Oil Company Ltd., *Q. J. geol. Soc.*, 104: 339-364.
- Whittaker, A., 1972. Intra-Liassic structures in the Severn Basin area. *Inst. Geol. Sci. Rep. No. 72/3*: 5pp.
- Whittaker, A., 1975. A postulated post-Hercynian rift valley system in Southern Britain. *Geol. Mag.*, 112: 137-149.
- Whittaker, A., 1980. Shrewton No. 1. Geological well completion report. *Rep. Deep Geol. Unit. Inst. Geol. Sci. No. DP/80*.
- Whittaker, A., (Editor) 1985. Atlas of Onshore sedimentary basins in England and Wales: Post-Carboniferous Tectonics and Stratigraphy. Blackie, Glasgow, 71 pp.
- Whittaker, A. and Chadwick, R.A., 1984. The large-scale structure of the Earth's crust beneath southern Britain. *Geol. Mag.*, 121: 621-624.
- Williams, G.D., and Brooks, M. 1985. A reinterpretation of the concealed Variscan structure beneath southern England by section balancing. *J. geol. Soc. London.*, 142: 689-696.
- Williams-Mitchell, E., 1956. the stratigraphy and structure of the chalk of the Dean Hill anticline, Wiltshire. *Proc. Geol. Assoc. London.*, 67: 221-227.
- Wills, L.J., 1973. A palaeogeological Map of the Palaeozoic Floor below the Permian and Mesozoic Formations in England and Wales. *Mem. Geol. Soc. London.*, No. 7, 23 pp.
- Wills, L.J., 1978. A palaeogeological map of the Lower Palaeozoic floor below the cover of upper Devonian, Carboniferous and later formations. *Mem. geol. Soc. London.*, 8: 36pp.
- Wooldridge, S.W. and Linton, D.L., 1938. Some episodes in the Structural evolution of south-east England considered in relation to the Concealed Boundary of Meso-Europe. *Proc. Geol. Assoc. London.*, 49: 264-92.

- Worssam, B.C. and Ivimey-Cook, H.C., 1971. The stratigraphy of the Geological Survey Borehole at Warlingham, Surrey. Bull. Geol. Surv. G.B. No. 36: 1-46.
- Wright, J.K., 1981. The Corallian rocks of north Dorset. Proc. Geol. Assoc. London., 92: 17-32.
- Ziegler, P.A., 1981. Evolution of sedimentary basins in North-West Europe. In: L.V. Illing and G.D. Hobson (Editors). Petroleum Geology of the Continental Shelf of North-West Europe. Heyden and Son Ltd: 3-39.
- Ziegler, P.A., 1982. Geological Atlas of Western and Central Europe. Shell International Petroleum Mag. BV, The Hague.
- Ziegler, P.A., 1983. Inverted basins in the Alpine foreland. In: A.W. Bally (Editor). Seismic Expression of Structural Styles - a picture and work Atlas. Am. Assoc. petrol. Geol. studies in Geology., Series No. 15., 3: 3.3.3-3.3.12.
- Ziegler, P.A., 1984. Caledonian and Hercynian crustal consolidation of Western and Central Europe - A working hypothesis. Geologies en Minbouw., 63: 93-108.
- Ziegler, P.A., 1986. Late Cretaceous and Cenozoic intra-plate compressional deformations in the Alpine Foreland - a geodynamic model. Tectonophysics, 000:000-000.

APPENDIX A

LOC 1	CAEN HILL PIT	ST 9831	6141	ALBIAN	GAU
LOC 2	SEEND	ST 9371	6101	APTIAN	GS
LOC 3	SEEND CLEEVE	ST 9331	6091	APTIAN	GS
LOC 4	BRADFORD ON AVON	ST 8261	5991	BATHONIAN	FM (BC)
LOC 5	STOWFOLD FARM	ST 8091	5781	BATHONIAN	FM
LOC 6	CASTLE FARM	ST 8031	5751	BATHONIAN	GO, FM
LOC 7	CASTLE FARM BARN	ST 8081	5741	BATHONIAN	FM
LOC 8	STEEPLE ASHTON	ST 9061	5591	OXFORDIAN	C
LOC 9	SPINNEY FARM	ST 7951	5511	BATHONIAN	FM
LOC 10	RODE CUTTING	ST 8671	5491	BATHONIAN	FM
LOC 11	WOOLVERTON	ST 7921	5311	BATHONIAN	FM
LOC 12	WESTBURY WORKS	ST 8851	5301	KIMMERIDGIAN	K
LOC 13	WESTBURY	ST 8661	5251	OXFORDIAN	C
LOC 14	WATERSLADE FARM	ST 8241	5221	BATHONIAN	FM
LOC 15	BECKINGTON	ST 8021	5171	BATHONIAN	FM
LOC 16	LULLINGTON	ST 7831	5311	BATHONIAN	FM
LOC 17	OLDFORD	ST 7921	5051	BAJOCIAN?	IO?
LOC 18	VALLIS VALE	ST 7606	4950	CARB/RHAETIAN	-, R
LOC 19	VALLIS CENTRE	ST 7555	4920	CARB/BAJOCIAN	-, IO
LOC 20	VALLIS	ST 7656	4870	BATHONIAN	FM
LOC 21	FROME CUTTING	ST 7931	4781	CALLOVIAN	KC
LOC 22	KEYFORD	ST 7831	4731	BATHONIAN	FM
LOC 23	CHANNY QUARRY	ST 7191	4571	CARB/BAJOCIAN	-, IO
LOC 24	HOLWELL QUARRY	ST 7261	4501	TRIAS/BAJOCIAN	T, IO
LOC 24	HOLWELL NORTH	ST 7271	4541	CARB/BAJOCIAN	-, IO
LOC 25	MARSTON ROAD	ST 7311	4491	CARB/RHAET/HETT	-, R, BL
LOC 26	CLOFORD QUARRY	ST 7181	4411	CARB/HETT-BAJOCIAN	-, BL?, JB
LOC 27	WINDSOR HILL	ST 6153	4512	NORIAN?/HETTANGIAN?	T, BL?
LOC 28	WINDSOR HILL S	ST 6171	4491	HETTANGIAN	(DSS)
LOC 29	HOBBS DOWNSIDE	ST 6231	4471	CARB/HETTANGIAN?	-, (DSS)
LOC 30	SHEPTON MALLET RR	ST 6351	4481	HETTANGIAN?	(DSS)
LOC 31	VIADUCT QUARRY	ST 6221	4421	HETTANGIAN?	(DSS)
LOC 32	COOMBE RISE SM	ST 6111	4381	HETT/SINEMURIAN	BL (DSS?)
LOC 33	CHELYNCH EAST	ST 6531	4381	BAJOCIAN	IO
LOC 34	CHELYNCH QUARRY	ST 6501	4371	BAJOCIAN	IO
LOC 35	STUMP CROSS	ST 6021	4291	RHAETIAN	R
LOC 36	SHEPTON RAILWAY B	ST 6291	4261	HETTANGIAN?	(DSS)
LOC 37	DOULTING	ST 6481	4251	TOARCIAN/BAJOCIAN	BS, IO
LOC 38	DOULTING RAILWAY	ST 6501	4251	BAJOCIAN	IO
LOC 39	WANSTROW	ST 7081	4075	BATHONIAN	FM
LOC 40	BEARD HILL	ST 6297	4080	SINEMURIAN	BL
LOC 41	BATCOMBE	ST 6866	3942	PLIENSBAACH/TOARCIAN	JB
LOC 42	WESTCOMBE	ST 6762	3950	PLIENSBAACH/TOARCIAN	JB
LOC 43	EVERCREECH	ST 6456	3882	HETTANGIAN	BL
LOC 44	EDMUND HILL	ST 5061	3925	PLIENSBAACHIAN	PS
LOC 45	STONE DOWN HILL	ST 5075	3920	PLIENSBAACHIAN	PS
LOC 46	GILCOMBE FARM	ST 6931	3616	BATHONIAN	FM
LOC 47	CREECH HILL SOUTH	ST 6690	3525	PLIENSBAACH/TOARCIAN	JB, BS
LOC 48	BRUTON ESTATE	ST 6865	3512	BATHONIAN	FE
LOC 49	BRUE RIVER	ST 6921	3521	BATHONIAN	FE
LOC 50	SOUTH BREWHAM	ST 7275	3448	CALLOVIAN	KC
LOC 51	GODMINSTER FARM	ST 6845	3243	BATHONIAN	FER
LOC 52	CASTLE GROUND	ST 8011	3181	OXFORDIAN	C
LOC 52	ZEALS PARK	ST 8001	3181	OXFORDIAN	C
LOC 53	HADSPEN QUARRIES	ST 6541	3141	BAJOCIAN	IO
LOC 54	HADSPEN QUARRIES	ST 6541	3151	BAJOCIAN	IO
LOC 55	KEINTON MANDEVILL	ST 5481	3031	HETTANGIAN?	BL
LOC 56	GODS HILL YARLING	ST 6611	2981	BAJOCIAN	IO
LOC 57	UPPER CHICKSGROVE	ST 9621	2951	TITHONIAN	P, PB
LOC 58	GREENS QUARRY	ST 9311	2901	TITHONIAN	P

List of localities visited during this study

LOC 59	TUCKING MILL	ST 9361	2901	TITHONIAN	P
LOC 60	TISBURY RAILWAY	ST 9451	2881	TITHONIAN	P
LOC 61	MITCHELS FARM	ST 7331	2851	OXFORDIAN	C
LOC 62	CHARLTON ADAM	ST 5371	821	HETTANGIAN?	BL
LOC 63	WOOLSTON FIELD	ST 6591	2771	BAJOCIAN	IO
LOC 64	WOOLSTON CUTTING	ST 6631	2771	BAJOCIAN	IO
LOC 65	UPTON QUARRY	ST 4548	2704	HETTANGIAN	BL
LOC 66	HIGHBROOKS QUARRY	ST 4911	2601	HETTANGIAN?	BL
LOC 67	CAMEL HILL	ST 5691	2551	HETTANGIAN	BL
LOC 68	SPARKFORD HILL	ST 6021	2541	RHAETIAN	R
LOC 69	PEN HILL	ST 6321	2521	BAJOCIAN	IO
LOC 70	BLACKFORD	ST 6660	2550	BAJOCIAN	IO
LOC 71	MAPERTON CUTTING	ST 6681	2542	BAJOCIAN	IO
LOC 72	NORTH CHERITON	ST 6891	2591	BATHONIAN	FM
LOC 74	ABBAS COMBE	ST 6988	2219	BATHONIAN	FE, BB, FM
LOC 75	HATCH BEAUCHAMP	ST 3055	2044	HETTANGIAN	BL
LOC 76	FIVEHEAD RIVER	ST 2931	1901	HETTANGIAN?	BL
LOC 77	SANDFORD ORCAS	ST 6221	2071	PLIENSBAACHIAN	PS
LOC 78	HOLLOWAY	ST 6341	2041	TOARCIAN	BS
LOC 79	TODBER EAST SIDE	ST 7975	1995	OXFORDIAN	C
LOC 80	TODBER PLANT	ST 7971	1991	OXFORDIAN	C
LOC 81	GANNETS, TODBER	ST 7951	1981	OXFORDIAN	C
LOC 82	PATSON HILL	ST 6271	1941	TOARCIAN	BS
LOC 83	STALBRIDGE	ST 7161	1851	BATHONIAN	FM
LOC 84	CHARLOCK HILL	ST 6171	1831	TOARCIAN	BS
LOC 85	OBORNE	ST 6491	1841	BAJOCIAN	IO
LOC 86	QUARR LANE	ST 6376	1780	BAJOCIAN	IO
LOC 87	SHERBOURNE NORTH	ST 6300	1760	BAJOCIAN	IO
LOC 88	BARRINGTON	ST 3951	1781	PLIENSBAACHIAN	PS
LOC 89	SHEPTON BEAUCHAMP	ST 4021	1781	PLIENSBAACHIAN	PS
LOC 90	STOKE SUB HAMDON	ST 4724	1763	PLIENSBAACH/TOARCIAN	JB
LOC 91	MONTACUTE CUTTING	ST 5041	1741	PLIENSBAACH/TOARCIAN	JB
LOC 92	MONTACUTE PARK B	ST 4981	1680	PLIENSBAACH/TOARCIAN	JB
LOC 93	HAM HILL	ST 4780	1720	TOARCIAN	BS (HS)
LOC 94	HALFWAYHOUSE N	ST 6020	1640	BAJOCIAN	IO
LOC 95	HALFWAY HOUSE	ST 6021	1631	BAJOCIAN	IO
LOC 96	PRESTON PLUCKNETT	ST 5371	1621	PLIENSBAACH/TOARCIAN	JB
LOC 97	LUPTON	ST 5191	1641	PLIENSBAACH/TOARCIAN	JB
LOC 98	LOUSE HILL QUARRY	ST 6095	1609	BAJOCIAN	IO
LOC 99	TILLYS HILL ROAD	ST 5781	1571	TOARCIAN	BS
LOC 100	TILLYS HILL HOLL	ST 5771	1551	TOARCIAN	BS
LOC 101	ODCOMBE	ST 5080	1565	TOARCIAN	PS
LOC 102	DANCING HILL	ST 6361	1521	BATHONIAN	FE
LOC 103	WEST HILL	ST 6421	1481	BATHONIAN	FM
LOC 104	COUNCIL TIP	ST 4941	1471	TOARCIAN	BS
LOC 105	WESTLANDS ROAD	ST 5351	1461	TOARCIAN	BS
LOC 106	YEOVIL STATION	ST 5701	1421	TOARCIAN	BS
LOC 107	SEAVINGTON	ST 4003	1447	BAJOCIAN	IO
LOC 108	DONYATT	ST 3451	1404	PLIENSBAACH/TOARCIAN	JB
LOC 109	LOPEN SW	ST 4131	1381	BAJOCIAN	IO
LOC 110	CHINNOCK BRIDGE	ST 5051	1341	TOARCIAN	BS
LOC 111	OKER HILL	ST 5161	1331	TOARCIAN	BS
LOC 112	HOLYWELL	ST 5291	1311	TOARCIAN	BS
LOC 113	HINTON-ST-GEORGE	ST 4231	1301	TOARCIAN	BS
LOC 114	WEST CHINNOCK	ST 4622	1273	TOARCIAN	BS
LOC 115	BROADHILL FARM	ST 4941	1211	BATHONIAN	FM
LOC 116	FURLAND	ST 4321	1191	BAJOCIAN	IO
LOC 117	BEER HACKETT	ST 5924	1200	CALLOVIAN	KC
LOC 118	SUTTON BINGHAM	ST 5521	1151	CALLOVIAN	KC
LOC 119	SUTTON BINGHAM E	ST 5531	1151	CALLOVIAN	KC

LOC 120	HARDINGTON MOOR	ST 5181	1181	BATHONIAN	FM
LOC 121	HARDINGTON MANDEV	ST 5136	1188	BATHONIAN	FM
LOC 122	YETMINSTER	ST 5991	1061	CALLOVIAN	KC
LOC 123	WARREN HILL	ST 4035	1030	ALBIAN	GS
LOC 124	CREWKERNE	ST 4361	0951	TOARCIAN/BAJOCIAN	BS, IO
LOC 125	CREWKERNE SOUTH	ST 4361	0761	BAJOCIAN	IO
LOC 126	LIBERTY FARM	ST 4579	0800	BATHONIAN	FM
LOC 127	MELBURY OSMOND	ST 5700	0810	BATHONIAN	FM
LOC 128	CALFHAY FARM	ST 6151	0621	OXFORDIAN	O
LOC 129	BROADWINDSOR CUT	ST 4391	0271	TOARCIAN/BAJOCIAN	BS, IO
LOC 130	HOLLIS HILL	ST 4425	0275	BAJOCIAN	IO
LOC 131	BURSTOCK	ST 4781	0261	BATHONIAN	FM
LOC 132	HORN PARK QUARRY	ST 4581	0211	BAJOCIAN	IO
LOC 133	WADDON HILL	ST 4471	0175	BAJOCIAN	IO
LOC 134	WADDON HILL SOUTH	ST 4473	0172	BAJOCIAN	IO
LOC 135	TOLCIS TIP	ST 2801	0101	HETTANGIAN?	BL
LOC 136	COOMBE, MAPPERTON	SY 4962	9987	BAJOCIAN	IO
LOC 137	MARLPITS	SY 4985	9715	BAJOCIAN	IO
LOC 138	POWERSTOCK WEST	SY 5101	9611	TOARCIAN	BS
LOC 139	OLD STATION, NETTL	SY 5225	9552	BAJOCIAN	IO
LOC 140	BELL QUARRY EAST	SY 5011	9501	BAJOCIAN	IO
LOC 141	BELL QUARRY WEST	SY 4981	9491	BAJOCIAN	IO
LOC 142	LODERS RAILWAY	SY 5021	9461	BAJOCIAN	IO
LOC 143	LODERS CUTTING	SY 4961	9430	TOARCIAN	BS
LOC 144	QUARRY HILL HOLL	SY 4331	9381	PLIENSBAACHIAN	DS?, TS?
LOC 145	COLMERS HILL	SY 4365	9381	PLIENSBAACHIAN	DS?, TS?
LOC 146	SYMONDSBURY	SY 4468	9380	TOARCIAN	BS
LOC 147	QUARRY HILL	SY 4350	9320	BAJOCIAN	IO
LOC 148	UPLDERS	SY 5131	9361	BAJOCIAN	IO
LOC 149	MATRAVERS	SY 5131	9331	BAJOCIAN	IO
LOC 150	VINNEY CROSS	SY 5091	9301	BAJOCIAN	IO
LOC 151	UPLDERS CUTTING	SY 5075	9290	TOARCIAN/BAJOCIAN	BS, IO
LOC 152	EAST LODERS HILL	SY 4981	9301	BAJOCIAN	IO
LOC 153	INNSACRE, SHIPTON	SY 4961	9261	BAJOCIAN	IO
LOC 154	BONSCOMBE WEST	SY 4841	9231	BAJOCIAN	IO
LOC 155	BONSCOMBE EAST	SY 4851	9221	BAJOCIAN	IO
LOC 156	SMACOMBE FARM	SY 5011	9171	BAJOCIAN	IO
LOC 157	CROSS ROADS, SHIPA	SY 5001	9151	BAJOCIAN	IO
LOC 158	CROSS ROADS, SHIPB	SY 5001	9141	TOARCIAN/AALENIAN	BS, IO
LOC 159	CAINS FOLLY E	SY 3845	9262	PLIENSBAACHIAN	BM
LOC 160	CAINS FOLLY W	SY 3810	9275	PLIENSBAACHIAN	BM
LOC 161	STONEBARROW S	SY 3806	9273	SINEMURIAN	BV
LOC 162	ST GABRIELS W	SY 3875	9250	PLIENSBAACHIAN	BM, GA
LOC 163	STONEBARROW S	SY 3806	9273	SINEMURIAN	BM
LOC 164	ST GABRIELS E	SY 3900	9246	PLIENSBAACHIAN	BM, GA
LOC 165	GOLDEN CAP	SY 4036	9220	TOARCIAN	BS
LOC 165	WEAR CLIFFS	SY 4078	9182	PLIENSBAACHIAN	DS
LOC 166	RIDGE CLIFF B	SY 4286	9135	PLIENSBAACHIAN	EC
LOC 166	RIDGE CLIFF A	SY 4285	9135	PLIENSBAACHIAN	EC
LOC 166	RIDGE CLIFF C	SY 4287	9135	PLIENSBAACHIAN	EC
LOC 167	THORNCOMBE BEACON	SY 4330	9140	PLIENSBAACHIAN	TS
LOC 168	EAST EBB COVE	SY 4375	9124	PLIENSBAACHIAN	EC
LOC 169	HAVEN CLIFF	SY 2650	8960	NORIAN/RHAETIAN	T, R
LOC 170	CULVERHOLE GULLYA	SY 2720	8941	RHAETIAN	R
LOC 171	CULVERHOLE GULLYB	SY 2715	8940	RHAETIAN	R
LOC 172	HUMBLE POINT	SY 3080	9040	HETTANGIAN	BL
LOC 173	SHAPWICK GRANGE A	SY 3118	9190	SENONIAN	UC
LOC 173	SHAPWICK GRANGE B	SY 3117	9190	SENONIAN	UC
LOC 173	SHAPWICK GRANGE C	SY 3119	9188	SENONIAN	UC
LOC 174	WEST CLIFF 7	SY 3320	9138	HETTANGIAN	BL

LOC 175	WEST CLIFF 5A	SY 3320 9138	HETTANGIAN	BL
LOC 176	WEST CLIFF 5B	SY 3320 9136	HETTANGIAN	BL
LOC 177	DEVONSHIRE HEAD	SY 3280 9110	HETTANGIAN	BL
LOC 177	DEVONSHIRE HEAD	SY 3282 9112	HETTANGIAN	BL
LOC 178	CHARTON BAY	SY 2965 9000	NORIAN/RHAETIAN	T, R
LOC 179	DEVONSHIRE HEAD	SY 3300 9125	HETTANGIAN	BL
LOC 180	WEST CLIFF ANTI	SY 3300 9129	HETTANGIAN	BL
LOC 181	WEST CLIFF 1,2	SY 3308 9132	HETTANGIAN	BL
LOC 182	WEST CLIFF 4,5	SY 3306 9130	HETTANGIAN	BL
LOC 182	WEST CLIFF 3	SY 3307 9131	HETTANGIAN	BL
LOC 183	WEST CLIFF 6	SY 3305 9130	HETTANGIAN	BL
LOC 184	WEST CLIFF 5C	SY 3320 9137	HETTANGIAN	BL
LOC 185	SEVEN ROCK POINTA	SY 3272 9083	HETTANGIAN	BL
LOC 186	SEVEN ROCK POINTB	SY 3258 9088	HETTANGIAN	BL
LOC 187	POKERS POOL	SY 3320 9133	SINEMURIAN	SB
LOC 188	SEVEN ROCK POINTC	SY 3256 9088	HETTANGIAN	BL
LOC 189	PINHAY BAY NORTH	SY 3178 9080	RHAETIAN/HETTANGIAN	R, BL
LOC 189	PINHAY BAY SOUTH	SY 3177 9078	HETTANGIAN	BL
LOC 190	WEST CLIFF W	SY 4381 9097	PLIENSBAACHIAN	TS
LOC 191	WEST CLIFF BEACH	SY 4520 9087	PLIENSBAACH/TOARCIA	JB
LOC 191	FAULT CORNER	SY 4518 9090	PLIENSBAACH/TOARCIA	JB
LOC 192	WEST CLIFF UPPER1	SY 4540 9072	BATHONIAN	FE, BB
LOC 193	WEST CLIFF UPPER2	SY 4540 9071	BATHONIAN	FE
LOC 194	WEST CLIFF E	SY 4540 9078	BATHONIAN	FE
LOC 195	SHIPTON GORGE W	SY 4951 9161	BAJOCIAN	IO
LOC 196	BOTHENHAMPTON	SY 9121 9121	BATHONIAN	FM
LOC 197	HAVEN CLIFF WEST	SY 2585 8985	ALBIAN/CENOMANIAN	GS
LOC 198	COOMBE FARM	ST 6288 1777	BAJOCIAN	IO
LOC 199	EAST CLIFF A	SY 4650 9019	TOARCIA	BS
LOC 200	EAST CLIFF B	SY 4650 9020	TOARCIA	BS
LOC 201	EAST CLIFF C	SY 4651 9019	TOARCIA	BS
LOC 202	EAST CLIFF D	SY 4652 9018	TOARCIA	BS
LOC 203	EAST CLIFF E	SY 4653 9017	TOARCIA	BS
LOC 204	EAST CLIFF F	SY 4654 9016	TOARCIA	BS
LOC 205	EAST CLIFF G	SY 4655 9015	TOARCIA	BS
LOC 206	EAST CLIFF H	SY 4655 9014	TOARCIA	BS
LOC 207	EAST CLIFF I	SY 4656 9013	TOARCIA	BS
LOC 208	EAST CLIFF J	SY 4656 9012	TOARCIA	BS
LOC 209	EAST CLIFF K	SY 4657 9012	TOARCIA	BS
LOC 210	EAST CLIFF L	SY 4657 9011	TOARCIA	BS
LOC 211	EAST CLIFF M	SY 4658 9010	TOARCIA	BS
LOC 212	EAST CLIFF O	SY 4658 9009	TOARCIA	BS
LOC 212	EAST CLIFF P	SY 4680 8998	TOARCIA	BS
LOC 213	EAST CLIFF CEN B	SY 4680 8999	TOARCIA	BS
LOC 213	EAST CLIFF CEN A	SY 4680 9000	TOARCIA	BS
LOC 214	EAST CLIFF CENTRE	SY 4678 9000	TOARCIA	BS
LOC 215	EAST CLIFF GULLYB	SY 4702 8991	TOARCIA	BS
LOC 215	EAST CLIFF GULLYD	SY 4703 8990	TOARCIA	BS
LOC 215	EAST CLIFF GULLYA	SY 4701 8991	TOARCIA	BS
LOC 215	EAST CLIFF GULLYE	SY 4703 8989	TOARCIA	BS
LOC 215	EAST CLIFF GULLYC	SY 4702 8990	TOARCIA	BS
LOC 216	EAST CLIFF N	SY 4717 8983	TOARCIA	BS
LOC 217	FRESHWATER WEST	SY 4738 8975	TOARCIA	BS
LOC 218	SPYWAY QUARRIES	SZ 0321 7681	TITHONIAN/RYAZANIAN	P, PB
LOC 218	FRESHWATER PARK	SY 4790 8990	BAJOCIAN	IO
LOC 219	FRESHWATER A	SY 4785 8958	TOARCIA	BS
LOC 220	FRESHWATER C	SY 4787 8956	TOARCIA	BS
LOC 221	FRESHWATER D	SY 4786 8956	TOARCIA	BS
LOC 222	FRESHWATER B	SY 4803 8935	TOARCIA	BS
LOC 223	BURTON CLIFF W	SY 4800 8945	TOARCIA/BAJOCIAN	BS, IO

LOC 224	FRESHWATER D	SY 4788	8956	TOARCIAN	BS
LOC 224	BURTON CLIFF E1	SY 4803	8944	TOARCIAN/BAJOCIAN	BS, IO
LOC 225	BURTON CLIFF E2	SY 4804	9840	TOARCIAN	BS
LOC 226	CLIFF HILL	SY 4875	8938	TOARCIAN/BAJOCIAN	BS, IO
LOC 227	SOUTHOVER	SY 4980	3885	TOARCIAN	BS
LOC 228	CLIFFEND	SY 4930	8870	BATHONIAN	FM
LOC 229	COGDEN FARM	SY 5058	8910	BATHONIAN	FM
LOC 230	LOCKE FARM	SY 5481	8971	BATHONIAN	FM
LOC 231	EAST BEXINGTON	SY 5585	8445	OXFORDIAN	C
LOC 232	EAST BEXINGTON 2	SY 5587	8443	OXFORDIAN	C
LOC 233	ABBOTSBURY ROAD	SY 5635	8520	KIMMERIDGIAN	K
LOC 234	BLIND LANE, ABBOTS	SY 5761	8561	KIMMERIDGIAN	K(AIO)
LOC 235	RED LANE, ABBOTS	SY 5761	8551	KIMMERIDGIAN	K(AIO)
LOC 236	PORTESHAM QUARRY	SY 6105	8595	TITHONIAN	P, PB
LOC 237	WADDON QUARRY	SY 6241	8581	TITHONIAN	P
LOC 238	CORTON FARM	SY 6361	8551	TITHONIAN	P
LOC 239	FRIAR WADDON	SY 6501	8581	TITHONIAN	PB
LOC 240	WADDON HILL UPWEY	SY 6451	8541	TITHONIAN	P
LOC 241	GRANERY, UPWEY	SY 6611	8541	TITHONIAN	PB
LOC 242	RIDGEWAY	SY 6711	8521	TITHONIAN	PB
LOC 243	REDCLIFFE FARM	SY 9331	8671	EOCENE	BAG
LOC 244	LINTON HILL WEST	SY 5821	8451	OXFORDIAN	C
LOC 245	LINTON HILL EAST	SY 5861	8431	OXFORDIAN	C
LOC 246	CHESTERS HILL	SY 5761	8361	CALLOVIAN	KC
LOC 247	CHALBURY CAMP	SY 6945	8381	TITHONIAN	P, PB
LOC 248	NOIGNS DOWN	SY 7535	8381	TITHONIAN	P
LOC 249	POXWELL LODGE QU	SY 7441	8356	TITHONIAN	P, PB
LOC 250	NOTTINGTON HO	SY 6635	8240	OXFORDIAN	KC, O
LOC 251	HERBURY	SY 6111	8101	BATHONIAN	FM, BB?, FE
LOC 252	FLEET COMMON	SY 6296	7983	CALLOVIAN	KC
LOC 253	EAST FLEET	SY 6345	7990	CALLOVIAN	KC
LOC 254	CROOKHILL PIT	SY 6435	7975	CALLOVIAN/OXFORDIAN	O
LOC 255	BOWLEAZE COVE	SY 7061	8181	OXFORDIAN	C
LOC 256	REDCLIFF POINT	SY 7118	8165	OXFORDIAN	C
LOC 257	REDCLIFF SOUTH	SY 7132	8169	OXFORDIAN	C
LOC 258	REDCLIFF NORTH	SY 7145	8178	OXFORDIAN	C
LOC 259	SHORTLAKE	SY 7230	8195	OXFORDIAN	C
LOC 260	OSMINGTON MILLS C	SY 7351	8161	OXFORDIAN	C
LOC 260	OSMINGTON WATERF	SY 7357	8158	OXFORDIAN	C
LOC 261	OSMINGTON CLIFF	SY 7401	8138	OXFORDIAN	C
LOC 262	OSMINGTON POINT	SY 7431	8135	OXFORDIAN	C
LOC 263	BRAN POINT	SY 7431	8131	OXFORDIAN	C
LOC 264	HOLWORTH HOUSE	SY 7621	8158	TITHONIAN	P, PB
LOC 265	WHITE NOTHE	SY 7728	8067	SENONIAN	UC
LOC 266	DURDLE DOOR	SY 8045	8035	TITHONIAN-SENONIAN	PB-UC
LOC 267	OSMINGTON MILLS	SY 7355	8164	OXFORDIAN	C
LOC 268	MAN'O'WAR COVE	SY 8077	3037	CENOMANIAN/TURONIAN	LC, MC
LOC 269	DUNGY HEAD	SY 8151	8001	TITHONIAN	P, PB
LOC 270	LULWORTH CENTRAL	SY 8267	8000	CENOMANIAN/TURONIAN	LC, MC?
LOC 271	PEPLARS POINT	SY 8275	7975	TITHONIAN/RYAZANIAN	PB
LOC 272	MUPE ROCKS	SY 8391	7961	TITHONIAN	P
LOC 273	MUPE POINT	SY 8441	7921	TITHONIAN/RYAZANIAN	PB
LOC 274	BACON HOLE	SY 8405	7970	TITHONIAN	PB
LOC 275	MUPE BAY	SY 8441	8001	'NEOCOMIAN'	W
LOC 276	BLACK ROCK, MUPE	SY 8461	8011	CENOMANIAN/TURONIAN	LC, MC?
LOC 277	COW CORNER	SY 8605	8040	CENOMANIAN/TURONIAN	LC, MC?
LOC 278	WORBARROW BAY CEN	SY 8871	8021	'NEOCOMIAN'	W
LOC 279	WORBARROW BAY	SY 8701	7961	RYAZANIAN	PB
LOC 280	FLOWERS BARROW	SY 8661	8041	ALBIAN/CENOMANIAN	GS, LC
LOC 281	WORBARROW BAY 2	SY 8682	7951	TITHONIAN/RYAZANIAN	PB

LOC 282	WORBARROW TOUT	SY 8681	7951	TITHONIAN	P
LOC 283	BRANDY BAY 1	SY 8901	7931	KIMMERIDGIAN	K
LOC 284	GAD CLIFF BRANDY	SY 8901	7951	KIMMERIDGIAN	K
LOC 285	BRANDY BAY 2	SY 8911	7941	KIMMERIDGIAN	K
LOC 286	BRANDY BAY 3	SY 8931	7931	KIMMERIDGIAN	K
LOC 287	HORBARROW BAY 2	SY 8961	7911	KIMMERIDGIAN	K
LOC 288	HORBARROW BAY 2	SY 8971	7901	KIMMERIDGIAN	K
LOC 289	HORBARROW LEDGES2	SY 8971	7891	KIMMERIDGIAN	K
LOC 290	HORBARROW BAY 1	SY 8961	7901	KIMMERIDGIAN	K
LOC 291	HORBARROW LEDGES3	SY 8981	7881	KIMMERIDGIAN	K
LOC 292	CHANEL, KIMMERIDGE	SY 9011	7901	KIMMERIDGIAN	K
LOC 293	KIMMERIDGE LEDGES	SY 9031	7901	KIMMERIDGIAN	K
LOC 294	KIMMERIDGE	SY 9030	7901	KIMMERIDGIAN	K
LOC 295	KIMMERIDGE OIL	SY 9041	7921	KIMMERIDGIAN	K
LOC 296	KIMM, OIL WELL 2	SY 9041	7921	KIMMERIDGIAN	K
LOC 296	KIMMERIDGE BAY	SY 9051	7821	KIMMERIDGIAN	K
LOC 297	GAULTER GAP	ST 9081	7901	KIMMERIDGIAN	K
LOC 298	SMEDMORE HILL W	SY 9181	8001	TITHONIAN	P
LOC 299	SMEDMORE HILL E	SY 9191	8011	TITHONIAN	P, PB
LOC 300	CUDDLE	SY 9121	7821	KIMMERIDGIAN	K
LOC 301	KIMMERIDGE LEDGE2	SY 9200	7775	KIMMERIDGIAN	K
LOC 302	CLAVELLS HARD	SY 9181	7771	KIMMERIDGIAN	K
LOC 303	ROPE LAKE	SY 9251	7751	KIMMERIDGIAN	K
LOC 304	ROPE LAKE HEAD	SY 9271	7741	KIMMERIDGIAN	K
LOC 305	COCKNOMLE QUARRY	SY 9321	8231	SENONIAN	UC
LOC 306	CORFE CASTLE VIEW	SY 9591	8251	SENONIAN	UC
LOC 307	CORFE CASTLE CUT	SY 9611	8241	CENOMANIAN-SENONIAN	LC, MC, UC
LOC 308	BRENSCOMBE HILL	SY 9861	8201	SENONIAN?	UC?
LOC 309	REDEND POINT	SZ 0385	8282	EOCENE	BAG
LOC 310	STUDLAND	SZ 0455	8240	SENOMANIAN	UC
LOC 311	CURRENDON FARM	SZ 0161	8135	SENONIAN?	UC?
LOC 312	ROUND DOWN	SZ 0181	8111	SENONIAN?	UC?
LOC 313	BALLARD POINT	SZ 0471	8131	CENOMANIAN/TURONIAN	GS, LC
LOC 314	LONDON DOORS QU	SY 9491	7921	TITHONIAN	P
LOC 315	DOWNSAY WOOD	SY 9805	7911	TITHONIAN/RYAZANIAN	PB
LOC 316	ACTON QUARRIES	SY 9881	7861	RYAZANIAN	PB
LOC 317	BLACKLANDS	SY 9891	7811	TITHONIAN/RYAZANIAN	PB
LOC 318	ULWELL WORKS	SZ 0211	8041	'NEOCOMIAN'	W
LOC 319	ACTON QUARRIES	SY 9861	7831	TITHONIAN/RYAZANIAN	PB
LOC 320	SWANWORTH QUARRY	SY 9691	7831	TITHONIAN	P
LOC 321	FRESHWATER	SY 9381	7735	KIMMERIDGIAN	K
LOC 322	FRESHWATER STEPS	SY 9401	7731	KIMMERIDGIAN	K
LOC 323	CHAPMANS POOL	SY 9561	7691	KIMMERIDGIAN	K
LOC 324	ALDHAMS QUARRY	SY 9641	7641	TITHONIAN	P
LOC 325	ST ALDHAMS HEAD	SY 9621	7541	TITHONIAN	P
LOC 326	WINSPIT	SY 9771	7601	TITHONIAN	P
LOC 327	WINSPIT CLIFF	SY 9771	7611	TITHONIAN	P
LOC 328	SEACOMBE	SY 9841	7661	TITHONIAN	P
LOC 329	SEASPRAY	SY 9945	7750	TITHONIAN	P
LOC 330	SEA SPRAY LEDGE U	SY 9921	7681	TITHONIAN	P
LOC 331	SEA SPRAY LEDGE L	SY 9931	7681	TITHONIAN	P
LOC 332	DANCING LEDGE	SY 9971	7691	TITHONIAN	P
LOC 334	SPYWAY QUARRIES A	SZ 0321	7681	TITHONIAN	P
LOC 335	SPYWAY QUARRIES B	SZ 0321	7681	TITHONIAN	P
LOC 336	CUCKOO POUND	SZ 0161	7741	TITHONIAN/RYAZANIAN	PB
LOC 337	CALIFORNIA FARM	SZ 0211	7761	TITHONIAN/RYAZANIAN	PB
LOC 338	TILLY WHIM CAVES	SZ 0301	7691	TITHONIAN	P
LOC 339	DURLSTON HEAD	SZ 0351	7721	TITHONIAN	P, PB
LOC 340	DURLSTON HEAD B	SZ 0351	7723	TITHONIAN	P, PB
LOC 341	PEVERIL POINT	SZ 0401	7861	RYAZANIAN	PB

LOC 342	NOTHE FORT	SY 6851	7851	OXFORDIAN	C C C C P P P P PB
LOC 343	CENTRE LEDGES	SY 6791	7781	OXFORDIAN	
LOC 344	WESTERN LEDGES	SY 6771	7771	OXFORDIAN	
LOC 345	SANDSFOOT CASTLE	SY 6761	7741	OXFORDIAN	
LOC 346	WEST CLIFF	SY 6841	7191	TITHONIAN	
LOC 347	BLACKNOR	SY 6821	7181	TITHONIAN	
LOC 348	PORTLAND BILL A	SY 6750	6850	TITHONIAN	
LOC 349	PORTLAND BILL TIP	SY 6771	7121	TITHONIAN	
LOC 350	PORTLAND BILL B	SY 6750	6848	TITHONIAN	

KEY

BAGSHOT SANDS	BAG	
UPPER CHALK	UC	
MIDDLE CHALK	MC	
LOWER CHALK	LC	
UPPER GREENSAND	GS	
GAULT CLAY	GAU	
WEALDEN	W	
PURBECK	PB	
PORTLAND GROUP	P	
KIMMERIDGE CLAY	K	(AIO) ABBOTSBURY IRON ORE
CORALLIAN	C	
OXFORD CLAY	O	
KELLAWAYS/CORNBRASH	KC	
FOREST MARBLE	FM	
BOUETTI BED	BB	(GO) GREAT OOLITE L/ST. (BC) BRADFORD CLAY.
FULLERS EARTH	FE	
INFERIOR OOLITE	IO	
BRIDPORT/YEOVIL S.	BS	(HS) HAM HILL STONE
DOWNCLIFF CLAYS	DC	
JUNCTION BED	JB	
THORNCOMBE SANDS	TS	PS PENNARD SANDS
DOWNCLIFF SANDS	DS	
EYPE CLAY	EC	
GREEN AMMONITE BEDS	GA	
BELEMITE MARLS	BM	
BLACK VEN MARLS	BV	
SHALES WITH BEEF	SB	
BLUE LIAS	BL	(DSS) DOWNSIDE STONE LOCAL
RHAETIC	R	
TRIASSIC	T	
BASEMENT	-	CARBONIFEROUS/DEVONIAN

LOC 5	200/8 SE	LOC 231	248/59 N
LOC 8	354/4 E	LOC 233	295/18 N
LOC 9	346/4 E	LOC 234	234/15 S
LOC 12	272/4 S	LOC 235	290/15 SW
LOC 13	333/5 E	LOC 236	267/8 N
LOC 15	215/2 E	LOC 237	283/12 N
LOC 16	220/16 SE	LOC 238	290/10 NE
LOC 17	266/4 N	LOC 239	260/8 N
LOC 19	244/3 N	LOC 240	280/9 N
LOC 22	184/4 E	LOC 242	286/4 NE
LOC 24	284/8 S	LOC 244	224/10 N
LOC 25	306/17 S	LOC 246	281/16 N
LOC 31	250/6 S	LOC 247	298/10 SW
LOC 32	228/6 N	LOC 249	276/19 S
LOC 33	266/3 S	LOC 250	288/11 SW
LOC 39	202/4 W	LOC 251	274/7 S
LOC 42	354/8 E	LOC 252	254/10 S
LOC 43	300/3 W	LOC 257	326/10 SW
LOC 44	300/5 SW	LOC 258	342/12 SW
LOC 45	315/10 SW	LOC 259	281/44 N
LOC 53	183/2 SE	LOC 260	236/5 SE
LOC 54	239/39 NW	LOC 261	321/10 E
LOC 57	218/5 S	LOC 263	310/6 NE
LOC 58	218/5 S	LOC 264	250/35 N
LOC 60	205/2 SE	LOC 266	272/75 N
LOC 62	352/5 E	LOC 269	248/36 N
LOC 68	260/7 N	LOC 271	320/24 N
LOC 69	230/7 S	LOC 274	265/25 N
LOC 73	220/7 S	LOC 275	285/84 N
LOC 76	310/10 S	LOC 278	293/28 NE
LOC 81	189/8 E	LOC 279	256/38 N
LOC 84	227/2 S	LOC 281	247/35 N
LOC 97	260/3 S	LOC 283	259/17 N
LOC 100	300/2 S	LOC 284	262/12 N
LOC 103	352/3 W	LOC 285	259/17 N
LOC 105	300/9 S	LOC 286	240/13 N
LOC 110	210/4 N	LOC 287	231/7 W
	290/8 S	LOC 290	193/4 NW
LOC 112	295/4 E	LOC 292	290/4 S
LOC 117	300/46 SW	LOC 293	296/2 SW
LOC 118	268/5 S	LOC 296	264/2 S
LOC 126	267/6 N	LOC 297	326/4 SE
LOC 128	252/28 S	LOC 298	310/26 E
LOC 132	294/3 N	LOC 299	268/23 N
LOC 133	260/3 S	LOC 301	194/3 E
LOC 135	184/20 E	LOC 303	191/2 E
LOC 137	350/2 W	LOC 317	266/3 S
LOC 140	265/7 S	LOC 318	256/16 N
LOC 142	263/8 S	LOC 319	314/10 NE
LOC 144	255/3 S	LOC 322	340/2 E
LOC 145	220/5 SE	LOC 324	241/3 SE
LOC 147	240/8 S	LOC 337	297/7 N
LOC 150	345/4 NE	LOC 338	220/2 SE
LOC 151	240/2 S	LOC 341	298/5 N
	304/11 S	LOC 342	260/9 S
LOC 155	334/7 E	LOC 343	250/4 S
LOC 158	270/2 S	LOC 344	212/6 S
LOC 169	354/9 E	LOC 345	245/5 S
LOC 171	193/3 E		
LOC 191	270/30 N		
LOC 196	275/12 N		
LOC 197	331/5 E		
LOC 213	290/2 N ?		
LOC 228	270/6 S		
LOC 229	280/25 N		
LOC 230	233/14 S		

Bedding dips recorded at individual localities

APPENDIX B

1	CAM	GS	61	BAGGERIDGE NO3	GS
2	HORSLEY	GS	62	BAGGERIDGE NO2	GS
3	CIRENCESTER EWEPENS	GS	63	BAGGERIDGE NO1	GS
4	CIRENCESTER LEWIS LANE	GS	64	STEEPLE ASHTON	WS
5	MEYSEY HAMPTON	GS	65	STEEPLE ASHTON WELL	WS
6	KEMBLE	GS	66	DEVIZES 1	D
7	TETBURY	GS	67	WEST LAVINGTON	B
8	TETBURY UPTON	GS	68	EASTERTON	WS
9	LATTON	WS	69	RUSHALL	WS
10	FARINGDON 1	F	70	CHUTE	WS
11	LEIGHTERTON AIRFIELD	GS	71	VERNHAM DEAN	V
12	LONG NEWTON 2	S	72	EAST BRENT	SS
13	COOLES FARM	U	73	BURTON ROW	B
14	CRICKLADE	WS	74	BURNHAM NO1	SS
15	HIGHWORTH REDOWN	WS	75	RODNEY STOKE WATERWORK	SS
16	HIGHWORTH MARSHALL DAV	WS	76	RODNEY STOKE BORING	SS
17	SHIPTON MOYNE	SS	77	KILMERSDON	SS
18	SHIPTON MOYNE	GS	78	HEMINGTON	SS
19	GREAT SHERTON	GS	79	FAULKLAND	I
20	RODBOURNE CHENEY	WS	80	MELLS	SS
21	SWINDON RODBOURNE LANE	WS	81	BUCKLAND DENHAM	SS
22	SWINDON G.W.R.	WS	82	ORCHARD LEIGH	GS
23	LYDIARD TREGOZE	WS	83	STAPLEMEAD MILLS	SS
24	WOTTON BASSET	WS	84	RODE	SS
25	FAULKLAND	GS	85	BECKINGTON SEYMOURS	SS
26	SEAGARY	WS	86	WESTBURY	WS
27	WROUGHTON	WS	87	UPTON SCUDAMORE G.W.R.	WS
28	BROAD HINTON	WS	88	UPTON SCUDAMORE TROW.	WS
29	OGBOURNE ST GEORGE	WS	89	TILSHEAD	WS
30	BAYDON	WS	90	HUNTSPILL	SS
31	WRAXALL	SS	91	WELLS EASTON	SS
32	PITMINSTER	SS	92	FROME GIBBET HILL	I
33	COLERNE	WS	93	FROME	SS
34	CHIPPENHAM	WS	94	CATCOTT	SS
35	CALNE	WS	95	PILTON	SS
36	MARLBOROUGH	WS	96	SHEPTON MALLET BREWERY	SS
37	CHARLOMBE	SS	97	WITHAM FRIARY	SS
38	BATH LANDSDOWN	SS	98	CORSLEY	WS
39	BATH BREWERY	SS	99	WESTBURY	D
40	BATH PINCHES WELL	SS	100	CODFORD ST PETER	I
41	BATHAMPTON DOWN	GS	101	SHREWTON 1	D
42	YATTON	SS	102	SELWORTHY 2	I
43	NORRINGTON	I	103	PURITON	U
44	BISHOP CANNINGS	WS	104	SWANG FARM 2	I
45	HORSECOMBE VALE 15	I	105	SHAPWICK	SS
46	STAVERTON	WS	106	STREET	SS
47	MELKSHAM SPA	WS	107	COMPTON DUNDON	SS
48	DEVIZES	WS	108	MAIDEN BRADLEY	WS
49	OARE	WS	109	BRIXTON DEVERILL	WS
50	PEASEY	WS	110	CODFORD ST PETER	WS
51	BURBAGE	WS	111	YARBURY CASTLE	*
52	HAM NO1	V	112	AMESBURY	WS
53	BUTTERMERE	WS	113	BARTON STACY	B
54	KINGSCLERE NO1	F	114	WIVELISCOMBE	SS
55	CHURCHILL	SS	115	TAUNTON	SS
56	CHEDDAR WOOD	SS	116	LANGPORT	SS
57	HARPTREE	SS	117	SOMERTON	SS
58	DUNKERTON	SS	118	KEINTON MANDEVILLE	SS
59	COMBE HAY	GS	119	EAST LYDFORD	SS
60	TWINHOE	GS	120	BRUTON 1	I

Western Wessex Basin borehole list
of II.A.1.

121	MERE	WS	175	YEOVIL WORKHOUSE	SS
122	EAST KNOYLE SUTTON	WS	176	YEOVIL IVELHAP LTD	SS
123	EAST KNOYLE WINDMILL	WS	177	YEOVIL WESTERN COUNTIE	SS
124	TISBURY	WS	178	YEOVIL GAS WORKS	SS
125	DINTON	WS	179	YEOVIL BWENS	SS
126	FOVANT WOOD	WS	180	THORNFORD	GS
127	BARFORD ST MARTIN	WS	181	SHERBOURNE WATERWORKS	DS
128	SAILSBURY	WS	182	OBORNE	GS
129	FARLEY SOUTH 1	S	183	MILBOURNE PORT	SS
130	LOCKERLEY 1	S	184	STOWELL	SS
131	WINCHESTER 4	I	185	BISHOPS CAUNDLE	DS
132	WINCHESTER 1	I	186	ABBAS TEMPLECOMBE	SS
133	WINCHESTER 5	I	187	HENSTRIDGE	SS
134	WINCHESTER 3	I	188	HENSTRIDGE BHA + BHB	DS
135	WINCHESTER 2	I	189	STALBRIDGE	DS
135A	UPHAM	H	190	LONG BURTON	DS
136	PITMINSTER	GS	191	HOLWELL	DS
137	ISLE ABBOTS	SS	192	LYDINCH	DS
138	CURRY RIVEL (HAMBRIDGE)	SS	193	STURMINSTER NEWTON	DS
139	LONG LOAD	SS	194	IWERNE COURTNEY	DS
140	ASH	SS	195	DURWESTON	DS
141	CHITHORNE DOMER	SS	196	BLANDFORD	DS
142	WEST CAMEL	SS	197	CRANBORNE 1	R
143	WESTON BANFYLD	SS	198	WOODLANDS	B
144	RIMPTON	SS	199	CLUMPHILL	B
145	BLACKFORD	SS	200	FORDINGBRIDGE 1	R
146	WINCANTON SUDDON GRAN.	SS	201	CADHAM	B
147	WINCANTON	SS	202	BUNKERS HILL	I
148	WYKE BREWERY	I	203	SOUTHAMPTON 1	I
149	SHAFTSBURY WATERWORKS	DS	203A	SOUTHAMPTON COMMON	H
150	DONHEAD ST MARY	WS	204	MARCHWOOD 1	I
151	DONHEAD ST ANDREW	WS	204A	SWANWICK	H
152	BOWER CHALKE	WS	205	RAMNOR PARKHILL	B
153	DOWNTON	WS	205A	DIBDEN	H
154	HOE 1	*	206	PORTSDOWN 2	I
154A	EASTLEIGH	H	206A	WICKHAM	H
155	HORNDEN	*	207	PORTSDOWN 1	I
156	MIDDLETON 1	D	207A	HAVANT	H
156A	BOSHAM	H	207B	PORTSMOUTH BREWERY	H
156B	CHICHESTER BREWERY	H	207C	PORTSMOUTH DOCKYARD	H
156C	CHICHESTER MENTAL HOS.	H	207D	HAYLING ISLAND	H
156D	CHICHESTER GATE HOUSE	H	208	WEST COWES	B
157	COMBE ST NICHOLAS	SS	209	SANDHILLS 1	*
158	ILMINSTER	SS	209A	NEWPORT	H
159	WHITE LACKINGTON	SS	210	ARRETON 1	F
160	SOUTH PETHERTON WATER.	SS	210A	BEMBRIDGE	H
161	SOUTH PETHERTON MANOR	SS	211	ARRETON 2	D
162	MERRIOT	SS	211A	BEMBRIDGE HOTEL	H
163	STOKE SUB HAMBDON COM.	SS	212	CHARD SNOWDON HILL	SS
164	MARTOCK	SS	213	CHARD MINTONS LANE	SS
165	STOKE SUB HAMBDON SITE	SS	214	CHARD WITHOUT SUNNY.SD	SS
166	STOKE SUB HAMSDON HED.	SS	215	CHARMINSTER	U
167	NORTON SUB HAMBDON	SS	216	CREWKERNE SOUTH STREET	SS
168	WEST OKER	SS	217	SEABOROUGH 1	D
169	PRESTON PLUCKNETT FAC.	SS	218	STOKE ABBOTT	DS
170	HENDFORD HILL BORING	SS	219	CRABBS BARN LANE	DS
171	EAST OKER	SS	220	FROME ST QUINTIN	DS
172	PRESTON PLUCKNETT FURZ	SS	221	CATTISTOCK	DS
173	LONGCROFT BORING	SS	222	MAIDEN NEWTON	DS
174	MUDFORD	SS	223	HILTON LOWER ANSTY	DS

224	SHAPWICK	B	294	STUDLAND	I
225	BUSHEY FARM A12	S	295	STUDLAND SCHOOL	DS
226	WINTERBORNE KINGSTON	I	296	SWANAGE SPRINGHEAD	DS
227	BERE REGIS	D	297	ULWELL	DS
228	CORFE MULLEN	DS	298	ULWELL WATERWORKS	DS
229	BOURNEMOUTH WATERWORKS	DS	299	BH 98/11-2	*
230	CANFORD MAGNA	DS	300	CORFE CASTLE	DS
231	WIMBORNE MINSTER	DS	301	CREECHBARROW	DS
232	BOURNEMOUTH	DS	302	ENCOMBE 1	B
233	LYMINGTON	B	303	KIMMERIDGE 1	B
234	MARSHWOOD	B	304	KIMMERIDGE 3	*
235	UPLYME	DS	305	BROADBENCH NO1	S
236	LYME REGIS	I	306	CHALDON DOWN 2	S
237	LYME REGIS	DS	307	CHALDON DOWN G2	S
238	LYME REGIS	DS	308	CHALDON HERRING 1	S
239	CHARMOUTH	DS	309	CHALDON HERRING G2	S
240	WOOTTON FITZPAINE	DS	310	CHALDON HERRING G3	S
241	CHARMOUTH 5	I	311	OVERMOIGNE	DS
242	NETTLECOMBE	D	312	POXWELL NO2	S
243	COGDEN FARM	DS	313	POXWELL NO3	S
244	COMPTON VALLANCE	DS	314	POXWELL	S
245	COMPTON VALLANCE	DS	315	RINGSTEAD	*
246	LITTLE BREDY	DS	316	LULWORTH BANKS 1	U
247	MANSFIELD SHALE SHAFT	U	317	SOUTHWELL	DS
248	PORTISHAM	I			
249	WADDON 4	I			
250	WADDON	DS			
251	LANGTON HERRING NORTH	I			
252	LANGTON HERRING SOUTH	I			
253	SEABARN FARM	B			
254	CORTON FARM	DS			
255	FRIAR WADDON DAIRY HOU	DS			
256	FRIAR WADDON	DS			
257	DORCHESTER BREWERY	DS			
258	BRYANTS PUDDLE	DS			
259	SPYWAY BORE	DS			
260	WADDOCKS CROSS	*			
261	POOLE GASWORKS	DS			
262	BH 98/11-1	*			
263	GOULDS BOTTOM	DS			
264	RADIPOLE 1	F			
265	LITTLEMOOR	U			
266	WEST ASHTON BINCOMBE	WS			
267	OSMINGTON 2	I			
268	OSMINGTON 1	I			
269	WEST KNIGHTON	GS			
270	WARMEWELL MILL	DS			
271	WOODSFORD AERODROME	DS			
272	WOOL	DS			
273	WORGRET HEATH	DS			
274	WAREHAM 1	*			
275	WAREHAM NO2	S			
276	STOBOROUGH NO1	D			
277	STOBOROUGH 2	S			
278	ARNE 1 + 3	S			
279	WYTCHE FARM B20 + B21	S			
280	WYTCHE FARM 3	D			
281	WYTCHE FARM 1	D			
282	WYTCHE FARM 4	D			
283	WYTCHE FARM 2	D			

KEY

B	BLOOMER 1980
D	D.O.E RELEASE
DS	WELLS AND SPRINGS OF DORSET
F	FALCON & KENT (1960)
GS	WELLS AND SPRINGS OF GLOUCESTER
H	WELLS AND SPRINGS OF HAMPSHIRE
I	B.G.S DATAFILES
O	SHELL CONFIDENTIAL BOREHOLE RELEASE
R	RHYS et al. (1982)
S	SCOTPET LTD, WESSEX BASIN BOREHOLE LIS
SS	WELLS AND SPRINGS OF SOMERSET
U	CONFIDENTIAL SOURCE
WS	WELLS AND SPRINGS OF WILTSHIRE
*	LIMITED OR NO DATA

Wells and springs = Mem. Geol. Surv.G

APPENDIX C

ARNE G1
ELV 26 FT
DOE RELEASE

SY 9575 8704
T.D. 3731 FT

M.Y	DEPTH (FT)
0.0	0.0
89.00	1436.00
91.00	1600.00
97.00	1749.00
113.00	1920.00
119.00	1959.00
163.00	1960.00
169.00	2390.00
175.00	3040.00
188.00	3045.00
194.00	3319.00
200.00	3492.00
213.00	3692.00
219.00	3762.00
238.00	5762.00
248.00	6312.00
258.00	9512.00

ARRETON 2
ELV 125 FT
DOE RELEASE

SZ 5320 8580
T.D. 9227 FT

M.Y	DEPTH (FT)
0.0	0.0
119.00	210.00
150.00	2659.00
156.00	3764.00
169.00	4540.00
175.00	4979.00
188.00	5210.00
194.00	5400.00
213.00	6468.00
219.00	6550.00
238.00	6994.00
258.00	7950.00

ASHDOWN 2
ELV 585 FT
FALCON & KENT 1960

TQ 512 295
T.D. 5630 FT

M.Y	DEPTH (FT)
0.0	0.0
138.00	640.00
150.00	1250.00
156.00	2910.00
169.00	3693.00
175.00	3957.00
188.00	4378.00
194.00	4665.00
200.00	4790.00
213.00	5630.00

BERE REGIS
ELV 227 FT

TERRIS & BULLERWELL 1965

SY 864 956
T.D. 5533 FT

M.Y	DEPTH (FT)
0.0	0.0
89.00	1028.00
91.00	1193.00
97.00	1355.00
113.00	1544.00
169.00	2248.00
175.00	2956.00
188.00	2998.00
194.00	3557.00
200.00	3900.00
213.00	4690.00
219.00	4816.00
238.00	5533.00
258.00	9283.00

BLETCHINGLY
ELV 69 M
BLOOMER 1980

TQ 362 477
T.D. 1910 M

M.Y	DEPTH (M)
0.0	0.0
144.00	338.00
150.00	619.00
156.00	987.00
169.00	1251.00
175.00	1323.00
188.00	1446.00
194.00	1542.00
197.00	1578.00
219.00	1842.00

BOBBING
ELV 120 FT
LAMPLUGH ET. AL. 1923

TQ 89 65
T.D. 1260 FT

M.Y	DEPTH (FT)
0.0	0.0
54.90	1.00
65.00	142.00
91.00	587.00
97.50	822.00
113.00	1000.00
144.00	1036.00
156.00	1037.00
169.00	1108.00
175.00	1190.00

Boreholes used in the backstripping analysis

BOLNEY
ELV 71 M
BLOOMER 1980

TQ 280 243
T.D. 2439 M

M.Y	DEPTH (M)
0.0	0.0
144.00	213.00
150.00	431.00
156.00	986.00
169.00	1172.00
175.00	1268.00
188.00	1418.00
194.00	1521.00
197.00	1682.00
213.00	1884.00
219.00	1898.00

BRABOURNE
ELV 7
STRAHAN ET. AL. 1916

TR 100 308
T.D. 2058 FT

M.Y	DEPTH (FT)
0.0	0.0
113.00	72.00
119.00	302.00
150.00	720.00
156.00	982.00
169.00	1515.00
175.00	1709.00
188.00	1753.00
213.00	1893.00
231.00	1974.00

BRIGHTLING
ELV 459 FT
FALCON & KENT 1960
(FAULT ACCOUNTED FOR)

TQ 685 210
T.D. 1322 FT

M.Y	DEPTH (FT)
0.0	0.0
150.00	474.00
156.00	1610.00
169.00	2314.00
175.00	2543.00
188.00	2845.00
194.00	3100.00
200.00	3213.00
213.00	3733.00

BRISTOL CHANNEL
ELV 0

SS 900 600
T.D. ?

LLOYD ET. AL. 1973
(THICKNESSES POSTULATED)

M.Y	DEPTH (M)
0.0	0.0
156.00	290.00
163.00	610.00
169.00	785.00
188.00	805.00
194.00	895.00
200.00	1065.00
213.00	1485.00
243.00	1760.00

BRUTON 1
ELV 96 M

ST 6896 3284
T.D. 385 M

HOLLOWAY & CHADWICK 1984

M.Y	DEPTH (M)
0.0	0.0
175.00	38.00
188.00	45.00
194.00	111.00
200.00	119.00
213.00	268.00
219.00	285.00
238.00	293.00

BURTON ROW
ELV 50 M

ST 336 521
T.D. 1105 M

EDMUNDS & BURLEY 1977

M.Y	DEPTH (M)
0.0	0.0
200.00	37.00
213.00	405.00
219.00	423.00
238.00	907.00
243.00	954.00
258.00	1200.00

CHANNEL AREA
ELV 0

SY 75 75
T.D. 0

(THICKNESSES POSTULATED)

M.Y	DEPTH (M)
0.0	0.0
97.00	400.00
138.00	1200.00
213.00	2000.00
258.00	3800.00

CLIFFE
ELV 12 FT

TQ 74 76
T.D. 1063 FT

LAMPLUGH ET. AL. 1923

M.Y	DEPTH (FT)
0.0	0.0
88.50	500.00
97.50	733.00
113.00	941.00
119.00	1037.00

COLLENDEAN
ELV 84 M
BLOOMER 1980

TQ 248 443
T.D. 1755 M

M.Y	DEPTH (M)
0.0	0.0
144.00	456.00
150.00	724.00
156.00	1169.00
169.00	1472.00
175.00	1557.00
188.00	1726.00
219.00	2176.00

COOLESFARM
ELV 310 FT
CONFIDENTIAL

SP 04 93
T.D. 11525 FT

M.Y	DEPTH (FT)
0.0	0.0
169.00	100.00
175.00	404.00
188.00	531.00
194.00	975.00
200.00	2000.00
213.00	2015.00
219.00	2040.00
238.00	3372.00
248.00	3952.00

COWDEN 1
ELV 410 FT
DOE RELEASE

TQ 467 428
T.D. 6036 FT

M.Y	DEPTH (FT)
0.0	0.0
138.00	950.00
150.00	1750.00
156.00	3000.00
169.00	3850.00
188.00	4400.00
194.00	4700.00
200.00	4800.00
213.00	5400.00
219.00	5420.00

CRANBOURNE 1
ELV 60 M
DOE RELEASE

SU 03408 07073
T.D. 2041 M

M.Y	DEPTH (M)
0.0	0.0
89.00	249.00
91.00	304.00
97.00	371.00
113.00	445.00
156.00	491.00
169.00	697.00
175.00	844.00
188.00	892.00
194.00	959.00
200.00	1020.00
213.00	1162.00
243.00	1593.00

DEVIZES
ELV 190 FT
DOE RELEASE

ST 96026 56987
T.D. 3506 FT

M.Y	DEPTH (FT)
0.0	0.0
175.00	1000.00
188.00	1216.00
194.00	1448.00
200.00	1626.00
213.00	2182.00
243.00	3104.00

ELHAM
ELV 275 FT
LAMPLUGH ET. AL. 1923

TR 18 44
T.D. 1598 FT

M.Y	DEPTH (FT)
0.0	0.0
97.50	290.00
113.00	406.00
144.00	719.00
150.00	720.00
156.00	918.00
169.00	1300.00
175.00	1491.00
188.00	1499.00
194.00	1540.00
197.00	1560.00
213.00	1598.00

FARINGDON 1
ELV 298 FT
FALCON & KENT 1960

SU 324 947
T.D. 3131 FT

M.Y	DEPTH (FT)
0.0	0.0
169.00	565.00
175.00	745.00
188.00	810.00
194.00	885.00
200.00	935.00
213.00	1465.00
219.00	1525.00
238.00	2150.00

FARLEY SOUTH
ELV 214 FT
SHELL CONFIDENTIAL

SU 2358 2852
T.D. 5510 FT

M.Y	DEPTH (FT)
0.0	0.0
73.00	115.00
97.00	1438.00
113.00	1752.00
119.00	1810.00
150.00	2065.00
156.00	2672.00
169.00	3376.00
175.00	3746.00
188.00	3883.00
213.00	4723.00
219.00	4774.00
238.00	5510.00

FOLKESTONE
ELV 113 FT
LAMPLUGH ET. AL. 1923

TR 23 37
T.D. 1487 FT

M.Y	DEPTH (FT)
0.0	0.0
119.00	335.00
144.00	553.00
145.00	554.00
156.00	763.00
163.00	1375.00
188.00	1376.00
194.00	1430.00
197.00	1447.00
213.00	1487.00

FORDINGBRIDGE
ELV 229 FT
FALCON & KENT 1960

SU 1876 1180
T.D. 4487 FT

M.Y	DEPTH (FT)
0.0	0.0
56.00	678.00
73.00	679.00
89.00	1600.00
91.00	1775.00
97.00	1997.00
113.00	2251.00
156.00	2461.00
169.00	3104.00
175.00	3512.00
188.00	3630.00
200.00	4020.00
213.00	4317.00
219.00	4379.00
248.00	5037.00

FORDON 1
ELV ?
DOE RELEASE

TA 05 75
T.D. 7559 FT

M.Y	DEPTH (FT)
0.0	0.0
113.00	89.00
138.00	535.00
156.00	1815.00
169.00	2059.00
188.00	2252.00
194.00	2340.00
198.00	2366.00
219.00	2810.00
238.00	3138.00
248.00	4743.00
258.00	6610.00

HARMANSOLE
ELV 200 FT
LAMPLUGH ET. AL. 1923

TR 14 52
T.D. 1730 FT

M.Y	DEPTH (FT)
0.0	0.0
97.50	561.00
113.00	741.00
144.00	814.00
156.00	815.00
169.00	1137.00
175.00	1231.00
194.00	1232.00
197.00	1246.00
213.00	1249.00

HENFIELD
ELV 36 FT
FALCON & KENT 1960

TQ 182 151
T.D. 5105 FT

M.Y	DEPTH (FT)
0.0	0.0
138.00	1080.00
150.00	1538.00
156.00	2620.00
169.00	3480.00
175.00	3818.00
188.00	4193.00
194.00	4388.00
200.00	4500.00
213.00	4890.00

HERNE
ELV 95 FT
LAMPLUGH ET. AL. 1923

TR 18 67
T.D. 1187 FT

M.Y	DEPTH (FT)
0.0	0.0
65.00	206.00
97.50	828.00
113.00	1088.00

HIGHWORTH
ELV 352 FT
DOE RELEASE

SU 18314 91528
T.D. 3820 FT

M.Y	DEPTH (FT)
0.0	0.0
169.00	502.00
188.00	805.00
194.00	1022.00
200.00	1695.00
213.00	1916.00
219.00	2020.00
225.00	2390.00
238.00	3070.00
243.00	3493.00

IRISH SEA
ELV 0
COLTER & BARR 1975

SD 10 10
T.D. 2990 M

M.Y	DEPTH (M)
0.0	0.0
243.00	940.00
258.00	2710.00
286.00	2990.00

KEMPSEY 1
ELV 86 FT
DOE RELEASE

SO 86090 49334
T.D. 9794 FT

M.Y	DEPTH (FT)
0.0	0.0
238.00	1297.00
243.00	3851.00
258.00	4398.00
286.00	7476.00

KINGSCLERE
ELV 538 FT
FALCON & KENT 1960

SU 499 589
T.D. 5125 FT

M.Y	DEPTH (FT)
0.0	0.0
113.00	395.00
138.00	1020.00
150.00	1720.00
156.00	2641.00
169.00	3190.00
175.00	3440.00
188.00	3800.00
194.00	3940.00
200.00	4225.00
213.00	4970.00
219.00	5060.00
243.00	5560.00

LARNE
ELV ?
NAYLOR & SHANNON 1982

NW 54 57
T.D. 1283 M

M.Y	DEPTH (M)
0.0	0.0
213.00	88.00
219.00	108.00
238.00	1075.00
248.00	3000.00

LOCKERLEY
ELV 118 FT
SHELL CONFIDENTIAL

SU 3067 2591
T.D. 6725 FT

M.Y	DEPTH (FT)
0.0	0.0
91.00	1106.00
97.00	1353.00
113.00	1647.00
138.00	1762.00
150.00	2072.00
156.00	2684.00
169.00	3400.00
175.00	3778.00
188.00	3991.00
194.00	4386.00
213.00	5374.00
219.00	5435.00
243.00	6725.00

LYDDEN VALLEY
ELV 11 FT
LAMPLUGH ET. AL. 1923

TR 37 53
T.D. 2027 FT

M.Y	DEPTH (FT)
0.0	0.0
97.50	770.00
113.00	850.00
119.00	922.00
144.00	939.00

MAGILLIGAN
ELV ?
NAYLOR & SHANNON 1982

NV 90 96
T.D. 1346 M

M.Y	DEPTH (M)
0.0	0.0
65.00	111.00
213.00	201.00
219.00	208.00
238.00	580.00
286.00	976.00

MALTON 1
ELV 7
DOE RELEASE

SE 75516 76394
T.D. 6258 FT

MIDDLETON 1
ELV 8 FT
DOE RELEASE

SU 9739 0150
T.D. 6982 FT

M.Y	DEPTH (FT)
0.0	0.0
150.00	52.00
156.00	147.00
169.00	718.00
188.00	1106.00
213.00	2059.00
219.00	2093.00
238.00	2714.00
248.00	3935.00
258.00	5052.00
286.00	5084.00

MARCHWOOD
ELV 28 FT
DOE RELEASE

SU 3991 1118
T.D. 8580 FT

M.Y	DEPTH (FT)
0.0	0.0
89.00	600.00
91.00	820.00
97.00	1119.00
113.00	1392.00
119.00	1514.00
138.00	1652.00
150.00	1940.00
156.00	2683.00
175.00	3530.00
188.00	3712.00
194.00	4027.00
200.00	4228.00
219.00	4304.00
258.00	5271.00

M.Y	DEPTH (FT)
0.0	0.0
54.00	642.00
56.00	722.00
89.00	1566.00
91.00	1731.00
97.00	1986.00
113.00	2212.00
156.00	2634.00
169.00	3289.00
175.00	3657.00
188.00	3748.00
194.00	4110.00
200.00	4249.00
213.00	4724.00
219.00	4842.00
238.00	5439.00
248.00	5632.00

MARSHWOOD
ELV 318 FT
DOE RELEASE

SY 3885 9880
T.D. 6229 FT

M.Y	DEPTH (FT)
0.0	0.0
213.00	417.00
219.00	456.00
238.00	1155.00
248.00	3193.00
258.00	3315.00
286.00	4396.00

MOCHRAS

ELV 0
BARR ET. AL. 1981

SH 55 26
T.D. 1939 M

M.Y	DEPTH (M)
0.0	0.0
24.60	601.00
194.00	863.00
200.00	1240.00
206.00	1768.00
213.00	1908.00
248.00	2108.00

N. CELTIC SEA AREA

ELV 0
NAYLOR & SHANNON 1982
(FROM SEISMIC RELECTION DATA)

51° 10' N
08° 33' W
T.D. 5400 M

M.Y	DEPTH (M)
0.0	0.0
97.50	1400.00
125.00	1700.00
131.00	2150.00
144.00	2300.00
150.00	3000.00
163.00	3400.00
188.00	3900.00
213.00	4650.00
248.00	5400.00

NETTLECOMBE
ELV 371 FT
DOE RELEASE

SY 5053 9543
TD 7005 FT

M.Y	DEPTH (FT)
0.0	0.0
188.00	22.00
194.00	353.00
200.00	806.00
213.00	1568.00
219.00	1648.00
243.00	3808.00
258.00	6267.00

PORTMORE NR 25 02
ELV ? T.D. 1864 M
 NAYLOR & SHANNON 1982

M.Y	DEPTH (M)
0.0	0.0
65.00	77.00
97.50	168.00
213.00	438.00
219.00	442.00
238.00	1095.00
248.00	1574.00
286.00	2400.00

PORTSDOWN 2 SU 638 078
ELV 225 FT T.D. 6556 F
 FALCON & KENT 1960

M.Y	DEPTH (FT)
0.0	0.0
89.00	520.00
91.00	730.00
97.00	1070.00
113.00	1358.00
119.00	1450.00
138.00	2275.00
150.00	2566.00
156.00	3668.00
169.00	4270.00
175.00	4717.00
194.00	5386.00
200.00	5672.00
213.00	6474.00
219.00	6540.00
248.00	7461.00

PREES 1 SJ 55 34
ELV ? T.D. ?
 COLTER & BARR 1975

M.Y	DEPTH (M)
0.0	0.0
213.00	600.00
219.00	630.00
231.00	1510.00
243.00	1760.00
248.00	2600.00
258.00	2752.00
286.00	3250.00

PURITON ST 319 409
ELV ? T.D. 2000 FT
 RICHARDSON 1928

M.Y	DEPTH (FT)
0.0	0.0
231.00	695.00
248.00	1465.00
286.00	2047.00

RINGSTEAD AREA SY 76 82
ELV 0 T.D. ?
 (THICKNESSES POSTULATED)

M.Y	DEPTH (M)
0.0	0.0
97.00	400.00
119.00	437.00
138.00	503.00
150.00	593.00
156.00	843.00
169.00	1159.00
175.00	1262.00
188.00	1266.00
194.00	1419.00
200.00	1560.00
213.00	1760.00
219.00	1786.00
258.00	2980.00

SEABOROUGH ST 4348 0620
ELV 108 M T.D. 1555 M
 CONFIDENTIAL

M.Y	DEPTH (M)
0.0	0.0
188.00	19.00
194.00	138.00
200.00	255.00
213.00	465.00
219.00	490.00
243.00	966.00
258.00	1555.00

SELWORTHY 2 SS 9244 4618
ELV 118 M T.D. 60 M
 I.G.S.

M.Y	DEPTH (M)
0.0	0.0
213.00	25.00
219.00	51.00
238.00	60.00

SHALFORD 1
ELV 49 M
FALCON & KENT 1960

SU 985 475
T.D. 1742 M

M.Y	DEPTH (M)
0.0	0.0
144.00	673.00
150.00	874.00
156.00	1255.00
169.00	1389.00
175.00	1514.00
188.00	1584.00
213.00	1615.00
219.00	1636.00

SONNINGEYE
ELV 134 FT
DOE RELEASE

SU 742 759
T.D. 2862 FT

M.Y	DEPTH (FT)
0.0	0.0
97.00	578.00
113.00	1070.00
119.00	1089.00
160.00	1104.00
169.00	1250.00
175.00	1270.00
188.00	1356.00

SHERBOURNE 1
ELV 640 FT
CONFIDENTIAL

SP 22 60
T.D. ?

M.Y	DEPTH (FT)
0.0	0.0
188.00	374.00
213.00	747.00
219.00	921.00
243.00	1759.00

SOUTHAMPTON 1
ELV 25 FT
DOE RELEASE

SU 41559 12018
T.D. 5994 FT

M.Y	DEPTH (FT)
0.0	0.0
54.00	489.00
56.00	573.00
89.00	1420.00
91.00	1596.00
97.00	1863.00
113.00	2091.00
119.00	2115.00
150.00	2275.00
156.00	2720.00
169.00	3403.00
175.00	3771.00
188.00	3884.00
194.00	4221.00
200.00	4396.00
213.00	4951.00
219.00	5018.00
238.00	5674.00
248.00	5894.00

SHREWTON
ELV 468 FT
DOE RELEASE

SU 03137 41989
T.D. 9824 FT

M.Y	DEPTH (FT)
0.0	0.0
89.00	203.00
91.00	369.00
97.00	530.00
113.00	903.00
150.00	1182.00
156.00	2080.00
169.00	2870.00
175.00	3462.00
188.00	3534.00
194.00	3921.00
200.00	4411.00
213.00	4946.00
219.00	5000.00
243.00	5489.00
258.00	5810.00

SOLE PIT BASIN 48/76-4

ELV 0 FT T.D. ?
GLENNIE & BOEGNER 1981

M.Y	DEPTH (FT)
0.0	0.0
65.00	1.00
144.00	3900.00
213.00	8800.00
248.00	13500.00
286.00	16000.00

SOLWAY BASIN
ELV 0
COLTER & BARR 1975

NY 10 60
T.D. 0

M.Y	DEPTH (M)
0.0	0.0
213.00	20.00
219.00	50.00
243.00	370.00
258.00	1115.00
286.00	1415.00

STOBOROUGH 1
ELV 36 FT
DOE RELEASE

SY 9126 8659
T.D. 4035 FT

M.Y	DEPTH (FT)
0.0	0.0
54.00	305.00
56.00	368.00
89.00	1269.00
91.00	1512.00
97.00	1652.00
113.00	1810.00
119.00	1818.00
169.00	2424.00
175.00	3072.00
188.00	3080.00
194.00	3374.00
200.00	3718.00
213.00	3918.00
219.00	3988.00
238.00	5187.00
248.00	5737.00
258.00	8937.00

STRAT A1
ELV 42 M
BLOOMER 1980

SU 948 528
T.D. 963 M

M.Y	DEPTH (M)
0.0	0.0
65.00	172.00
97.50	436.00
113.00	543.00
119.00	570.00
150.00	676.00
156.00	739.00
169.00	802.00
175.00	833.00
181.00	857.00
213.00	882.00

TATSFIELD 1
ELV 180 M
EDMUNDS & BURLEY 1977

TQ 41 57
T.D. 1405 M

M.Y	DEPTH (M)
0.0	0.0
144.00	650.00
188.00	1150.00
213.00	1323.00

WAREHAM 1
ELV ?
CONFIDENTIAL

SY 908 874
T.D. ?

M.Y	DEPTH (FT)
0.0	0.0
73.00	100.00
97.00	1600.00
163.00	1800.00
188.00	2700.00
219.00	5400.00
258.00	5775.00

WAREHAM 3
ELV 75 FT
DOE RELEASE

SY 9059 8721
T.D. 3599 FT

M.Y	DEPTH (FT)
0.0	0.0
54.00	348.00
56.00	416.00
89.00	1319.00
91.00	1564.00
97.00	1702.00
113.00	1866.00
119.00	1886.00
156.00	1991.00
175.00	2789.00
188.00	2796.00
194.00	3089.00
200.00	3453.00
213.00	3653.00
219.00	3703.00
238.00	5703.00
248.00	6253.00
258.00	9453.00

WARLINGHAM
ELV 346 FT
WORSSAM & IVIMEY-COOK 1971

TQ 3476 5719
T.D. 5001 FT

M.Y	DEPTH (FT)
0.0	0.0
91.00	188.00
97.00	395.00
113.00	739.00
119.00	1047.00
138.00	1889.00
150.00	2275.00
156.00	2987.00
163.00	3330.00
169.00	3483.00
175.00	3679.00
181.00	3694.00
188.00	3839.00
194.00	4018.00
200.00	4177.00
213.00	4498.00
219.00	4501.00

WESTBURY
ELV 200 FT
PRINGLE 1922

ST 872 429
T.D. 1948 FT

M.Y	DEPTH (FT)
0.0	0.0
156.00	396.00
169.00	695.00
175.00	993.00
188.00	1122.00
213.00	1297.00
219.00	1341.00
238.00	4297.00

WESTHAM 1
ELV 30 FT
BLOOMER 1980

TQ 6097 0535
T.D. 5213 FT

M.Y	DEPTH (FT)
0.0	0.0
138.00	540.00
150.00	850.00
156.00	1385.00
169.00	1790.00
175.00	2100.00
188.00	2250.00
194.00	2420.00
200.00	2485.00
213.00	2905.00
219.00	2910.00

WEYMOUTH BAY
ELV 0

SY 75 75
T.D. 0

(THICKNESSES POSTULATED)

M.Y	DEPTH (M)
0.0	0.0
73.00	1.00
89.00	297.00
91.00	363.00
97.00	408.00
113.00	460.00
119.00	706.00
138.00	1121.00
150.00	1253.00
156.00	1761.00
169.00	2121.00
175.00	2486.00
188.00	2490.00
194.00	2644.00
200.00	2786.00
213.00	3036.00
219.00	3071.00
243.00	3436.00
258.00	3590.00
286.00	4505.00

WILLESDEN 1
ELV 60 M
BLOOMER 1980

TQ 21 83
T.D. 817 M

M.Y	DEPTH (M)
0.0	0.0
54.90	42.00
65.00	60.00
88.50	113.00
91.00	183.00
97.50	243.00
113.00	308.00

WINTERBOURNE KINGSTON
ELV 61 M
DOE RELEASE

SY 8470 9796
T.D. 3043 M

M.Y	DEPTH (M)
0.0	0.0
97.00	287.00
113.00	345.00
119.00	349.00
156.00	397.00
169.00	679.00
175.00	906.00
188.00	927.00
194.00	1114.00
213.00	1574.00
219.00	1602.00
245.00	2467.00
258.00	3500.00

WYTFARM 1-4
ELV 9 M
DOE RELEASE

SY 980 853
T.D. 1141 M

M.Y	DEPTH (M)
0.0	0.0
54.00	125.00
73.00	142.00
89.00	456.00
91.00	511.00
97.00	555.00
113.00	612.00
169.00	764.00
175.00	891.00
188.00	893.00
194.00	1040.00
200.00	1147.00
213.00	1179.00
219.00	1200.00
238.00	1815.00
258.00	2968.00

WYCHFARM D5
ELV 33 FT
DOE RELEASE

SY 9956 8552
T.D. 9020 FT

M.Y	DEPTH (FT)
0.0	0.0
54.00	424.00
56.00	477.00
89.00	1500.00
91.00	1694.00
97.00	1840.00
113.00	2028.00
169.00	2426.00
175.00	2994.00
188.00	2998.00
194.00	3342.00
200.00	3614.00
213.00	3960.00
219.00	4028.00
243.00	5667.00
258.00	8600.00

SELECTED BOREHOLES FROM UNITED KINGDOM
CONTINENTAL SHELF AND ONSHORE
USED IN BACKSTRIPPING.

BRISTOL CHANNEL 102/28-1
ELV 0 T.D. 8389 FT
KAMERLING 1979

M.Y	DEPTH (FT)
0.0	0.0
65.00	630.00
97.50	1775.00
119.00	1875.00
213.00	3832.00
219.00	4110.00
248.00	7965.00

CARDIGAN BAY 103/2-1
ELV 0 T.D. 3146 M
BARR ET. AL. 1981

M.Y	DEPTH (M)
0.0	0.0
24.60	215.00
175.00	410.00
181.00	530.00
200.00	580.00
213.00	950.00
219.00	970.00
223.00	1400.00
231.00	2700.00
248.00	2965.00

CARDIGAN BAY 106/24-1 (INC 106/28-1)
ELV 0 T.D. 2775 M
BARR ET. AL. 1981

M.Y	DEPTH (M)
0.0	0.0
24.60	730.00
150.00	1170.00
156.00	1715.00
163.00	2000.00
169.00	2230.00
175.00	2545.00
181.00	2845.00
213.00	3345.00
219.00	3400.00
231.00	4880.00
248.00	5130.00

FASNET BASIN 55/30-1
ELV 0 T.D. 2800 M
ROBINSON ET. AL. 1981

M.Y	DEPTH (M)
0.0	0.0
65.00	850.00
113.00	1090.00
144.00	1290.00
206.00	1900.00
213.00	2210.00
248.00	2800.00

W. APPROACHES 83/24-1 49° 10' 35.1" N
08° 20' 34.3" W
ELV 0 T.D. 1044 M
CONFIDENTIAL

M.Y	DEPTH (M)
0.0	0.0
11.30	249.00
54.90	406.00
65.00	431.00
83.00	540.00
88.50	657.00
91.00	720.00
97.50	806.00
113.00	853.00
213.00	854.00
286.00	904.00

CHANNEL BASIN 98/22-1 50° 14' 39" N
01° 39' 22" W
ELV 0 T.D. 2384 FT
CONFIDENTIAL

M.Y	DEPTH (FT)
0.0	0.0
169.00	508.00
175.00	1334.00
188.00	1413.00
194.00	1657.00
197.00	1737.00
213.00	2297.00
219.00	2384.00
248.00	2689.00

ERA	SUB-ERA	EPOCH	AGE	M A AGE	LITHOSTRATIGRAPHIC FORMATIONS	
CENOZOIC	QUATERNARY					
	NEOGENE	PLIOCENE		2.0		
		MIOCENE		5.1		
		OLIGOCENE		24.6		
	PALAEO- GENE	EOCENE		38.0	Hamstead Beds	
		PALAEOCENE		54.6	Bembridge, Solent, Barton, Bracklesham Groups and London Clay	
				65.0	Reading Beds	
	UPPER CRETACEOUS	SENONIAN	Maastrichtian	73.0	Upper Chalk	
			Campanian	83.0		
			Santonian	87.5		
			Coniacian	88.5		
	LOWER CRETACEOUS		Turonian	91.0	Middle Chalk	
			Cenomanian	97.5	Lower Chalk	
			Albian	113.0	Upper Greensand and Gault	
			Aptian	119.0	Lower Greensand	
			Barremian	125.0	Wealden	
		NEOCOMIAN	Hauterivian	131.0		
			Valanginian	138.0		
			Berriasian	144.0		
		JURASSIC	MALM	Tithonian	150.0	Purbeck Beds
				Kimmeridgian	156.0	Portland Group Kimmeridge Clay
Oxfordian				163.0	Corallian Beds Oxford Clay and Kellaways Beds	
Callovian				169.0	Great Oolite Series	
DOGGER	Bathonian		175.0	Inferior Oolite		
	Bajocian		181.0			
	Aalenian		188.0			
	LIAS		Toarcian	194.0	Upper Lias	
Piensbachian			200.0	Middle Lias		
Sinemurian			206.0	Lower Lias		
Hettangian			213.0			
Rhaetian			219.0		Rhaetic	
UPPER			Norian	225.0	Upper Keuper	
			Carnian	231.0		
	MIDDLE		Ladinian	238.0	Lower Keuper (Keuper Marl, Waterstones) Upper Bunter (Bunter s/st, L. Keuper s/st)	
Anisian		243.0				
SCYTHIAN	Spathian		Lower and Middle Bunter (Budleigh Salterton Pebble Beds and Aylesbeare Group in part)			
	Smithian					
	Dienerian					
	Griesbachian					
PERMIAN	LATE	Tatarian	248.0	(Aylesbeare Group in part local sands, mudstones and breccias)		
		Kazanian	253.0			
		Ufimian	258.0			
		Kungurian	263.0			
		Artinskian	268.0			
		Sakmarian				
	EARLY	Asselian	286.0			
			BASEMENT			

APPENDIX D

APPENDIX D

B. Remote Sensing Techniques

Introduction

Remote sensing is generally restricted to methods that employ reflected or omitted electromagnetic energy as a means of detecting, measuring and interpreting phenomena from afar (Goetz & Rowan 1981).

Historically the technique was based on aerial photography which had the advantage of high spatial resolution and stereo capability in the visible portion of the electromagnetic spectrum. In southern England panchromatic stereopairs were obtained for small areas to test their viability in recording fractures, bedding traces, lithological variations and vegetation patterns which may reflect the same phenomena. However, the results from a photogeological interpretation of the available aerial photos did not extend the structural information much beyond the knowledge gained by the Geological Survey over the past 100 years.

This prevented the areal extent and relative importance of various linear features with respect to basement reactivation could not be resolved without a wider more expansive areal coverage. The absence of publically accessible air photo coverage at comparable scales for large areas of southern England made the use of air photographs inappropriate.

Satellite remote sensing only really began with the launch of Landsat 1 in 1972. This system provided the geologist with multispectral data of the Earth's surface at small scales but with the advantage of a large synoptic coverage (34,000 sq km). Multispectral data were recorded for four bands using a multispectral scanner (MSS). The MSS acquired radiance data for the green and red parts of the visible

spectrum, and for two bands in the near infrared, of ground elements covering wavelengths 0.5 - 1.1 μm . The initial success of the MSS data led to the deployment of the system on Landsats 2 and 3. However, recognition of the inherent limitations of the MSS system particularly in terms of its spatial resolution and spectral coverage resulted in the development and deployment of a derivative known as the Thematic Mapper (TM) the system was deployed on Landsats 4 and 5. In contrast to the MSS, the TM has spectral bands of Band 5 1.55 - 1.75 μm and Band 7 at 2.08 - 2.35 μm (Goetz et al., 1983) and a spatial resolution of TM 40 metres pixel scale compared to the 80 metre pixel scale of the MSS data.

In addition to the analysis of imaging from the Landsat Series of satellites, the opportunity was presented to examine data from Seasat SAR (Synthetic Aperture Radar) data optically processed imaging at approximately 1:100, 000 scale and at 1:500, 000 scale (Seasat 1 Radar Mosaic, (sheets 3 & 4)) constructed by Huntings Surveys Ltd. Radar imaging/data as distinct from information acquired in the visible and near infrared, can be recorded in the presence of cloud, and from any predefined look direction. This has the advantage of removing the illumination biased of Landsat MSS and TM data sets. The results of these analyses in southern England are more fully summarized in Lake et al., 1984, and Dixon et al., 1985, however, a brief summary is outlined.

Landsat Interpretation

Landsat images are especially suitable for studying the relationships between landforms and major structural features because of the large synoptic coverage with uniform illumination and the relatively high spatial resolution (80 - 40µm).

Many previous studies which have used Landsat imagery have been concerned with the recognition of unmapped linear features termed lineaments (O'leary et al., 1976). These features comprise aligned regional morphological features such as river valley, ridges and scarps which are presumed to reflect some subsurface phenomena. Some such linear features have been related to faults, joints and fracture zones (eg. Canich & Gold 1976, Boccaletti et al., 1980). Saunders & Hicks (1976) have described lineaments mapped from Landsat MSS data that can be correlated with deeply buried structural features with no apparent surface exposures. Similarly, Vincent & Coupland (1980) identified structurally related lineaments in the Michigan Basin through a glaced drift cover of some 200 m. Thus it was thought feasible that pre Aptian structures under the chalk outcrop which maybe reactivated could show some surface expression in southern England.

A lineament mapping exercise using both Landsat MSS and TM imagery was undertaken in the central southern part of England between London and Bristol, following a more regional study of the MSS imagery in Southern England.

The upper Cretaceous sediment drape which covers most of the survey area, obscures the subsurface pre-Aptian structure evidence. However, the importance of reactivation associated with inversion may have

reactivated these earlier structures and hence be expressed through the upper Cretaceous cover which may or may not be visible on satellite imaging.

This combined with closely spaced borehole data (see Appendix A and Fig. II.A.1.) indicated possible subsurface structural controls of sedimentation, therefore linear orientations and lengths needed to be determined in those areas and to what extent they may be important in the basin kinematics. Lastly, local subsurface information allowed direct comparison with the lineament interpretation, further delineating the importance of various trends. In addition the subsurface structure in the area was generally poorly understood with most interpretations held commercial in confidence by exploration companies.

The regional study distinguished both linear and curvilinear features in the basement and the overlying Mesozoic sedimentary cover and indicated a lateral continuity of lineaments between the two. The spacing of these lineaments and their orientations between the two areas indicated basement reactivation.

The central portion of the basin was chosen for a more detailed study both to examine trends and frequencies but in addition to delineate its possible use as an exploration tool in southern England where most successful discoveries have been encountered to date.

A large body of geological and geophysical information was utilized to determine the geological significance of lineaments mapped from MSS, TM and SR data sets.

Lineament mapping was undertaken using two data sets at 1:250,000 scale comprising a Landsat MSS Band 7 image (path 218, row 24) and a TM Band 5 image (path 202, row 24). Both images were acquired covering a winter period, where low sun angles rendered interpretation of lineaments significantly easier. This accords with the findings of Larson (1982) among others. The final maps were screened to remove lineaments related to cultural features such as railways and roads. Two lineament types were identified: 1) Clear lineaments, which were defined as those clearly expressed in the imagery by distinct tonal discontinuities; and 2) Subtle lineaments, which were expressed on the image by diffuse tonal boundaries. The two images differed not only in respect of resolution, but also because the MSS scene was recorded when a snow cover lay on the ground, whereas no such cover was present at the time of TM data acquisition. The two lineament maps derived from each image are presented in figures 1, 2, II.A.2 and II.A.3. Length, orientation and frequencies were subsequently extracted from these maps and summarised in Figures 3 & 4. The MSS data revealed dominant lineament trends running NNE-SSW and E-W. Similar trends were also identified from the interpretation of the TM image.

Orientations

Many of the lineament orientations discussed below can be structures both individually and regionally. Where evidence exists, age of structures and rejuvenation and the effects of such structures on sedimentation will be summarised. Lineament orientations are discussed in order of significance, with the most prominent trend examined first.

4.1 ESE-WNW & E-W Trending Lineaments

These trends are orientated parallel with the main Variscan grain seen in the Variscan basement of SW England. This trend is dominated by faults, folds, thrusts, bedding and cleavage, so clearly developed in the basement during the Variscan Orogeny. There is also evidence of strike-slip movement along these orientations. Kellaway and Hancock (1983) gave evidence for sinistral strike-slip movements along this trend by correlating the Malvern magnetic anomaly with the Great magnetic anomaly of France and the 110 km offset of the Hercynian 'V' of England and France. Sanderson (1984) conversely summarized evidence for dextral strike-slip movements based on a variety of minor structures observed throughout the Variscan basement. However, within the Wessex basin, structures along this trend developed as listric growth faults, caused by backthrusting along shallow southward dipping Variscan thrusts (Chadwick et al., 1983). Lineaments 1 and 2 on figure 2 correspond to such features. A well documented example of the history of one of these trends lies just south of the study area, the South Dorset-Isle of Wight structural belt (Stoneley, 1982), which may have originally developed as a Variscan thrust, then during the Triassic developed as a growth fault with a downthrow to the north. The belt was then inverted before the Jurassic with a downthrow to the south. During the Jurassic many phases of accelerated subsidence occurred along this belt particularly in the Kimmeridgian. The Ringstead phase (Dewey, 1982) of uplift and folding occurred in pre-Aptian times although largely confined to the north of the belt. A large swell area developed across it in Upper Albian to Upper Cenomanian times (Drummond, 1970), followed by apparent stability until the Maastrichtian when further inversion along the belt confined

subsequent Tertiary sedimentation north of the belt, with the area south of the belt remaining emergent and a localized source area particularly during the Eocene (Plint, 1983). The whole of southern England became emergent by the Miocene when the belt was reactivated as a listric thrust due to northward Alpine compression.

Faults of this trend also form boundaries to the basin and to basement 'high's such as the London platform along lineament 1 (Figs 1 and 2) (Smalley & Westbrook, 1982) and the Portsdown-Paris Plage ridge (Taitt & Kent, 1958) the Regneses Hinge of Sellwood et al., (1985) along lineament 3 (Figs 1 and 2).

4.2 NNE-SSW & NE-SW trending lineaments

These are both Caledonian and late Variscan in age, however some of the late Variscan structures of this trend developed postumously over Caledonian trends. South of the Variscan front fault structures of this trend developed as a conjugate wrench pair to the NW-SE and NNW-SSE faults discussed later, in the late Variscan (Hobson & Sanderson, 1983) and movements along this trend are predominantly sinistral. Bevan (1985a) identified that two dominant lineament trends NNW-SSE and NNE-SSW augmented the mesofracture investigation. The trends were thought to reflect verticle conjugate shears with a σ_1 N-S compression and a σ_3 E-W extension during the Mid Oligocene to Mid Miocene. A later NW-SE trending fracture system truncates these earlier structures, which Bevan & Hancock (in press) related to NW directed Alpine convergence of Miocene to recent age. Lineament 4 (Figs 1 and 2) almost truncates a series of E-W en-echelon antiforms which are possibly related to an E-W basement wrench zone. Lineaments 4 and 5 (Figs 1 and 2) control river valleys,

emphasizing the importance of underlying tectonic control influencing geomorphology. The spacing of longer lineaments of this orientation is constant throughout the basin.

4.3 N trending lineaments

Structures of this orientation are generally interpreted as Pre-Caledonian in age; e.g the Malvern axis. Structures of this trend are generally north of a line from Reading to Bristol via Swindon, the postulated position of the 'Variscan Front' (Shackleton, 1984). However the continuation of such trending structures into the Wessex basin to the south favours a thin-skinned tectonic model for the Variscan Orogeny (Shackleton, 1984), the so called Bath axis (Kellaway & Welch 1948) is supposed to be a classic example of this, however this structure is undoubtedly non-existent (see Chapter 3). North-south Variscan and younger structures developed north of the 'Variscan Front' postumously over the older Malvernoid structures, such as the intra Liassic structures in the Severn valley studied by Whittaker (1972) were thought to be superimposed on N-S basement faults. Similar trending structures nearby were shown by Arkell (1933) to have influenced pre Bathonian sedimentation. Individual lineaments can be correlated to basement faults, such as lineament 11 (Fig. 2) which corresponds to the Batsford/Marlborough fault in the pre Devonian basement (Wills 1978).

4.4 ENE-WSW trending lineaments

Structures of this trend are both Caledonian (Gardiner & Sheridan 1981) and or Variscan reactivation of Cadomian structures (Shackleton 1984). Structures of this trend within the study area clearly are not reactivated basement structures e.g area A (Fig. 2) where no known

presumed basement involved gravity or magnetic anomaly is coincident with this trend.

4.5 NNW-SSE & NW-SE trending lineaments

This orientation developed in the late Variscan (Hobson & Sanderson 1983), was intermittently active throughout the Mesozoic, such as Drummond's (1970) Mid-Sorset swell affecting upper Albian and Cenomanian sedimentation, however was most prominent in the Tertiary, locally causing the development of small pull-apart basins as soon as seen in S.W. England along its trend. This trend developed as the conjugate wrench pair to the NE-SW trending faults with demonstrably dextral strike slip movements along its strike. Although this trend is not clearly seen due to azimuth angle of the sun looking directly down such an orientation, it has a significant underlying control in the development of the Wessex basin (Drummond 1970, Melville & Freshney 1983). Lineaments 6,7,8 (Fig. 2) defined on the TM imagery only, are just such examples, which correspond with Melville & Freshney's (1983) postulated deep basement faults. Lineaments 10 (Fig. 1) and 11 (Fig. 2) correspond to the axial trend of a residual gravity anomaly (Falcon & Tarrant 1951) and to Arkell's (1933) Birdlip axis, which is known to have been intermittently active throughout the Jurassic; this lineament also noticeably dextrally offsets the Shalbourne and Kingsclere Lower Greensand inliers along lineament 1 (Figs 1 and 2). Further west of the study area this orientation dominates gravity and magnetic maps and is clearly related to dextral strike slip faults. A new TM image clearly displays NW-SE faults across the Purbeck-Isle of Wight fault which are shown on figure II.A.3.

Lengths and Frequency

The lengths have been subdivided into four groups (Figs 3 and 4) to show if length plays an important role in relation to certain orientations. The frequency of each group has been summarized in Figures 3 & 4 and Table 1 so that a comparison between the two data sets could be carried out.

A larger number of lineaments at 5km and less were mapped on the MSS image by comparison with that of TM. This was somewhat surprising given the higher spatial resolution in the latter case. This discrepancy can be explained in part by the differences in the nature of cover. The snow in the MSS data enhances very subtle small linear patterns which are lost in the 'noise' of high spatial frequency cover variations seen in the TM image. At larger scales however these variations become less significant in the TM data and the number of lineaments (clear & subtle) increases by comparison with the MSS data. The MSS data shows more subtle lineaments than clear ones at all lengths, whereas the TM data shows more clear lineaments at lower lengths with subtle lineaments dominating lengths more than 5km. Again these differences can be explained in part by the different cover conditions at the time of imaging.

Table 1 summarizes the frequency percentage for both data sets:

TABLE 1
PERCENTAGE FREQUENCY OF LINEAMENTS FOR TM AND MSS AS A
FUNCTION OF LENGTH

LENGTHS	<2.6km	2.6-5km	5.1-10km	>10km	TOTAL
MSS TOTAL	17.5%	16%	11.5%	3%	48%
TM TOTAL	8%	16%	18%	10%	51%

There are only 4% more lineaments defined on the TM data in comparison to the MSS data; this difference could be ignored if the cloud cover on the MSS data is taken into account. Some data sets pick out one orientation in preference to others, for example clear lineaments from the TM data distinguish more E-W lineaments. Subtle lineaments from the TM data with lengths greater than 5km, appear to emphasise some of the deeper N-S Malvernoid basement structures.

Given the differences in land cover conditions between the two image data sets, it has proved very difficult to objectively evaluate the relative merits and/or demerits of TM versus MSS except at a very general level. A more effective comparison awaits the use of imagery for similar sun elevation angles, and comparable land cover conditions.

Conclusion

It has been shown that the lineaments derived from Landsat data can be directly correlated with known geology. Many are directly related to

faults, thrusts, joints, gravity (White, 1948) and magnetic trends (Falcon & Tarrant, 1951). Some lineaments represent the upward propagation of basement features, others (c.f. Chadwick & Kirby, 1982) show no correlation. It has already been discussed that the NW-SE structures play an important role in the development of the basin, however they are poorly represented on the imagery. The reason is primarily due to sun azimuth angle at the time of imaging. In the data examined here the sun looks directly along these features, thereby suppressing their appearance. Those linear features oriented perpendicular to the azimuth angle are preferentially enhanced. The result is a biased data set. Analysis of the Seasat SAR imagery for the area indicates the presence of NW-SE lineaments, indeed the Seasat data showed them to be as prominent as the other major lineaments trends running NE-SW and E-W.

These en-echelon structures may indicate a more deep seated control by the underlying basement. Many faults were reactivated before the Aptian and therefore the lineaments observed in the post Aptian cover may reflect these earlier structures. This can be clearly seen by examining the similarity between the total fault orientations derived from the Portland sheet (Fig. 3) with the total lineament orientations on the TM data (Fig. 4).

Both MSS and TM data provided structurally related information complementary to that acquired by other data collection techniques. However, effective utilization of lineament information provided by the MSS and TM data requires ancillary geological information such as maps, 'field data', and geophysical data, because the significance of many

lineaments cannot be fully appreciated from the imagery alone. Lineaments trends and patterns can only be used to infer new geological associations when their relationships to known geological features have been established. Therefore some major basement trends are expressed through the upper Cretaceous and Tertiary sedimentary cover implying rejuvenated basement structures.

Figure 1. MSS Lineament map.

Figure 2. TM Lineament map.

Figure 3. Clear lineament frequencies, lengths and orientations derived from MSS and TM data. Total fault orientations derived from the Portland map sheet are also shown.

Figure 4. Subtle lineament frequencies, lengths, and orientations derived from MSS and TM data. Total figures for both clear and subtle lineaments are also shown.

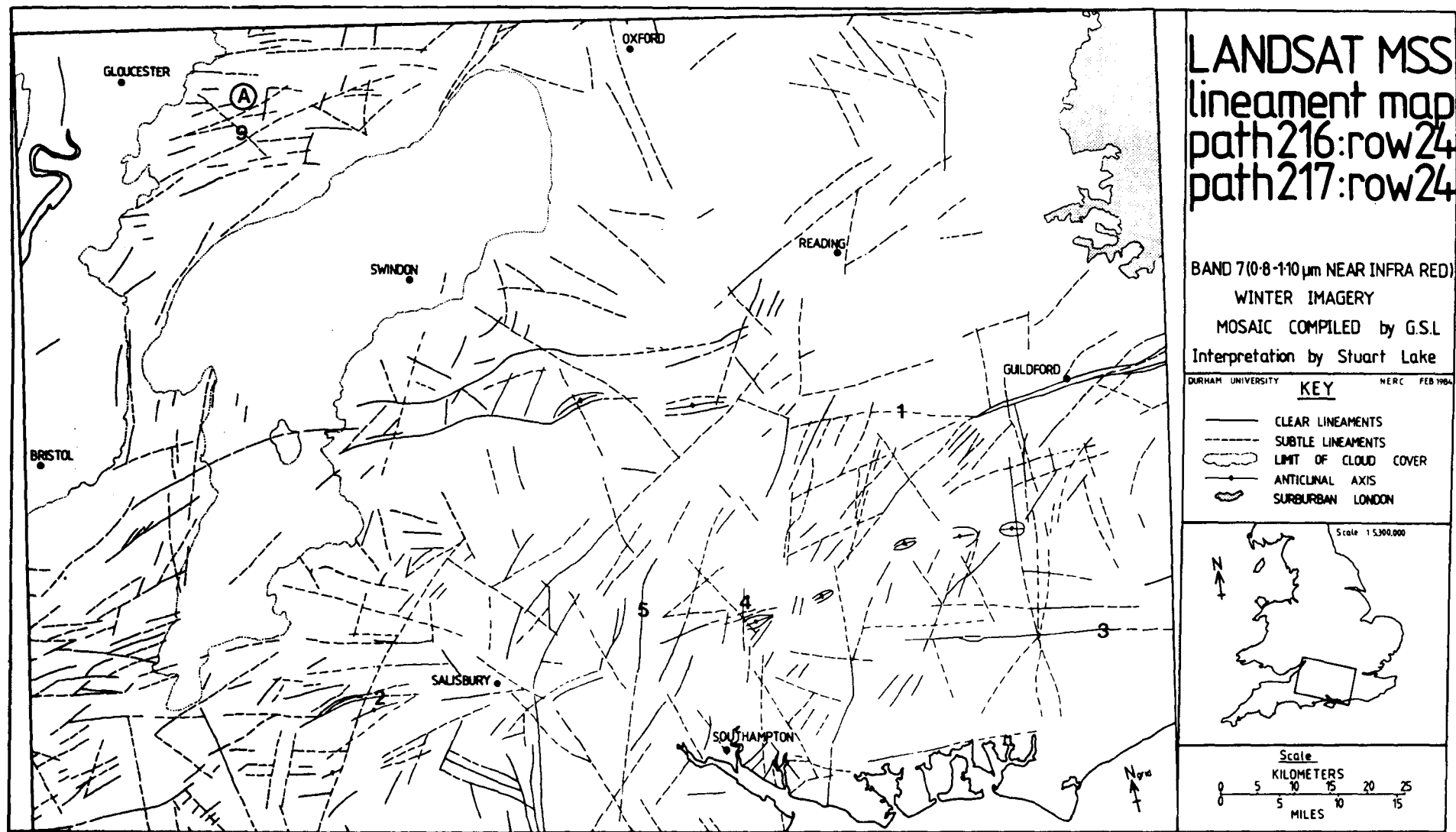


FIG 1

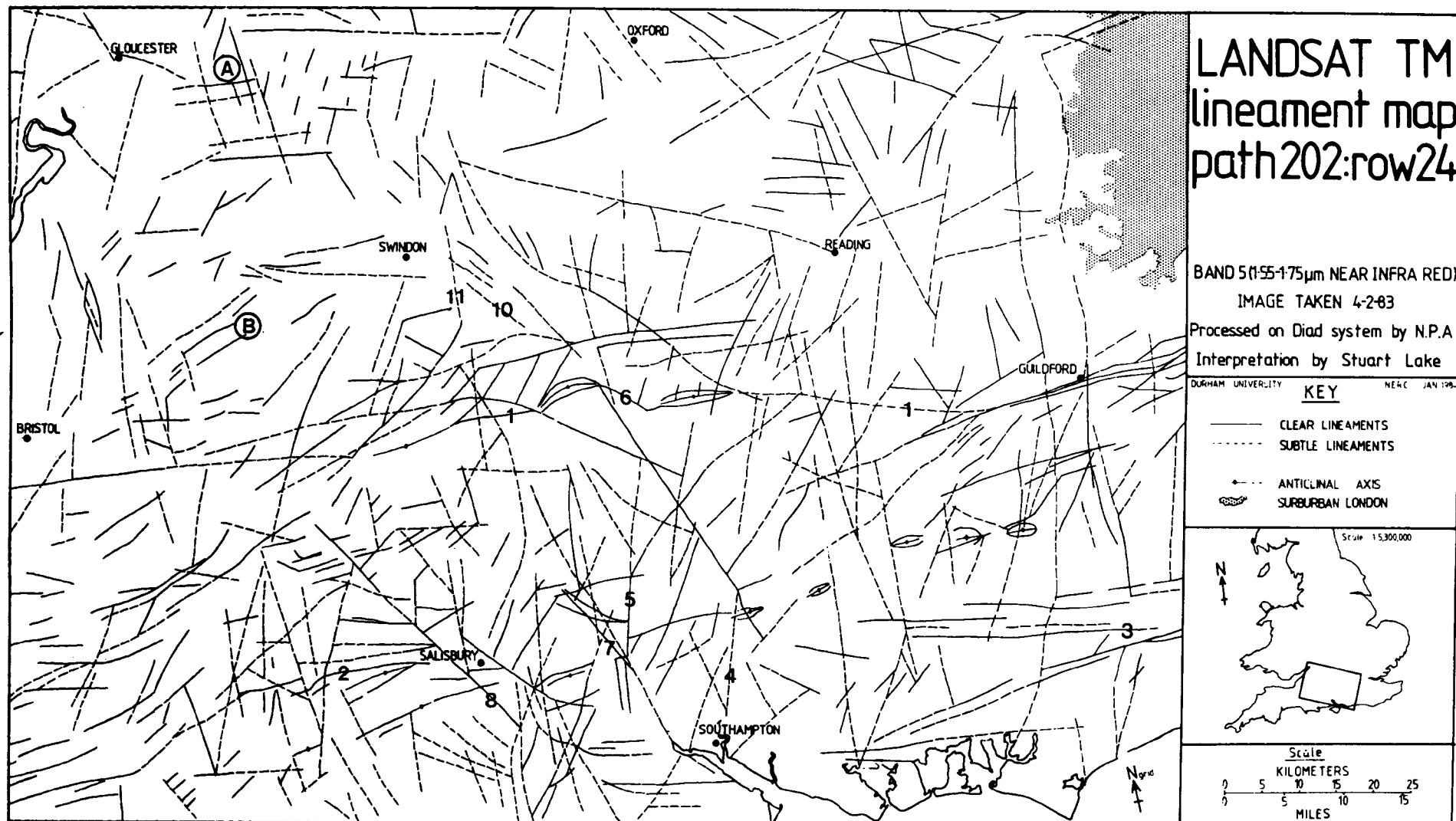


FIG 2

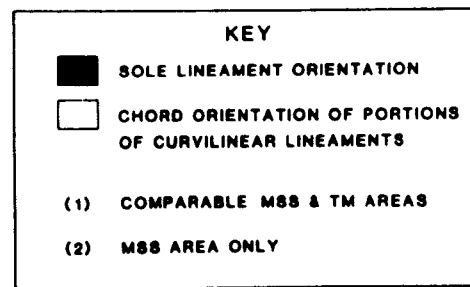
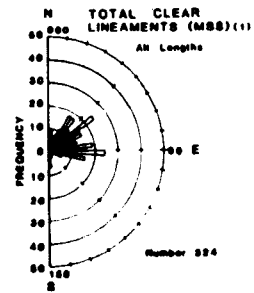
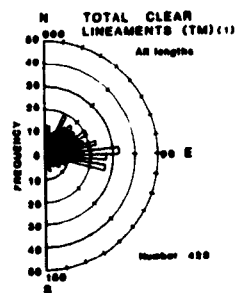
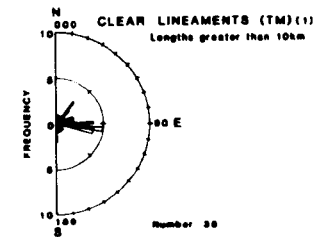
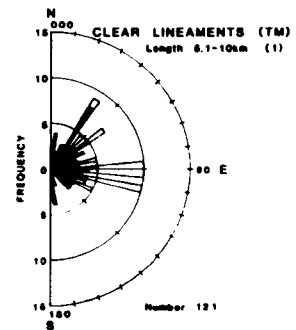
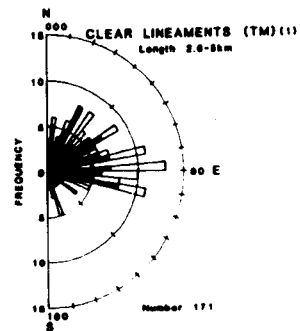
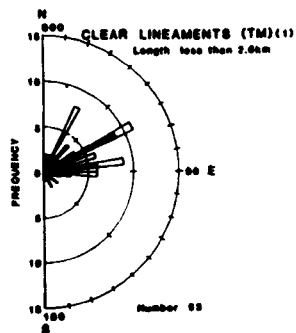
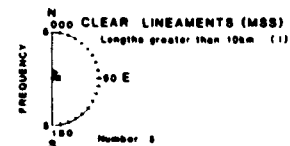
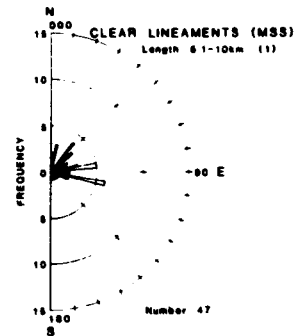
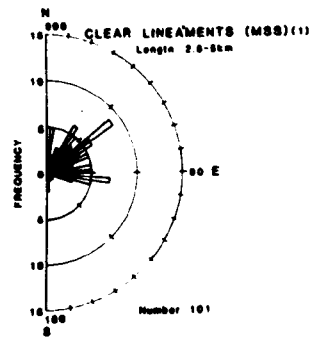
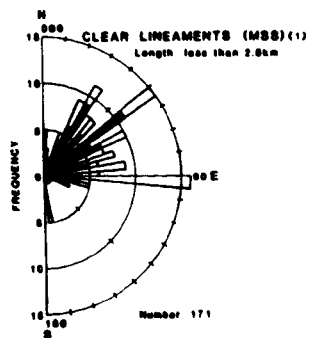
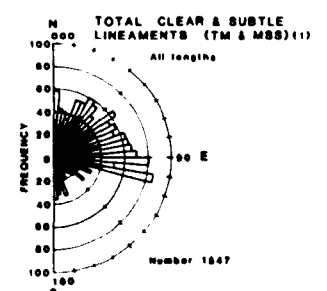
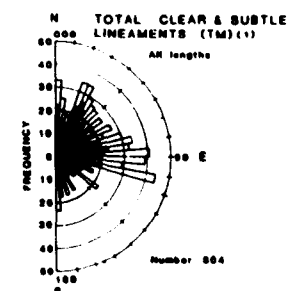
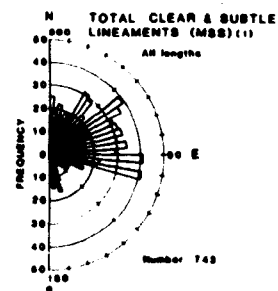
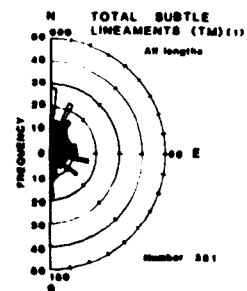
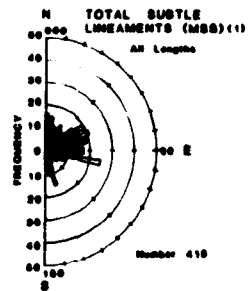
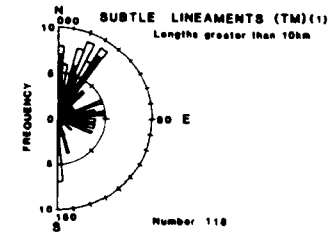
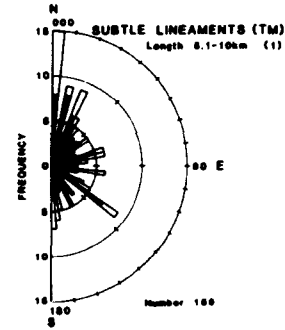
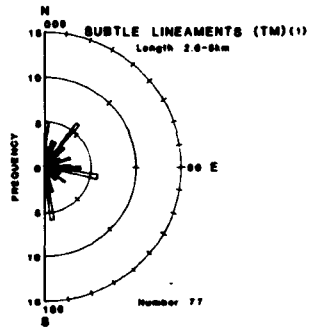
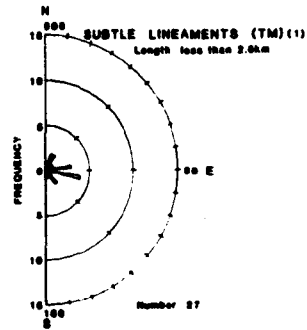
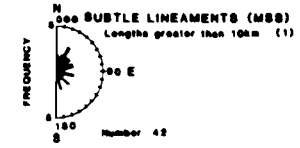
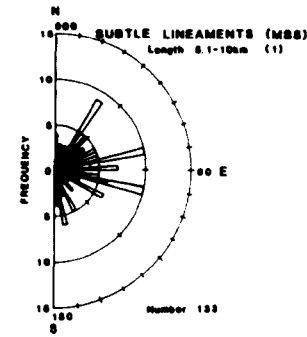
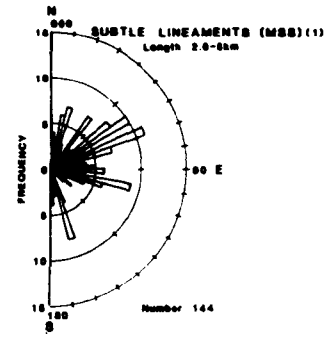
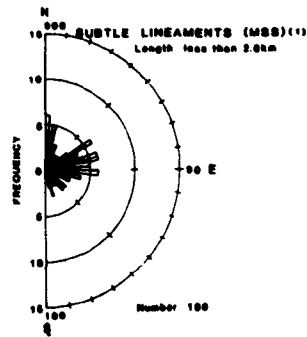


FIG. 3

FIG. 4



APPENDIX E

APPENDIX E

BRECCIATED PIPES AND THE BROKEN BEDS, PURBECK LIMESTONE FORMATION

S.D. Lake (Department of Geological Sciences, University of Durham, South Road, Durham DH1 3LE)

Abstract

Previously unrecorded breccia pipes extend up from the underlying Broken Beds into the undisturbed sedimentary cover. These have been identified at Bacon Hole and Durdle Door in south Dorset. The likely causes for the formation of the Broken Beds are re-evaluated. The results imply both diagenetic and tectonic effects during the Tertiary uplift of the Isle of Wight/Purbeck monocline along a former Mesozoic roll-over anticline.

The Purbeck Formation has attracted considerable interest over the past 200 years, in particular the remarkable limestone breccias at the base of the sequence that constitutes the Broken Beds. Various hypotheses have been suggested to explain their formation, these are reviewed by West (1960) and he advanced both a tectonic and sedimentary origin (West 1964 & 1975) whereupon removal of evaporites provided a place of weakness which was acted upon by tectonic forces.

Recent fieldwork by the author led to the discovery of breccia pipes that extend, in some cases, at least 10 metres from the Broken Beds into the overlying Lower Purbeck sequence. Therefore these hypotheses listed by West (1960) must somehow explain this phenomena or alternative hypotheses put forward.

The occurrence of the breccia pipes is particularly well exhibited at Bacon Hole (N.G.R. SY 842 797) where the largest upstanding stack has a peculiar knoll at the top (fig. 1 and Plate A.1). This is particularly well seen on the dust jacket-frontispiece of Arkell's (1947) memoir. On close examination this knoll displays the typical limestone brecciation associated with the Broken Beds, yet lies at least 5 metres above the main Broken Bed horizon. Examination from the seaward (southern) side of the stack particularly well displays the upward extension from the main Broken Bed horizon. A small scale example is well displayed on the eastern side of the stack, the brecciation extends some 4m into the overlying "Cypris" Freestone Member (Fig. 1). The width of both these pipes is approximately 4 meters.

Durdle Door eastern promontory (NGR SY 807 803) also displays a similar feature. The bedding planes of the "Cypris" Freestone member



← Plate A.1 A view of a brecciated pipe within the Purbeck Beds extending up through the 'Cypris freestones' from the 'Broken Bed' horizon, Mupe rock, Bacon Hole (N.G.R. SY 840 797). The detailed description of this structure is outlined in Appendix E.

↑ Plate A.2 Strong asymmetric folds exposed in the Purbeck Beds at Bacon Hole, with short, (N.G.R. SY 840 797) almost vertical north limbs. Axial planes dip 30°S. The relative movement is implied to be down dip to the north.

show a hemispherical brecciated body at beach level between the beach and the promontory. This breccia is definitely part of the Broken Beds, yet lies some distance above the main Broken Bed horizon. A lack of cross sectional exposure makes this somewhat speculative due to known local limestone partings within the Broken Beds, e.g. Worbarrow Tout (NGR SY 869 796) (see West, 1975; Ensom, 1985). Clearly these 'breccia pipes' are very important in the evolution of the Broken Bed horizon.

It can be shown from borehole evidence that further east on the Isle of Wight that the same stratigraphic horizon predominantly comprises anhydrite and gypsum. The Broken Beds are absent on the Isle of Portland. That conditions were hypersaline when these sediments were deposited is clearly demonstrated both ostracod and palynomorph assemblages (Anderson and Bazley, 1971; Hunt, 1980), algal remains (Brown, 1963) and the local presence of celestine (West, 1960).

The overlying "Cypris" Freestone member comprises laminated ostracodal biosparites, similar to the limestone blocks observed in the upper part of the Broken Beds sequence.

The diagenetic history of the Broken Beds was superbly demonstrated by West (1964) who showed that primary gypsum was converted to secondary anhydrite and locally replaced by chert prior to brecciation, although by no means all the silicification predated the gypsum-anhydrite change.

In the light of this work a further contribution can be made resulting from the observed breccia pipes and new structural evidence. The evolution of the Broken Beds is envisaged as follows, primary gypsum developed prior to burial (West, 1964) intercalated with thin layers of laminated ostracodal biosparite. Increasing depth of burial of the unit resulted in dehydration of the gypsum to anhydrite. This undoubtedly

occurred prior to the Eocene and the initiation of uplift. The depth of burial was probably less than 1500 metres based on known sedimentary thickness of the overlying units. The dehydration resulted in approximately 38% volume decrease (Blatt et al., 1972) thus resulting in abnormal fluid pressures. Fluids were undoubtedly additionally derived from the nearby algal limestones or clays. Locally the dirt beds (the Great dirt bed in particular) that lie at the base of the Broken Bed sequence may have acted partly as an impermeable layer preventing downward percolation of fluids. This combined with increasing lithostatic pressure associated with burial may have caused the pressurised fluids to outflow diapirically or resulted in hydrofracturing into the overlying "Cypris" Freestone member prior to flexuring.

Inversion undoubtedly initiated in the Palaeocene from structural evidence presented by Lake and Karner (1986) and was intermittent throughout the Tertiary, culminating in the Miocene. Gradual uplift, like that described, would result in rehydration of the anhydrite to gypsum. However the rate of uplift probably resulted in the rehydration having an insignificant effect on large scale volume changes. Later the sequence was calcitized resulting in small scale volume reduction.

Arkell (1938) convincingly demonstrated the tectonic control on brecciation. This is clearly evidenced by "asymmetric" northward facing monoclinial flexures confined solely within the Broken Beds, particularly at Bacon Hole, thus suggesting that the Broken Beds acted as an incompetent bed (Plate A.2). Enhanced by rehydration, initiation of downslope movement associated with increasing monoclinial flexuring and bedding plane slip, would further brecciate and deform the horizon. Therefore the Broken Beds are a result of combined dehydration and

collapse associated with anhydrite formation followed by subsequent rehydration and dissolution, as well as the tectonic monoclinal flexuring and uplift of the Isle of Wight-Purbeck monocline during the Palaeogene.

The absence of the Broken Beds to the east and west may reflect original sedimentological differences, the permeability of the surrounding lithologies, the absence of tectonic control and the timing of rehydration.

Acknowledgements

I thank the Natural Environment Research Council for the award of an NERC studentship and Marc Helman and Maurice Tucker for invaluable discussion and Mrs. C. Blair for typing this contribution.

References

- Arkell, W.J., 1938. The Purbeck Broken Beds. *Geol. Mag.*, vol. 75, p. 333-334.
- Arkell, W.J., 1947. The geology of the country around Weymouth, Swanage, Corfe and Lulworth. *Mem. geol. Surv. G.B.*
- Anderson, F.W. and Bazley, R.A.B., 1971. The Purbeck Beds of the Weald (England). *Bull. geol. Surv. G.B. No. 34.*
- Blatt, H., Middleton, G. and Murray, R., 1972. *Origin of Sedimentary Rocks.* Prentice-Hall, New Jersey.
- Brown, P.R., 1963. Algal Limestones and Associated Sediments in the Basal Purbeck of Dorset. *Geol. Mag.*, vol. 100, p 565-573.
- Ensom, P.C., 1985. An Annotated Section of the Purbeck Limestone Formation at Worbarrow Tout, Dorset. *Dorset Proceedings*, vol. 106, p. 87-91.
- Fisher, O., 1856. On the Purbeck Strata of Dorsetshire. *Trans. Camb. phil. Soc.*, vol. 9, p. 555-581.
- Hunt, C.O., 1980 A palynological investigation of the Lulworth Beds of Durlston Bay, Dorset, Unpublished M.Sc. thesis, University of Sheffield.
- Lake, S.D., and Karner, G.D., 1986. The structure and evolution of the Wessex Basin, Southern England: An example of inversion tectonics. *Tectonophysics*, vol. 000, p. 000-000.
- Sedgwick, A. and Murchison, R., 1840. On the Physical Structure of Devonshire. *Trans. Geol. Soc., Series II*, v. p. 633-703.
- Webster, T., 1816. Letters from Dorset (In: Enqlefield, H.C., *Picturesque Beauties of the Isle of Wight*, p. 117-238).

- West, I.M., 1960. On the occurrence of celestine in the Caps and Broken Beds at Durlston Head, Dorset. Proc. Geol. Assoc., vol. 71, p. 391-401.
- West, I.M., 1964. Evaporite diagenesis in the Lower Purbeck Beds of Dorset. Proc. Yorks. geol. Soc., vol. 34, p. 315-330.
- West, I.M., 1975. Evaporites and associated sediments of the basal Purbeck Formation (Upper Jurassic) of Dorset. Proc. Geol. Assoc., vol. 86, p. 205-225.

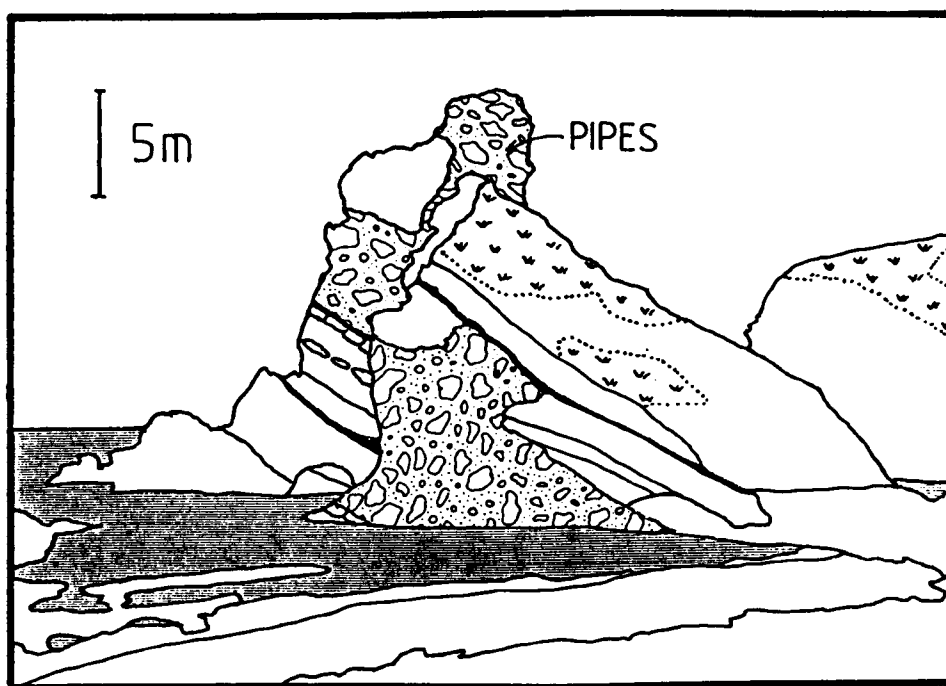


Figure Captions

- Fig. 1** Breccia pipes extending into the overlying Cypris Freestone Series from the Broken Beds. Looking south-westwards at Mupe Rocks, Bacon Hole (NGR SY 842 797)

APPENDIX F

APPENDIX F

EVIDENCE FOR BATHONIAN AND TITHONIAN SYNSEDIMENTARY FAULT MOVEMENTS IN
DORSET

S.D. Lake (Department of Geological Sciences, University of Durham).

ABSTRACT

Two localities are described at which synsedimentary fault movements can be inferred, based on sedimentary thickness variations across faults. Movement can be demonstrated in the Bathonian, Fullers Earth at Herbury, and in the Tithonian, Portland/Purbeck boundary at Durlston Head. These localities are structurally significant in describing the evolution of the area.

Dorset lies in the western portion of a large Late Palaeozoic-Cenozoic sedimentary basin within which at least four sub-basins can be distinguished, which extends from the 'Kent coast', in the east to the Dartmoor area in the west. The evolution of this area has been recently reviewed by Stoneley (1982), and Whittaker (1985). Many authors have demonstrated the importance of large scale E-W intermittent synsedimentary faulting in the basin particularly in the Mesozoic, however only one record to date of synsedimentary fault movement demonstrable at outcrop has been published (Jenkyns and Senior, 1977). Jenkyns and Senior (1977) reported on demonstrable synsedimentary movement occurring along the Eype mouth fault at Watton Cliff near

Bridport in the Toarcian (Junction Bed) horizon. During a much larger investigation of the structural evolution of Southern England by the author, at least two other localities show similar synsedimentary fault movement of differing ages.

The first locality at Herbury (N.G.R. SY 612 811) shows Fullers Earth clay overlain by the Forest Marble. The base of the Forest Marble is marked by a distinctive, brachiopod-rich limestone called the Boueti Bed (Arkell, 1947) seen at the top of the Cliff. Some 2 metres below the Boueti bed lies a distinctive calcilutite bed within the Fuller's Earth which dips approximately 7° to the south eventually cropping out on the beach at the north-west extremity of the Herbury promontory (Plate A.3). The bed is disrupted by at least two faults striking 190° and dipping approximately 87° SE and shows abrupt thickness changes across the faults, for example between the two exposed faults, the bed thickens from 9 cm on the immediate upthrown side to 28 cm on the downthrown side. Thus the limestone bed thickens up against the fault on the footwall downthrown side (Fig. 2). The Fullers Earth immediately above the limestone bed demonstrably thickens up against the fault, in addition the overlying Fuller's Earth overlaps eastward onto the upper bedding plane of the limestone Bed, implying N-S synsedimentary fault movement during the Bathonian in the Herbury area.

The second locality, Durlston Head (N.G.R. SZ 036 773) displays the complicated character of the the Portland/Purbeck boundary. The locality on the foot of the cliff ENE of Durlston Castle (Fig. 2, plate A.4) shows a series of dominant northward dipping normal faults, for example F1 which has a 7m normal downthrow. F2 shows a small displacement, whilst F3 shows a remarkable contrast in thickness on



Plate A.3 A detailed view of the Bathonian section at Herbury (N.G.R. SY 611 810) reveals growth faulting within the Fullers Earth. This is exemplified by the thickening of the limestone in the centre of the section from left to right against the fault, and progressive onlap to the left of the picture, (see Appendix F).

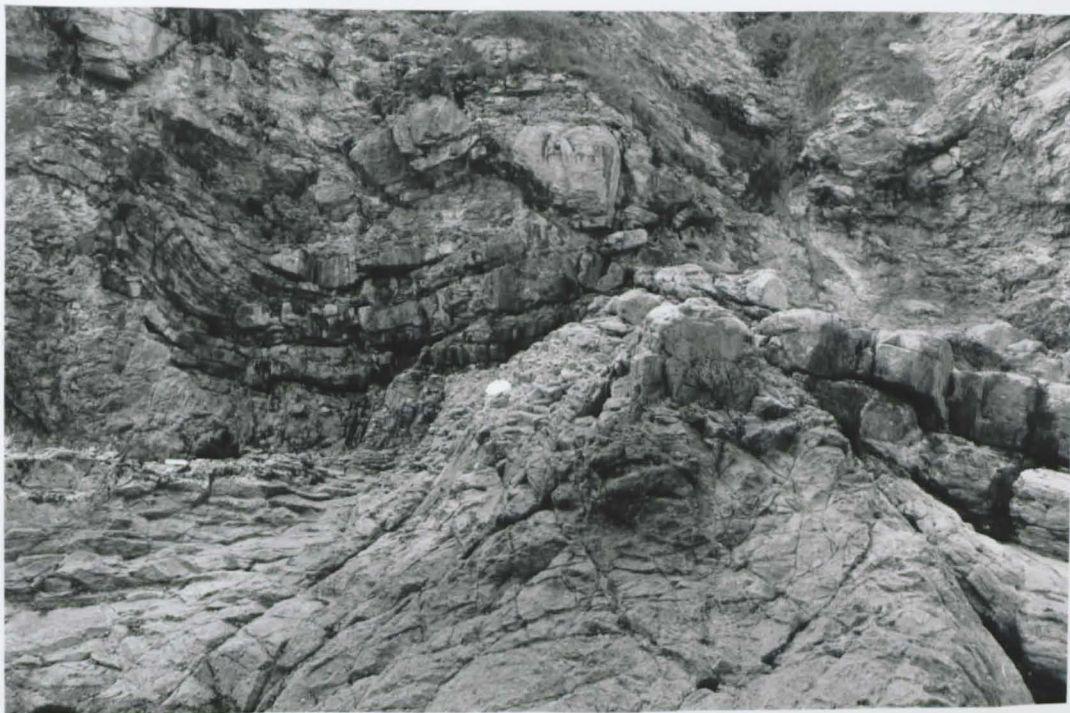


Plate A.4 Looking due west at the Tithonian growth fault described in Appendix F at Durlston Head (N.G.R. SZ 036 773). Fault 3 (see Appendix F) displayed in the centre of the picture. A major increase in thickness in the lower Purbeck stromatolitic units is displayed across the fault zone.

either side as noted by West (1960). Additionally, F3 also has well developed sub-horizontal E-W slickenside lineations, suggesting some oblique slip motion along the E-W faults. The difference in thickness on the two sides of F3 in particular is emphasised by measuring the thickness from the Portland/Purbeck junction up succession to a conspicuous impure laminated limestone, the basal bed of the "Cypris" freestone member (West, 1960). On the hanging wall southern side of F3, this succession just exceeds 2m whilst on the downthrown footwall side it exceeds 8m. Ordinarily this thickness variation could be attributed to removal of mineral solutions from the Broken Bed horizon, however the thickness change is too rapid, considering the small throw along F3. In addition the limestone beds immediately below the Broken Beds on either side of F3 do show a significant thickness variation from 3m plus on the northern footwall side to less than 1m on the southern hanging wall side. The lack of brecciation provides clear evidence that removal by mineral solution of the sequences cannot account for such thickness variations. Alternatively the presence of subhorizontal slickensides could indicate that similar thicknesses may exist across the fault except that one side has been moved by E-W oblique slip motion out of the plane of section. Though this may be partly true, from the author's own analysis, there is no clear evidence to suggest substantial E-W oblique slip motion either in this area or elsewhere. In addition the immediate footwall side of F3 displays a complex step faulted 'micro graben' some 5 m across and some 1.5m deep at the Purbeck/Portland boundary in the Hard Cap - a basal Purbeck limestone individual fault blocks within this 'micrograben' also display small scale thickness variations.

Thus this locality displays clear evidence of Portlandian

synsedimentary faulting previously not documented in the Dorset area. However breaks in sedimentation have been recorded at this boundary from subsurface data in Sussex, where the break is widespread and uniform without signs of erosion.

Acknowledgements

I thank the Natural Environment Research Council for the award of a N.E.R.C. studentship, Alastair Baird, Antony Dixon, Tim Palmer, and Paul Ensom for helpful comments on the manuscript, and Mrs. C. Blair for typing this contribution.

References

- Arkell, W.J., 1947. 'The geology of the country around Weymouth, Swanage, Corfe and Lulworth', Mem. geol. Surv. G.B.
- Jenkyns, H.C. and Senior, J., 1977. 'A Liassic palaeofault from Dorset'. Geol. Mag., vol. 114, p. 47-52.
- Stoneley, R., 1982. 'The structural development of the Wessex Basin'. J. geol. Soc. London, vol. 139, p. 543-554.
- West, I.M., 1960. 'On the occurrence of celestine in the Caps and Broken Beds at Durlston Head, Dorset', Proc. Geol. Assoc., Vol. 71, 391-401.
- Whittaker, A., (ed.), 1985. 'Atlas of Onshore Sedimentary Basins in England and Wales: Post-Carboniferous Tectonics and Stratigraphy', Blackie, Glasgow.
- Wimbledon, W.A. and Hunt, C.O., 1983. The Portland-Purbeck junction (Portland-Berriasian) in the Weald, and correlation of latest Jurassic-early Cretaceous rocks in Southern England, Geol. Mag. vol. 120, p. 267-280.

Figure 1 Field sketch of N-S Bathonian growth faulting at Herbury (N.G.R. SY 612 811). Bouetti Bed thickness exaggerated to show thickness variations across faults. Large subhorizontal arrow indicates onlap of the overlying Fuller's Earth onto the Bouetti Bed.

Figure 2 Field sketch of E-W Portlandian growth faulting at Durlston Head (N.G.R. SZ 036 773). A rapid thickness variation is clearly seen across F3. More localised thickness variations are recorded in the 'micrograben' at the junction between the base 'Caps' (Basal Purbeck beds) and top Portland Stone. Inset shows an expanded view of the Durlston Head succession. Horizontal lines in inset represent the Portland Stone.



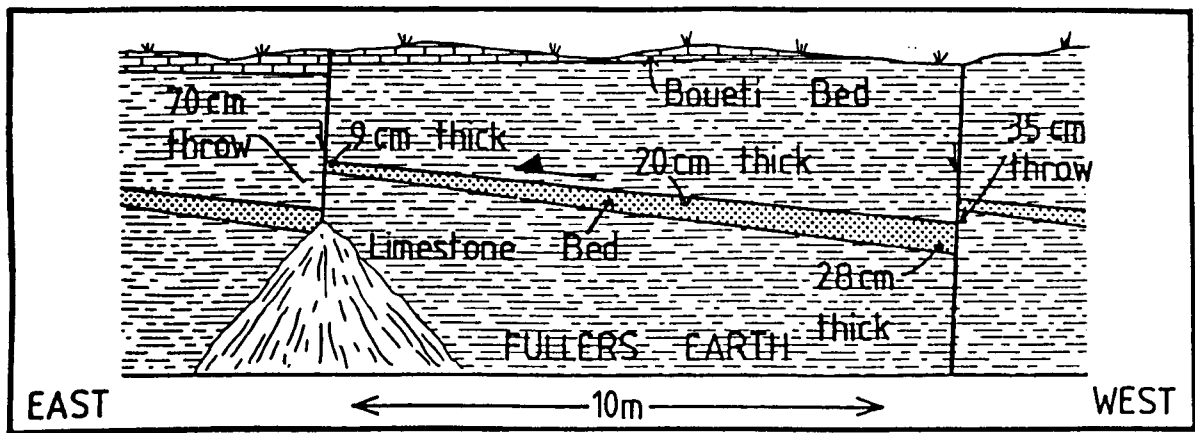


FIG. 1.

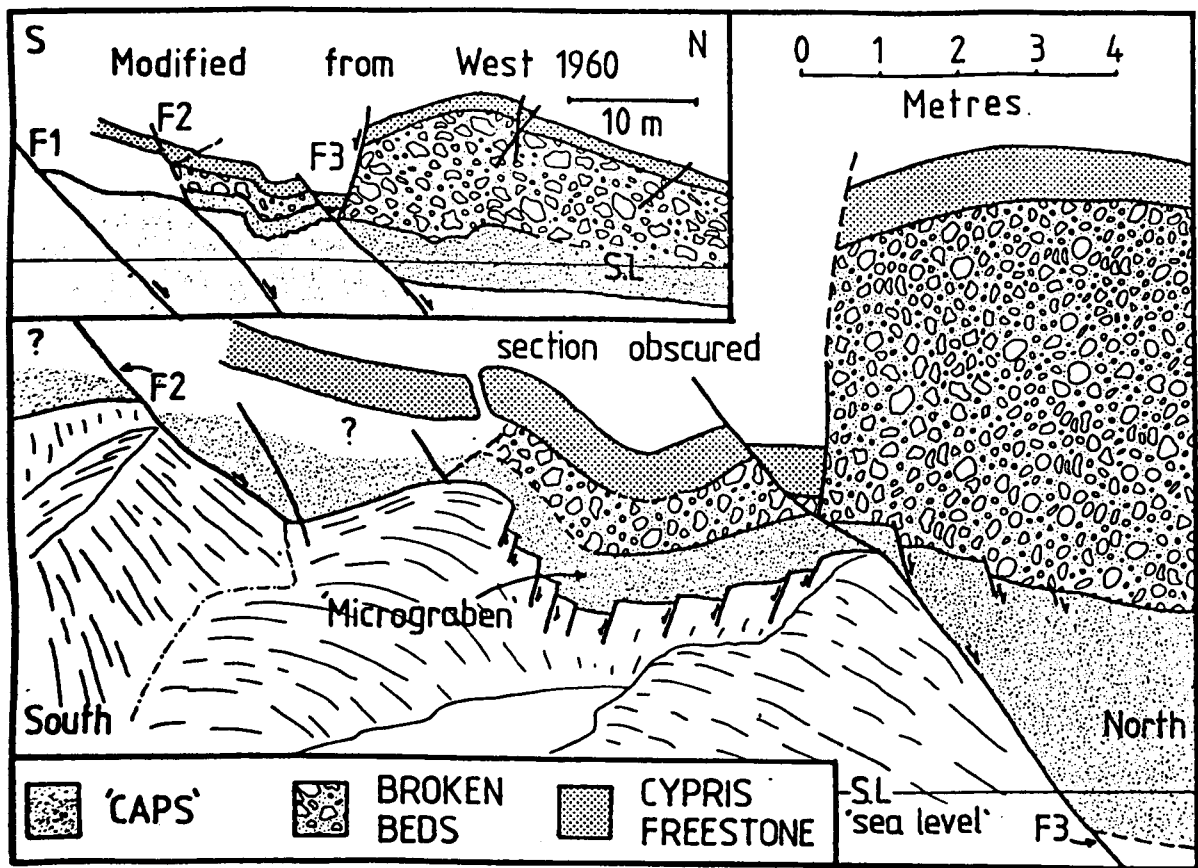


FIG. 2.

Figure 1. Field sketch of E-W section of Boueti Bed and Limestone Bed at Boueti. (N.B. 25 613 811). Boueti Bed thickness measured as shown. Thickness variations across Boueti Bed are indicated by arrows. Indicated units of the Boueti Bed are the Boueti Bed.

Figure 2. Field sketch of E-W section of Boueti Bed and Limestone Bed at Boueti. (N.B. 25 613 811). A rapid thickness variation is clearly seen across F2. Note localized thickness variations are recorded in the 'micrograben' at the junction between the Boueti Bed and Limestone Bed. (Note Boueti Bed and Limestone Bed are shown in expanded view of the Boueti Bed section. Horizontal lines in inset between the Boueti Bed and Limestone Bed.

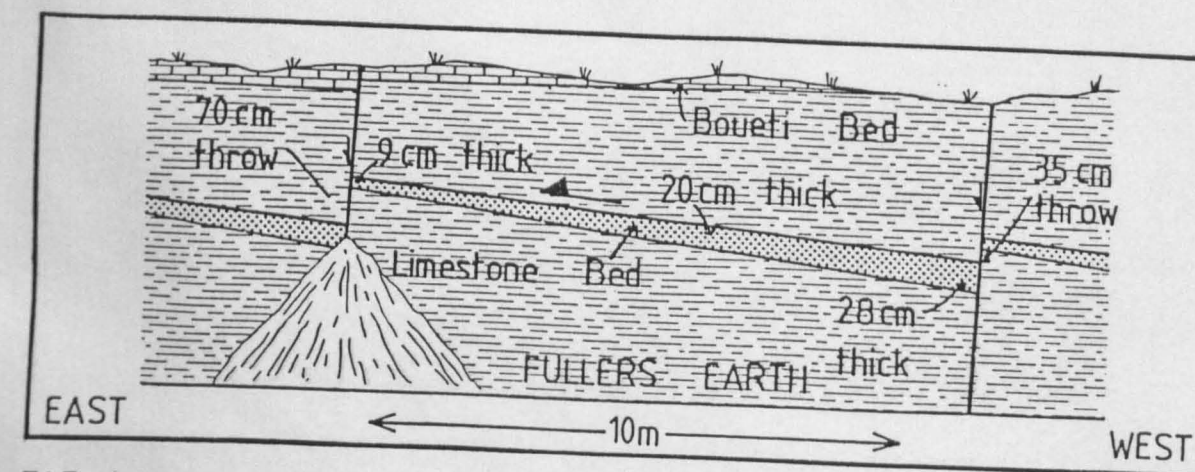


FIG. 1.

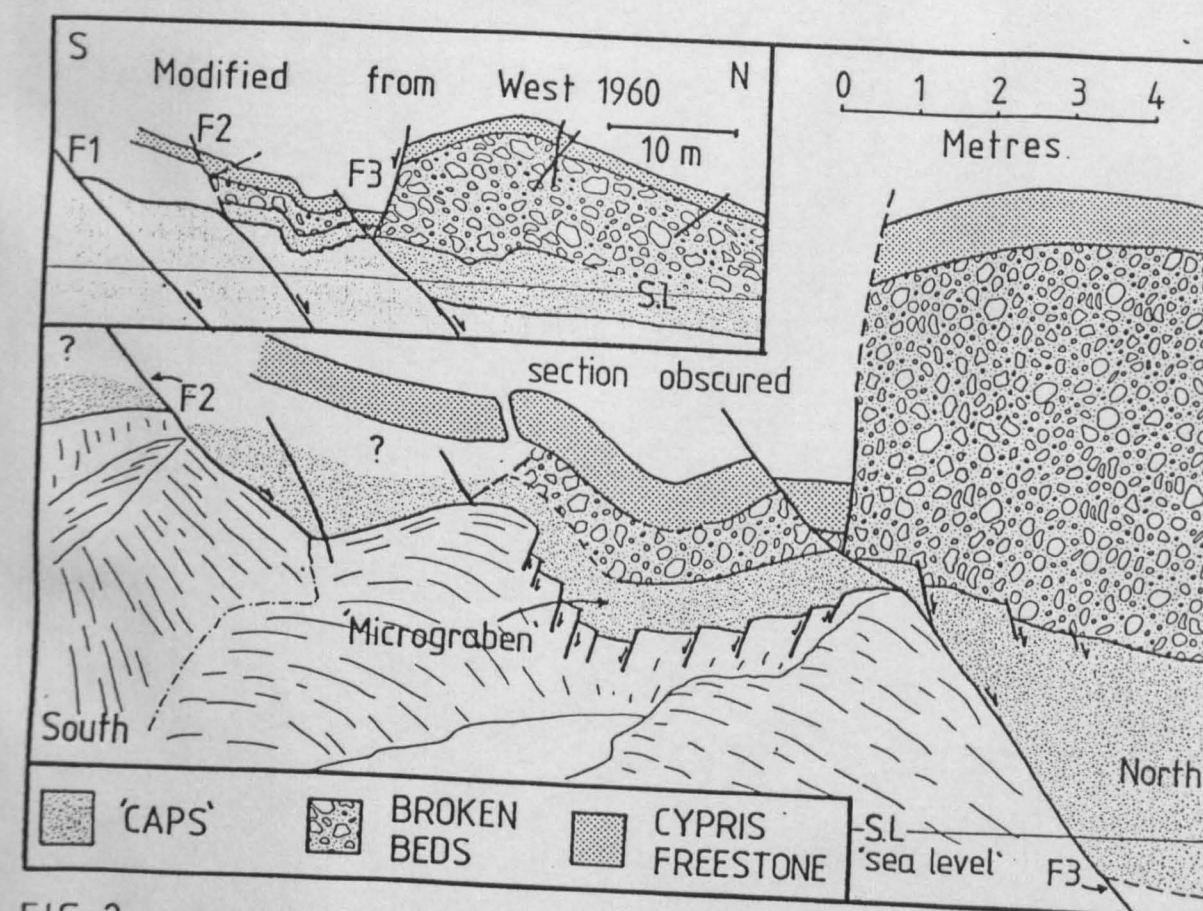


FIG. 2.